NASA Contractor Report   187598

NASA/AMERICAN SOCIETY FOR ENGINEERING EDUCATION (ASEE) SUMMER FACULTY FELLOWSHIP PROGRAM 1991

Surendra N. Tiwari   (Compiler)

OLD DOMINION UNIVERSITY
Norfolk, Virginia

Grant   NGT 47-003-029
September 1991

NASA
National Aeronautics and
Space Administration

Langley Research Center
Hampton, Virginia 23665

TABLE OF CONTENTS

i

LIST OF TABLES

LIST OF ABSTRACTS - RESEARCH FELLOWS

Section I

Organization and Management

The 1991 Old Dominion University (ODU)-NASA-Langley Research Center (LaRC) Summer Faculty Fellowship Research Program, the twenty-eighth such institute to be held at LaRC was planned by a committee consisting of the University Co-Director, LaRC staff members from the research divisions and the Office of University Affairs. It was conducted under the auspices of the Langley Research Center's Chief Scientist, Dr. Michael F. Card.

Each individual applying for the program was provided a listing of research problems available to the LaRC Fellows. Each individual was requested to indicate his or her problem preference by letter to the University Co-Director. The desire to provide each Fellow with a research project to his or her liking was given serious consideration.

An initial assessment of the applicant's credentials was made by the NASA-LaRC University Affairs Officer and the University Co-Director. The purpose of this assessment was to ascertain to which divisions the applicant's credentials should be circulated for review. Each application was then annotated reflecting the division to which the applications should be circulated. After the applications had been reviewed by the various divisions, a committee consisting of staff members from the various divisions, the University Affairs Officer and the University Co-Director met. At this meeting the representatives from the various divisions indicated those individuals selected by the divisions.

The University Co-Director then contacted each selected Fellow by phone extending the individual the appointment. The University Co-Director also forwarded each selected Fellow a formal letter of appointment confirming the phone call. Individuals were given ten days to respond in writing to the appointment. As letters of acceptance were received, contact was made with each Division Coordinator advising them of their Fellows for the summer program.

Each Fellow accepting the appointment was provided material relevant to housing, travel, payroll distribution and a listing of all NASA-LaRC Research Fellows. Each Fellow, in advance of commencing the program, was contacted by his or her Research Associate or a representative of the branch.

At the assembly meeting, Dr. Michael F. Card, Chief Scientist of the Langley Research Center, introduced the Langley Center Director, Mr. Richard Petersen who formally welcomed the summer Fellows and presented the video entitled "An Overview of Langley Research Center. Dr. mark Nataupsky briefed the Fellows on the benefits of the Visitor's Center. Mr. George Roncaglia from the Technical Library Branch briefed the Fellows on the use of the library. Mr. Richard Weeks, manager of the LaRC cafeteria, briefed the Fellows relevant to the cafeteria policies, hours, etc. Dr. John Shoosmith of the Analysis

and Computation Division briefed the Fellows on the Computational Facilities. The subject of security at LaRC was discussed by O. J. Cole from the Security Branch. Safety procedures were discussed by Mr. Clarence Breen from the Safety Branch. Mrs. Pam Verniel presented programs and activities sponsored by the Activities Center. Peter Edgette discussed the Occupational Health Services available through the clinic. Further information was disseminated by Dr. Surendra Tiwari, ODU, Dr. John Whitesides, George Washington University (GWU), and Dr. Lois S. Miller, ODU. Mr. Edwin J. Prior introduced the Langley Associates.

Throughout the program the University Co-Director served as the principal liaison person and had frequent contacts with the Fellows. The University Co-Director also served as the principal administrative officer. At the conclusion of the program, each Fellow submitted an abstract describing his/her accomplishments. Each Fellow gave a talk on his/her research within the division. The Research Associate then forwarded to the Co-Director the name of the person recommended by the division for the final presentation. Fifteen excellent papers were presented to the Fellows, Research Associates, and invited guests.

Each Fellow and Research Associate was asked to complete a questionnaire provided for the purpose of evaluation of the summer program.

Section II

Recruitment and Selection of Fellows

Returning Fellows

An invitation to apply and participate in Old Dominion University (ODU)-Langley Research Center (LaRC) Program was extended to those individuals who held 1990 LaRC Fellow appointments. Twenty individuals responded to the invitation, however, only thirteen were selected (Table 1). Twenty-nine applications were received from Fellows from previous years or from other programs. Five were selected .

New Fellows

Although ASEE distributed a combined brochure of the summer programs, many personal letters were mailed to deans and department heads of various engineering schools in the East, South and Midwest, by Dr. Surendra Tiwari of Old Dominion University (ODU), and by Professor John Spencer of Hampton University (HU) requesting their assistance in bringing to the attention of their faculties the ODU/HU-LaRC program. In addition, to the above, a number of departments of chemistry, physics, computer science and mathematics at colleges (including community colleges) and universities in the State of Virginia as well as neighboring states were contacted regarding this program. Although minority schools (Table 2) in Virginia and neighboring states were included in the mailing, the Co-Director from HU made site visits to minority schools soliciting applicants, and sent over three hundred letters to deans and department heads. These efforts resulted in a total of eighty-eight formal applications, all indicating the ODU/HU-LaRC Program as their first choice and a total of forty indicating the ODU/HU-LaRC Program as their second choice. The total number of applications received came to one hundred twenty-nine (Table 3).

Forty-one applicants formally accepted the invitation to participate in the program. Nine applicants declined the invitation. Several Fellows delayed their decision while waiting for acceptance from other programs. The top researchers seem to apply to more than one program and will make their selection based on research interest and stipend. Twenty-six positions were initially budgeted by NASA. Fifteen positions were funded by the LaRC divisions (Table 4).

The average age of the participants was 41.5.

TABLE I
RETURNEE/FIRST YEAR FELLOWS

41 (100%)

13 (31.7%)

28 (68.2%)

NO. OF FELLOWS
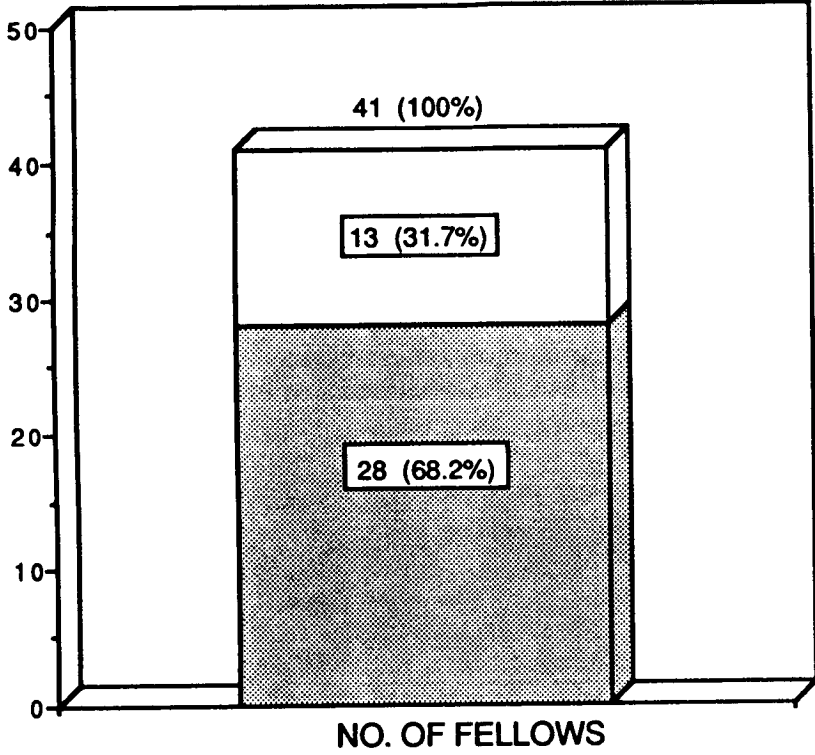
☐ RETURNEE

▨ FIRST YEAR

TABLE 2
DISTRIBUTION BY UNIVERSITY

31 (100%)

2 (6.5%)

3 (9.7%)

26 (83.9%)

NO. OF FELLOWS

☐ OMU

▦ HBCU

▩ NON-MINORITY
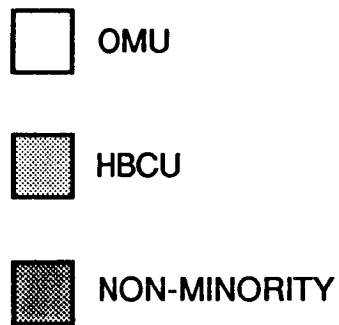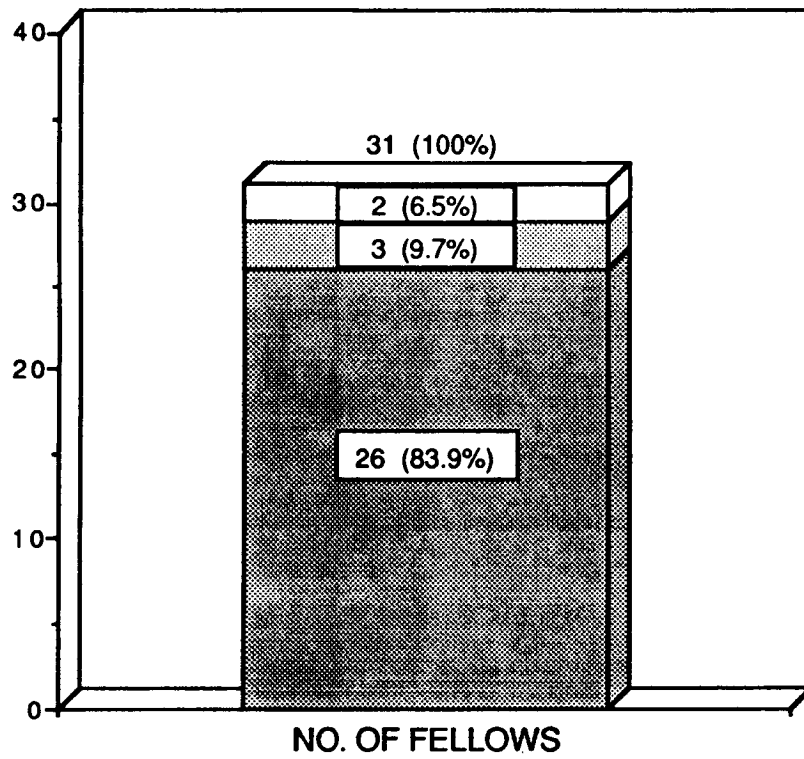
TABLE 3
APPLICATIONS/SELECTED

129 (100%)

41 (31.7%)

88 (68.3%)

NO. OF APPLICATIONS

200

100

0
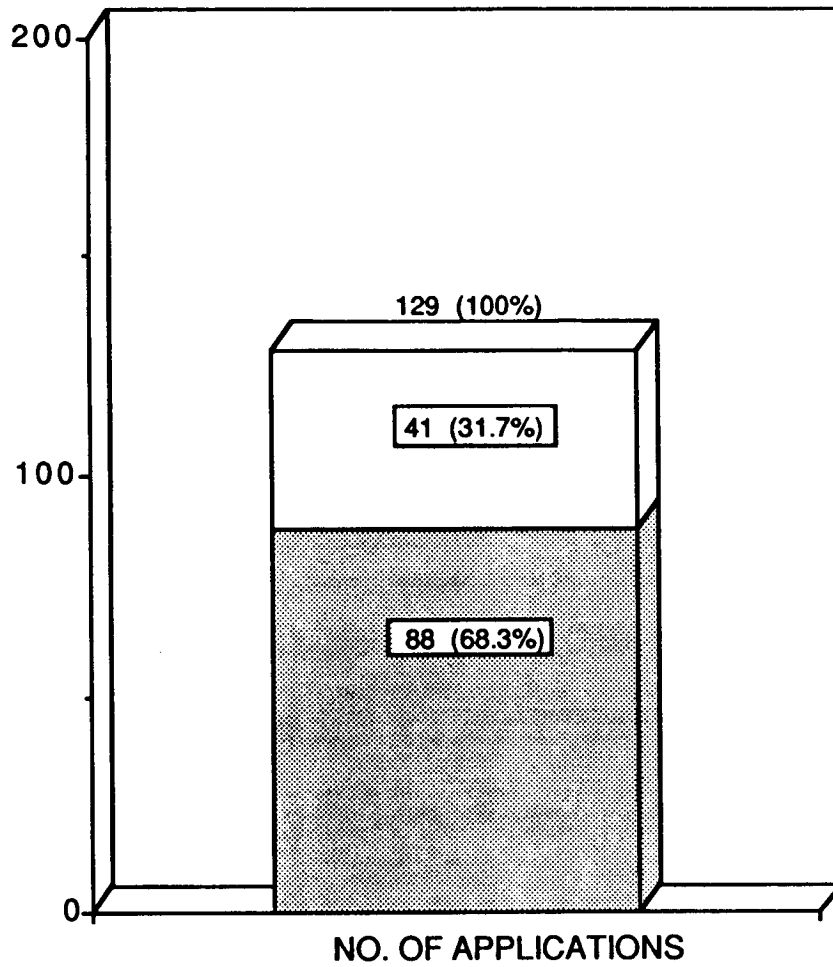
SELECTED

NON SELECTED

TABLE 4
DISTRIBUTION BY FUNDING

NO. OF FELLOWS

FUNDING SOURCE

41 (100 %)

15 (37%)

26 (63%)

☐ LOCAL PURCHASES

▨ HEADQUARTERS
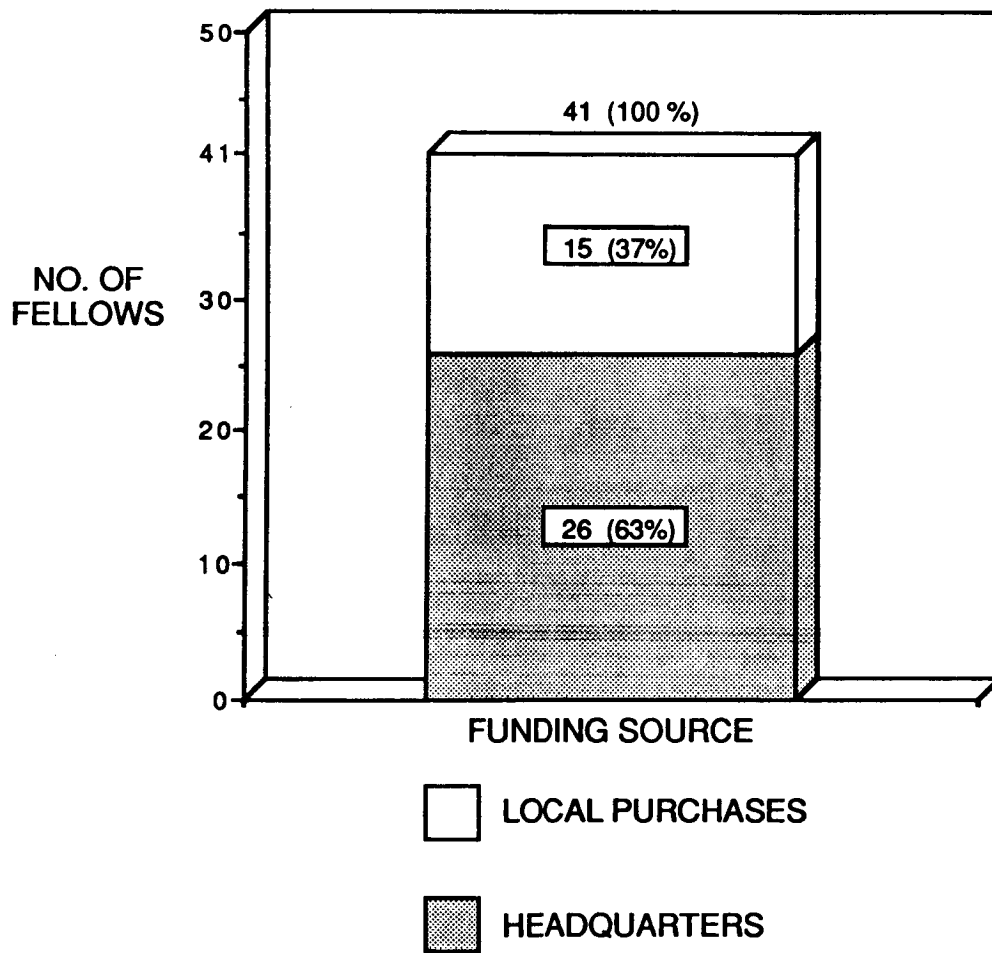
Section III

Stipend and Travel

A ten week stipend of $9,000 was awarded to each Fellow. Although this stipend has improved over previous years, it still falls short (for the majority of Fellows) of matching what they could have earned based on their university academic salaries. This decision to participate in the summer faculty research program does clearly reflect the willingness of the Fellow to make some financial sacrifice in order to participate in the summer program.

Travel expenses incurred by the Fellows from their homes to Hampton, Virginia, and return were reimbursed in accordance with current ODU regulations. A relocation allowance of $1,000.00 was provided for the Fellows traveling a distance of 50 miles or more.

Section IV

Lecture Series, Picnic, Dinner and Unsolicited Proposals Workshop

Lecture Series

In response to statements made by the Fellows, the Lecture Series was again arranged around research being done at LaRC and the speakers were LaRC research scientists.

Appendix III contains the agenda for the special ASEE Summer Lecture Series .

Picnic and Dinner

A picnic for the Fellows, their families, and guests was held on June 14, 1991. A seminar/dinner was held on August 5, 1991.

Unsolicited Proposals Workshop

An Unsolicited Proposals workshop was held on July 30, 1991.

SECTION V

Research Participation

The ODU-LaRC Research Program, as in the past years, placed greatest emphasis on the research aspects of the program. Included in this report are abstracts from the Fellows showing their accomplishments during the summer. These abstracts, together with the comments of the LaRC Research Associates with whom the Fellows worked, provide convincing evidence of the continued success of this part of the program. The Fellow's comments during the evaluation of the program indicated their satisfaction with their research projects as well as with the facilities available to them.

The research projects undertaken by the Fellows were greatly diversified as is reflected in their summer research assignments. Their assignments were as follows:

Number of Fellows Assigned	Division
2	Applied Aerodynamics Division
1	Analysis and Computational Division
2	Acoustics Division
2	Atmospheric Sciences Division
2	Office of the Chief Scientist
1	Flight Applications Division
3	Flight Electronics Division
1	Facilities Engineering Division
3	Fluid Mechanics Division
3	Flight Management Division
2	Guidance and Control Division
3	Instrument Research Division
1	Information Systems Division
7	Materials Division
3	Structural Dynamics Division
1	Structural Mechanics Division
2	Space Exploration Initiative Office
2	Space Systems Division

Thirty-seven (95%) of the participants were holders of the doctorate degree. Two (5%) held the masters degree. The group was a highly diversified one with respect to background. Areas in which the last degree was earned:

Number	Last Degree
2	Aeronautics/Astronautics
2	Aerospace Engineering
1	Chemical Engineering

9

Number	Last Degree
1	Chemical Physics
1	Chemistry
3	Civil Engineering
1	Computer Science
2	Education
3	Electrical Engineering
1	Engineering Management
1	Industrial Engineering
1	Information Systems
1	Inorganic Chemistry
1	Management
2	Materials Science & Engineering
2	Mathematics
1	Mechanical and Aerospace
6	Mechanical Engineering
2	Nuclear Chemistry
1	Organic Chemistry
1	Physical Chemistry
4	Physics
1	Psychology

Extensions

A portion of the funds remaining in the travel and relocation budget was used to grant extensions to eight Fellows in the program. To be considered for the extension, the Fellow submitted a statement of justification which was supported by the Research Associate. The requests were reviewed by the University Co-Director and the University Affairs Officer. The following individuals were granted extensions:

Sheri Beam	1 Week	Abu Masud	1 Week
Dave Johnson	1 Week	Steve Hodge	1 Week
Jim Sirkis	1 Week	N. K. Suleman	1 Week
Milton Ferguson	1 Week	Eric Spina	5 Weeks

Attendance at Short Courses, Seminars, and Conferences

During the course of the summer there were a number of short courses, seminars, and conferences, the subject matter of which had relevance to the Fellows research projects. A number of Fellows requested approval to attend one or more of these conferences as it was their considered opinion that the knowledge gained by their attendance would be of value to their research projects. Those Fellows who did attend had the approval of both the

Research Associate and the University Co-Director. The following is a listing of those Fellows attending either a short course, seminar or conference:

Sherilee Beam attended the Sony Tech Expo 91 in Washington, DC and a one week hands-on workshop with Composium and Software applications.

Bill Carpenter attended the conference Canadian Congress of Applied Mechanics.

Ed Celarier attended the NSF-Sponsored workshop on Molecular Orbital Theory at Georgia Institute of Technology, Atlanta, GA.

Linda Deans attended Indian Culture Day, Jamestown Settlement, Jamestown, VA and a short course Riding in Gliders, Wakefield, VA.

Mark Glauser was invited to give the keynote lecture at the Second World Conference on Experimental Heat Transfer, Fluid Mechanics and Thermodynamics in Dubrovnik, Yugoslavia. He also attended the ICASE Workshop Seminars on transition and turbulence.

Steve Hodge attended the AIAA Short Course on Aeroacoustics.

Dave Johnson attended four short courses: 1. Fiber Optics 2. Artificial Intelligence Concepts 3. Artificial Intelligence Applications 4. Satellite Communications Systems Engineering.

Ranga Narayanan attended International Congress on Industrial and Applied Mathematics.

Duc Nguyen attended the Fourth International Conference on Recent Advances in Structural Dynamics. Institute of Sound and Vibration Research, University of South Hampton, England.

Eric Spina attended the 22nd Fluid Dynamics , Plasma Dynamics and Lasers Conference in Hawaii.

Dennis Wilson attended "Hypersonic Propulsion Conference" July 29-31 and "Transition and Turbulence Workshop" sponsored by NASA and ICASE.

Chivey Wu attended the Aircraft Design Education Course at the University of Kansas.

Omar Zia attended American Control Conference in Boston, MA.

In addition to the above there was attendance and participation in conferences, seminars, and short courses held at LaRC.

Papers Presented

"Comparison of Polynomial Approximations and Artificial Neural Nets for Response Surfaces in Engineering Optimization " AIAA/ASME/ ASCE/AHS/ASC 33nd Structures, Structural Dynamics, & Materials Conference - Carpenter, William C., Dr.

"Education Initiative Project" Hampton City Schools Restructuring Team - Deans, Linda W., Dr.

"Proper Orthogonal Decomposition Based Turbulence Modeling" - Glauser, Mark, Dr.

"Relativistic Inertial Drag in Rotating Gravitational Fields from Classical Retarded Time Potentials" - Hafele, Joseph C., Dr.

"Locus of Pre/Post-Stall Longitudinal Eigenvalues", AIAA - Hall, Charles E. Jr., Dr.

"Evaluation and Ranking of Space Exploration Initiative Architectures using a Multi-Criteria Method" "Multiple Criteria Modeling in Space Exploration Initiative Design, Journal of the Operational Research Society, - Masud, Abu S.M., Dr.

Use of Artificial Neural Networks in Aerodynamics", Artificial Neural Networks in Engineering Conference - Meade, Andrew, Dr.

"Development of a Flow Visualization Technique for Characterization Convection in Liquid Metals - Metallurgical Transactions", "Convection in Tin in A Bridgman System" , "Gravitational Effects in Rayleigh-Marangoni Convection" - Narayanan, Ranganathan, Dr.

"Parallel-Vector for Control-Structure Integrated Methodology" - Nguyen, Duc T., Dr.

"Measurements of Air-, Nitrogen- and Oxygen- Broadened Half-widths and Shifts of Ozone Lines Near 3 um" - Prochaska, Eleanor, Dr.

"Response of Interferometric Optical Fiber Sensors Driven Beyond Glass Transition", Journal of Light Wave Technology, "Failure Analysis of Glass Optical Fiber Sensors Embedded Titanium Matrix Composites Driven Well Above Glass Transition", Journal of Applied Mechanics - Sirkis, James, Dr.

Anticipated Papers

"Atmospheric Spectroscopy with the SDT Revolving Mirror" - Hafele, Joseph C., Dr.

"Post-Stall Flight of Missiles", "Longitudinal/Lateral Post-Stall Flight Vehicle Mechanics" - Hall, Charles E. Jr., Dr.

"A Numerical Method for an Unsteady Flow via Acoustics" - Hodge, Steven, Dr.

"Doppler Global Velocimetry Measurements of the Vertical Flow Above a Thin Delta Wing" Meyers, J. F. , Usry, J. W., **Miller, L.Scott, Dr.**

"Effects of Low and High Workload Levels on Decision Making in a Monitoring Task" - Nygren, Thomas E., Dr.

"Use of Carboranes as Oxidation Inhibitors in Carbon-Carbon Composites" - Petty, John T., Dr.

"Electromagnetic Compensation for Surface Errors in Large Reflector Antennae" Smith, William T., Dr.

"Hypersonic Constant - Temperative Anemometry" Spina, Eric F., Dr.

"Spacecraft Design Optimization Using Taguchi Analysis" - Unal, Resit, Dr., "Application of Taguchi Methods to Dual Mixture Ratio Propulsion System Optimization for SSIO Vehicles" - Stanley, Douglas, Joyner, Russ, **Unal, Resit, Dr.**

"Critical Review of Transition Reynolds Number for Supersonic Shock Layers" - Wilson, Dennis, Dr.

"Object Oriented Development of Engineering Software Using CLIPS"- Yoon, C. John, Dr. Other Fellows are planning publications based on their research but have not solidified their plans at this time.

Anticipated Research Proposals

Videotapes about Space systems Division and Analysis and Computational Division - Sherilee Beam

Preliminary proposal submitted to Office of Interdisciplinary Research - Bill Carpenter

"Investigation of Polymer Crystallinity with Application to Polyimides and Polyarylethers" - NASA HBCU sponsored research program - Ed Celarier

"Atmospheric Spectroscopy with the SDI Revolving Mirror" - Joe Hafele

"Use of Artificial Neural Networks in Experimental Data Acquisition and Aerodynamic Design" - NASA, Andrew Meade

"The effect of Vetch on 2-D and 3-D Textile Composite Materials" - Tim Norman, NASA LaRC

"Phenomenological Model for Type III and IV Shock/Shock Interaction" - Dennis Wilson.

Funded Research Proposals

"Semi-discrete Galerkin Modeling of the Compressible Boundary Layer About An Airfoil"
NASA Langley Research Center - Andrew Meade

"Doppler Global Velocimetry Application and Evaluation" - NASA Langley Research Center -
L. Scott Miller.

"Parallel-Vector Finite Element Analysis for the CSM Testbed" - NASA Langley Research
Center - Duc T. Nguyen.

"Facilitating Pilot Use of Operations and Procedures Manuals Using Hypertext-Based
Strategies" - NASA Langley Research Center - C. Ray Russell.

"Center of Excellence in Hypersonics" - NASA Langley Research Center - Dennis Wilson.

Section VI

Summary of Program Evaluation

A program evaluation questionnaire was given to each Fellow and to each Research Associate involved with the program. A sample of each questionnaire is in Appendix V of this report. The questions and the results are given beginning on the next page.

A.	Program Objectives

1. Are you thoroughly familiar with the research objectives of the research (laboratory) division you worked with this summer?

   Very much so __25__ (71%)
   Somewhat __29__ (83%)
   Minimally __0__ (0%)

2. Do you feel that you were engaged in research of importance to your Center and to NASA?

   Very much so __33__ (94%)
   Somewhat __1__ (3%)
   Minimally __1__ (3%)

3. Is it probable that you will have a continuing research relationship with the research (laboratory) division that you worked with this summer?

   Very much so __25__ (71%)
   Somewhat __7__ (20%)
   Minimally __2__ (6%)

4. My research colleague and I have discussed follow-up work including preparation of a proposal to support future studies at my home institution, or at a NASA laboratory?

   Yes __25__ (71%)   No __10__ (29%)

5. What is the level of your personal interest in maintaining a continuing research relationship with the research (laboratory) division that you worked with this summer?

   Very much so __32__ (91%)
   Somewhat __3__ (9%)
   Minimally __0__ (0%)

B.	Personal Professional Development

1. To what extent do you think your research interests and capabilities have been affected by this summer's experience? You may check more than one?

   Reinvigorated __15__ (43%)
   Redirected __13__ (37%))
   Advanced __24__ (69%)
   Just Maintained __1__ (3%)
   Unaffected __0__ (0%)

2. How strongly would you recommend this program to your faculty colleagues as a favorable means of advancing their personal professional development as researchers and teachers?

   With enthusiasm __26__ (74%)
   Positively __9__ (26%)
   Without enthusiasm __0__ (0%)
   Not at all __0__ (0%)

3. How will this experience affect your teaching in ways that will be valuable to your students? (you may check more than one)

   By integrating new information into courses __25__ (71%)

   By starting new courses __4__ (11%)

   By sharing research experience __30__ (86%)

   By revealing opportunities for future employment in government

   agencies __22__ (63%)

   By deepening your own grasp and enthusiasm __9__ (26%)

   Will affect my teaching little, if at all __0__ (0%)

4. Do you have reason to believe that those in your institution who make decisions on promotion and tenure will give you credit for selection and participation in this highly competitive national program?

Yes __24__ (69%)   No __9__ (26%)   Unsure __2__ (6%)

| C. | Administration |

1. How did you learn about the Program? (Please check appropriate response)

    __14__ (40%)   Received announcement in the mail.

    __2__ (6%)   Read about in a professional publication.

    __21__ (60%)   Heard about it from a colleague.

    __2__ (6%)   Other (explain). Returnee, home institution research foundation.

2. Did you also apply to other summer faculty programs?

Yes __12__ (34%)   No __23__ (66%)

    __2__ (6%) DOE

    __6__ (17%) Another NASA Center

    __6__ (17%) Air Force

    __4__ (11%) Navy

3. Did you receive an additional offer of appointment from one or more of the above?   No __23__ (66%)   Yes __3__ (9%)

4. Did you develop new areas of research interest as a result of your interaction with your Center and laboratory colleagues?

Many __9__ (26%)

A few __25__ (71%)

None __1__ (3%)

5.   Would the amount of the stipend ($900 per week) be a factor in your
      returning as an ASEE Fellow next summer?

      Yes __19__ (54%)   No __15__ (43%)

      If not, why   My main reason for coming to Langley was to do
      research, not to make money. Research is the most important
      factor. Nine hundred per week seems reasonable.

6.   Did you receive any informal or formal instructions about submission
      of research proposals to continue your research at your home
      institution?

      Yes ____24____ (69%)   No ____10____ (29%)

7.   Was the housing and programmatic information supplied prior to the
      start of this summer's program adequate for your needs?

      Yes __29__ (83%)   No _3_ (9%)   N/A Local __1__ (3%)

8.   Was the contact with your research colleague prior to the start of the
      program adequate?

      Yes __28__ (80%)   No __7__ (20%)

9.   How do you rate the seminar program?
      Excellent ____11____ (31%)
      Very good ____15____ (43%)
      Good __7__ (20%)
      Fair __0__ (0%)
      Poor __1__ (3%)

10. In terms of the activities that were related to your research assignment, how would you describe them on the following scale?

Check one per activity	Time Was			
Activity	Adequate	Too Brief	Excessive	Ideal
Research	11	13	0	10
Lectures	27	1	4	2
Tours	14	8	1	4
Social/Recreational	19	3	2	8
Meetings	26	1	2	2

11. What is your overall evaluation of the program?

Excellent ____22____ (63%)

Very good ____11____ (31%)

Good ____1____ (3%)

Fair ____0____ (0%)

Poor ____0____ (0%)

12. If you can, please identify one or two significant steps to improve the program.

__See Fellow's Comments and Recommendations__

13. For second-year Fellows only. Please use this space for suggestions to improve the second year.

__See Fellow's Comments and Recommendations__

D.	Stipend

1. To assist us in planning for appropriate stipends in the future would you indicate your salary at your home institution.

    SALARY MEDIAN WAS
    $_42,128_ per Academic year _29_ (83 %) or Full year _1_.(3 %)
    (Check one)

2. Is the amount of the stipend the primary motivator to your participation in the ASEE Summer Faculty Fellowship Program?

    Yes _0_ (0%)   No _22_ (63 %)   In part _13_ (37%)

3. What, in your opinion, is an adequate stipend for the ten-week program during the summer of 1992?

    $9,000-8 (23 %) 10,000-14 (40 %) 11,000-1 (3 %) 12,000-3 (9 %)

    $12,500-2 (6 %) 13,000-4 (11 %)). $2,000 for Relocation. 80% of

    salary.

E.	American Society for Engineering Education (ASEE) Membership Information

1. Are you currently a member of the American Society for Engineering

    Education?

    Yes _4_ (11 %)   No _29_ (83 %)

Percentages have been rounded off to next whole number.

Percentage figures are based on the number of responses to the specific question.

Ninety-seven percent of the Fellows responding felt that their research was of importance to the center (LaRC) and to NASA. Note that this is an increase from eighty-one percent in 1990.

Ninety-one percent of the Fellows responding indicated a high level of personal interest in maintaining a continuing research relationship with the Lab/Division where they worked this summer. This figure is up from eighty-six percent in 1990.

Sixty-nine percent of the Fellows responding felt their research capabilities have been advanced as a result of the summer experience. forty-three were reinvigorated and thirty-seven were redirected.

Seventy-four percent of those responding would give a strong positive recommendation for the program to faculty colleagues. Twenty-six percent responding would give a positive recommendation for the program to faculty colleagues.

Forty-three percent responding indicated that salary (stipend) was not the p[rimary motivation to participate in the program.

Ninety-four percent of those responding gave a program evaluation from good (20 %) to excellent (31 %).

Twenty-three percent indicated a stipend range of $9,000.00 for the ten weeks as satisfactory.

Forty percent indicated a stipend range of $10,000.00 for the ten weeks as satisfactory.

Twelve percent indicated $11,000.00 to 12,000.00 for the ten weeks as satisfactory.

Seventeen percent indicated $12,500.00 to 13,000.00 for the ten weeks as satisfactory.

Eighty-three percent of the Fellows responding indicated that they **are not** currently members of the American Society for Engineering Education.

Fellow's Comments

The technical interaction is the most important thing. Experience is worth more than money, although additional money would be helpful. The opportunity to do research is the primary factor. The opportunity to do research is the primary factor. The stipend is quite reasonable. I would rather see an increase in the number of fellowships offered rather than an increase in salary. The entire staff is to be complimented on the professional and friendly manner in which they conducted ASEE affairs. I found the people working in University Affairs at LaRC to be top-notch. Excellent program! Thanks! The seminars were quite good. I would like to be able to come back for a second year. Research is more important to me than the stipend. Make sure Langley Associates understand the spirit of the program and want to be active supervisors; encourage them to make more in depth evaluation of fellows before they arrive to start work. I would have hoped to do collaborative research, leading to joint papers. I can make more money teaching summer school. I don't know how to improve it, but living arrangements (and their costs) have been the biggest problems including being away from family. Provide some incentive for associates to actively participate in the research. NASA researchers have a set of priorities which does **not** include actively supporting ASEE fellows. The program has made a big difference in my life, thank you! The program is great! Excellent director, staff and program. Great! Wonderful!

Fellow's Recommendations

Arrange to have fellows contact/meet with LaRC associates prior to first day of program. Have Unsolicited Proposal's Workshop sooner, or information about proposal procedure distributed sooner. Separate funds set aside for pre-summer visit. Increase relocation allowance to $2,000.00. Should have more seminars. An in-depth tour of the facility would be interesting. Host separate meetings and activities for LARSS and ASEE. Remove the restriction of a two summer limit on the program. Include some summer stipend for our Phd students. Need more access to personal computers. Make sure professors have necessary tools to do significant research. House faculty and students in one area. Automated procedure for after-hours privileges. I would like to have continued access to LaRC with library privileges, etc. - after my tenure maybe some form of "contractor" status with badge and pass, etc. would be adequate. Subsidize housing. Send offers earlier. Increase the stipend and length of tenure. Help locate good basic low cost

housing for a ten week period. The fellowship level should be related to the salary, about 80%. Earlier notification of fellows regarding program activities. Need to make appointments for physicals well in advance so they can be all done during first week or earlier. Have proposals workshop earlier in the summer to motivate thinking about continuation of research collaboration. Langley Associates who are not familiar with the Faculty Fellows should be encouraged to give some advanced planning toward getting their Fellow started in their research group. Encourage "networking" within their areas of interest. Make the program easier to extend beyond ten weeks - that is too short. Require written communication between ASEE Fellow and NASA Associate to discuss project two to three months prior to arrival. Provide a list of participants and a brief bio at entry to program. Better match between the research areas of a participant and the LaRC associate.

Research Associates' Survey

Ninety-six percent of the responses indicated that the Fellows were adequately prepared for their research assignments. Several Fellows already had a good background in the area of research and brought an advanced level of knowledge to the project. The one negative response was due to a lack of definition of the research problem by the Research Associate.

All of the Research Associates responding indicated satisfaction with the diligence, interest, and enthusiasm of the Research Fellow.

Ninety-three percent of the Research Associates responding expressed an interest in serving in the program again.

Eighty-nine percent of the Research Associates responding expressed an interest in having the Fellow, if eligible, return for a second year. One negative response felt the Fellow should be allowed to participate in a field more compatible with his experience.

Research Associates' Comments

Ten weeks is too short! I think the program is quite good and the interaction between universities and NASA is beneficial to both groups. Keep up the good work! Great as it is! Appreciated being involved in real-world engineering problems relating to control law design for advanced aircraft. Outstanding! The research we are doing...and what the Fellow is doing at the university compliment each other.

25

Thanks for the flexibility and letting him (the Fellow) come early, otherwise he would not have been able to participate. I value the exchange of ideas and approaches to achieve the research objectives with outside researchers. Also, it opens up new research areas for my future research programs. Excellent technical background. Excellent! This is a very good program when the skills and interests of the individual match an active branch research program. Obviously, based on this experience, the program seems to be an "everybody's a winner" type of activity. Insufficient lead time for LaRC Associates to respond to administrative requests. Interaction with new people interested in similar research activities is very enlightening and often generates new concepts and ideas.

Research Associates' Recommendations

Recommend we prepare a booklet describing our computer system and send it to the Fellow before he/she comes. After the Fellow arrives here, assign him/her a computer user number so that he/she can use computer immediately. Better access to PC's. Contact with the Fellow four to six weeks prior to arrival would help the Research Associate better prepare by ordering the necessary supplies and equipment so that everything would be in place and the Fellow could begin research immediately. Funding for more than two terms for those who are excellent. If there was any way to lengthen the project duration within typical academic summers, we would improve the likelyhood of productive cooperation. Selecting a fellow on the basis of resumes can be risky. It may be worthwhile to provide for an interview, at least by phone. It would have been helpful to get earlier notice of reporting requirements. Assignments of Fellows should be made far enough ahead to allow for interchanges between Langley Research Associates and the Fellow before on-site arrival. Each fellow should have a specific research plan prior to his/her arrival at Langley and should have an up-to-4 pages research summary at the conclusion of his/her summer work. The research summary is to replace the presentation currently required of each fellow. The research report has a permanent value whereas the presentation is short-lived and is often poorly attended. Organize your review process so that the reviews are done once in a manner satisfactory to all parties involved?

SECTION VII

Conclusions and Recommendations

Conclusions

Comments from the Research Fellows and the Research Associates indicates a very high level of satisfaction with the program. The Fellows feel their research activities to be important to them in terms of professional growth, and important to the Center and NASA. The Associate indicated the importance of the research to the Center and a few commented on how rewarding the experience was to them at a personal level.

The Research Fellows all stated that they would strongly recommend the program to faculty colleagues.

There is still a need for improved communications between the Fellow and the Associate prior to arrival. It was also noted that communications between the Fellow, the Associate and others working within the Division could be improved.

There were several statements early in the program about the lack of work space (desk, chair, etc.).

There is an indication of a need for greater access to computers (more PCs).

Although the stipend is not the primary motivator towards participation in the program, there is an indication that a larger stipend is needed.

There is a need for more informal communications between the Research Fellows. An opportunity to discuss research along with the recreational activities.

While there are some small frustrating items, the kind that go with any large and complicated operation, it can be stated that the overall indication from Research Fellows and Research Associate is that the program is highly successful and certainly achieves the goal of facilitating research interests between NASA and university faculty.

Recommendations

Continue to urge increased contact by the Research Associate prior to arrival.
Suggest that the Research Fellow contact the Research Associate for information.

Urge greater communications between Research Associate and Research Fellow
during the ten week research period. Broaden the communications base to
include other persons and activities within the Division. Establish work area and
office equipment prior to arrival of Research Fellow. Arrange for required computer
access by Research Fellow.

Urge increase in stipend to a minimum of $10,000.00 for the ten week period.

APPENDIX I

PARTICIPANTS - ASEE/NASA LANGLEY

SUMMER FACULTY RESEARCH PROGRAM

RETURNEES

1991 NASA-ASEE-ODU FELLOWS RETURNEES

FELLOW	DIVISION	RESEARCH ASSOCIATE
Dr. Doria, Michael Associate Professor Mechanical Engineering Valparaiso University Valparaiso, IN 46383	Fluid Mechanics Division	Perry Newman Building 1192T Mail Stop 128 Tel. 864-2247
Dr. Hafele, Joseph C. Professor Physics Christopher Newport College Newport News, VA 23606	Flight Electronics Division	Steve Sandford Building 1202 Mail Stop 474 Tel. 864-1836
Dr. Hodge, Steven L. Assistant Professor Mathematics Hampton University Hampton, VA 23668	Acoustics Division	David Chestnutt Building 1298T Mail Stop 460 Tel. 864-3626
Dr. Lee, Byung-Lip Associate Professor Engineering Science & Mechanics Pennsylvania State University University Park, PA 16802	Materials Division	Ruth Pater Building 1293A Mail Stop 226 Tel. 864-4277

30

FELLOW	DIVISION	RESEARCH ASSOCIATE
Dr. Meade, Andrew Assistant Professor Mechanical Engineering Rice University Houston, TX 77251-1892	Applied Aerodynamics Division	James Luckring Building 641 Mail Stop 361 Tel. 864-2869
Dr. Miller, Leonard S. Assistant Professor Aerospace Engineering Wichita State University Wichita, KS 67208	Flight Applications Division	Jimmy W. Usry Building 1230 Mail Stop 235A Tel. 864-4598
Dr. Nguyen, Duc Thai Associate Professor Civil Engineering Old Dominion University Norfolk, VA 23529	Structural Dynamics Division	Dr. Keith Belvin Building 1293B Mail Stop 230 Tel. 683-3761
Dr. Prochaska, Eleanor S. Coordinator, MTRC, & Instructor Math & Computer Science Western Carolina University Cullowhee, NC 28723	Atmospheric Sciences Division	Mary Ann Smith Building 1247D Mail Stop 401A Tel. 864-2701
Dr. Rogers, Joel C. W. Associate Professor Mathematics Polytechnic University Brooklyn, NY 11201	Acoustics Division	Dr. Jack Preisser Building 1208 Mail Stop 461 Tel. 684-3618

FELLOW	DIVISION	RESEARCH ASSOCIATE
Dr. Russell, Carl R. Assistant Professor Mathematical Sciences Virginia Commonwealth University Richmond, VA 23284	Flight Management Division	Terence S. Abbott Building 1168 Mail Stop 152 Tel. 864-2009
Dr. Unal, Resit Assistant PRofessor Engineering Management Old Dominion University Norfolk, VA 23529	Space Exploration Initiative Office	Ed Dean Building 1244T Mail Stop 253 Tel. 864-8213
Dr. Wilson, Dennis E. Associate Professor Mechanical Engineering University of Texas Austin, TX 78712	Structural Mechanics Division	Bob Nowak Building 1265 Mail Stop 395 Tel. 864-1391
Dr. Wu, Chivey Associate Professor Mechanical Engineering California State University, LA Los Angles, CA 90032	Applied Aerodynamics Division	Lawrence Putnam Building 1236 Mail Stop 267 Tel. 864-5116

32

APPENDIX II

PARTICIPANTS-ASEE/NASA LANGLEY

SUMMER FACULTY RESEARCH PROGRAM

FIRST YEAR

1991 NASA-ASEE-ODU FELLOWS
FIRST YEAR

FELLOW	DIVISION	RESEARCH ASSOCIATE
Dr. Abbitt, John D. Assistant Professor Aerospace, Mechanical & Engineering Science University of Florida Gainesville, FL 32611-2031	Information Systems Division	Reginald J. Exton Building 1230 Mail Stop 235A Tel. 864-4605
Ms. Beam, Sherilee Assistant Professor Mass Media Arts Hampton University Hampton, VA 23669	Analysis and Computation Division	Don Lansing Building 1268 Mail Stop 125A Tel. 864-6714
Dr. Carpenter, William C. Professor Civil Engineering & Mechanics University of South Florida Tampa, FL 33620	Structural Dynamics Division	Dr. J.-F. Barthelemy Building 1229 Mail Stop 246 Tel. 864-2809
Dr. Celarier, Edward A. Assistant Professor Chemistry Hampton University Hampton, VA 23669	Materials Division	Jeffrey Hinkley Building 1293A Mail Stop 226 Tel. 864-4259

34

FELLOW

Dr. Cobb, Stephen H.
Assistant Professor
Physics
Murray State University
Mayfield, KY 42066

Dr. Deans, Linda W.
Professor
Urban Education
Norfolk State University
Norfolk, VA 23504

Mr. Ferguson, Milton W.
Assistant Professor
Chemistry/Physics
Norfolk State University
Norfolk, VA 23504

Dr. Glauser, Mark N.
Assistant Professor
Mechanical & Aeronautical Engineering
Clarkson University
Potsdam, NY 13699

Dr. Hall, Charles
Assistant Professor
Mechanical & Aeronautical Engineering
North Carolina State University
Raleigh, NC 27695-7910

DIVISION

Space Systems Division

Office of the Chief Scientist

Information Systems Division

Fluid MEchanics Division

Guidance and Control
Division

RESEARCH ASSOCIATE

Ja Lee
Building 200
Mail Stop 493
Tel. 864-1473

Marchelle Cainright
Building 1153
Mail Stop 154
Tel. 864-3313

Min Namkung
Building 1230B
Mail Stop 231
Tel. 864-4962

Tom Gatski
Building 1192D
Mail Stop 156
Tel. 864-5552

F. R. Morrell
Building 1298
Mail Stop 489
Tel. 864-4004

35

FELLOW	DIVISION	RESEARCH ASSOCIATE
Dr. Hawk, Jeffrey A. Assistant Professor Metallurgic & Materials Engineering University of Alabama Tuscalossa, AL 35487-0202	Materials Division	W. Barry Lisagor Building 1148 Mail Stop 188A Tel. 864-3135
Mr. Johnson, David Professor Business/Information Systems St. Paul's College Lawrenceville, VA 23005	Facilities Engineering Division	Bob Feldhousen Building 209 Mail Stop 436 Tel. 864-7295
Dr. Kasturi, Rangachar Acting Director Electrical & Computer Engineering Pennsylvania State University University Park, PA 16803	Flight Management Division	Randall L. Harris Building 1268A Mail Stop 152E Tel. 864-6641
Dr. Masud, Abu S. M. Associate Chairman Industrial Engineering Wichita State University Wichita, KS 67208-1595	Space Exploration Initiative Office	Ed Dean Building 1244T Mail Stop 253 Tel. 864-8213
Dr. Miller, Lois S. Chairperson Management Hampton University Hampton, VA 23668	Office of the Chief Scientist	Dr. Surendra Tiwari Building 1312 Mail Stop 105A Tel. 864-5214

FELLOW	DIVISION	RESEARCH ASSOCIATE
Dr. Narayanan, Ranganathan Associate Professor Chemical Engineering University of Florida Gainesville, FL 32611	Information Systems Division	Dr. Archie Fripp Building 1202 Mail Stop 473 Tel. 864-1503
Dr. Norman, Timothy L. Assistant Professor Mechanical & Aerospace Engineering West Virginia University Morgantown, WV 26506-6101	Materials Division	Charles E. Harris Building 1205 Mail Stop 188E Tel. 864-3473
Dr. Nygren, Thomas E. Associate Professor Psychology Ohio State University Columbus, OH 43210	Flight Management Division	Alan T. Pope Building 1168 Mail Stop 152 Tel. 864-8384
Dr. Petty, John T. Associate Professor Natural Sciences Longwood College Farmville, VA 23901	Materials Division	Wallace L. Vaughn Building 1205 Mail Stop 191 Tel. 864-3509
Dr. Plaza-Rosado, Heriberto Professor Electrical & Computer Engineering University of Puerto Rico-RUM Mayaguez, PR 00709-5000	Space Systems Division	John Healy Building 1232 Mail Stop 365 Tel. 864-4412

37

FELLOW	DIVISION	RESEARCH ASSOCIATE
Dr. Sirkis, James Assistant Pressor Mechanical Engineering University of Maryland College Park, MD 20742	Information Systems Division	Robert S. Rogowski Building 1230 Mail Stop 231 Tel. 864-4990
Dr. Smith, William T. Assistant Professor Electrical Engineering University of Kentucky Lexington, KY 40506-0046	Guidance and Control Division	M. C. Bailey Building 1299 Mail Stop 490 Tel. 864-1802
Dr. Spina, Eric F. Associate Professor Mechanical & Aerospace Engineering Syracuse University Syracuse, NY 13244	Fluid Mechanics Division	S. K. Robinson Building 1247A Mail Stop 163 Tel. 864-8022
Dr. Suleman, Naushadalli K. Assistant Professor Chemistry Hampton University Hampton, VA 23668	Materials Division	Dr. Sheila Long Building 1293A Mail Stop 229 Tel. 864-4250
Dr. Tompson, Robert Research Assistant Professor Nuclear Engineering University of Missouri Columbia, MO 65211	Atmospheric Sciences Division	Dr. Glenn Yue Building 1250A Mail Stop 475 Tel. 864-2678

FELLOW	DIVISION	RESEARCH ASSOCIATE
Dr. Tortorelli, Victor J. Associate Professor Chemistry Ursinus College Collegeville, PA 19426	Materials Division	P. M. Hergenrother Building 1293 Mail Stop 226 Tel. 864-4270
Dr. Watson, George H. Assistant Professor Physics & Astronomy University of Delaware Newark, DE 19716	Flight Electronics Division	Norm Barnes Building 1202 Mail Stop 474 Tel. 864-1630
Dr. Yoon, Chongyul John Assistant Professor Civil & Environmental Engineering Polytechnic University Brooklyn, NY 11201	Structural dynamics Division	Dr. J. Sobieski Building 1229 Mail Stop 242 Tel. 864-2799
Dr. Zia, Omar Associate Professor Electronic Engineering Technology California Polytechnic State University San Luis Obispo, CA 93407	Flight Electronics Division	Lenny McMaster Building 1299 Mail Stop 476 Tel. 864-1733

APPENDIX III

LECTURE SERIES

PRESENTATIONS BY RESEARCH FELLOWS

1991
ASEE/NASA
Old Dominion University - Langley Research Center

LECTURE SERIES

Location: Activities Center Auditorium, Bldg. 1222
Time: 10:00 a.m. to 11:15

DATE	TOPIC	SPEAKER
June 11	Global Warming	Dr. Joel Levine Atmospheric Sciences Division - Space Directorate
June 18	High Speed Civil Transport	Donald Maiden Advanced Vehicles Division - Aeronautics Directorate
June 25	Long Duration Exposure Facility	Dr. William Kinard Materials Division - Structures Directorate
July 2	Nondestructive Evaluation: What's Up Doc?	Dr. Joseph Heyman Instrument Research Division - Electronics Directorate
July 9	HL 20 Personnel Launch System	Dr. Kelli Willshire Information Systems Division - Flight Systems Directorate
July 23	Artificial Neural Networks	Donald Soloway Information Systems Division - Flight Systems Directorate

Schedule of Final Presentations by Faculty Fellows

Location: Building 1212, Room 200
Date: AUGUST 8, 1991
Time: 8:00 A.M. TO 4:30 P.M.

NAME/DIVISION/BRANCH	TOPIC
Eleanor Prochaska ASD/CDB	Analysis of Pressure-Broadened Ozone Spectra in the 3-um Region
John Petty MD/AMB	The Use of Carboranes as Oxidation Inhibitors for Carbon-Carbon Composites
Sherilee Beam ACD/FSGB	The HL-20 as The Personnel Launch System
Leonard Scott Miller FAD/FRB	An Evaluation of Preliminary Doppler Global Velocimetry Measurements
Thomas Nygren FLTMD/CVIRB	Incorporating Affective Bias in Models of Human Decision Making
Joseph Hafele FED/ESB	The Role of Time and Speed in NASA's SUNLITE Program
William T. Smith GCD/AMRB	Further Evaluation of the Constrained Least Squares Electromagnetic Compensation Method
John Abbitt IRD/OSS	Calibration of a Tunable Excimer Laser Using the Optogalvanic Effect
Abu Masud SEIO	Application of Multiple Criteria Decision Methods in SEI Design and Planning
Dave Johnson FENGD/PICO	Project and Manpower Planning
R. Narayanan ISD/IPTB	Convection in a Bridgman Geometry
Andrew Meade AAD/TAB	The Use of Artificial Neural Networks in Aerodynamic Design and Experimental Data Acquisition
Mark Glauser FLDMD/TFPBB	Proper Orthogonal Decomposition Based Turbulence Models

42

NAME/DIVISION/BRANCH	**TOPIC**
Heriberto Plaza-Rosado SSD/VAB	Naturally Induced Secondary Radiation in Interplanetary Space: Preliminary Analysis for Gamma Radiation and Radioisotope Production From Thermal Neutron Activation
Duc Thai Nguyen SDYD/SDB	Implementation of the Lanczos Eigen-Solver for the CSI Code on High Performance Computers

APPENDIX IV

GROUP PICTURE OF RESEARCH FELLOWS

45
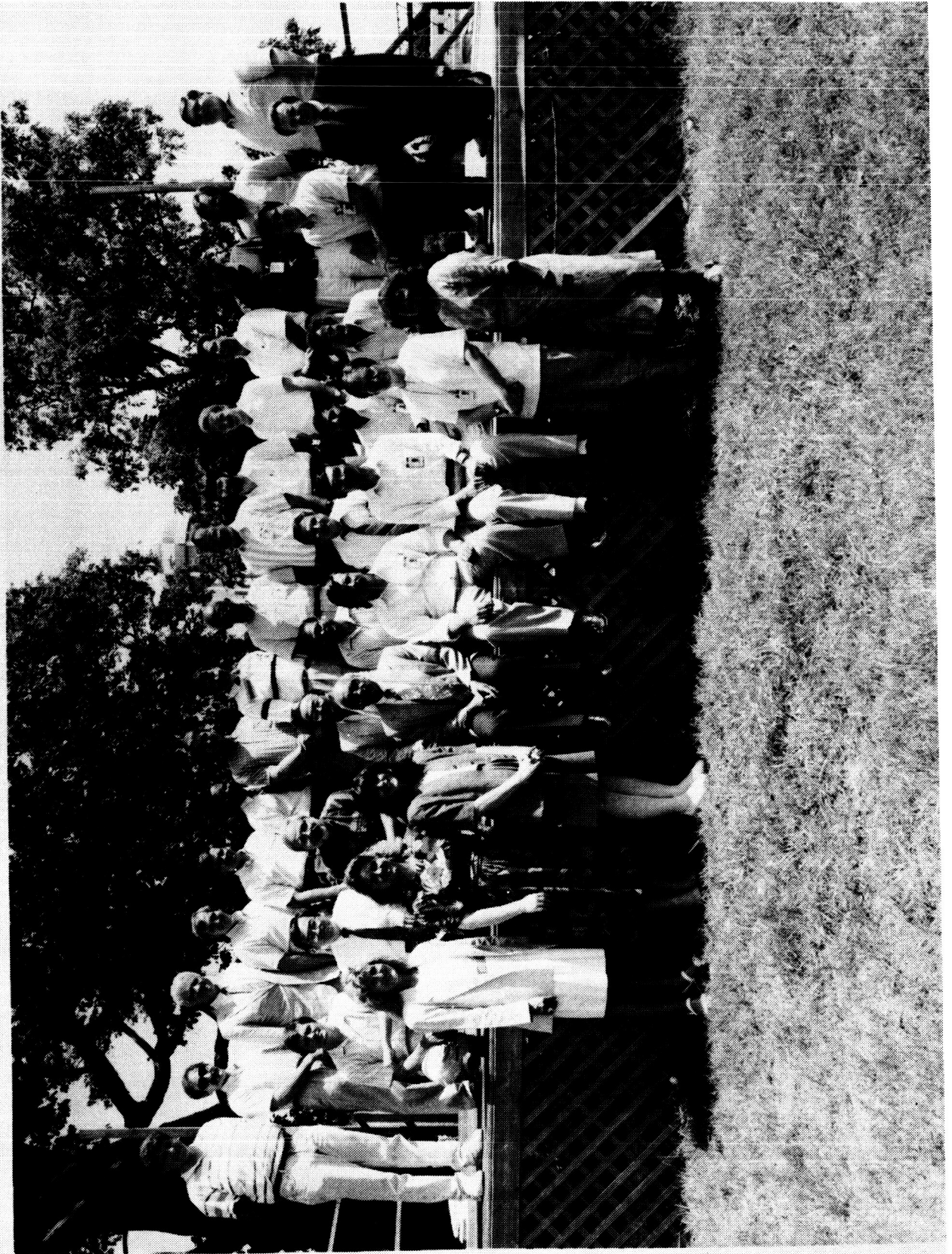
NASA/ASEE SFFP
Summer 1991
List of Attendees

Back Row: Left to Right

Dr. Michael Doria, Dr. Victor J. Tortorelli, Dr. Joel C. W. Rogers, Dr. Steven L. Hodge, Dr. Jeffrey A. Hawk, Dr. Rangachar Kasturi, Dr. John D. Abbitt, Dr. John T. Petty, Prof. Milton W. Ferguson, Dr. Daniel Nohl(JOVE), Dr. L. Scott Miller, Dr. William T. Smith, Dr. Andrew Meade, Dr. William C. Carpenter, Dr. Edward A. Celarier, Dr. Robert Tompson.

Middle Row: Left to Right

Dr. George H. Watson, Dr. Byung Lip (Les) Lee, Dr. Thomas E. Nygren, Dr. Chongyul John Yoon, Dr. Abu S. M. Masud, Dr. Omar Zia, Dr. Naushadalli K. Suleman, Dr. Heriberto Plaza-Rosado, Dr. Stephen H. Cobb, Dr. C. Ray Russell

Front Row: (Left to Right)

Prof. Sherilee Beam, Ms. Debby Young, Ms. Mary Fagley, Dr. Surendra N. Tiwari(seated), Dr. Charles Hall, Dr. Chivey Wu,Dr. Eleanor S. Prochaska (standing), Dr. Lois S. Miller.

Not Pictured:

Dr. Linda W. Deans, Dr. Mark N. Glauser, Dr. Joseph C. Hafele, Prof. David Johnson, Dr. Ranganathan Narayanan, Dr. Duc Thai Nyuyen, Dr. Timothy L. Norman, Dr. James Sirkis, Dr. Eric F. Spina, Dr. Resit Unal, Dr. Dennis E. Wilson.

APPENDIX V

DISTRIBUTION OF FELLOWS BY DIVISION

NASA LANGLEY RESEARCH CENTER
1991 ASEE (SFFP)
DISTRIBUTION OF FELLOWS BY DIVISION
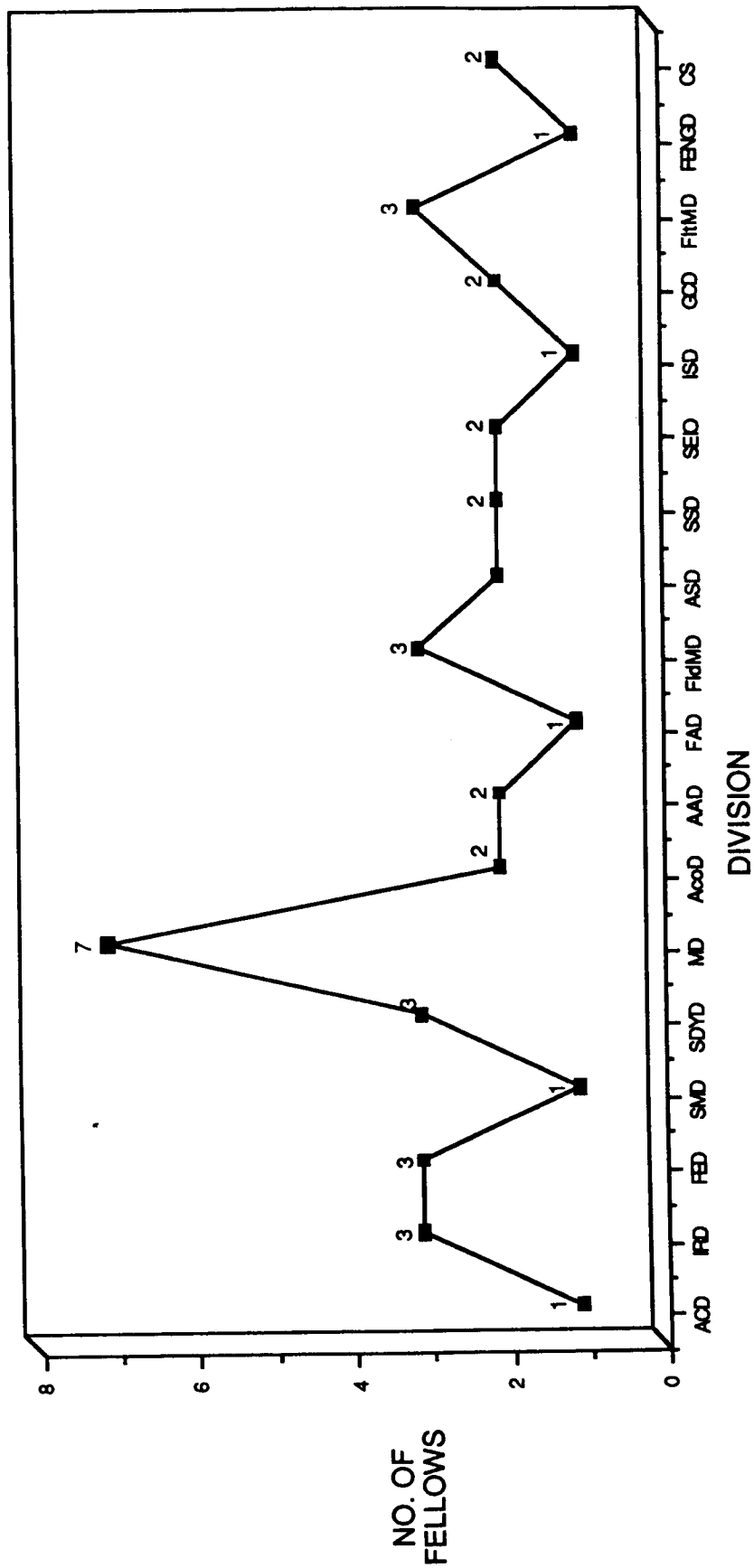
APPENDIX VI

DISTRIBUTION OF FELLOWS BY DIRECTORATE

1991 ASEE (SFFP)
DISTRIBUTION OF FELLOWS BY DIRECTORATE*

NO. OF FELLOWS

20

10

0

Electronics 7 (17%)

Structures 13 (31%)

Aeronautics 6 (15%)

Space 5 (12%)

Flight Systems 6 (15%)

Systems Engineering & Operation 1 (2%)

Office of the Chief Scientist 2 (5%)

DIRECTORATE
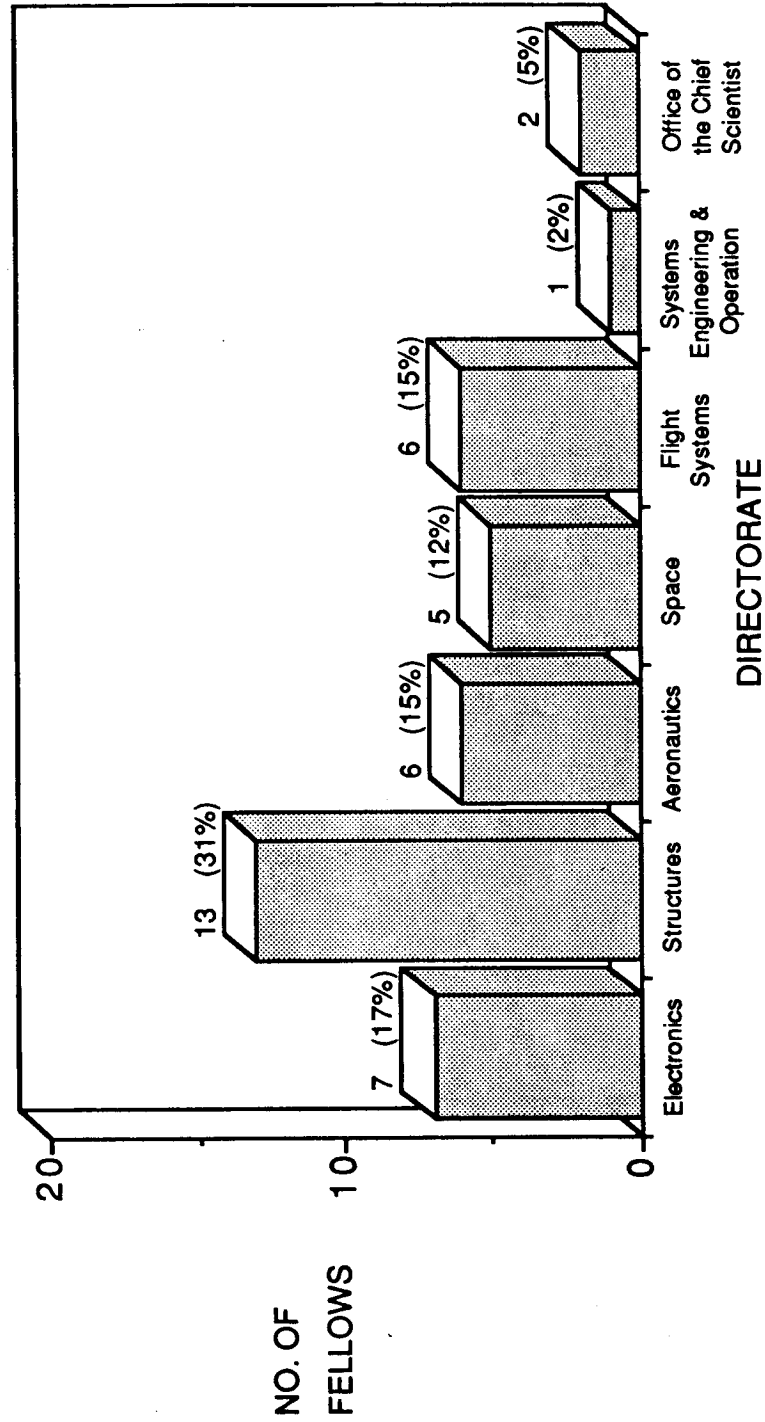
*Including the Office of the Chief Scientist

50

APPENDIX VII

DISTRIBUTION OF FELLOWS BY ETHNICITY/MALE

1991 ASEE (SFFP)
DISTRIBUTION OF MALE FELLOWS BY ETHNICITY

NO. OF FELLOWS

ETHNICITY

- Black: 2 (5%)
- Hispanic: 1 (2%)
- Asian: 9 (22%)
- Nonminority: 25 (61%)

52
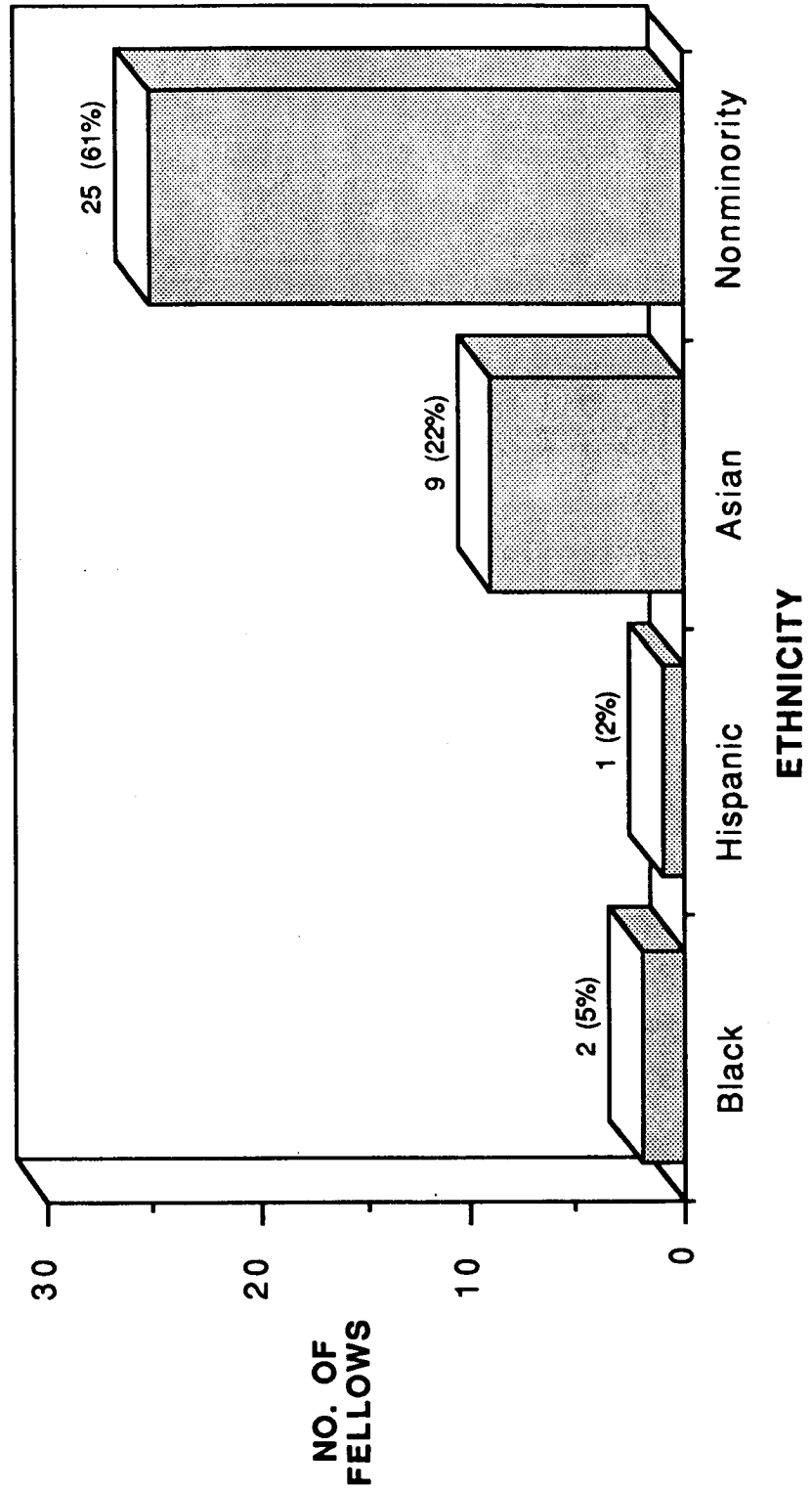
APPENDIX VIII

DISTRIBUTION OF FELLOWS BY ETHNICITY/FEMALE

1991 ASEE (SFFP)
DISTRIBUTION OF FEMALE FELLOWS BY ETHNICITY

NO. OF
FELLOWS

ETHNICITY

Black   Hispanic   Asian   Nonminority

2 (5%)   0   0   2 (5%)
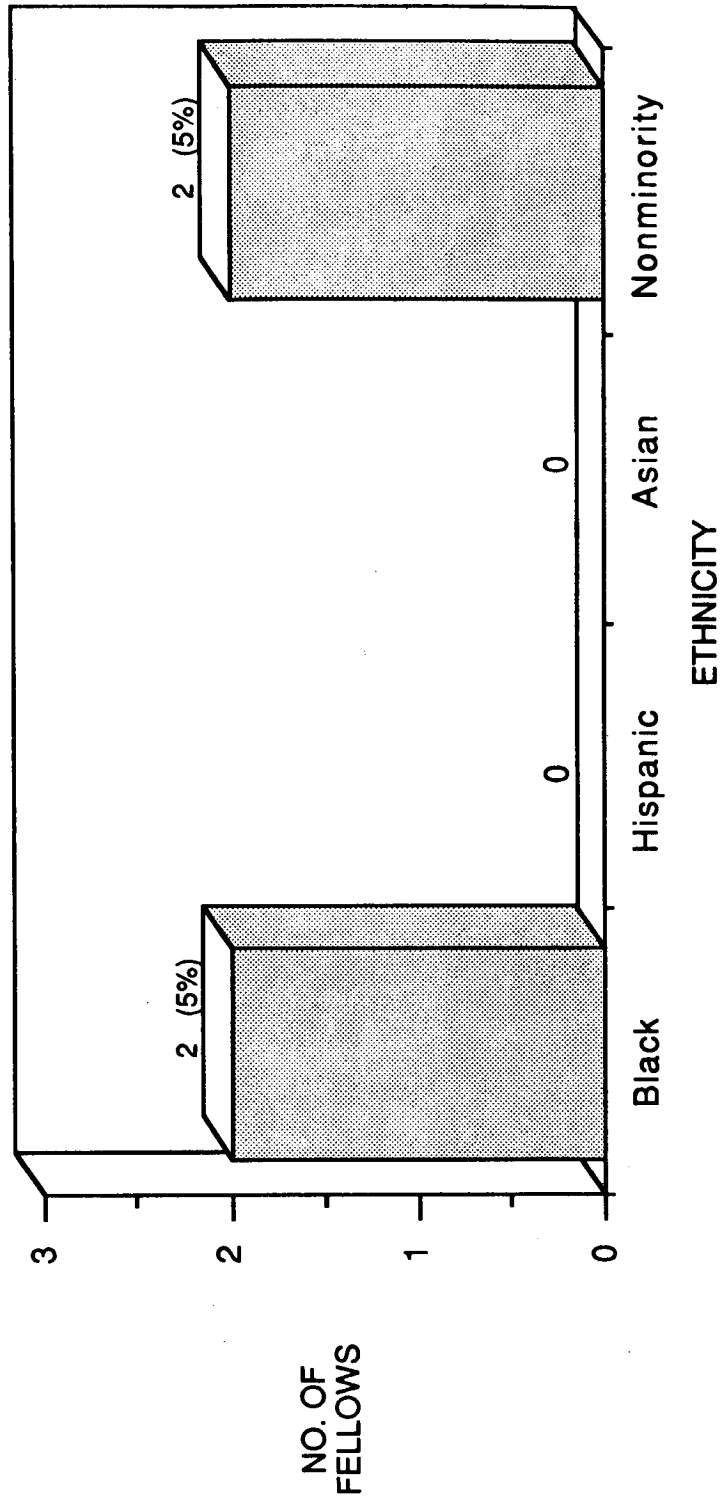
APPENDIX IX

DISTRIBUTION OF FELLOWS BY UNIVERSITY RANKS

1991 ASEE (SFFP)

DISTRIBUTION OF FELLOWS BY UNIVERSITY RANKS

NO. OF
FELLOWS

30

20

10

0

5 (12%)

Professor

12 (29%)

Associate
Professor

UNIVERSITY RANK

20 (49%)

Assistant
Professor

4 (10%)

*Other

* Instructor
Acting Director
Associate Chairperson
Chairperson
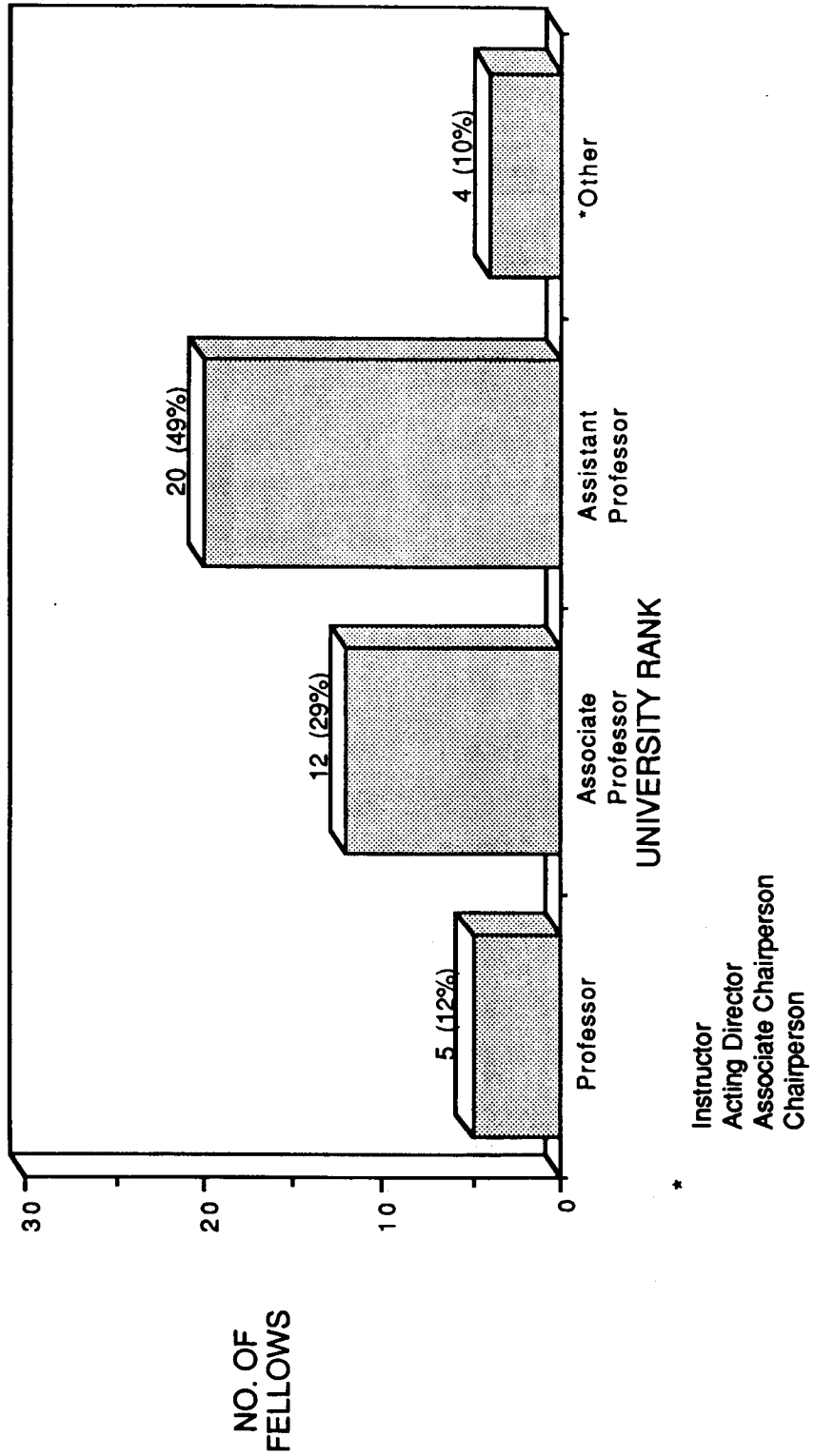
APPENDIX X

ABSTRACTS - RESEARCH FELLOWS

Calibration of a Tunable Excimer Laser
Using the Optogalvanic Effect

by

John D. Abbitt
Assistant Professor
Department of Aerospace Engineering, Mechanics,
and Engineering Science
University of Florida
Gainesville, FL   32611-2031

A device for the calibration of a tunable excimer laser is currently under development. The laser provides ultraviolet radiation at three principal wavelengths, 193, 248, and 308 nm and is tunable over a range of 1 nm at each of these wavelengths. The laser is used as a non-intrusive optical probe to excite electronic transitions, and thereby induce fluorescence, of the principal molecules or atoms of interest in supersonic flowfields, both reacting and non-reacting. The fluorescence resulting from the excitation is observed with an intensified camera. Over the range of tunability at the three wavelengths are a number of transitions that can be observed. The intensity of the fluorescence depends in part on the local temperature and density. The nature of this thermodynamic dependence is variable among transitions, thus, requiring identification of the transition under observation. The specific transition excited corresponds directly to the wavelength of the radiation.

The present technique used in this laboratory for transition identification consists of scanning the laser across the range of tunability and observing the fluorescence resulting from various molecular transitions. The distance between transitions can be plotted and compared with a known spectrum. Although this method is valid, there are not always enough transitions under the gain profile to make an accurate determination. Also, accuracy is diminished by the fact that most of these species are molecular and not atomic.

The optogalvanic effect has been suggested as a simple alternative for determining laser wavelength. The optogalvanic effect is induced by illuminating a self-sustained gaseous discharge with radiation that is resonant with the metastable states of the atomic or molecular elements with the discharge. The absorption of a photon changes the probability of ionization of the atom or molecule which changes the electrical properties of the discharge. This change can be observed as an increase or decrease in

the conductivity of the discharge. The change in conductivity is known as the optogalvanic effect.

The optogalvanic effect appears to be especially well-suited for laser wavelength calibration. Commercial hollow cathode tubes that are powered by the laser itself are available as discharge sources with various atomic fill gases and electrode materials. Atomic species are desirable since the transition linewidths are very narrow thus providing high resolution. The ideal cell would contain elements that have well-isolated, easily identifiable transitions. When two transitions have been located, a device could be set up to interpolate between transitions and provide a 0-5 volt signal to the operator.

The first phase of an experimental investigation into the use of the optogalvanic effect for laser calibration was initiated this summer. The intent of this phase is to increase the understanding of the behavior of a low-pressure electrical discharge, and to set up a discharge cell and observe the optogalvanic effect using the visible light from a Nd: YAG pumped pulsed dye laser.

A schematic of typical apparatus used to observe the optogalvanic effect is shown in Figure 1.[1] High voltage passes through a current limiting ballast resistor and into one electrode of a hollow cathode lamp or low-pressure discharge. The other electrode is connected to ground. The signal is received through a capacitor which is connected to a boxcar averager. The output from the boxcar is sent to a chart recorder.

First attempts to observe the optogalvanic effect have been made using a normal discharge cell. The cell consists of a glass tube with quartz window mounted on each end through which the laser beam passes. The electrodes consist of circular rings mounted 8 mm apart inside the tube and are oriented so that the beam passes through their center. The beam is focused to a point between the electrodes.

We have not been able to observe the optogalvanic effect to date. It is suspected that spatial positioning of the focal point of the beam is critical. Most of the voltage drop in the cell occurs within a small region near the cathode, and it is likely that the focused beam must be positioned within this area. Future plans include purchasing a commercial hollow cathode lamp in which more accurate positioning of the beam can be accomplished.

---

1.   Narayanan, K., Ullas, G., and Rai, S. B., Chemical Physics Letters, Vol. 156, No. 1, 1989, 55-60.
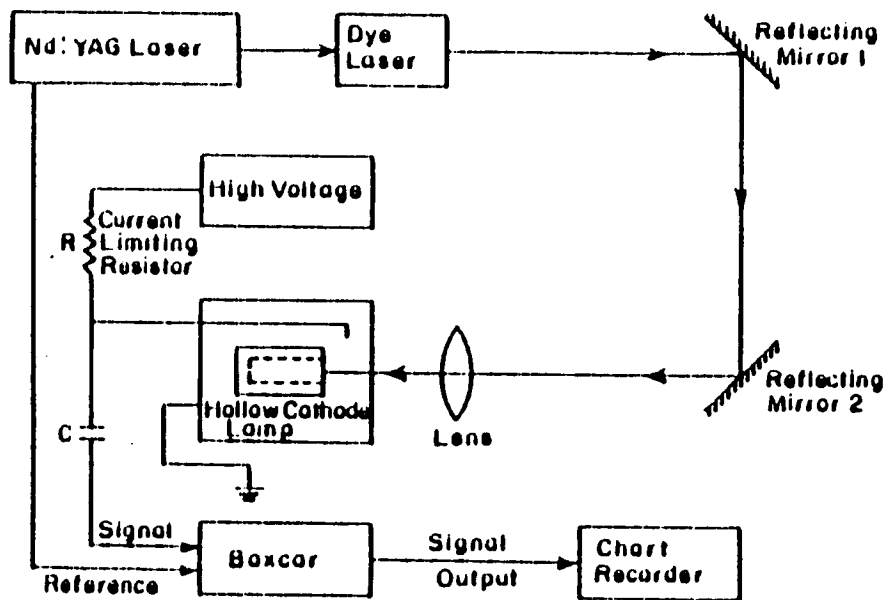
Figure 1. Experimental set-up for optogalvanic effect.

THE HL-20
AS
THE PERSONNEL LAUNCH SYSTEM

by

Sherilee F. Beam
Assistant Professor
Department of Mass Media Arts
Hampton University
Hampton, Virginia 23668

To ensure manned access to space, the Personnel Launch System is under consideration by NASA as a complement to the Space Shuttle (fig.1). Its primary mission will be to transport crew and passengers to and from Space Station Freedom in low-earth orbits. There are currently two design studies being funded: a biconic, ballistic-shaped vehicle at the Johnson Space Center and a lifting body concept at Langley Research Center.

In the late 1950's, both NASA and the Air Force were engaged in the study of lifting bodies for low-earth orbit vehicles. Projects included the M2F2 series, the X24 series, and the HL-10 (developed here, at Langley) (fig. 2). These lifting bodies drive their lift solely from the shape of the fuselage. By the mid-1960's, full-scale models were actually built and tested with some success and some failure. Langley's HL-10 was one of the most successful of these projects. However, these studies were temporarily shelved while work progressed on the Space Shuttle. Some of the test results from these studies actually led to concept refinements on certain aspects of the Shuttle development.

Due to the more recent successes of the Shuttle program and a directive to place a Space Station in orbit, there has been renewed interest in developing a lifting body vehicle as the Personnel Launch System. The vehicle, the HL-20, is a Langley Research Center project in the Space Systems Division, involving the efforts of a number of individuals (figs.3,4,5).

Data on the research carried out thusfar for peer and lay review has been available in hard copy formats, but a need existed for actual video footage, combined with scientific visualization technology, for presentation and archival purposes (figs.6,7,8,9,10,11). This ASEE project will satisfy that need. An informational videotape is being produced which briefly identifies and explains the research conducted on the Personnel Launch System in development at Langley.

Areas of investigation to be covered include Computational Fluid Dynamics, Wind Tunnel Testing, Human Factors Research, and Flight Simulation. Since the individuals involved are more knowledgeable and hold far more credibility in their content areas than any producer, interviews with each them, including the Project Manager and the Chief of the Division, serve as the storyline for the narration of the visuals. Both the interviews and scientific visualization data have been collected by videotaped field recordings, Ethernet, and/or video laser disc (figs.6,7,8,9,10,11).

As indicated above, the target audience, identified by the Space Systems Division, would actually be two separate classes of viewers. This makes the producer's job of content explanation much more complicated. In an effort to resolve this, the technical scientific visualization data will be underscored by a simpler voice-over narration process whenever necessary.

The editing process is accomplished using the Composium, a state-of-the-art, high-end computer in the Analysis and Computational Division. The computer allows one to multi-layer up to four separate images. In addition, it is possible to enhance the image, simulate motion and actual environments (e.g., space), or to include titling on static and real images. As the Composium has been designed primarily for multi-layering and graphics, it is not typically a real-time videotape editing system. Therefore, the editing process is much more time-consuming; yet, the editor is capable of performing many additional features. Some of the visualization, including the actual model, will be placed in simulation situations for the purpose of explanation and clarification (fig. 12).

To date, all of the first phase (preproduction) has been completed. This included considerable time spent on researching hypersonic technology and the history behind the HL-20 in order to ask specific questions relevant to each area of investigation in an effort to have the correct content information necessary for the videotape, securing necessary equipment (Sony Betacam video camera, audio equipment and facilities for voice-over production, a field lighting kit and videotapes) and personnel (an employee in the Flight, Software & Graphics Branch was trained by the Producer), and scheduling. The Producer also attended an intensive week-long workshop on Composium Operations. Most of the second phase (production) has been completed. To date, one interview and additional cover video shots remain to be videotaped. The final phase (postproduction) will take place during the last two weeks of the program. The videotape will begin with an opening shot of the current HL-20 full-scale model simulated in a flight situation; then, a historical overview (with actual footage of predecessors of the vehicle), will be presented. At this point, the project participants will be the basis of audio portion with only connective or explanatory narration supplied. During their soundbites, video footage of their research will be edited in to accompany the explanations. However, due to unforeseen circumstances involving the equipment, a request has been made for an extension to complete the project.

References

1. Erwin, H., "Personnel Launch System (PLS) Lifting Body and Low L/D," AIAA 90-3815, NASA Johnson Space Center, Texas, 1990.

2. Hallion, Richard P., ed., The Hypersonic Revolution, Eight Case Studies In The History of Hypersonic Technology, From Max Valier to Project Prime, Volume I, 1924-1967, Special Staff Office, Aeronautical Systems Division, Wright-Patterson Air Force Base Office, Ohio, 1987.

3. Hallion, Richard P., On The Frontier, Flight Research at Dryden, 1946-1981, The NASA History Series, Scientific and Technical Information Branch, NASA, Washington, D.C., 1984.

4. Piland, William M., Theodore A. Talay, and Howard W. Stone, "Personnel Launch System Definition," IAF-90-160, NASA Langley Research Center, Virginia, 1990.

5. Wilkinson, Stephan, "The Legacy of Lifting Body," Air & Space, April/May 1991, pp. 50-62.
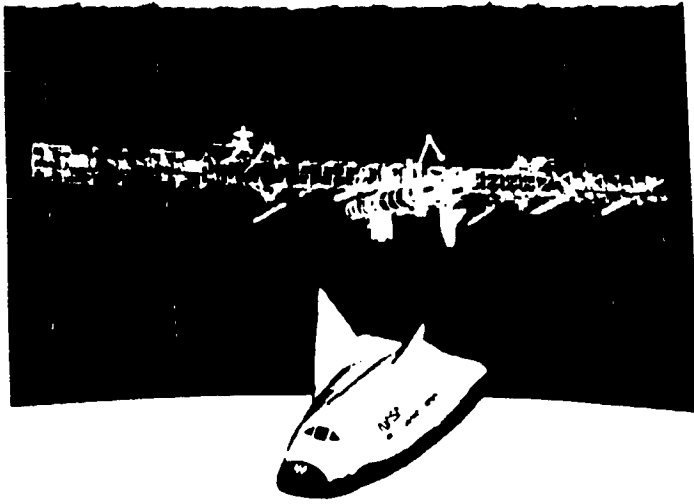
Figure 1. NASA Langley lifting-body PLS.
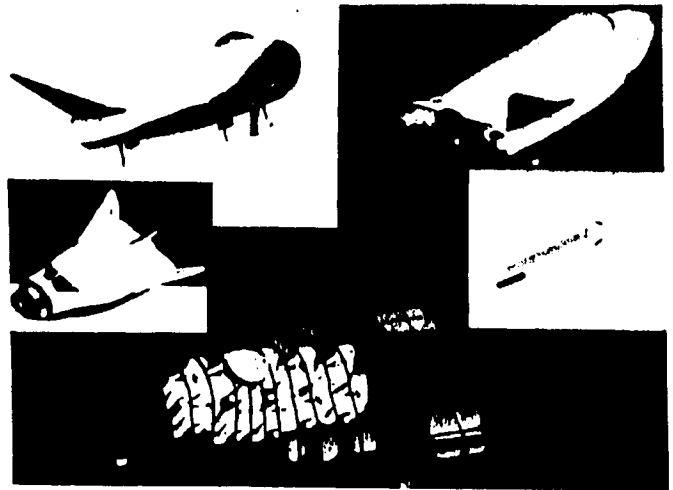
Figure 3 Aspects of the NASA Langley PLS.

Northrop M2-F2

Northrop 111-10

Martin X-24A

Martin X-24B
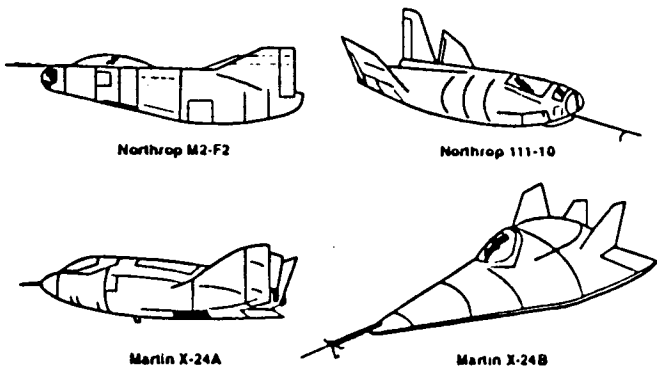
Figure 2. U.S. lifting-body configurations (1960's-1970's).

121.5 ft

78.1 ft

29.5 ft

23.5 ft

USA
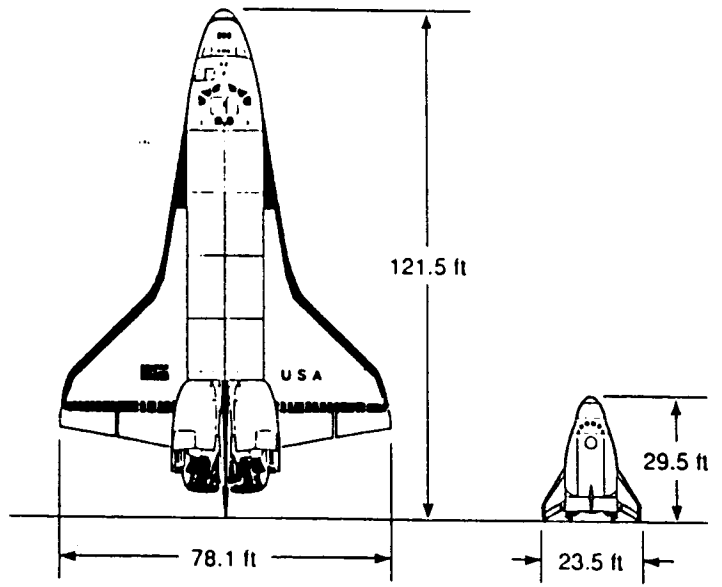
Figure 4. STS Orbiter and PLS planform comparison. (Courtesy Rockwell International Corp.)

63
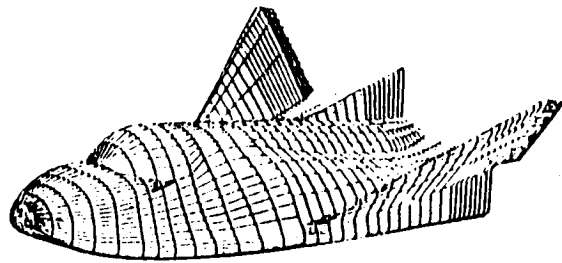
Fig. 5. A PLS Shape Proposed by LaRC.
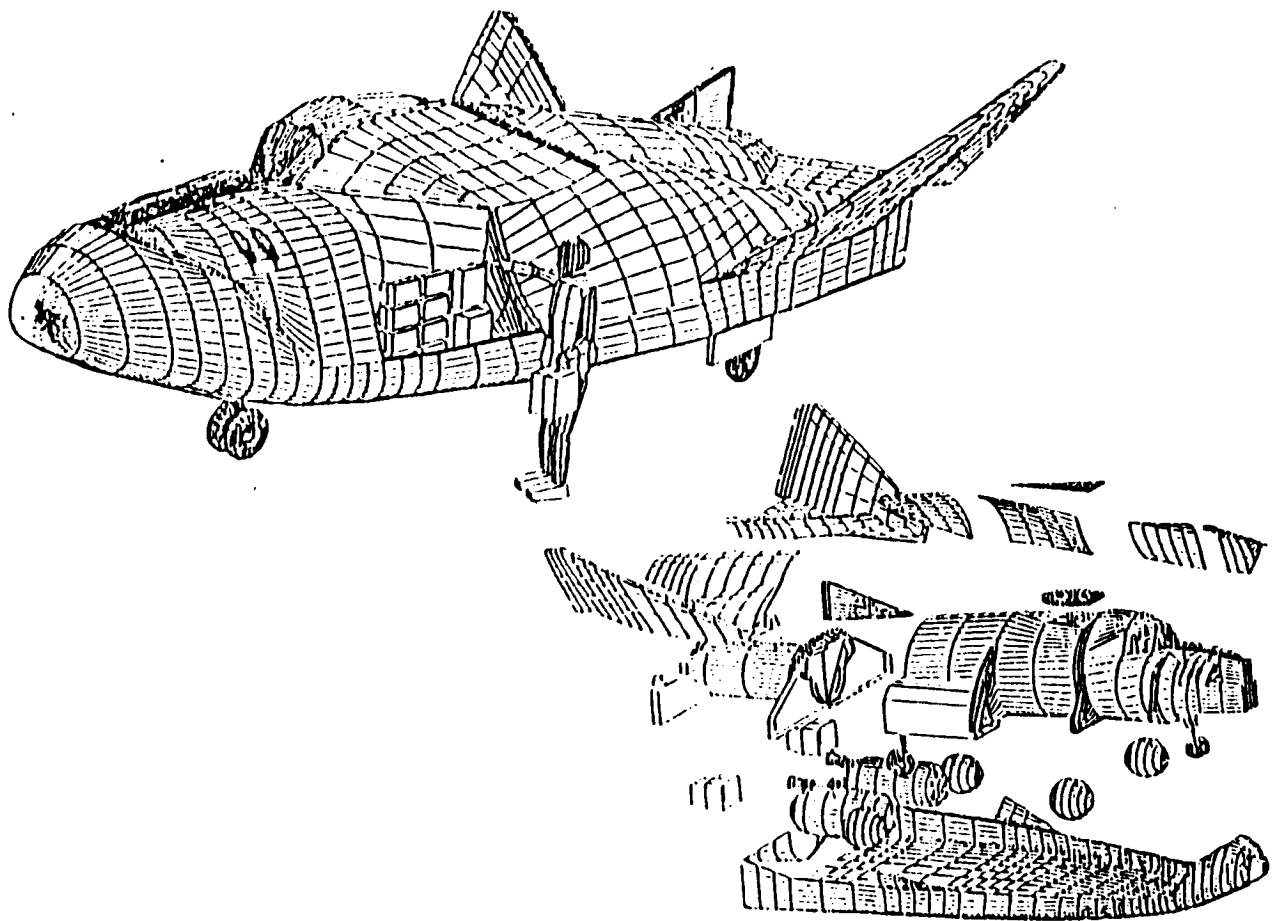
Figure 6. PLS hypersonic test model.
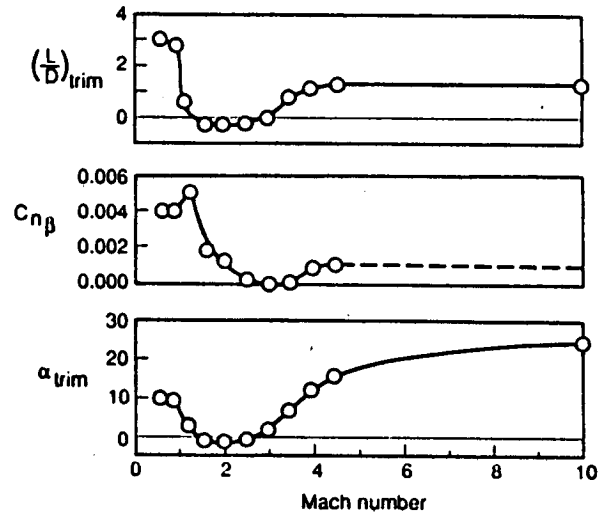
Figure 7. Summary PLS aerodynamic characteristics.
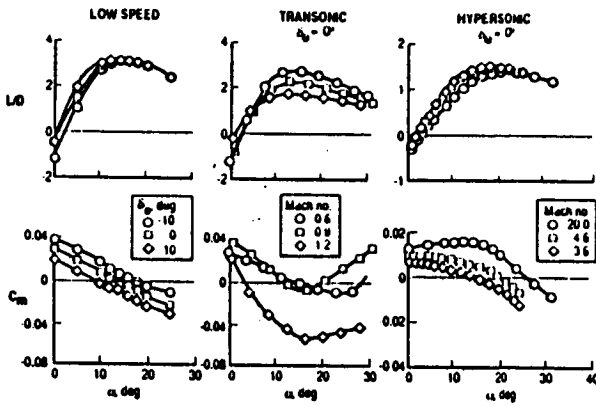
Figure 8. PLS longitudinal aerodynamic characteristics (moment ref. = 0.54L).

Real-gas simulation; M=6

Test gas	Density ratio
O Air	5.23
□ CF$_4$	11.90
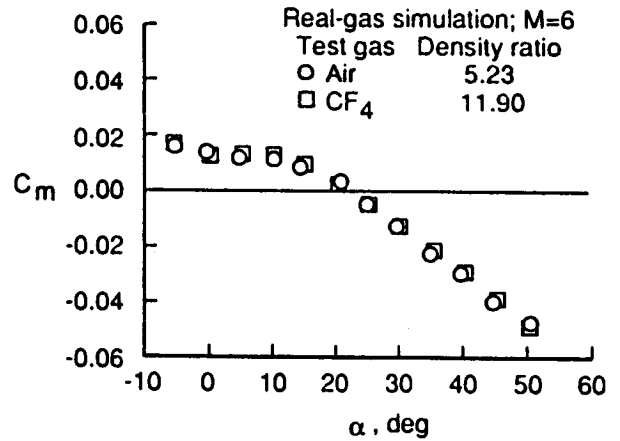
Figure 9. Hypersonic aerodynamic real-gas effects.

65
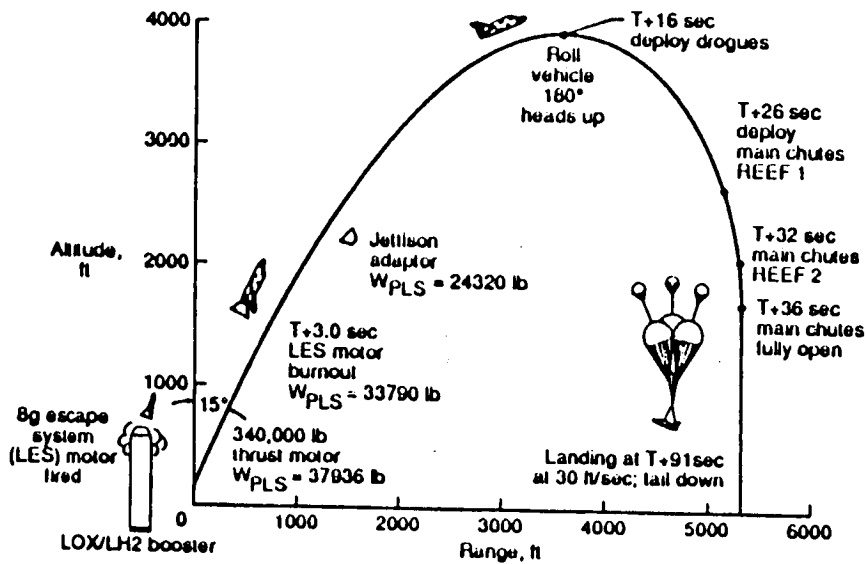
Figure 10 . On-pad launch escape sequence.

Supplementary flotation system
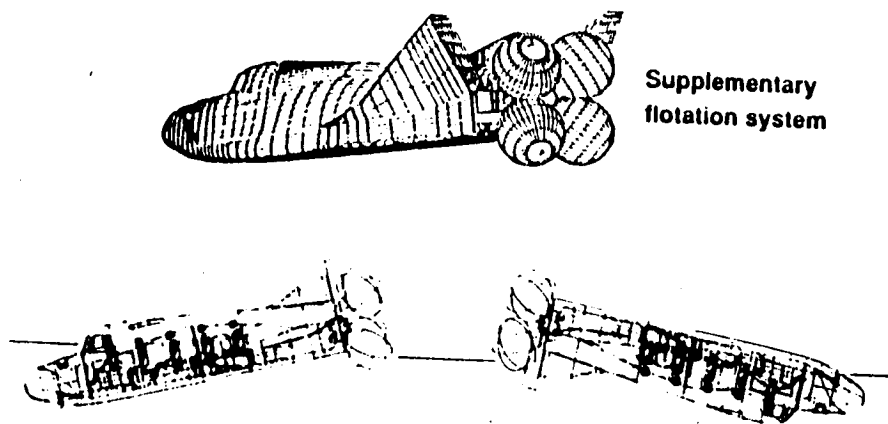
Figure 11 . Flotation concept for dry aft hatch.
(Courtesy Rockwell International Corp.)

66

PLS OPERATIONS SCENARIO
DRM-1
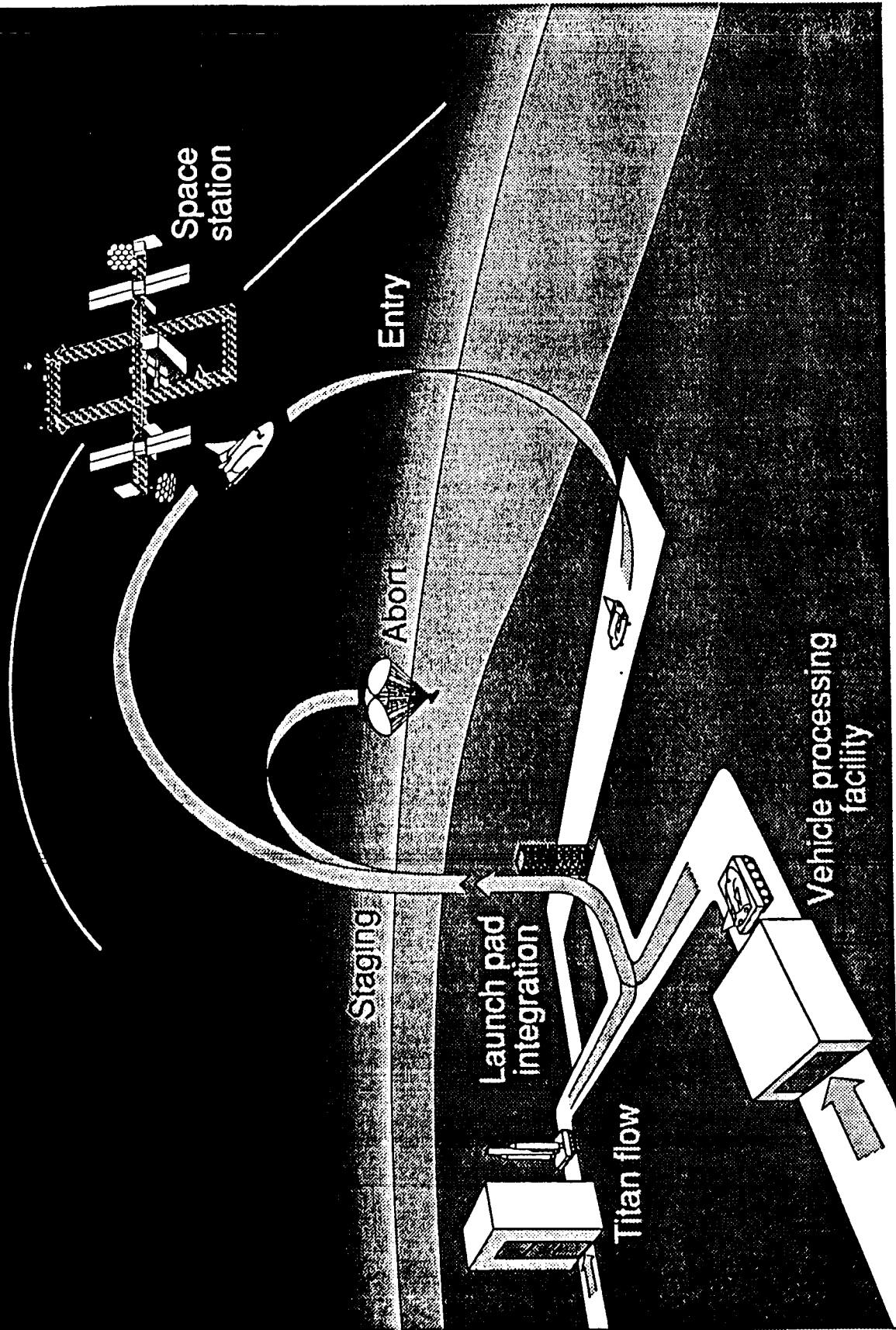
Space station

Entry

Abort

Staging

Launch pad integration

Titan flow

Vehicle processing facility

Figure 12

67

Comparison of Polynomial Approximations and
Artificial Neural Nets for Response Surfaces in
Engineering Optimization

by

William C. Carpenter
Department of Civil Engineering and Mechanics
University of South Florida
Tampa, Florida 33620

ABSTRACT

Engineering optimization problems involve minimizing some function subject to constraints. In areas such as aircraft optimization, the constraint equations may be from numerous disciplines such as structures, aerodynamics, environmental engineering, etc. The transfer of information between these disciplines and the optimization algorithm presents a problem. Response surfaces are a convenient way of transferring information between disciplines to the optimization algorithm. They are also suited to problems which may require numerous re-optimizations such as in multi-objective function optimization or to problems where the design space contains numerous local minima, thus requiring repeated optimizations from different initial designs. Their use has been limited, however, by the fact that development of response surfaces requires a number of initial functional evaluations either at randomly selected or preselected points in the design space. Thus, they have been thought to be inefficient compared to algorithms that sequentially perform functional evaluations closer and closer to the optimum solution. A development has taken place in the last several years which may effect the desirability of using response surfaces. It may be possible that artificial neural nets are more efficient in developing response surfaces than polynomial approximations which have been used in the past. This paper is concerned with this development.

The performance of polynomial approximations and artificial neural nets are compared on a number of test problems. Different number of designs are used to generate polynomial approximations of various orders and to generate different artificial neural nets. The quality of fit of the approximations at the designs and over the region of interest are compared with respect to the number of designs needed to develop the approximations as well as to the number of undetermined parameters associated with the approximations. For polynomial approximations, the number of undetermined parameters involved in the approximation is the number of undetermined coefficients associated with approximation. With artificial neural nets, the number of undetermined parameters is the number of weights in the net.

The problems that are considered are typical to those found in engineering applications. In Example 1, the irregular shape Banana

Function in two variables by Fox [1] is approximated by polynomials of the order 1, 2, 3, and 4 and by artificial neural nets with 1, 2, 4, 6, and 20 nodes on a hidden layer. The shape of the Banana Function, two approximations that were developed, and typical performance comparisons are given at the end of this abstract.

In Example 2, the volume of a fully stress designed 6 bar truss subject to stress, buckling, and size constraints is determined in terms of the coordinates of one node of the truss. This type of response surface could then be used to find the optimum location of that node of the truss. Response surfaces are developed for the truss volume in terms of the coordinate variables using polynomials of order 2, 3, and 4 and artificial neural nets with 3, 5, and 7 nodes on a single hidden layer. Performance of the approximations are compared over a region of interest. The truss in question, the shape of the function being approximated, and a typical performance comparison is given at the end of this abstract.

The first two examples consider approximations of complicated functions in two variables. The third example is concerned with approximations of a less complicated function in 4 variables. A 35 bar truss is considered. The area of the bottom chord is taken to be A_1, the area if the top chord to be A_2, the area of the verticals and the diagonals to be A_3, and the height of the truss to be H. A response surface for the stress in one of the lower chord members is developed in terms of these variables. Polynomials of order 1 and 2 and artificial neural nets with 1, 2, and 3 nodes on the hidden layer are considered. The 35 bar truss and a table comparing the approximations is given at the end of this abstract.

In the fourth example, the same truss is considered but in this case a response surface for the stress in a member of the bottom chord is developed in terms of 15 area variables. A table comparing the approximations is given at the end of this abstract.

This paper yields valuable information as to the number of training sets required for the two types of approximations and to their relative performance. First, with both types of approximations, it was found that it is desirable to use at least 100% more training sets than the number of associated undetermined parameters. Secondly, it was found that performance is controlled by the number of undetermined parameters associated with the approximation.

Currently, selection of artificial neural nets and the number of designs used to train them is done largely by trial and error. Based on the above findings, this paper develops simple rules which can be used to make a reasonable selection of a neural net and the number of training designs required to train it.

References
1.   Fox, R.L., _Optimization Methods for Engineering Design_, Addison-Weslely Publishing Company, Reading, Mass (1971).

69

Figure 5. Fox's banana function

Level	func
7	20.00
6	17.50
5	15.00
4	12.50
3	10.00
2	7.50
1	5.00
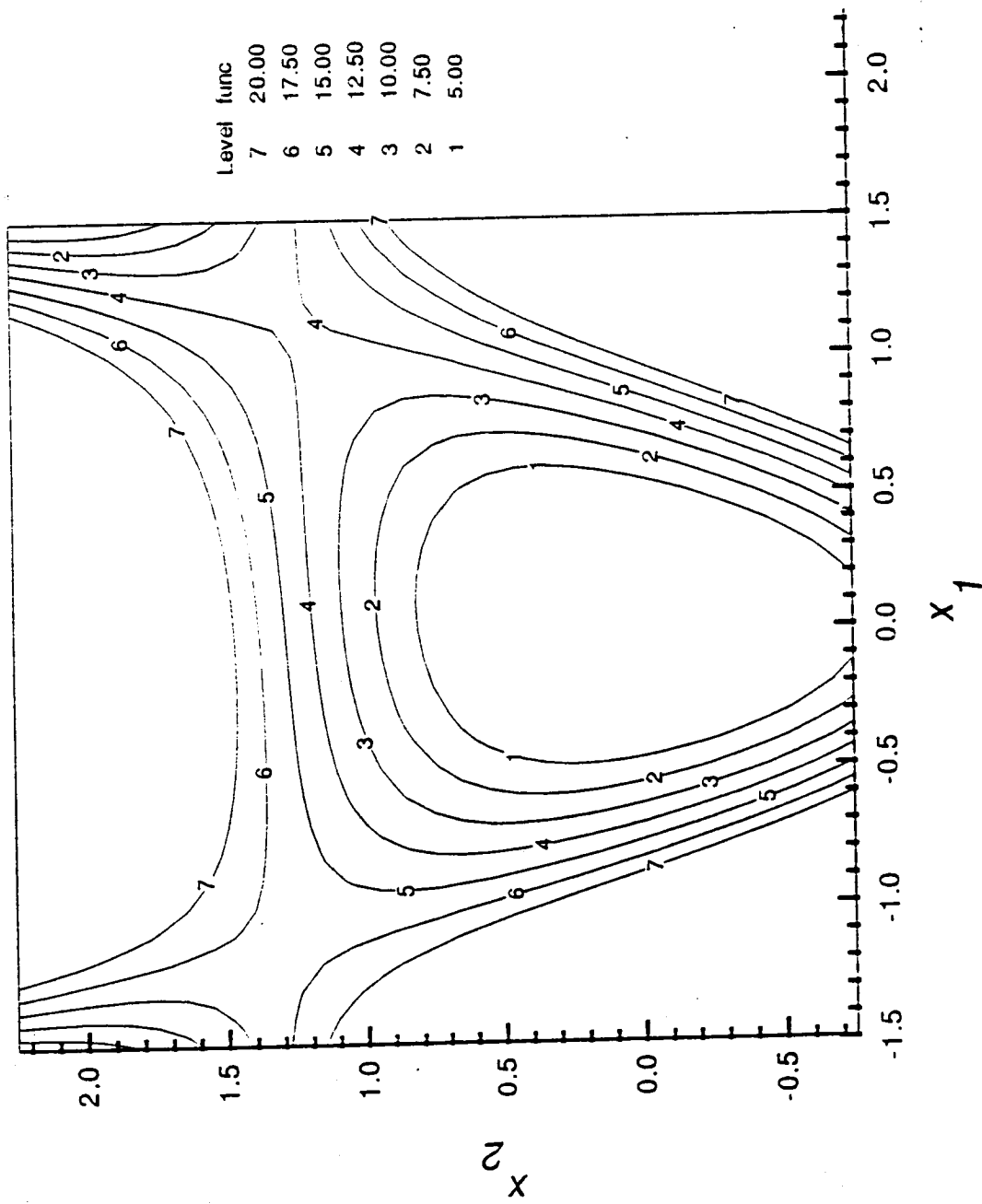
Figure 7. Third order polynomial approximation

71

Level	func
7	20.00
6	17.50
5	15.00
4	12.50
3	10.00
2	7.50
1	5.00
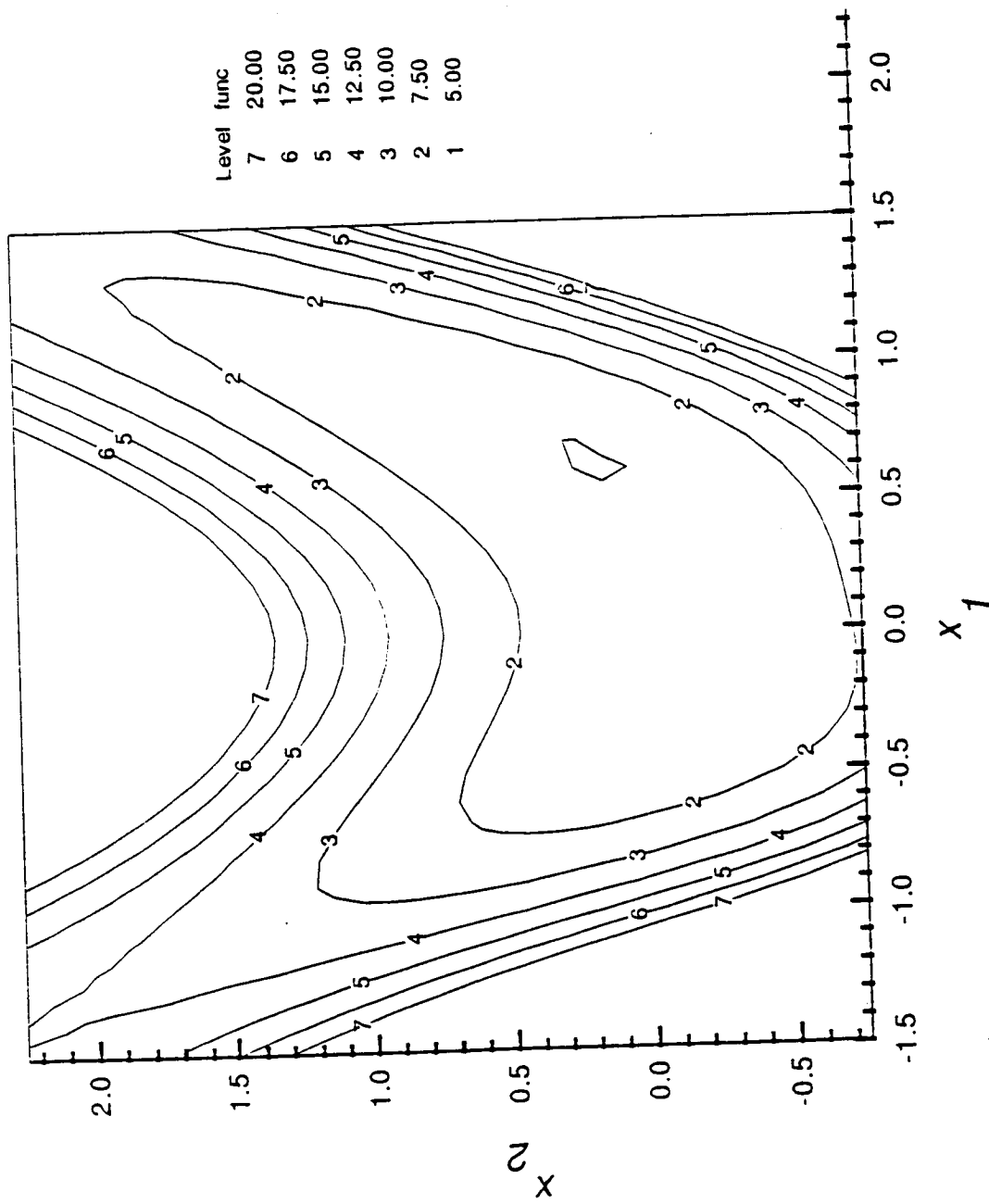
Figure 8. Artificial neural net--6 node hidden layer

Performance on Fox's Banana Function
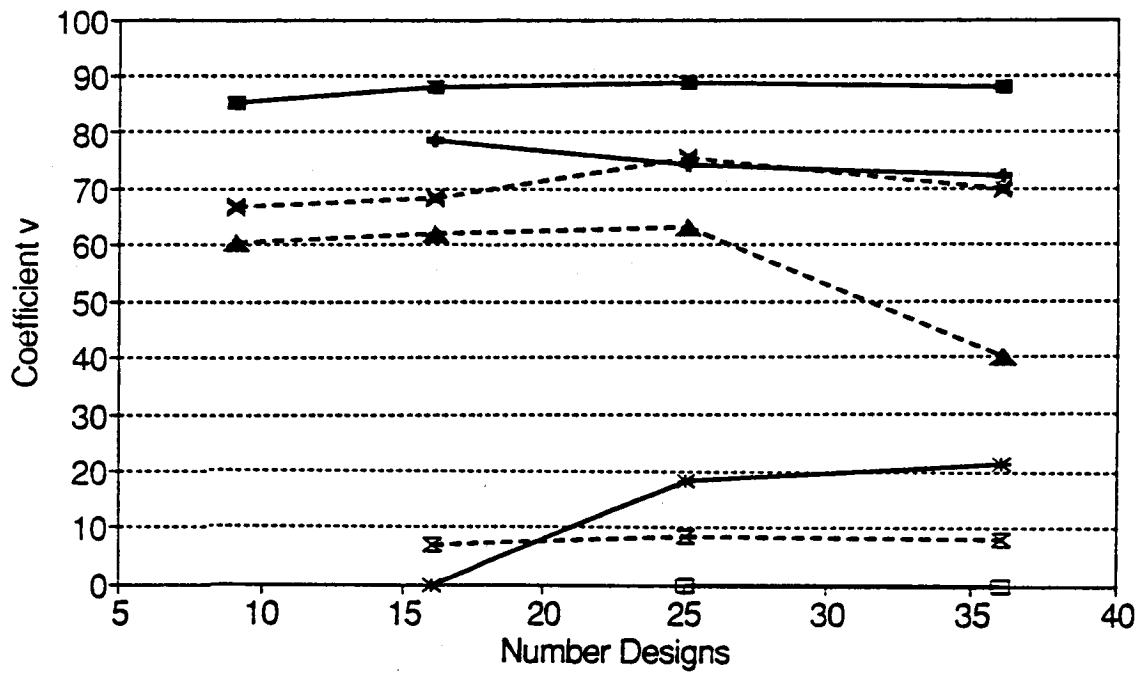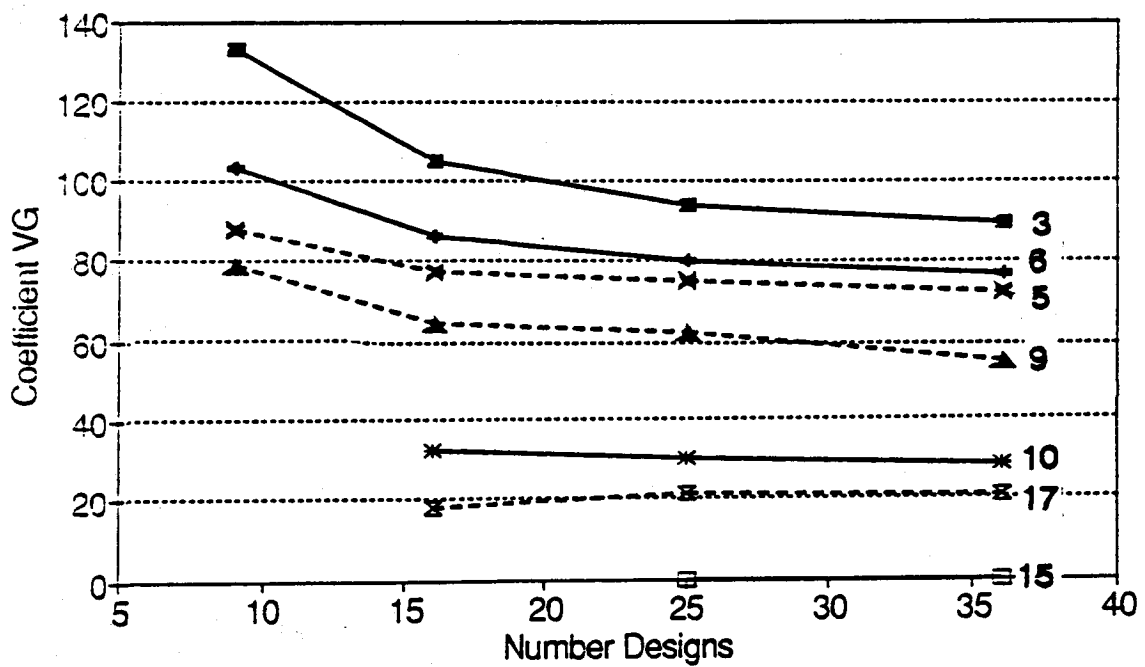
Figure 10. Non-dimensional RMS error

Figure 11. Variation of function explained by model

Figure 12. Non-dimensional RMS error at grid
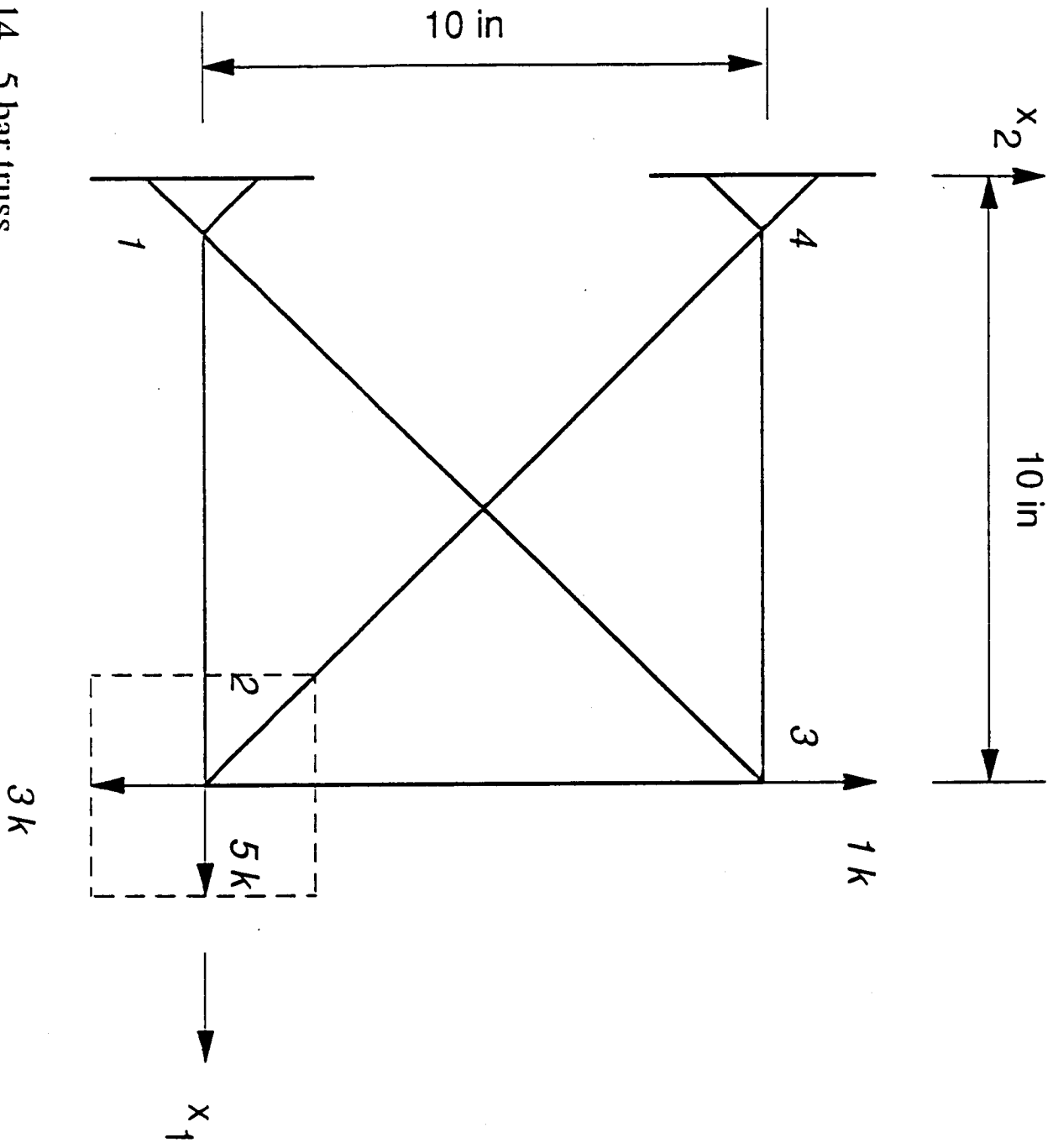
Figure 14. 5 bar truss

76
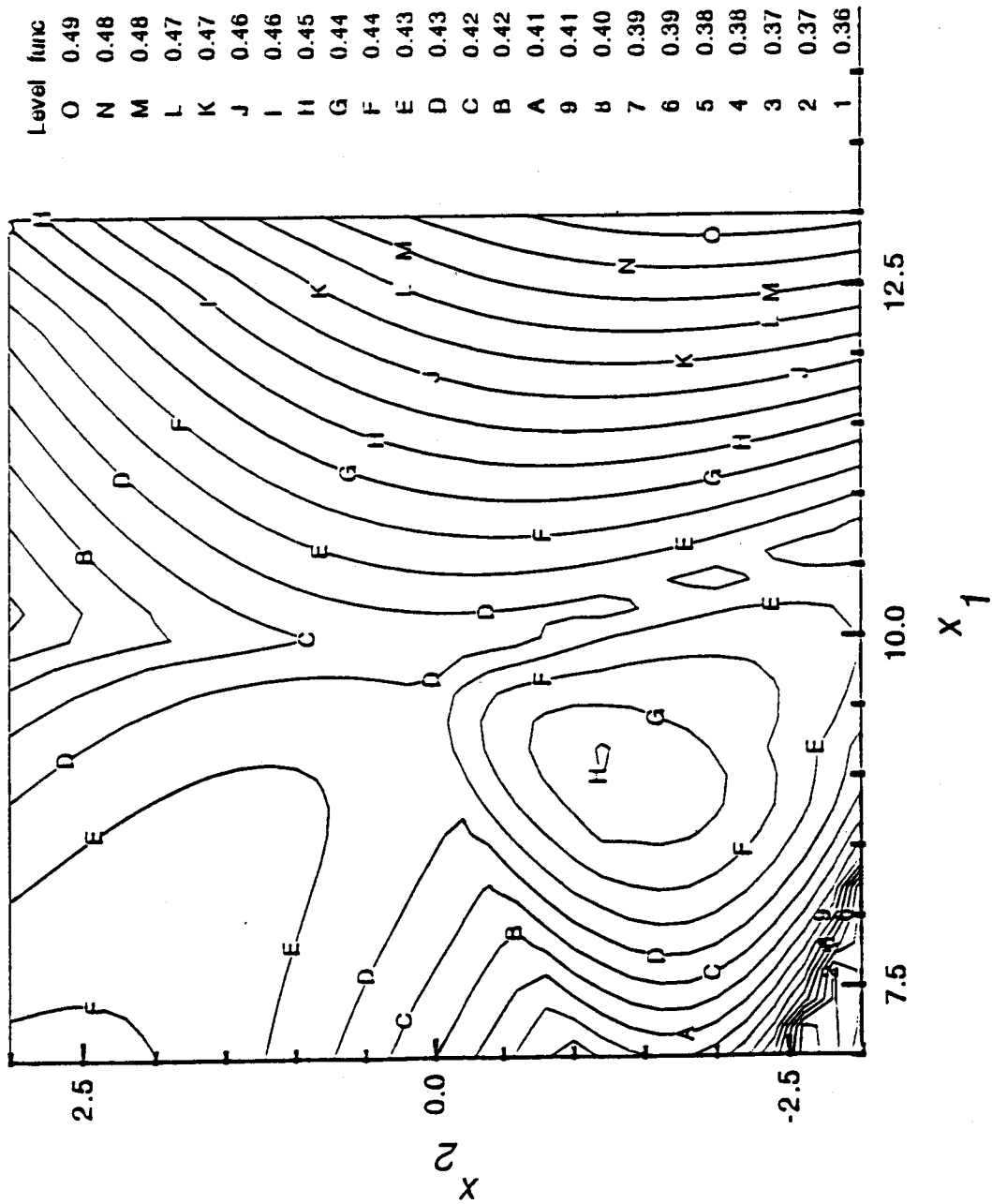
Figure 15. Optimum volumes

Performance on Five Bar Truss
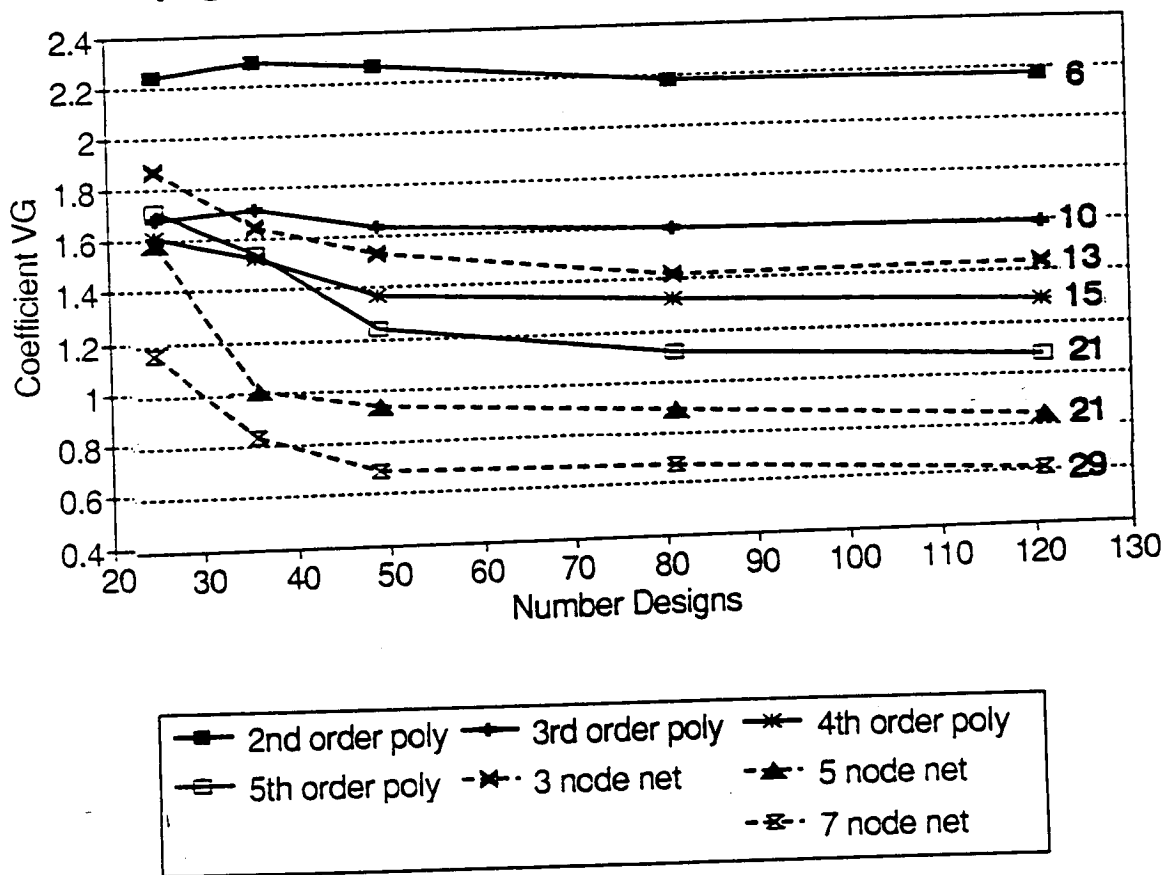
Figure 18. Performance of approximations
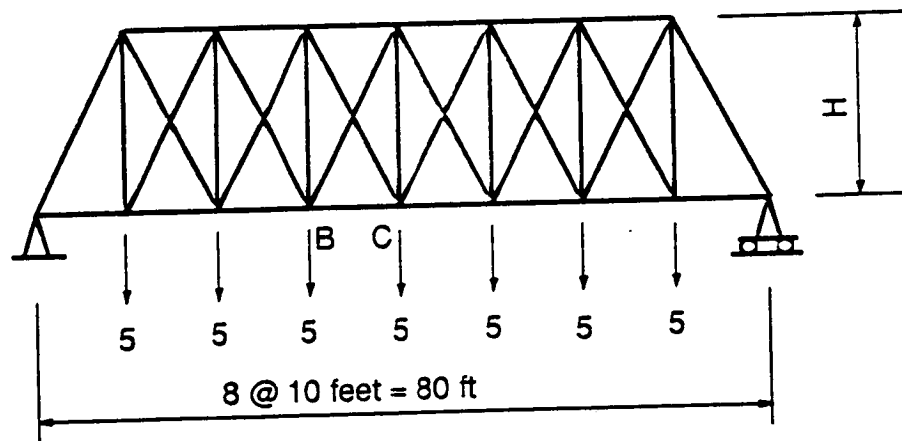
Figure 19. 35 bar truss

Table III. Performance of Approximations on the 35 Bar Truss
Response Surface.

Description	Number of undetermined parameters	coefficient v_G
1st Order Polynomial	5	8.37
Neural Net, H=1	7	7.56
Neural Net, H=2	13	3.75
2nd Order Polynomial	15	2.41
Neural Net, H=3	19	2.19

COMPUTATIONAL MODELLING OF POLYMERS

by

Edward A. Celarier
Department of Chemistry
Hampton University
Hampton, VA 23668

Polymeric materials and polymer/graphite composites show a very diverse range of material properties, many of which make them attractive candidates for a variety of high-performance engineering applications. Their properties are ultimately determined largely by their chemical structure, and the conditions under which they are processed. There are a great many variables involved.

It would be desirable to start with engineering specifications of material performance, and determine which of an infinite number of possible polymers would be best suited, and what processing methods should be employed. Unfortunately, the state of the art is not yet up to this point. Instead, polymer design is guided in large part by the intuitions of chemists and materials engineers, who must then synthesize candidate polymers, process them into material samples, and test the samples to see if they indeed have the desired properties. This method has some severe drawbacks: It is time-consuming, it is expensive, and it produces a great amount of chemical material that must somehow be disposed of.

It is the aim of computational chemistry to be able to simulate candidate polymers on a computer, and determine what their likely material properties will be. Generally, this involves simulations conducted at the level of atoms and molecules, from which one expects to obtain the properties of a macroscopic sample of the material. Some progress has been made toward this end over the last 15 years, and has been focussed on polymers and proteins, or biopolymers. However, there are a great many difficulties that have been encountered, and wildly inaccurate results are often the subtle consequences of assumptions that are made in order to cut a given problem down to a computable size. Thus, given a polymer system one is interested in, one must examine such factors to ensure that one's computed material properties are not dominated by artifact of the modelling process, by making a critical evaluation of the suitability of a chosen modelling method to the particular problem in hand.

A number of commercially available software packages purport to predict the material properties of samples, given the chemical structures of their constituent molecules. One such system, *Cerius*, produced by Cambridge Molecular Design, of Cambridge, England, has been in use at Langley Research Center. It is comprised of a number of modules, each of which performs a different kind of calculation on a molecule in the program's "workspace" We were particularly interested to evaluate the suitability of this program to aid in the study of microcrystalline polymeric materials.

One of the first model systems we examined was benzophenone (1), for which excellent crystallographic data on the molecular geometry in the crystalline state are available. We turned out to be up against the following difficulty: One module of *Cerius* performs a semiempirical quantum calculation, to determine the energy-optimized geometry of a *single* molecule (often referred to as a gas-state geometry, since there is no influence from other molecules). The optimized geometry was fairly close to the crystallographic geometry, and the small difference was acceptable, since the potential energy surface with respect to internal bond rotations is quite flat around this minimum. In order to determine the crystal packing of the molecule, one must freeze the internal molecular conformation, and adjust the lattice type, symmetry space-group, and lattice parameters to minimize the energy. In this program, this energy is computed from the sum of Lennard-Jones (6-12) potential energy functions, pairwise over the atoms, and, even though the electrostatic partial charges for each of the atoms is calculated for the gas-phase geometry, coulombic intermolecular interactions are negleced. Even specifying the space-group revealed by the crystallographic data, and some of the lattice parameters, this program did not give reasonable values for the remaining parameters. If different lattice types and different space-groups were specified, the energies were seen to be greater or less than that calculated for the *known* structure of the crystal. Thus, as far as this program is concerned, the known structure is not the minimum energy configuration. This raises serious questions as to the usefulness of this program in its current state to correctly calculate the energetics (and hence material and thermal properties) of candidate crystal structures, and thereby predict the crystalline structure of a novel polymer molecule which is, after all, much more complex than benzophenone.

Furthermore, it is uncommon to have a crystal of a polymeric material. Instead, we are interested in the behavior of materials which consist of microcrystallites embedded in an amorphous phase. Since the crystallites are very small, they are probably not well-modelled by this program, since this program assumes a crystal of infinite extent in at least one dimension.

Other difficulties encountered with this program include the fact that its interface to the semiempirical quantum calculation does not currently permit the user to control enough of the calculation to make it worthwhile. We have been in contact with Cambridge Molecular Design, and they are in the process of adopting a number of our suggestions in this regard.

Finally, over the period of this fellowship, some critical examinations were made into some of the theoretical underpinnings of calculations directed toward the prediction of the physical properties of polymeric materials. As a result of this process, the groundwork for a new approach was laid out and formalized into a proposal for funded research. We hope to soon be in a position to implement and demonstrate the utility of this new approach to explore the formation of microcrystalline domains in samples of high-performance polymers of interest to NASA.

Investigation of the Excited State Iodine Lifetime in the Photodissociation of Perfluoroalkyl Iodides

by

Stephen H. Cobb
Assistant Professor
Department of Physics and Astronomy
Murray State University
Murray, Kentucky 42071

The development of a space-based solar pumped laser system has been the focus of NASA research for several years. This laser would have application in power transmission to space vehicles and bases on the moon or Mars, where it could provide a means of electric power generation, propulsion, and communication[1]. An evaluation of prospective laser materials over the past decade has resulted in the identification of the iodine photodissociation laser as that system best suited to solar-pumped high energy operation[2]. The active medium for the solar-pumped iodine photodissociation laser is from the family of perfluoroalkyl iodides. These lasants have the general form $C_nF_{2n+1}I$, often abbreviated as RI. These iodides are known to exhibit photodissociation of their C-I bond when irradiated by near UV photons. Though many isomers have been tested with regard to their solar pumping properties, the iodide t-C_4F_9I has been identified as the most promising material for high-power application.

C_4F_9I is an attractive candidate for a lasant in that: 1) its absorption curve is shifted toward longer wavelengths in comparison to other iodides, allowing a greater absorption of the available solar radiation, and 2) the formation of R_2 dimers appears to be greatly limited. This subsequently results in greater recombination to the original RI molecule and a decreased production of the iodine molecule I_2, which is known to inhibit lasing action.

The excited state lifetime of the active medium is a very important parameter in a laser system. It governs the ability of a laser amplifier to store energy. The excited iodine atom has a long natural radiative lifetime (130 msec), giving the potential for high gain in the laser system[3]. However, non-radiative processes such as quenching by the parent RI molecule can shorten the lifetime considerably. If the lifetime is reduced too severely, the material ceases to be an effective lasant. Therefore, when attempting to develop theoretical models to

assess the performance of a potential laser system, knowledge of the excited state lifetime is of prime importance.

The focus of this work is to experimentally determine the lifetime of the excited iodine atom following photodissociation of C_4F_9I, and also to monitor fluorescence from the iodine molecule at 500 nm to determine if I_2 is being produced in the process. Photodissociation is achieved using a XeCl excimer laser with output wavelength of 308 nm. The XeCl beam is focused into the middle of a cylindrical quartz cell containing the lasant. The laser pulse is detected with a fast risetime photomultiplier tube (PMT) as it exits the cell. Fluorescence is recorded at 90 degrees to the XeCl beam by detection with a germanium photodiode fronted by a 1.315 micron filter to allow transmission of fluorescence due to excited atomic iodine only. The exponentially decaying fluorescence signal is measured to determine the time required for its intensity to fall to 1/e of its initial value. This time represents the lifetime of the excited iodine atom for a given pressure of RI vapor. Fluorescence from molecular iodine is also monitored at 90 degrees to the laser beam by a PMT fronted by a 500nm transmission filter. These experiments will be conducted at various pressures of RI to record any changes in lifetime versus pressure.

Work to date consists of experimental design, equipment acquisition and assembly, and initial checkout. The experiment is being brought on-line using the less expensive and readily available iodide C_3F_7I. Once completely operational, C_4F_9I will be inserted as the sample lasant.

References

1. Weaver, Willard R. and Lee, Ja H., "A Solar Pumped Gas Laser for the Direct Conversion of Solar Energy," J. Energy, Vol. 7, No. 6, Nov.-Dec. 1983, pp. 498-501.

2. Hwang, In Heon, Han, Kwang S., and Lee, Ja H., "XeCl Laser Pumped Laser Using t-C_4F_9I," Optics Comm., Vol. 70, No. 4, 15 March 1989, pp. 341-344.

3. Hwang, In Heon, Lee, Ja H., and Lee, Min H., "A Long-Pulse Amplifier for Solar Pumped Iodine Lasers," Optics Comm. , Vol. 58, No. 1, 1 May 1986, pp. 47-52.

MINI-CURRICULUM IN AEROSPACE CAREERS
FOR THE
VIRGINIA AIR AND SPACE CENTER
HAMPTON, VIRGINIA

AND

CONSULTANT FOR CONTRACTOR STEERING COUNCIL
EDUCATION INITIATIVE

BY

PROFESSOR LINDA W. DEANS
DEPARTMENT OF URBAN EDUCATION AND SCHOOL LEADERSHIP
NORFOLK STATE UNIVERSITY
NORFOLK, VIRGINIA 23504

A MINI-CURRICULUM IN AEROSPACE CAREERS
FOR THE
VIRGINIA AIR AND SPACE CENTER

AND

CONSULTANT TO THE CONTRACTOR STEERING COUNCIL EDUCATION INITIATIVE

BY

PROFESSOR LINDA W. DEANS
DEPARTMENT OF URBAN EDUCATION AND SCHOOL LEADERSHIP
NORFOLK STATE UNIVERSITY
NORFOLK, VIRGINIA 23504

The assignments of this professor at the NASA-Langley Research Center during the summer of 1991 as a participant in the ASEE Summer Fellows Program involved an array of activities and experiences as they relate to the Office of External Affairs and Public Service. Two major projects have evolved from these experiences: 1. Development of a mini-curriculum in aerospace careers for grades pre-kindergarten through twelve for the purpose of enrichment for students who will attend the new Virginia Air and Space Center, which will open during the Spring of 1992; and 2. Coordinating and serving as the education consultant to the NASA-Contractor Steering Council Education Initiative, which involves a series of career oriented briefings that can be utilized in the five local school divisions to inform students of career opportunities at the NASA-Langley Research Center and with its contractors.

The thrust of the first assignment, Development of a Mini-Curriculum in Aerospace Careers for the Virginia Air and Space Center, has involved the development of three levels of activities for each visit of a group of students. During a visit, the student would be given a general activity, which would aim to teach, generally, decision-making and cooperative learning. Three different activities of this type was designed for each grade level grouping (pre-k-3; 4-6; 7-9; and 10-12). This allows for any given student group to be able to visit the Center three times while a student is within a given grade level grouping and be given the opportunity to participate in a different activity during each visit. The justification for this was to provide variety and stimulate interest in the area of aerospace careers for students at all grade levels. Additionally, as a follow-up to this activity, a second series of activities specific to aerospace careers was designed in order to have the student focus on this significant area. Again, three different activities of this type was designed that correlated with the initial decision activity. Lastly, the third set of activities related directly to the exhibits that will be displayed at the new Virginia Air and Space Center.

These exhibits include exhibits that were once displayed at the Visitor's Center at NASA-Langley, as well as other exhibits designed by national and international scientists, engineers, sculptors/sculptresses, and artists. Even though many of these exhibits were available to the professor only as sketches in a brochure, the goal was attained to develop applicable activities. Samples of all three levels of activities will follow this abstract.

A second project in which the professor was involved was that of the NASA-Langley Research Center Contractors Steering Council's Education Initiative. The idea for this project originated with the Senior Staff of NASA-Langley. The primary goal was to further enhance NASA's involvement in promoting improved education at the local level. Further, the intent was to involve the many contractors who contribute to the NASA workforce in a cooperative effort, such as this Education Initiative. Instead of having the contractors compete with each other in order to provide a service for NASA-Langley, they would now work cooperatively to provide a viable service to NASA-Langley and the local community, by producing a program that will be used in the local school districts in an effort to improve the workforce in the future. The Office of External Affairs and Public Service at NASA-Langley was asked by the Senior Staff to coordinate this project. As an ASEE professor in the field of education, I was given this assignment. This assignment has involved extensive meetings with the Contractor Steering Council as a group, as well as with individuals on the Council. Individuals representing 25 job types were identified and given some general parameters to write career-related information concerning each of the 25 job types. The writing of these job descriptions has involved meeting as groups and with individuals representing job clusters. After the initial writing, the job descriptions are circulated for perusal by others in that particular job field, as well as by supervisors of that particular job type for accuracy. These writers were guided through the process with constant reminders of the age-level of the students who would be utilizing this product. After the writings are perused for the final time, the professor will complete the second component of this project by writing the courses and/or skills that the student will need to learn while in school in order to either be prepared to go directly into the workforce or to enter a post-high school training program that will prepare the student for the particular job.

As a part of the development of the project with the NASA Contractor Steering Council, the professor lead the team to visit the superintendents and central office staff of local school districts in order that they might give input for this project. The expertise of the professor was supported by the collaboration with the educators from the five local school districts. This project aims to be piloted in the five local school districts during the 1991-92 school term.

The aforementioned projects have afforded the professor the opportunity to actually utilize that body of knowledge that is taught to those graduate students in the Department of Urban Education and School Leadership at Norfolk State University, Norfolk, Virginia. The experience has been second-to-none for the professor at this stage in experiential professional development. This professor will be returning to the classroom at Norfolk State with new ideas and directions as a result of participation in the ASEE Summer Faculty Fellowship Program.

GENERAL ACTIVITY
WHAT IS IMPORTANT IN YOUR LIFE?
A BAKER'S DOZEN!

Objective:

The purpose of this activity is to help young people to recognize what is important to them in daily life. A theme which runs all through values clarification and career education is that in order to make some sense out of the bewildering array of alternatives in life, we have to set some priorities. This strategy gets at this issue in a fresh, personal way.

Materials Needed:

Pictures of all household electrical appliances and utensils
Large Envelope
Scissors
Glue
Pencils

Lesson Plan/Procedures:

This is an individual activity. Give each student an activity packet which will contain pages of pictures of electrical household appliances and utensils and a. Each student is to write her/his name at the top of the activity packet.

The teacher says: "Think of a list of 13 things (a baker's dozen) that you personally use around your house which make use of electricity. This includes anything at all with plugs and anything which you use fairly frequently or someone uses for you very frequently. Select these items from the pictures that you will find in your packet; cut them out; and place them in your envelope. You will have 15 minutes to find these thirteen pictures.

Now, remove the pictures of three things you could live without the easiest. Place these pictures face down on your desk. If, for example, the city had an acute power shortage, and every home was asked to cut down on its use of electricity which three could you give up most easily? These are the three you would remove from your envelope. Take a few minutes to think about this.

On the other hand, which three do you find very precious? These are items that you feel that you just absolutely cannot live without. Choose these three and glue them to the outside of your envelope. These would be the last ones you would want to give up.

Closing Activity:

The teacher then asks for volunteers to tell about their pictures which are placed on their tables, the ones that they can give up most easily. Then have the students to tell about the pictures that are glued to the outside of their envelopes, the ones that they absolutely cannot do without. Also, the class can make "I Learned Statements" about these 13 possessions, or about their material possessions in general.

The teacher should make sure that you share your own list durng the discussion and let your students know where you stand on the use of appliances. The teacher should be careful not to do excessive moralizing. Let the data speak for each person and to each person in its own way.

The teacher can play "devil's advocate" and suggest that everyone should give the three items they crossed out to needy individuals or families. The teacher will take a large envelope and walk around the room to collect all items that can be given to needy individuals and families.

AEROSPACE ACTIVITY
DESIGNING USEFUL PRODUCTS
FOR USE AT HOME AND IN SPACE

Objective:

In Activity 1A, the space ambassadors were told that they did not have to worry about problems of time, space, language, or life support because modern technology could fulfill these needs. However, there may exist day-to-day problems that have to be resolved in creative innovative ways by the space travelers. This activity will encourage thought processes that can allow for resolution of day-to-day obstacles to conveniences.

Materials Needed:

Four squares of paper; two of which are different shades of the same color and one slightly larger than the other.
Thread
Cotton balls
Glue
40 Plastic Drinking Straws
40 Dressmaker Straight Pins
2 - 100 gram masses
Meter Stick
4 Pieces of Ribbon
2 - 6 inch squares of paper
Space Spinoffs Activity Sheet

Lesson Plan/Procedures:

1. Divide the class into groups of 4-5 students so that there will be six total groups.

2. Place two groups on a team in order to have three teams.

3. Assign each group a "construction project". Choose: a. Paper Toy Making - Paper Basket; b. Soda Straw Strong Arm; or c. The Sun Box. The groups who receive the same construction project form a team.

4. Give each group the materials for the construction project. Allow 30 minutes for the construction. Upon completion of the projects, each group is to determine how this device can be used by the space ambassadors sent in Activity 1A. Record these thoughts on the "Space Spinoffs Activity Sheet." "Space Spinoffs" are new products, processes, and ideas that have come from the space program. If your designs can be used both in space and on planet earth, then you have produced a space spinoff.

Closing Activity:

1. Have the teams to collaborate concerning both their design and their lists of Space Spinoffs. Determine who had the most applications on the space spinoff list.

2. Allow the two groups to share ideas of design variations.
3. Have each team to share their experiences with the entire group.
4. Ultimately, facilitate a discussion in which the students may recognize the past experiences of astronauts in having to make adaptations while in outer space and/or have students to project possible adaptations for future space travel.

SPINOFF ACTIVITY SHEET

What's in it for me? That is a question that many people have asked about space technology. A lot of money and hard work have gone into the space program. What are the benefits of space research and construction similar to this that you have just completed? The answer is "space spinoffs." Space spinoffs are new products, processes, and ideas that have come from the space program. Space spinoffs are an example of technology transfer, which is technology used or invented for one job can be used to do jobs in other areas.

HOW MANY SPACE SPINOFFS CAN YOUR GROUP LIST?

1.

2.

3.

4.

5.

6.

7.

8.

9.

10.

11.

12.

13.

ETC.

GENERAL ACTIVITY
WHAT IS THE DIFFERENCE BETWEEN WORK AND PLAY?

Objective:

The purpose of this activity is to make students aware that the difference between work and play is simply a matter of opinion.

Materials Needed:

Activity: List of Adjectives for Work
Activity: Describing Activities as Work or Play
Pencils

Lesson Plan/Procedures:

1. Allow each student to work as an individual. Give each student a copy of the two activity sheets. Allow them to read and follow the directions and complete both.

2. Ask each student to find a partner to discuss his/her answers with. Ask the students to keep a count of how many answers are changed during the collaboration with this classmate.

3. Ask each student to find a different partner to discuss his/her answers with. Ask the students to keep a count of how many answers are changed during the collaboration with this classmate.

4. A large group discussion should follow with the facilitator listing the activities on the board (or on a overhead) in order for discussion to take place.

Closing Activity:

The facilitator should initiate a discussion about job satisfaction as it relates to "work" and "play", with the emphasis being that if an individual enjoys his/her work, then the two verbs can be intertwined.

Ask the students to think of some individuals who really enjoy their work and some who do not.

For each adjective, check whether the word describes work or play or both.

	Adjectives	Work	Play	Both
1.	hard			
2.	a grind			
3.	easy			
4.	tiring			
5.	enjoyable			
6.	physical			
7.	mental			
8.	exciting			
9.	useful			
10.	routine			
11.	repetitious			
12.	manual			
13.	menial			
14.	challenging			
15.	healthy			
16.	necessary			
17.	tedious			
18.	sloppy			
19.	interesting			
20.	boring			
21.	demanding			
22.	dangerous			
23.	dirty			

Activity #2 - Describing Activities as Work or Play

Activity		Work	Play	Both
1.	riding a bike	___	___	___
2.	mowing the lawn	___	___	___
3.	building a birdhouse	___	___	___
4.	solving math problems	___	___	___
5.	washing dishes	___	___	___
6.	tending a garden	___	___	___
7.	writing short stories	___	___	___
8.	pen and ink drawing	___	___	___
9.	repairing a radio	___	___	___
10.	telling stories	___	___	___
11.	solving puzzles	___	___	___
12.	decorating a room	___	___	___
13.	shopping	___	___	___
14.	trimming shrubs	___	___	___
15.	playing the piano	___	___	___
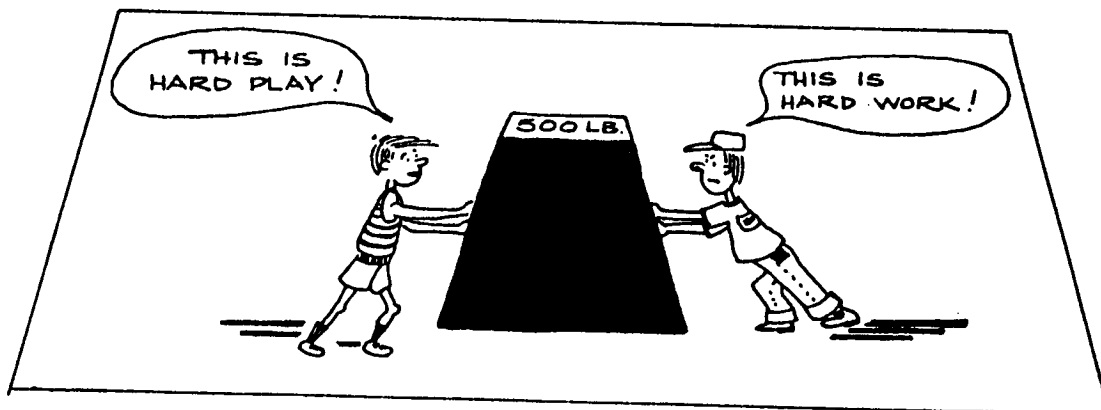
AEROSPACE ACTIVITY
IDENTIFYING WORK/PLAY ROLES
IN THE LIFE OF AN AEROSPACE WORKER

Objective:

The purpose of this activity is to differentiate between work and play of an aerospace worker.

Materials Needed:

Film: (See listing for appropriate title)
Poster Board
Fishing Line
Scissors
Magic Marker
Activity Sheet: Making a Mobile
paper
pencil

Lesson Plan/Procedures:

1. Divide the class into groups of 3-4 students. Give them the instructions to write down different verbs that relate to the jobs of the different aerospace workers who will be depicted in the film.

2. At the end of the film, ask two groups to choose at least five verbs that related to play and two groups to choose at least five verbs that related to work.

3. Ask a fifth group to construct two mobiles with space for ten words on each mobile. Have this group to collect the "play" verbs and mount them on one mobile and then collect the "work" verbs and mount them on the other mobile.

4. The facilitator will display each mobile and allow the class to compare the differences and the similarities.

Closing Activity:

Ask the students to give thoughts on what each of them would like to do to contribute to space exploration for the United States.

Activity 3C
Grades 4-6

EXHIBIT ACTIVITY
WORK OR PLAY

Objective:
    The purpose of this activity is to

Experiences with Optimizing Airfoil Shapes for

Maximum Lift over Drag

by

Michael L. Doria

Associate Professor

Department of Mechanical Engineering

Valparaiso University

Valparaiso, Indiana 46383

The goal of my work this summer was to find airfoil shapes which maximize the ratio of lift over drag for given flow conditions. For a fixed Mach number, Reynolds number and angle of attack, the lift and drag depend only on the airfoil shape. This then becomes a problem in optimization: find the shape which leads to a maximum value of lift over drag. The optimization was carried out using a package developed by Gregory A. Wrenn called KSOPT [1]. This is a self contained computer code for finding the minimum of a function subject to constraints. To find the lift and drag for each airfoil shape a flow solution has to be obtained. This was done using a two dimensional Navier Stokes code developed by Swanson, Turkel and Jameson.

The airfoil shape is defined analytically as a linear combination of orthonormal basis functions. The amplitudes of each term uniquely define a surface. Four terms are retained for both the upper and lower airfoil surface. Therefore there are a total of eight design parameters which characterize an airfoil shape. For fixed free stream flow conditions the lift and drag depend only on these eight design parameters.

The objective function is the quantity which is to minimized. In the present work the goal is to maximize lift over drag. This suggests two possibilities for the objective function — the negative of the ratio of lift over drag or the inverse, namely, the ratio of drag over lift. More success was obtained with the former.

It was found during the course of the work that several geometric constraints had to be put on the design space. These constraints were necessary to prevent the optimizer from specifying airfoil shapes which were impossible or unrealistic. A total of six geometric constraints were imposed. These included constraints on the airfoil area, the radius of curvature at the leading edge and minimum thickness.

Several problem areas became apparent as various cases were tried. First of all, even though constraints were imposed, the optimizer sometimes generated unrealistic shapes. This is because KSOPT allows constraints to be violated as it carries out its search for an optimum. For these cases a call to the flow code has to be skipped. Secondly, the

flow code becomes unsteady or divergent for some shapes, particularly at shapes with high lift. This presents a dilemma for the optimizer because it must generate shapes with high lift but not so high that the flow code cannot handle them. Its like asking the optimizer to go right up to the edge of the cliff and search around but not fall over. There is also a difficulty with resolution in the flow solution. The resolution in lift and drag may be less than the change in lift and drag caused by a change of shape. In this case, the optimizer may not get the correct sign for the gradient of the objective function and start the search in the wrong direction. The objective function has more than one local minimum. Therefore the optimizer may end up at a relative minimum instead of the absolute minimum. For this reason it is important to start with more than one guess for the initial shape. For the runs carried out this summer two initial shapes were used: a symmetric NACA 0012 and a NACA 0012 with five percent camber.

The optimization process was carried out for a number of cases. In all cases the free stream Mach number was kept at 0.3 and the Reynolds number at 5 million. In one case the angle of attack was 6.0 degrees. In all others the flow was kept at zero incidence. Airfoil shapes were obtained with lift over drag ratios as high as 113. Some general guidelines emerged as experience with the optimizer increased. Some of these are as follows

1. The optimization process seems to work better with the objective function equal to the negative of lift over drag.
2. There is more than one local minimum. So start with more than one initial shape, at least one with camber.
3. The final shape obtained depends on the mesh size and number of multigrid cycles used in the flow code.
4. Use the internal scaling option in KSOPT.
5. Additional constraints or modifications in the objective function may be necessary to avoid obtaining shapes which are too highly cambered or have very sharp trailing edges.

From experiences with KSOPT it is clear that airfoil optimization it is not yet at a point where it can be fully automated. Human intervention in the process is still necessary. However, if the user is persistent and provides some intelligent and patient prodding, the optimization process can lead to some good airfoil designs. In future work it would be interesting to investigate the effects of adding additional constraints on the maximum camber, the trailing edge angle, and the pitching moment. Also some additional investigation into other objective functions may prove useful.

Reference

1. Wrenn, Gregory A. , "An Indirect Method for Numerical Optimization Using the Kreisselmeier-Steinhauser Function", NASA Contractor Report 4220, March 1989.

EXPERIMENTAL DETERMINATION OF RESIDUAL STRESS

by

Professor M. W. Ferguson
Department of Chemistry and Physics
Norfolk State University
Norfolk, Virginia 23504

Residual stresses in finished parts have often been regarded as factors contributing to premature part failure and geometric distortion. Currently being investigated are residual stresses in welded structures and railroad components. High residual stresses formed in welded structures due primarily to the differential contractions of the weld material as it cools and solidifies can have a profound effect on the surface performance of the structure. In railroad wheels, repeated use of the brakes causes high residual stresses in the rims which may lead to wheel failure and possible derailment.

The goals of the study were: (1) to develop strategies for using X-ray diffraction to measure residual stress; (2) to subject samples of Inconel 718 to various mechanical and heat treatments and to measure the resulting stress using X-ray diffraction; and (3) to measure residual stresses in ferromagnetic alloys using magnetoacoustics.

X-ray diffraction is an effective nondestructive method for the measurement of residual surface stress. In crystalline materials, the residual stress causes a difference in the lattice spacings from the stress-free values. It may be shown (ref. 1) using elasticity theory that the residual stress is related to the difference in the measured d-spacing by the equation

$$\sigma_\phi = \frac{E}{(1 + \nu)\sin^2\psi} \frac{(d_i - d_n)}{d_n} \qquad (1)$$

where σ_ϕ is the calculated residual stress in the ϕ direction, d_n, the spacing of the planes parallel to the surface of the sample, d_i, the spacing of the planes whose normal makes an angle ψ with the normal to the surface, E, the Young's modulus, and ν, the Poisson's ratio. E and ν are material constants obtained from the appropriate tables. Since the angular position 2θ of the diffracted beam is measured directly with a diffractometer, it is convenient to express equation (1) in terms of 2θ rather than plane spacings. The relation between the spacing d and the diffraction angle θ is given by Bragg's law which states

$$d = \frac{\lambda}{2\sin\theta} \qquad (2)$$

where λ is the wavelength of the incident radiation. Substitution of Bragg's law into equation (1) leads to

$$\sigma_\phi = \frac{E \cot\theta}{2(1 + \nu)\sin^2\psi} (2\theta_n - 2\theta_i) \qquad (3)$$

where $2\theta_n$ is the observed value (in radians) of the diffraction angle in the normal measurement and $2\theta_i$ its value in the inclined measurement. Thus a measurement of $2\theta_n$ and $2\theta_i$ at a given diffraction peak allows a determination of the residual stress.

The X-ray diffraction system was used to determine residual stresses in samples of Inconel 718. Samples studied were a flat plate, an annealed flat plate, and a flat plate bent in the form of a semicircle. Although the stress in the annealed sample was negligible, stresses in the flat and bent samples were considerably higher. A concern in the investigations was the low intensity of the diffraction peaks in the desired angular range using molybdenum K_α radiation. Mechanical treatments of the surfaces of the samples produced no significant increase in the relative intensities of the diffraction peaks.

Low-field magnetoacoustic interaction has been successful in the investigation of residual stress in Fe-alloys (ref. 2). Young's modulus in ferromagnets depends not only on the degree of magnetization, but also on the stress; therefore, the acoustic natural velocity, which is E dependent, directly relates to the stress state. In this experiment, as a time-dependent magnetic field was passed through ferromagnets subjected to fixed amounts of stress (tension and compression), acoustic waves in the pulse-echo mode were propagated through the samples. Since it can be shown that the fractional change in natural velocity is approximately equal to the fractional change in frequency of a phase-locked acoustic wave, a pulsed-phase-locked-loop acoustic interferometer was used to measure the fractional frequency shifts of the acoustic waves as a function of the external magnetic field.

In the magnetoacoustic experiments, the magnetization was chosen to be parallel to the uniaxial stress axis. Compressional and shear acoustic waves were propagated perpendicular to the stress axis through various Fe-alloys. Preliminary results show a correlation between the fractional change in frequency of the acoustic waves and the external field as a function of the different stress states. An analysis of the magnetoacoustic results is in progress.

101

References

1. I. C. Noyan and J. B. Cohen, Residual Stress, Measurement, and Interpretation (Springer-Verlag, New York, 1987).

2. M. Namkung and D. Ultrata, Review of Progress in Quantitative Nondestructive Evaluation, edited by D. O. Thompson and D. E. Chimenti (Plenum Press, New York, 1988), Vol. 7B, pp. 1429-1438.

Proper Orthogonal Decomposition Based Turbulence Modeling

Mark N. Glauser
Assistant Professor
Dept. of Mechanical and Aeronautical Engineering
Clarkson University
Potsdam, NY 13699

August 6, 1991

ABSTRACT

The proper orthogonal decomposition (v. Lumley 1967) is utilized to provide one mode estimates of various turbulence quantities in the near-wall region of the turbulent boundary layer. The experimental data of Herzog (1986) and the direct numerical simulation (DNS) results of Zang (1991) provide the two-point correlation tensor. The correlation tensor is then used as the kernel in the integral eigenvalue problem from which the proper orthogonal modes are obtained. The one mode estimates of the turbulent kinetic energy, dissipation, and triple moments all exhibit the proper asymtotic behavior near the wall. As a validation test, a model for the triple moments is developed and its near-wall behavior is studied. This information can then be used to obtain an estimate of the damping function near the wall, which is then compared to known existing behavior.

Since this is an initial investigation the streamwise and spanwise dependence is suppressed and only the wall normal direction (y^+) behavior of various turbulence statistics near the wall is studied. Before examining one mode estimates of the triple moments and the dissipation (on which the model is based), various second order moments are examined. If these do not exibit the proper behavior near the wall (as discussed by Speziale et at 1990) it does not seem reasonable to expect the one mode estimate of the triple moment and dissipation to have the right behavior. Only the results obtained using the experimental data of Herzog will be discussed here since the results from the simulations of Zang exhibit similar behavior.

In all of the figures discussed the dashed line corresponds to the one mode reconstruction of the particular quantity and the solid line to the proper behavior near the wall (v. Speziale et al 1990). Figure 1 shows the one mode estimate of the turbulent kinetic energy. Note how well the slope from the one mode estimate matches the proper behavior near the wall which for the kinetic energy is y^{+2}. Figure 2 shows the one mode estimate of the Reynolds stress compared to the proper behavior which is y^{+3}. Again as was observed with the energy, the one mode estimate of the Reynolds stress is doing a remarkable job.

Since the one mode estimates of the kinetic energy and Reynolds stress clearly exhibit the right behavior it seems reasonable to inspect the behavior of the one mode estimates

of the triple moment and the dissipation near the wall. Figure 3 shows the one mode estimate of the triple moment compared to the proper behavior which is y^{+4}. Here, as was observed with the second moments, the one mode estimate is doing quite well. Figure 4 shows a one mode estimate of the dissipation. It should be a constant near the wall. In the results shown here the dissipation is seen to increase slightly but this is well within the experimental accuracy of the data of Herzog. It should be noted that the DNS results of Zang for the dissipation were constant. Figure 5 shows the one mode estimate of the model near the wall. It, as well, exhibits the proper behavior which is y^{+5}.

Since the one mode estimates of the triple moment, the model and the dissipation all exhibit the proper behavior near the wall, the wall damping function can be obtained as well. The damping function is calculated by dividing the one mode estimate of the triple moment by that of the model. This result is shown plotted in figure 6. Except for very near the wall the damping function has the right behavior which is $1/y^{+}$. This deviation near the wall is due to experimental problems in this region and not deficiences in the approach. This was verified by utilizing the simulations where the one mode estimate of the damping function was seen to have the right behavior up to the wall.

Future work will involve extending these ideas to more complex turbulent flows such as separated shear layers and various compressible flows where the proper behavior of the various quantities is not obvious. The ideas presented here then hold forth the possibility of helping us to predict more accurately these and other complicated turbulent flows.

References

Herzog, S. (1986), The Large Scale Structure in the Near-wall Region of Turbulent Boundary Layer, Ph.D. thesis, Cornell University.

Lumley, J.L. (1967), The Structure of Inhomogeneous Turbulent Flows, Atmospheric Turbulence and Radio Wave Propagation, Moscow 1967.

Speziale, C.G., Abid, R., and Anderson, E.C., (1990), A Critical Evaluation of Two-Equation Models for Near Wall Turbulence, AIAA 90-1481.

Zang, T.A. (1991), private communication.
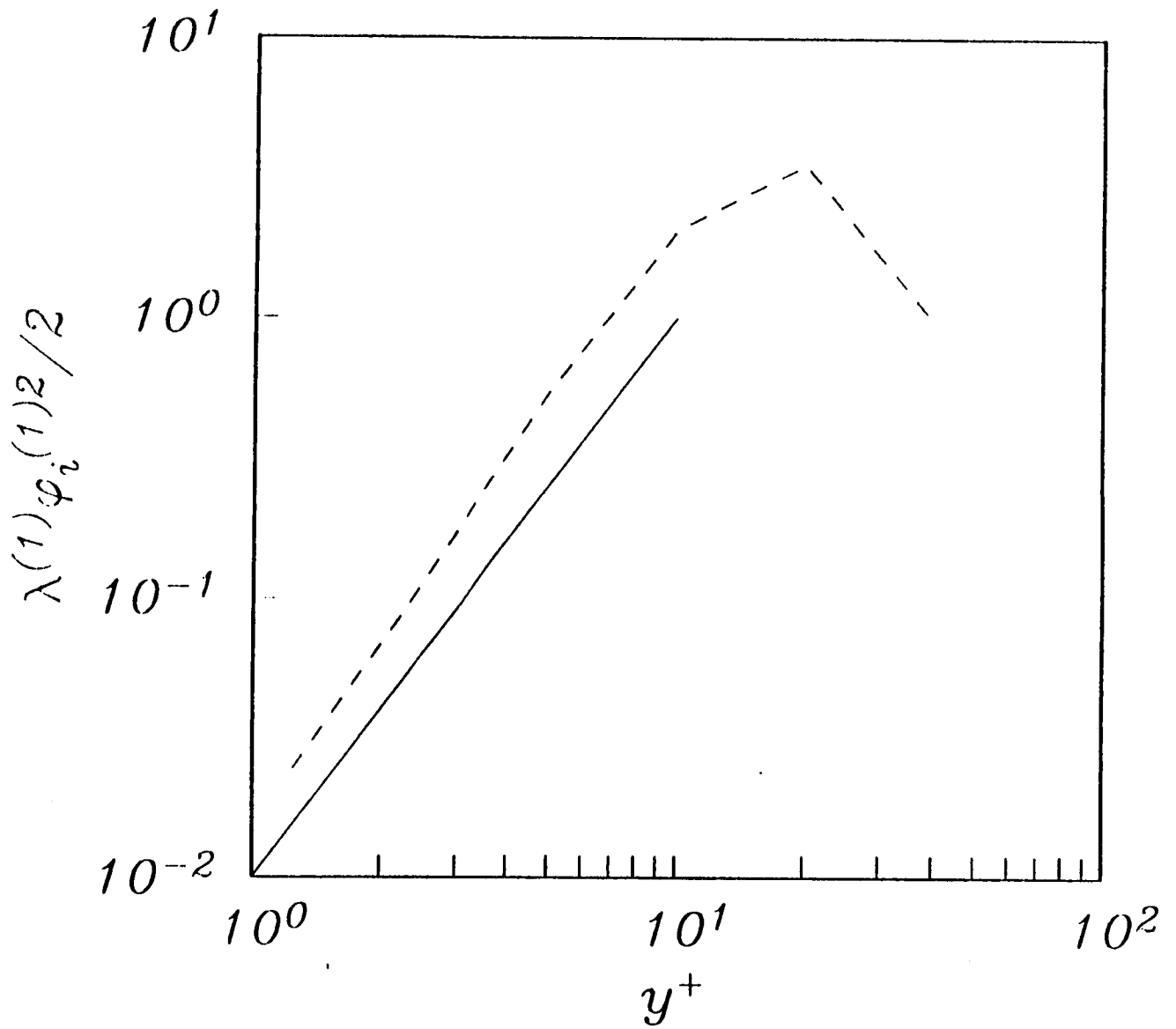
Figure 1.   One mode contribution to the turbulent kinetic energy.
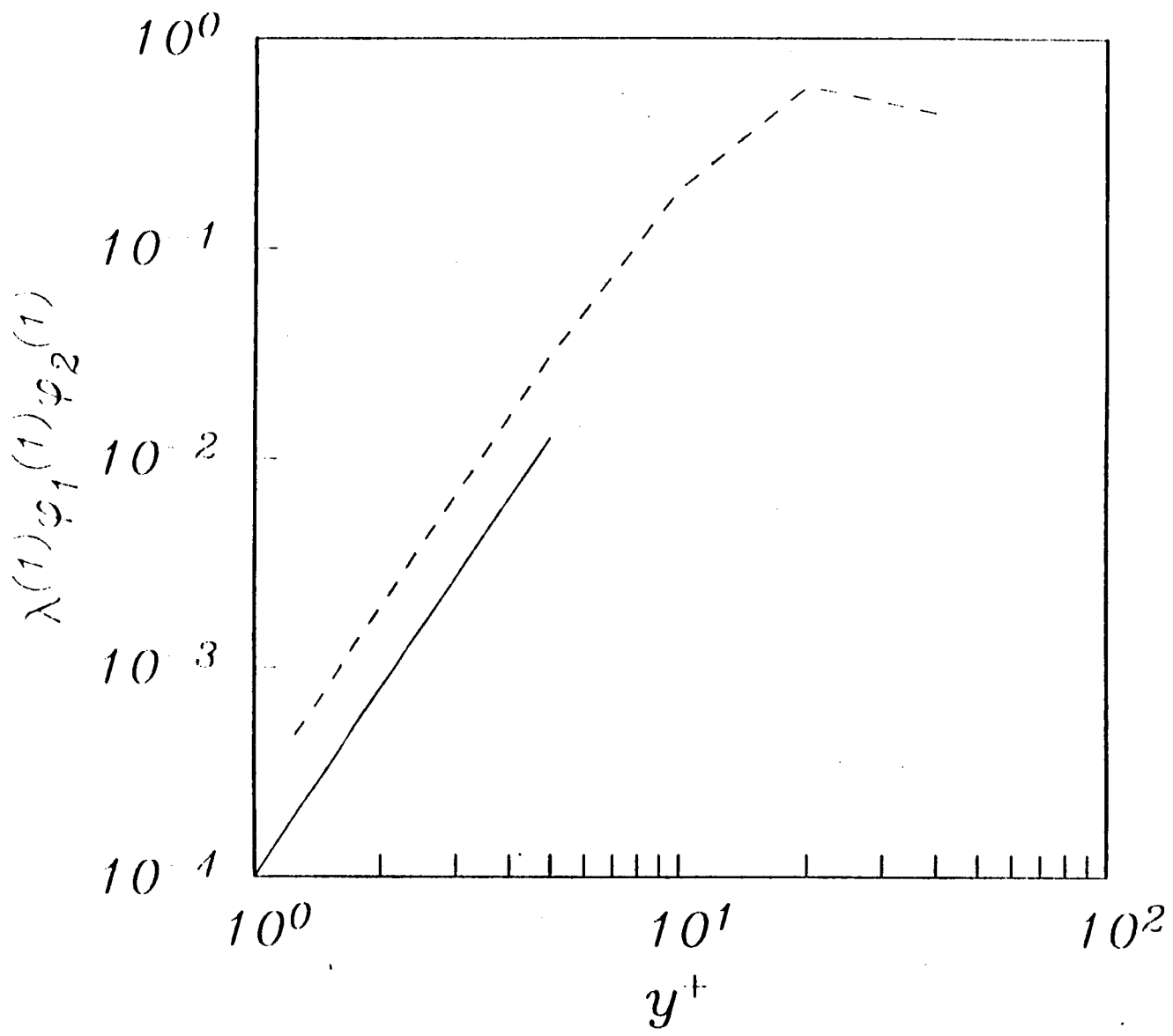
Figure 2. One mode contribution to the Reynolds stress.
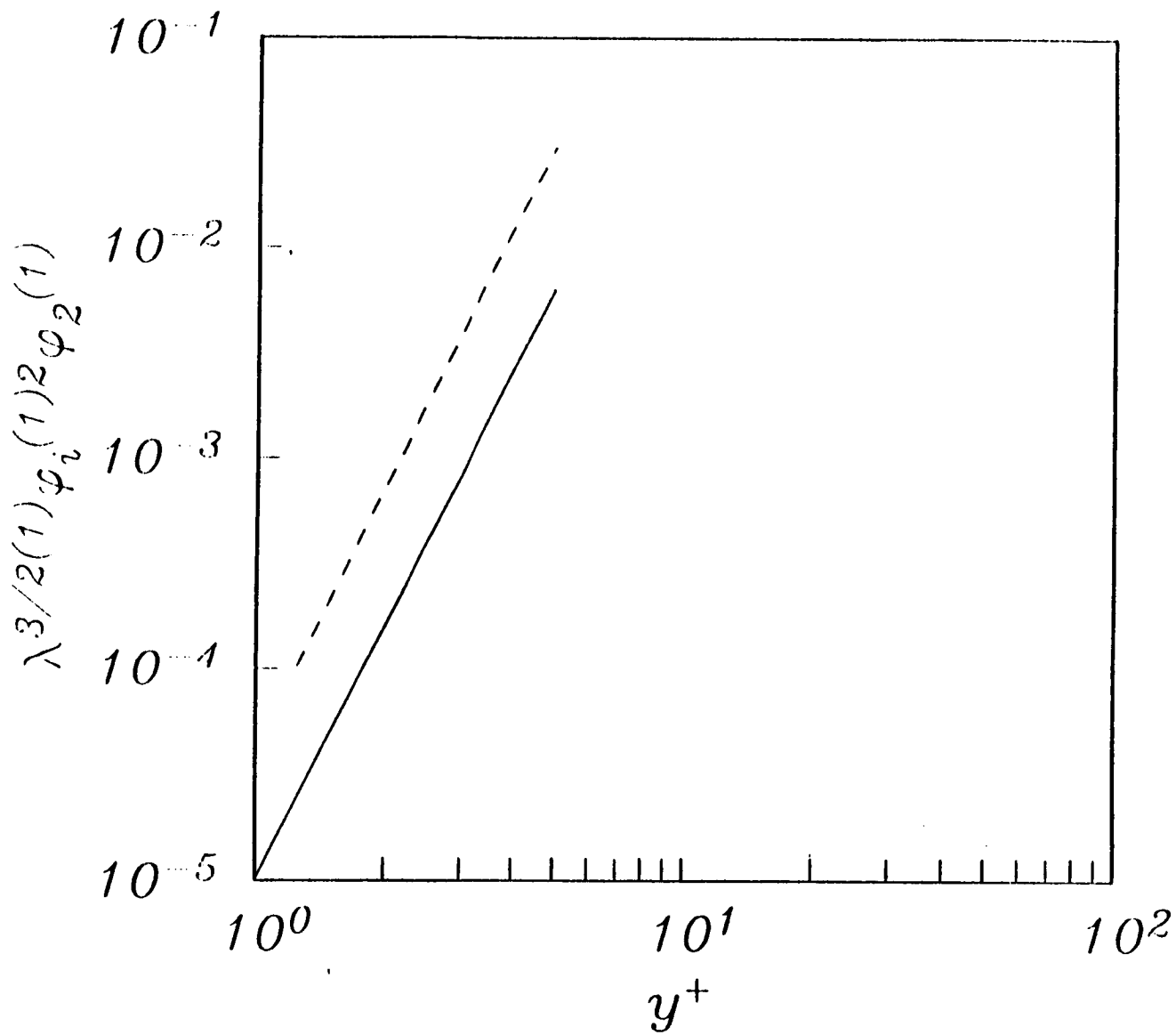
Figure 3. One mode contribution to the triple moment.
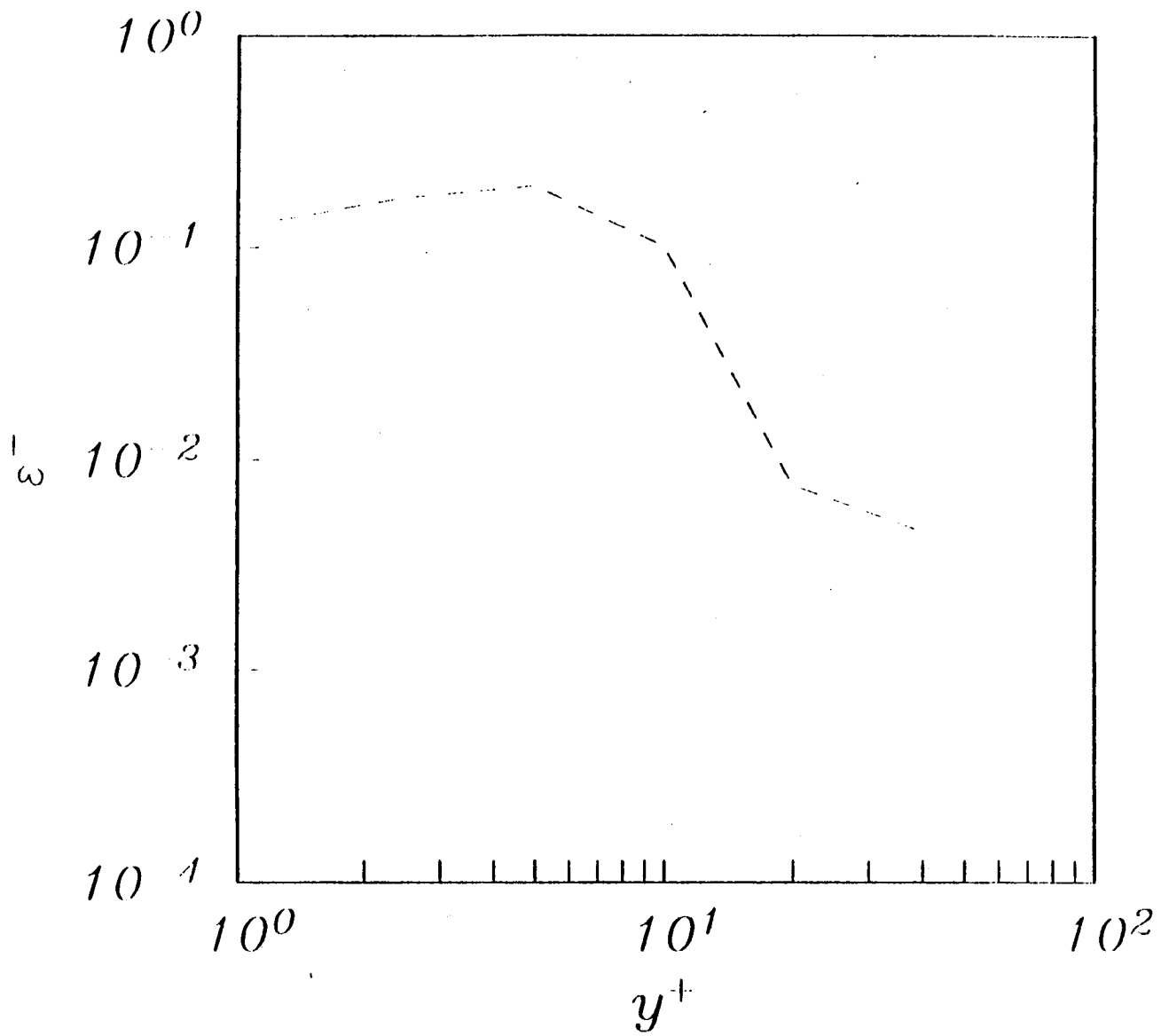
Figure 4. One mode contribution to the dissipation of kinetic energy.
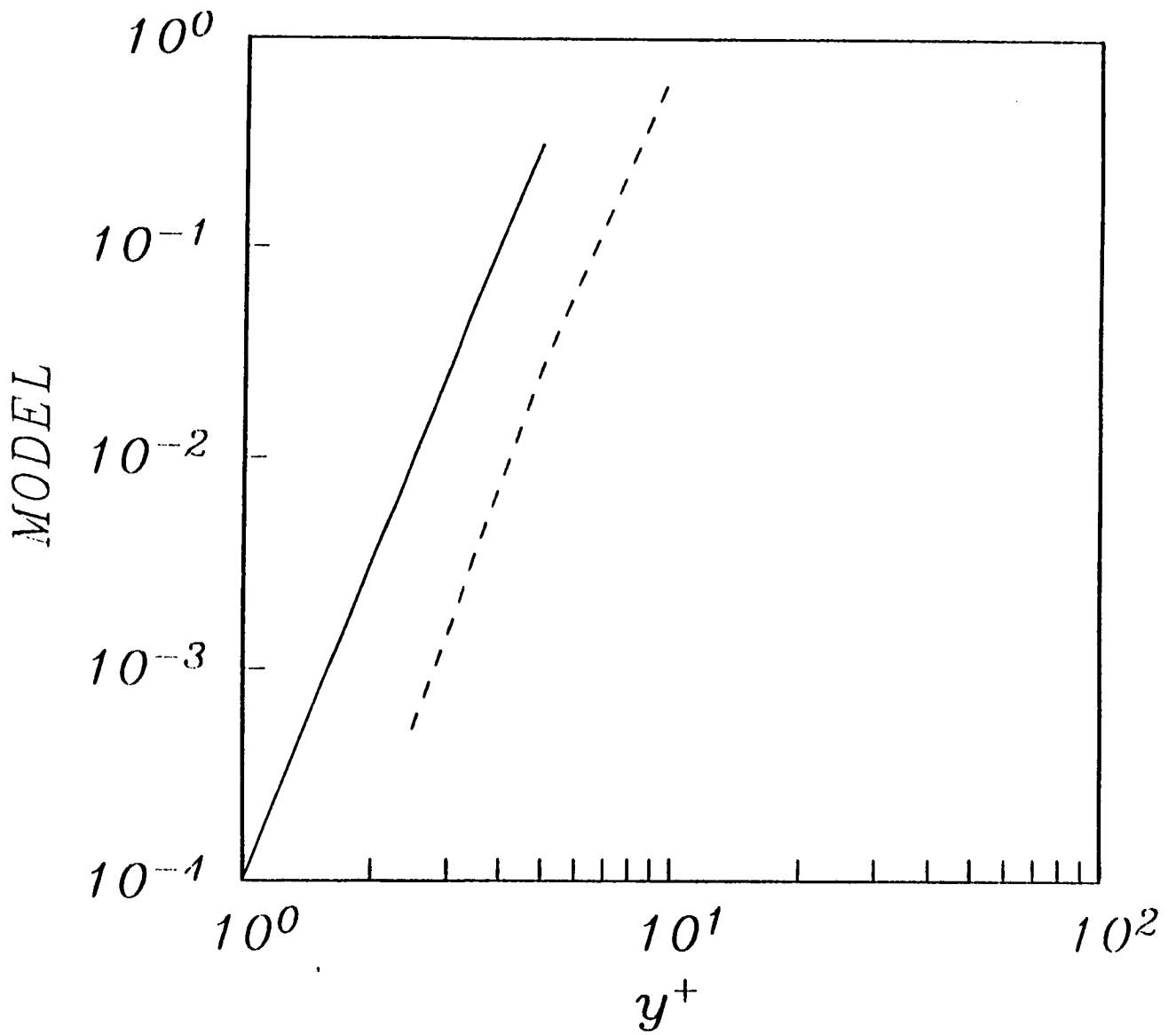
Figure 5. One mode contribution to the Model.
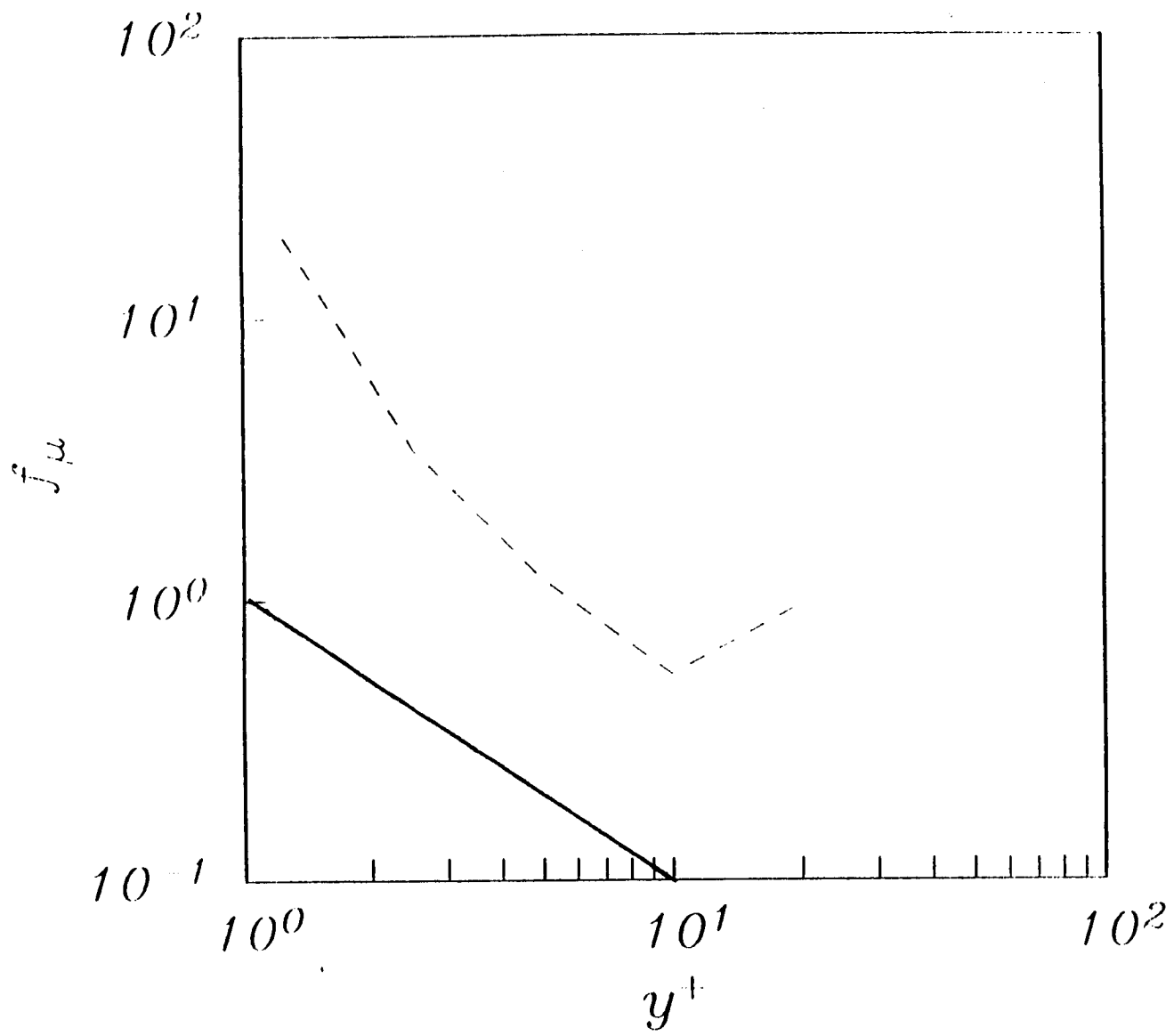
Figure 6. One mode contribution to the wall damping function.

The Role of Time and Speed in NASA's SUNLITE Program

Joseph C. Hafele
Research Professor of Physics
Christopher Newport College
Newport News, VA 23606

The SUNLITE program of NASA's Langley Research Center aims to demonstrate lower noise and better frequency stability for CW solid-state lasers in the microgravity environment of space. The program will utilize laser-diode-pumped non-planar-ring-oscillators regulated by ultra-stable high-finesse Fabry-Perot spectrometers to produce light beams with phase rate or frequency variations as low as 3 Hz. This translates into a stability ratio $\Delta f/f_o \sim 1E-15$, where Δf = FWHM Line-Width (Hz) and f_o = Line Center Frequency (Hz). Achieving this goal would increase previously achieved solid-state laser coherence lengths from 186 miles (1 light-msec, $\Delta f \sim 1$ kHz) to 62,000 miles (0.3 light-sec, $\Delta f \sim 3$ Hz). Such long coherence lengths would permit more efficient transmission of Earth-satellite and intersatellite communications. It would also permit large interferometric gravity wave antennas, and even interferometric detection of relativistic "inertial-drag" effects on low-Earth-orbit satellites.

SUNLITE will use the "period-method" to measure the phase rate and frequency stability of the lasers. The stability of a voltage, $v(t)$, that is periodic in time, t, could be measured by one of two basic methods: *i)* (FT(V)-method) Measure N voltages {v1,...,vN} at N successive times {t1,...,tN}, apply a preconditioning function $V(v)$ to the raw data, and then apply the Fourier Transform to the preconditioned data to get the spectral distribution of frequencies in $V(v)$. If $V = v$, the FT(v) gives the spectral distribution of frequencies in $v(t)$, from which the line-width Δf and line-center frequency f_o could be calculated (Fig. 1). *ii)* (P-method) Measure M successive periods {p1,...,pM} and reciprocate the periods ($f_i = 1/p_i$) to get M frequencies {f1,...,fM}. The mean frequency and Allan Variance can then be calculated from this sequence of frequencies. Notice that the P-method does not involve the Fourier Transform.

The P-method was chosen because it requires less memory space for the raw data (M < 3N), because frequencies can be analyzed on-line in real-time simply by reciprocating the periods ($f_i = 1/p_i$), and because the mean and variance of the frequencies can be calculated as fast or faster than they can be with the fastest FFT's. Furthermore, for a given signal-to-noise power ratio, the P-method requires less data and less computer time to extract the noise components. Although the P-method does require fast Time Interval Counters, the FT-method requires comparably fast Sampling Volt Meters. For either method, however, time and computer speed play a critical role.

The simple question "What time is it?" may not be as simple as it seems. According to Newton (cir. 1700 AD) "Absolute time flows equably, without relation to anything external", and a clock is only a futile attempt to measure the underlying absolute time. But according to Einstein (cir. 1900 AD) "Time is that which is indicated by a clock", and the time "here and now" cannot be separated from the clock located at the place "here" that is used to measure the time at the instant "now". The SUNLITE program is actually concerned with the question: "What is the time t_i for the i-th voltage v_i, and what is the time step, $\Delta t_i = t_{i+1} - t_i$, between the (i+1)-th voltage and the i-th voltage?" A computer clock will be used to measure these times.

Any clock consists of a periodic or oscillating element, and a memory to count the periods of the oscillator. Digital clocks contain an electronic oscillator and a counter/register which serves as the memory (Fig. 2). The performance of a clock can be determined by comparing it with another clock. Most computers contain two independent clocks, a "system clock" that drives the microprocessor, and a "24-hour time and date clock" that stays on all the time. A source code in BASIC that can be used to study the performance of the system clock "TIMER" is listed under Prog. 1.

The speed of a computer can be expressed in IOPS (Integer Operations Per Second) or in FLOPS (FLoating point Operations Per Second). A source code in BASIC to measure the speed for the integer operation K=K+1 is listed under Prog. 2. This program, in both the uncompiled form (interpreter) and in the compiled form (exe code), was used to measure the speed of various PC's. For 6 different PC's, IOPS ranged between 100 and 7000 K-counts per second. Mean values for 3 personal computers are shown in Fig. 3. Clearly, computer speed depends both on the computer model (hardware) and on the programming (software).

The higher the frequency of the oscillator in a clock, the better is the resolution or time interval between "ticks" of the clock. As important as resolution is uniformity in the time interval between successive ticks. Figure 4 is a graph of the K-counts of Prog. 2 for 260 seconds on a COMPAQ PORTABLEIII laptop computer. The "jitter" up-and-down from the general trend is due to phase noise, while the large step down near 70 seconds is caused by "digit rollover" in the reference clock (Fig.2). In this case, digit rollover caused more variance than did jitter. A more severe case of digit rollover is shown in Fig. 5. In this case, rollover caused a clearly visible "staircase" effect in the K-count.

To minimize the noise components from digitization and rollover, and to maximize memory reliability, SUNLITE will use a nonvolatile 32-bit memory to store the period data.

Fig. 1. Various functions V(v) which could be applied to the periodic voltage v(t) before applying the Fourier Transform.

FT(V)	Precond.Func.	Comment
FT(ω)	V = v	Identity Function (raw data)
FT(z)	V = (v-<v>)/σ	Normalized to Standard Deviation
FT(y)	V = (v-<v>)/<v>	Normalized to Mean
FT(power)	V = v^2	Power Spectrum
FT(τ)	V = v(t)v(t-τ)	Autocorrelation Function

Fig. 2. Schematic diagram for a 24-hour digital clock. Output of the divider has a frequency of 1 Hz. Digit rollover occurs between successive stages of the memory registers.
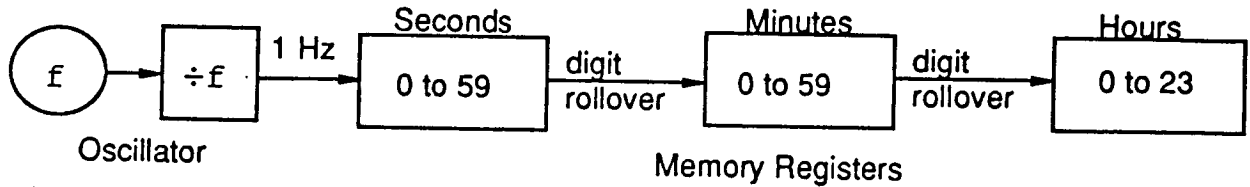
Fig. 3. Average values for the counter operation K=K+1 for various personal computers. The IOPS program listed below (Prog. 2) was used in each case. It was run by means of the GWBASIC interpreter and the QUICKBASIC compiler.

Software	IBM PC AT	MEGA PC AT	COMPAQ PORTIII
GWBASIC(interp.)	500	672	?
QUICKBASIC(comp.)	1292	1720	2512*

(* A NORTHGATE PC (w/64k nonvolatile cache memory) produced a K-count greater than 7000.)

Fig. 4. Time structure in the IOPS K-count of Prog. 2 for a COMPAQ PORTABLEIII laptop PC. This structure is similar to every other case studied. Total elapsed time (x-axis) = 250 seconds. Minimum K-count = 2501. Maximum K-count = 2529. Mean K-count = 2512.482.

Timing Loop Count. Elapsed Time: TIMER 260.89 TIMES 00:04:21
MaxCount: 2529 MinCount: 2501 Mean: 2512.481927718843

113
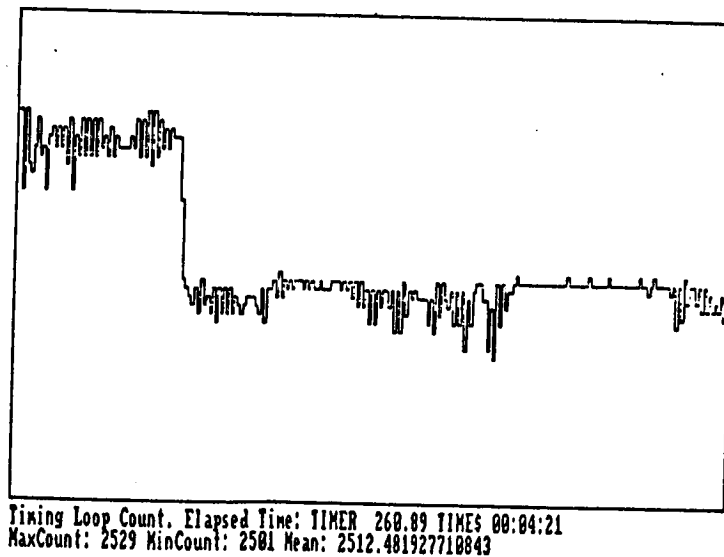
Fig. 5. Time structure in the K-count showing an extreme case for digit rollover. This case was measured with an EPSON LQ 510 laptop PC. Elapsed time = 260 seconds. Mean K-count = 626.488. Minimum K-count = 615. Maximum K-count = 630.


```
62486764200.000 = Start        Seconds(A0)        Stop = 62486764460.950
StartDATE$(TIME$Set 01-01-1980:00:00:00) MuaXvalue= 249 MeanXvalue=  626.4879
MinXvalue =   615    MaxXvalue =   630    ElapsedTime (seconds) =   260.950
```
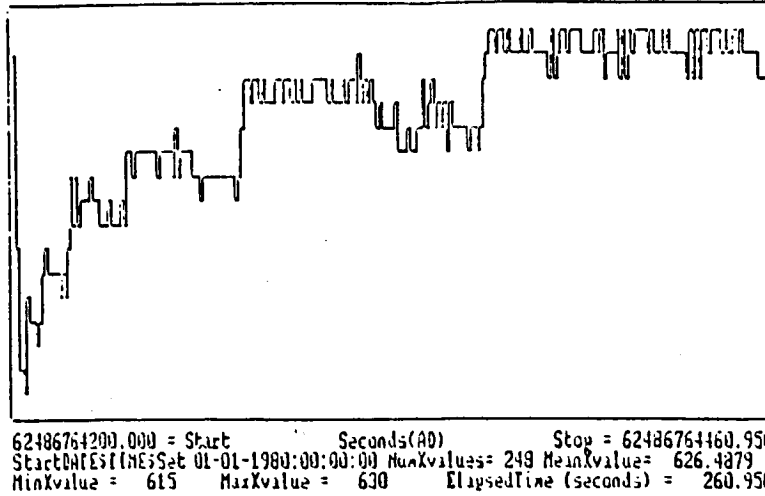
Prog. 1. Source code in BASIC to study the performance of the system clock TIMER. After setting the 24-hour clock to zero(line 20), the system clock is synchronized to it (line 30). Successive values for TIMER are recorded (line 30) in the array T(I).

```
10    CLEAR:DEFINT I-K:OPTION BASE 1:DIM T(1000)
20    TIME$="0:0:0":T=TIMER
30  ' WHILE TIMER=T:WEND
30 FOR I=1 TO 1000:T(I)=TIMER:NEXT I
40    FOR J=1 TO 1000
50      PRINT J,T(J)
60    NEXT J
70    END
```

Prog. 2. Source code in BASIC to measure a computer's speed. Line 40 counts the number of K=K+1 operations the computer can execute in successive 1-second time intervals IOPS. FLOPS could be measured by substituting X=X+1 in the WHILE/WEND loop (line 40).

```
10    CLEAR:DEFINT C,I-K:OPTION BASE 1:DIM C(100)
20    TIME$="0:0:0"
30    FOR I=1 TO 100: K=0: T=TIMER+1
40      WHILE TIMER<T: K=K+1: WEND
50      C(I)=K
60    NEXT I
70    FOR J=1 TO 100:PRINT J,C(J):NEXT J
80    END
```

114

Formulation of the Linear Model from the Nonlinear Simulation for the F18 HARV

Charles E. Hall, Jr.

Assistant Professor
Mechanical and Aerospace Engineering
North Carolina State University
Raleigh, North Carolina 27695

The F18 HARV is a modified F18 aircraft which is capable of flying in the post-stall regime in order to achieve superagility. The onset of aerodynamic stall, and continued into the post-stall region, is characterized by nonlinearities in the aerodynamic coefficients. These aerodynamic coefficients are not expressed as analytic functions, but rather in the form of tabular data. The nonlinearities in the aerodynamic coefficients yield a nonlinear model of the aircraft's dynamics. Nonlinear system theory has made many advances, but this area is not sufficiently developed to allow its application to this problem, as many of the theorems are existance theorems and that the systems are composed of analytic functions. Thus, the feedback matrices and the state estimators are obtained from linear system theory techniques. It is important, in order to obtain the correct feedback matrices and state estimators, that the linear description of the nonlinear flight dynamics be as accurate as possible.

The nonlinear simulation is run under the Advanced Continuous Simulation Language (ACSL). The ACSL simulation uses FORTRAN subroutines to interface to the look-up tables for the aerodynamic data. ACSL has commands to form the linear representation for the system. This is a two step process. The first step is to trim the system, which is identical to trimming the aircraft. This involves calculating the trim input, $\mathbf{u}^*$, for a given trim state, $\mathbf{x}^*$, such that the derivatives of the state vector, $\dot{\mathbf{x}}$, are zero. The state space for the simulation is $\mathbf{x} = (u, w, q, \theta)^T$ The second step is to calculate the Jacobians of the state transisiton map, $\mathbf{f}(\mathbf{x})$ with respect to $\mathbf{x}$ at $\mathbf{x}^*$, and the input map, $\mathbf{g}(\mathbf{x}, \mathbf{u})$ with respect to $\mathbf{u}$ at $\mathbf{x}^*$ and $\mathbf{u}^*$. For analytic functions this is accomplished by calculating the partial derivatives of the functions, but since analytic functions do not exist, and ACSL can not perform symbolic calculations, the Jacobians are formed by numeric differentiation. ACSL uses the central difference method to perform the numeric differentiation.

$$\frac{\partial f_i(\mathbf{x})}{\partial x_j}\Big|_{\mathbf{x}=\mathbf{x}^*} = \frac{f_i(\mathbf{x}^* + \delta_j \hat{\mathbf{e}}_j) - f_i(\mathbf{x}^* - \delta_j \hat{\mathbf{e}}_j)}{2\delta_j} \tag{1}$$

Where the perturbation vector is defined as $\delta = (U\cos(\alpha)/100, U\sin(\alpha)/100, 5°/s, 2°)^T$. This is used to calculate the A matrix for the linear representation, $\dot{\tilde{\mathbf{x}}} = A\tilde{\mathbf{x}} + B\tilde{\mathbf{u}}$ with $\tilde{\mathbf{x}} = \mathbf{x} - \mathbf{x}^*$ and $\tilde{\mathbf{u}} = \mathbf{u} - \mathbf{u}^*$. Similarly the B matrix is calculated by the numerical differentiation of $\mathbf{g}(\cdot)$. The result of this is that the A and B matrices are not only functions of $\mathbf{x}^*$ and $\mathbf{u}^*$, but also of δ.

The state transition map, $\mathbf{f}(\mathbf{x})$, and the input map $\mathbf{g}(\mathbf{x}, \mathbf{u})$, are derived from the equations of motion for the system. A predominant part of these equations are based on the aerodynamic forces and moments. These forces and moments are calculated via the standard methods by using a nondimensional coefficient. These coefficients are the results of wind tunnel testing and they are stored in data files. The data points are generally functions of two variables, α and Mach number. Occasionally, a third variable is added such as control surface deflection. For this work, emphasis was placed on the α-Mach space variables. There are different sets of α vaules and Mach number values at which the coefficients are known. For example, C_{m_0} are known for $\alpha \in \{-12., -4., -2., 0., \ldots\}$ and Mach number $\in \{0.2, 0.6, 0.8, 0.85, \ldots\}$ but C_{m_q} are known for $\alpha \in \{-4., 0., 4., \ldots\}$ and Mach number $\in \{0.2, 0.6, 0.8, 0.9, \ldots\}$. To calculate the particular coefficient, with α and Mach number either equal or not equal to values in the respective sets, a second order Lagrange interpolation is performed. If the desired α and M are both equal to elements in the respective sets, then the Lagrange interpolation yields the coefficient from the table. This is accomplished first by bracketting

the α and Mach number, M, between availible α_i and M_j, such that $\alpha_i < \alpha \leq \alpha_{i+1}$ and $M_j < M \leq M_{j+1}$. Letting $\Delta\alpha = \alpha_{i+1} - \alpha_i$ and $\Delta M = M_{j+1} - M_j$, and $C_{i,j}$ be the coefficient C at α_i and M_j, the following expression yeilds $C(\alpha, M)$.

$$C(\alpha, M) = \frac{C_{i,j}(\alpha_{i+1} - \alpha)(M_{j+1} - M) + C_{i,j+1}(\alpha_{i+1} - \alpha)(M - M_j)}{\Delta\alpha\Delta M} +$$

$$\frac{C_{i+1,j}(\alpha - \alpha_i)(M_{j+1} - M) + C_{i+1,j+1}(\alpha - \alpha_i)(M - M_j)}{\Delta\alpha\Delta M} \tag{2}$$

It can be seen from the form of Eq. 2 that for a constant α or M, the plot for the resulting one variable function $C(\cdot)$ is a series of connected straight line segments. Calculation of the various aerodynamic coefficients, not including coefficients in $\dot{\alpha}$, and summation into the total force and moment calculation are perform by the FORTRAN subroutine SFAERRF. SFAERRF takes into account the various sets of α and M that are availible.

When the system is linearized about some trim point and the eigenvalues are compared to those of the DMS simulation, some differences arise. The eigenvalues also exhibited a dependence on δ. With the need for accurate linear representations for the system, the following work addressed the problem of how to minimize the differences of the two systems.

Due to the dependence on the perturbation size, δ, in the numerical calculation of the Jacobian, elimination of the numerical differentiation would address this problem and possibly assist in minimizing the differences between the two models. The concept was to express the tabular data in a known functional form, that could have its derivative calculated analytically by a FORTRAN subroutine. Various possible functional forms were examined, such as the fourth order Lagrange, full order Lagrange, and quadratic, cubic, quartic splines. These functions were C^1 or greater over the entire α-Mach space, being at least C^1 on the boundaries of different α-Mach cells. The full order Lagrange interpolation and the various splines produced oscillations that were not desirable. The fourth order Lagrange interpolation required a data window, which developed discontinuities in the derivatives at the window boundaries. Applying these techniques to the many data tables during each iteration would be computer intensive, and discontinuities would still exist in the derivatives on the cell boundaries.

An intermediate approach has been followed. Numerical differentiation has been retained with a larger perturbation step size, and the data space for "sparcely" distributed data has been augmented. The larger perturbation step size is opposite to the expected limit in calculating a derivative. The use of the increased perturbation size has the effect of decreasing the magnitude of the second derivative of the particular coefficient. The perturbation step size has been set equal to one half of the minimum parameter step size, in this study $\delta_\alpha = 1°$. The α perturbation which is useful for operations with the aerodynamic data space, but α is not a state space variable but it is related to the state variable w. A function $\delta_w = f(\delta_\alpha)$ was calculated and included in the formulation of the linear model. The augmenting of the data space also provides the for the minimization of the second derivative. The data space is augmented by calculating intermediate values for the particular coefficient by using a fourth order Lagrange interpolation. For example for a function of one variable defined at $\alpha = 0, 4, 8, 12, \ldots$, a value of the function can be estimated at $\alpha = 2, 6, 10, \ldots$ by using the nearest four data points.

These techniques have been applied in a staged way to the ACSL simulation. The modified perturbation step size was applied to the linearization of the system, as were the unmodified perturbation step size. Then the data for C_{m_q} was augmented by using the fourth order Lagrange interpolation for intermediate data points in α. Nine different α values were set, and the longitudinal eigenvalues were calculated by each of the three methods at each α. The differences between the various longitudinal eigenvalues were small, except for two cases. The locus of the eigenvalues, as a function of α was generated as a result of this work.

Preliminary Investigations Into Candidate Materials and Accelerated Test Methodology for the High Speed Civilian Transport

by

Jeffrey A. Hawk
Assistant Professor
Department of Metallurgical & Materials Engineering
University of Alabama
Tuscaloosa, Alabama 35487

One of the major issues which must be addressed in programs related to the development of future high-speed aircraft is candidate materials for airframe components. Aerodynamic heating effects at cruise speeds of between mach 2.0 and 2.4 dictate that skin temperatures during service will typically be in the vicinity of 225°F to 370°F. At the present time, the most compatible alloys at the high end temperatures are based on the Ti-6Al-4V system. Near the lower end of the temperature range, i.e., mach 2.0, considerable experience has been gained from the materials development program for the Concord. Aluminum alloy RR58 (i.e., 2618) was used as the main airframe material. The specific properties and fabrication technology related to these alloys are well established, such that they may readily be adapted to such applications. However, there are disadvantages associated with the use of the Ti-6-4 alloy which are related to material costs and alloy density. Recently, these factors have generated a considerable driving force for research directed at alternative alloy systems. The prime candidates in this category are elevated temperature aluminum alloys which may be considerably cheaper in terms of raw material costs and offer potential for significant weight savings.

Conventional, age-hardenable aluminum alloys exhibit a significant diminution of mechanical properties at temperatures approaching 300°F because the fine strengthening precipitates coarsen rapidly and lose their coherency. This has encouraged the use of novel powder-metallurgy (PM) techniques such as rapid solidification processing (RSP) to extend the solid solubility of certain alloying additions (e.g., of transition metals and rare earths), refine the microstructure, reduce chemical segregation and morphological changes of the eutectic or primary phase, and allow the formation of metastable phases. During powder manufacture and processing to bulk form, these alloys develop high volume fractions of thermally stable, non-shearable precipitates. This approach offers a means of producing uniform dispersions of fine intermetallic phases which resist coarsening and provide significant strength at temperatures up to 650°F.

Current commercial ingot-metallurgy (IM) techniques are not capable at present of producing the fineness and homogeneity of dispersoids afforded by PM techniques. This is due to the limit on the maximum achievable cooling rate during solidification which ultimately determines the size and distribution of the precipitates. However, one of the major problems that has been encountered using PM consolidation and processing techniques to produce components from aluminum alloys has been the tendency of powders to form tenacious oxide films. These layers can restrict, or inhibit, the fabrication of material of good metallurgical integrity following

current commercial consolidation techniques. Therefore, in order for elevated temperature aluminum alloys to become a viable alternative, it is necessary to demonstrate that the specific mechanical properties of consolidated material in the temperature range of 225°F to 450°F are comparable to or better than those of commercial titanium alloys.

Since the airframe will see a wide range of temperatures, a number of alloy systems must be investigated. These include conventional IM alloys similar to 2219 but with Ag additions, Al-Li alloys (primarily 8090 and Weldalite), PM alloys based on Fe additions (e.g., Al-Fe-Ce and Al-Fe-V-Si), and various aluminum metal matrix composites which use SiC as the reinforcing phase. The mechanical properties of each alloy must be carefully explored to insure adequate performance at room and elevated temperatures. Therefore, the first part of this research program has focused on accumulating a data base of available mechanical properties (i.e., tensile, fracture toughness, fatigue, fatigue crack propagation, creep and creep rupture) for the various candidate alloys. This process is necessarily ongoing, as many of the candidate alloys are still under development. Thus, this portion of the research is essentially open ended.

The specification of candidate aluminum alloys and the collation of their mechanical properties, however, addresses only a minor portion of the selection procedure. Once candidate materials have been identified, they must be thoroughly tested under static and cyclic conditions in the range of service temperatures and stresses. Of primary interest are the reaction kinetics of the candidate alloys as they pertain to creep, creep rupture, and microstructural stability. Generally speaking, information on these particular properties for the candidate alloys is generally inadequate for design purposes. In order to facilitate timely determination of the aforementioned properties for creep and creep rupture design, an acceleration of the test methodology is needed. The acquisition of information on accelerated creep testing methodology forms the second part of this research program.

Creep tests and microstructural stability investigations, by their very nature, are long term propositions. The major thrust in this area is to predict long time behavior, i.e., component lifetime, from short term creep rupture tests. The duration of the test can be shortened by increasing the stress and/or the temperature of the test. Care must be taken, however, to insure that microstructural changes do not occur as a result of increases in temperature/stress as this would invalidate lifetime predictions. A review of creep rupture testing methodology and lifetime extrapolation techniques has been initiated in order to better understand the number and types of tests needed to produce adequate creep and creep rupture design information. Normal extrapolation techniques (e.g., Larson-Miller, Manson-Haferd, etc.) are valid only if creep rupture information is available for at least 1/3 of the projected component lifetime. Since the HSCT has a minimum design lifetime of 60,000 hours, creep rupture tests must be performed for times in excess of 20,000 hours. One accelerated creep technique, the θ-projection concept, is an attractive alternative to conventional creep rupture testing. The θ-projection method reduces the total number of creep tests needed to generate design information.

Work to date has focused on three areas: (1) property information on candidate alloys (continuation of work initiated by S. Hales, AS&M); creep and creep rupture testing, i.e., accelerated test method assessment; and (3) microstructural stability considerations for high temperature applications. A white paper on each topic will be the result of the summer research.

A NUMERICAL METHOD FOR
UNSTEADY AERODYNAMICS VIA ACOUSTICS

STEVE HODGE[*]

Abstract. Formal solutions to the wave equation may be conveniently described within the framework of generalized function theory. Here generalized function theory gives a formulation and formal solution of a wave equation describing oscillation of a flat plate from which a numerical method may be derived.

Summary. Wave equations describe vibrations and spatial perturbations ("waves") of physical terms away from certain ambient terms. In acoustics vibration terms are generally described as "sound" though they are of a wider range than audible sound. In general, think of wave equations as describing any moderately small variation in space or time. Acoustics and aeronautics parallel in that the governing equations of linearized compressible aerodynamics and acoustics are the same. The linear acoustic wave equation for the velocity potential $\phi(x,t)$ is

$$(1) \qquad \frac{\partial^2 \phi}{\partial t^2} - \frac{1}{c^2}\frac{\partial^2 \phi}{\partial x^2} = 0$$

where c is the "speed of sound." The nature and scope of the infinite possible solutions to (1) vary enormously. Usually a particular physical situation or other specifies "initial conditions" or "boundary conditions" which narrow the admissible solutions down to one. However, there is an enormous gulf between knowing that a unique solution is there and writing it down with a particular equation or function from which to calculate. There are many ingenious techniques for bridging this gulf. In particular, sound generated from physical situations which involve moving objects may be described by wave equations with "generalized derivatives" and have formal solutions which involve integrals of generalized functions. Generalized derivatives are a useful formal method roughly equivalent to a "weak" formulation [1], but with the benefit of derivative formalism in which the work of integration by parts is automatically incorporated. The generalized functions and derivatives are useful in describing discontinuous phenomena such as the intrusion of a wing in free space or a "shock" in flow quantities on the surface of the wing [2].

In thin airfoil theory the boundary conditions are specified on the mean chord surface [3]. In terms of generalized derivatives and linearized momentum equation $p = -\rho_0 \frac{\partial \phi}{\partial t}$, the wave equation becomes

$$(2) \qquad \frac{\bar{\partial}^2 p}{\partial t^2} - \frac{1}{c^2}\frac{\bar{\partial}^2 p}{\partial x^2} = \frac{\bar{\partial}}{\partial t}\left[\rho_0 v_n |\nabla f_{mc}|\Delta(f_{mc})\right] + \bar{\nabla}\cdot\left[\Delta p \nabla K \delta(K)\right]$$

where f_{mc} is the mean chord surface, K is the mean chord surface and wake, v_n is the normal velocity due to thickness and the bars over the derivatives denote generalized derivatives [4]. This equation is similar to the Ffowcs Williams-Hawkings (FW-K)

$$(3) \qquad \frac{\bar{\partial}^2 p}{\partial t^2} - \frac{1}{c^2}\frac{\bar{\partial}^2 p}{\partial x^2} = \frac{\bar{\partial}}{\partial t}\left[\rho_0 v_n |\nabla f|\Delta(f)\right] + \bar{\nabla}\cdot\left[p\nabla f \delta(f)\right]$$

which is a formal restatement of the equations of continuity and momentum [5]. Since pressure is continuous across the wake, this may be rewritten

$$(4) \qquad \frac{\partial^2 p}{\partial t^2} - \frac{1}{c^2}\frac{\partial^2 p}{\partial x^2} = \frac{\partial}{\partial t}\left[\rho_0 v_n |\nabla f_{mc}|\Delta(f_{mc})\right] + \nabla \cdot \left[\Delta p \nabla f_{mc}\delta(f_{mc})\right].$$

Equation (3) has formal solution

$$(5) 4\pi p(x,t) = \frac{1}{c}\frac{\partial}{\partial t}\int_{f_{mc}=0}\left(\frac{\rho_0 c v_n + \Delta p\cos(\theta)}{r|1 - M_r|}\right)_{\tau^*} dS + \int_{f_{mc}=0}\left(\frac{\Delta p\cos(\theta)}{r^2|1 - M_r|}\right)_{\tau^*} dS$$

Here τ^* is the emission time of a signal received by the observer at time t. Integration of (5) with respect to t and the identity $p = -\rho_0\frac{\partial}{\partial t}\phi$ leaves

$$4\pi\rho_0\phi(x,t) = -\frac{1}{c}\int_{f_{mc}=0}\left(\frac{\rho_0 c v_n + \Delta p\cos(\theta)}{r|1 - M_r|}\right)_{\tau^*} dS + \int_{-\infty}^{t}\int_{f_{mc}=0}\left(\frac{\Delta p\cos(\theta)}{r^2|1 - M_r|}\right)_{\tau^{*\prime}} dSdt'.$$
$$(6)$$

Here $\tau^{*\prime}$ is the emission time of the signal received at time t'.

Generally (6) is separated into two terms. We are interested in the so called "lifting" terms (corresponding to aerodynamic lift), namely:

$$(7) 4\pi\rho_0\phi(x,t) = -\frac{1}{c}\int_{f_{mc}=0}\left(\frac{\Delta p\cos(\theta)}{r|1 - M_r|}\right)_{\tau^*} dS + \int_{-\infty}^{t}\int_{f_{mc}=0}\left(\frac{\Delta p\cos(\theta)}{r^2|1 - M_r|}\right)_{\tau^{*\prime}} dSdt'.$$

Refer figure 1 for the following. We assume that the mean chord surface is a flat plate moving with uniform velocity in direction shown. Assume that the pressure is piecewise of the form $\Delta p e^{i\Gamma t}$ over individual surface panels of the plate. This corresponds to an unsteady aerodynamic loading. On individual panels P_{ij} in the coordinate system shown in figure 1 the individual integrals restated in terms of normal velocity reduce to

$$4\pi v_n(x,t) = 1/c\frac{\partial}{\partial x_3}\int_{P_{ij}}\left(\frac{\Delta p\cos(\theta)}{r|1 - M_r|}\right)_{\tau^*} dS + \frac{\partial}{\partial x_3}\int_{-\infty}^{t}\int_{P_{ij}}\left(\frac{\Delta p\cos(\theta)}{r^2|1 - M_r|}\right)_{\tau^{*\prime}} dSdt'$$
$$(8)$$

where v_n is the velocity in the normal direction and M_r is the Mach number in the r-direction. Since we are interested in aerodynamic lifting, the observer point will be on the lifting surface and consequently (8) will be singular on panel on which the observer lies. Although divergent, a physically correct solution may be extracted when the integral is considered in the Cauchy principle value sense with corresponding "Hadamard finite part" [6]. After a good choice of coordinate systems, reducing $\frac{\partial}{\partial x_3}$ to a limit definition, using a principle value, and alot of summertime work, the integrals remarkably reduce to $\lim_{h\to 0+}\frac{\partial}{\partial h}(I_1 + I_2)$ where

$$(9) \qquad I_1 = h/ce^{i\Gamma t}\int_{r_1}^{r_2}\frac{e^{-i\Gamma r/c}}{r}\left\{sin^{-1}\left[\frac{y_2(r)}{\sqrt{r^2 - h^2}}\right] - sin^{-1}\left[\frac{y_1(r)}{\sqrt{r^2 - h^2}}\right]\right\} dr$$

and

$$(10) I_2 = h\int_{-\infty}^{t}e^{i\Gamma t'}\int_{r_1}^{r_2}\frac{e^{-i\Gamma r/c}}{r^2}\left\{sin^{-1}\left[\frac{y_2(r)}{\sqrt{r^2 - h^2}}\right] - sin^{-1}\left[\frac{y_1(r)}{\sqrt{r^2 - h^2}}\right]\right\} drdt'$$

(the endpoints r_i are the range of r over panel P_{ij} and quantities in the 2nd integral y_i and r depend on t'). We are now ready to consider the global effect of simultaneous

observers in each panel. This leaves a system of algebraic equations which may be solved for unknowns Δp. At present a numerical method for this system is being formed with the aid of Mathematica.

REFERENCES

[1] G.B. Whitham(1974) *Linear and Nonlinear Waves.* Wiley Interscience, New York.

[2] R. Kanwal(1983) *Generalized Functions: Theory and Technique.* Academic Press, New York.

[3] H. Ashley and M. Landahl(1965) *Aerodynamics of Wings and Bodies.* Addison Wesley, Reading, Massachesetts.

[4] R.L. Millikan(1984) *A New Lifting Surface Method: An Acoustic Approach.* NASA CR 4329 Vol 1.

[5] M. Goldstein(1971) *Aeroacoustics.* NASA SP-346.

[6] A.H. Zemanian(1965) *Distribution Theory and Transform Analysis.* McGraw Hill, New York.
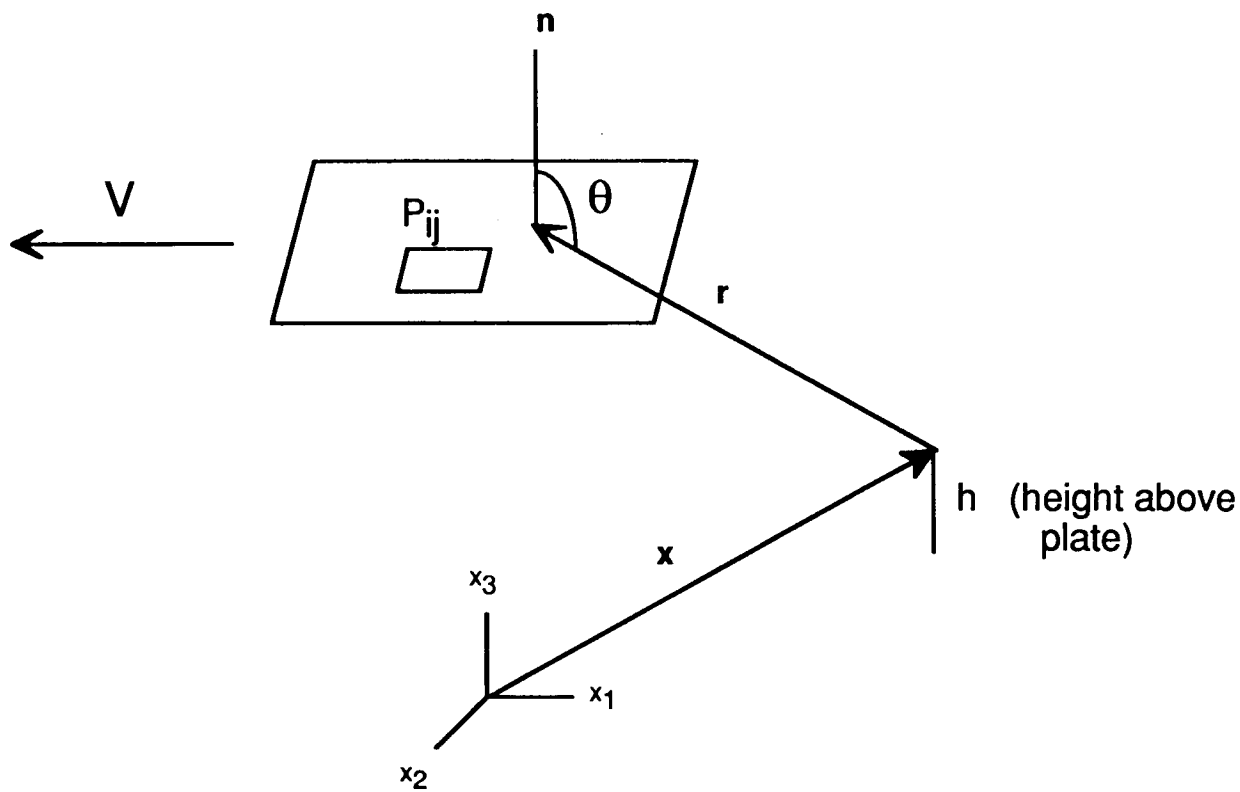
Figure 1

MANPOWER AND PROJECT PLANNING

by

Professor David W. Johnson
Business and Education Department
Saint. Paul's Collage
Lawrenceville, Virginia 23868

N92-13844

Client Organization

The client for this project is the Facilities Engineering Division (FENGD) within the Systems Engineering and Operations Directorate of the Langley Research Center, NASA, Hampton, Virginia. The Division's primary responsibility is to manage projects assigned to it, usually for the construction or rehabilitation of facilities and ensure that the project meets its technical objectives on schedule and within budget. In the the period of June 1, 1990 to May 31, 1991, FENGD managed 120 construction projects with a total estimated construction cost of $357.7 million.

The complexity of this management environment can be judged in part by the number and size of these projects further multiplied by the fact that these are multiple year, multiple phase projects. For instance, one project---Modifications to the 8 Foot High Temperature Tunnel has already spanned six fiscal years, while another, Refurbishment of the Hypersonic Facilities Complex, entails work on five facilities.

The purpose of this project was to study how manpower and projects are planned at the Division and to make recommendations for improving the effectiveness and productivity of the tools that are used.

Findings

The existing manpower and project planning processes (including the managemant plan for the Division, existing manpower planning reports, project reporting to LaRC and NASA Headquarters, employee time reporting, financial reporting, and coordination/ tracking reports for procurement) were discussed with several people and project planning software was evaluated.

1. **None of the tools now in use directly supports initial project planning or manpower planning.**

2. **The tools now in use are stand-alone tools and their usefulness is limited to their special purpose.**

3. **Considerable effort is needed to produce and maintain data about FENGD projects. Yet, the return on this investment is further limited since much of it uses manual or only partially automated systems.**

4. **These tools do not give FENGD management a ready ability to evaluate the impact of a new project or the many changes to existing projects.** One need that has been voiced often, for instance, is to assess the impact of slippage or early completion in one project upon another project or upon the manpower that is committed to both.

5.   There exists project planning software that is economical to purchase and that can be implemented on existing PCs within the Division.

6.   There is experience using project management software within the Division. One major project, the Hypersonics Facilities Complex, has been using MacProject II and Excel as project planning and tracking tools.

7.   There is a requirement for quality graphics. In the formal monthly project review meetings and day-in and day-out, Facilities Engineering people meet NASA management, their peers, and contractors to discuss a very large number of project tasks. Accurate communication is mandatory

8.   The Division's administrative support staff is experienced in using Macintosh PCs and is enthusiastic for the quality of graphics that they currently obtain from them.

Recommendations and Status

Software   The recommendations are: (1) Select the MacProject II, Excel, and the 4th Dimension software packages for project planning, spreadsheet analysis, and database management and each includes graphics capabilities; (2) Order two sets of this software: one for the Assistant, Program Integration and the other for the Program Analyst who supports him.   **Status** Just prior to drafting this report, these three software packages were installed on PCs for both people.

Manpower Planning   The recommendations are: (1) Train the Program Analyst in the 4th Dimension software; and (2) build an initial Manpower database with the 4th Dimension software package. This would then become a working tool with the data used and maintained by the Program Analyst   **Status** Training for the Program Analyst has begun and the initial manpower database is now being developed.

Project Planning   The recommendation are: (1) Train the Assistant, Program Integration and the Program Analyst in the MacProject II software; (2) Develop a prototype project plan for the major CoF project, the Minor CoF project with Preliminary Study and the Minor CoF project without Preliminary Study. Identify standard tasks for use as the starting point for new project planning; (3) Develop a demonstration of manpower and project tracking using MacProject II and 4th Dimension to be used as a briefing and training tool; (4). Direct that new project planning will use MacProject II and will be supported by the Program Analyst; and,. (5) .If continued MacProject II support is required for the Hypersonics Project, move the project data and responsibility for its maintenance to the Program Analyst.   **Status** Training for the Program Analyst has begun. The standard administrative milestones have been defined by FENGD management for the prototype projects and are being used in MacProject II. An example of the typical construction and engineering milestones in a project is now being developed and a dictionary of standard data elements has been started.

August 5, 1991

Reference: Kerzner, Harold. Project Management: A Systems Approach To Planning, Scheduling, and Controlling, New York: Van Nostrand Reinhold, 1989.

Analysis of Simulated Image Sequences from Sensors for Restricted-Visibility Operations

Rangachar Kasturi
Department of Electrical and Computer Engineering
Penn State University
University Park, Pennsylvania 16802

Abstract

As part of the Advanced SenSor and Imaging System Technology (ASSIST) program, imaging systems and interface requirements are being evaluated in order to enhance a pilot's view of the outside environment under restricted visibility conditions. A sequence of simulated images as seen from an aircraft as it approaches a runway was obtained from a model of a passive millimeter wave sensor operating at 94 GHz. Atmospheric attenuation is known to be a local minimum at this frequency. These images were analyzed to delineate objects of interest such as runways, taxiways, buildings, etc. Information about the position and motion of various objects on the ground may be computed by tracking the regions in such segmented image sequence. This information can be combined with data from other sensors to alert the pilots of any objects which are likely to be a hazard for continuing the flight.

1. Introduction

Enhancing the safety of operation of aircraft under restricted visibility conditions has been an important research topic for many years [1]. There is a great deal of interest in imaging sensors with the capability to *see through* fog and produce a *real-world* display which, when combined with symbolic or pictorial guidance information, could provide the basis for a landing system with lower visual minimum capability than those presently being used operationally [2]. An example of the interest in sensor and imaging systems technology is the FAA/DOD/Industry program entitled, *Synthetic Vision* [3].

Since the attenuation of radiation in the visible spectrum due to fog is very large [4] (Figure 1), sensors are being designed to operate at lower frequencies at which the attenuation is smaller (providing the ability to *see through* fog). One such frequency of choice is 94 GHz since the clear-air attenuation at this frequency is a local minimum and fog attenuation is low (Figure 1). In a joint research project, NASA Langley Research Center and TRW are developing an imaging system to capture images using a passive sensor operating at this frequency. The goal of this project is to establish a foundation for imaging sensor and pictorial graphics display technology and their integration into future cockpit systems to enable transport operations under restricted-visibility conditions [2]. Extensive enhancement and analysis of images acquired using such sensors is essential in order to identify and track various objects such as buildings, runways, vehicles, etc. as the aircraft approaches a runway for landing. Information extracted from such an analysis is useful to generate warning signals to the pilot of any potential hazards.

A real-time model of the visible output from a 94 GHz sensor, based on a radiometric simulation of the sensor, has been developed. A sequence of images as seen from an aircraft as it approaches for landing has been simulated using this model. Thirty frames from this sequence of 200 x 200 pixel images (For: H x V) were analyzed to identify and track objects in the image using the *Cantata* image processing package within the visual programming environment provided by the *Khoros* software system [5]. The image analysis operations are described in this paper.

2. Analysis of Simulated Images

The image analysis operations include noise filtering, edge detection, edge closing, region labeling, and matching of corresponding objects in the image sequence. An example of the iconic *Cantata* workspace used in this analysis is shown in Figure 2. Three frames from the simulated image sequence on which this analysis was performed are shown in Figure 3. The image analysis operations are described in this section.

Noise Filtering: Since a model for the noise phenomena is not yet available, random noise was added to the images during simulation. A simple weighted spatial averaging filter (module marked *vconvolve* in Fig. 2) [6] was then used to decrease the effect of this additive noise. Although this is adequate to filter noise in these simulated images, a filter designed to match the noise in actual, real-world images will have to be developed later, when such data is available.

Edge Detection: Edge pixels in the images were detected using the Difference Recursive Filter (DRF; *vdrf* in Fig. 2) [7]. This filter, which is based on principles similar to those of the well-known Laplacian of Gaussian filter [8], has been shown to be an optimal filter for detection of step edges in white noise [7]. The smoothing function used by this filter is a symmetrical exponential function.

Edge Closing: Edge pixels detected by the DRF filter are not guaranteed to form closed object boundaries. Such gaps in boundaries are bridged using an edge-closing operator (*vclose* in Fig. 2). The edge-closing operator uses as its input two images: the output of the DRF filter and a gradient image (eg., output of a Sobel edge detector - *vdiff* in Fig. 2). It follows a path of maximum gradient between the two end points being bridged. The resulting closed edges detected in corresponding images of Figure 3 are shown in Figure 4.

Region Labeling: Connected pixels belonging to the same object in the image are given a unique label. 4-connectivity [6] is used in this labeling scheme (pixels which are connected at the top, bottom, left, and right - but not diagonally - are said to be four-connected to the pixel at the center). The region labeling operator (*vlabel* in Fig. 2) uses the output of the edge-closing module; alternatively, it is also possible to label objects by operating directly on the noise filtered image using region growing techniques.

Region Matching: Objects in consecutive frames of the image sequence are compared to identify corresponding objects. The matching (*vrmatch* in Fig. 2) is done using a probabalistic rule which is based on the size and shape of regions. It computes the similarity of objects in successive frames. To illustrate objects which are matched they are assigned the same gray level in both frames in the displayed image. Two such frames after matching are shown in Figure 5.

3. Conclusions

A software system for analyzing simulated image sequences from a passive millimeter wave imaging system was described in this paper. The analysis/tracking system consists of the following stages: smoothing using a spatial averaging filter for noise reduction; detection of edge pixels using a recursive filter; bridging discontinuities in detected edges using an edge-linking operator; labeling objects in each image in the sequence; and comparing objects in consecutive frames to locate corresponding objects.

The passive millimeter wave imaging system will facilitate operation in restricted visibility conditions. Automated analysis of sensor-captured images to locate and track moving objects will provide critical information necessary for detecting potential runway incursions. Quantifying the amount of apparent motion of static objects in the scene from consecutive image frames is also useful as a cross-check of the position and velocity of the approaching aircraft. The preliminary results presented here using simulated images clearly demonstrate the potential of image analysis methods for detecting and tracking objects in a dynamic scene. Analysis of real images is well known to be a much more difficult task, however, particularly in real-time. To realize a practical system, new vision algorithms for analyzing sensor-captured images, and new display concepts for fusing information from various sensors, are necessary.

References

1. Glines, C.V., "Synthetic vision will let pilots see through precipitation," *Professional Pilot, Vol. 24*, pp. 62-67, Aug. 1990.
2. Hatfield, J.J and R. V. Parrish, "Advanced cockpit technology for future civil transport aircraft," *Proc. 11th Annual IEEE/AESS Dayton Chapter Symposium*, pp. , Dayton, Ohio, Nov. 1990.

3. Burgess, M.A., "Safety in future aircraft systems," *Proc. Flight Safety Foundation's 34th Corporate Aviation Safety Seminar*, pp. 76-99, Dearborn, Michigan, April 1989.

4. Young, S.K., R.A. Davidheiser, B. Hauss, P.S.C. Lee, M. Mussetto, M.M. Shoucri, L. Yujiri, "Passive millimeter-wave imaging," *TRW Space & Defense - Quest, Vol. 13*, No. 2, pp. 3-20, Winter 1990/91.

5. Rasure, J., D. Argiro, T. Sauer, and C. Williams, "A visual language and software development environment for image processing," *Intl. J. Imaging Systems and Technology, Vol. 2*, pp. 183-199, 1990.

6. Gonzalez, R.C. and P. Wintz, *Digital Image Processing*, second edition, Addison-Wesley, Reading, Massachusetts, 1987.

7. Shen, J. and S. Castan, "An optimal linear operator for edge detection," *Proc. IEEE Conf. Computer Vision and Pattern Recognition*, pp. 109-114, Miami Beach, Florida, 1986.

8. Marr, D. and E. Hildreth, "Theory of edge detection," *Proc. Royal Society, London, Ser. B, Vol. 207*, pp. 187-217, 1980.
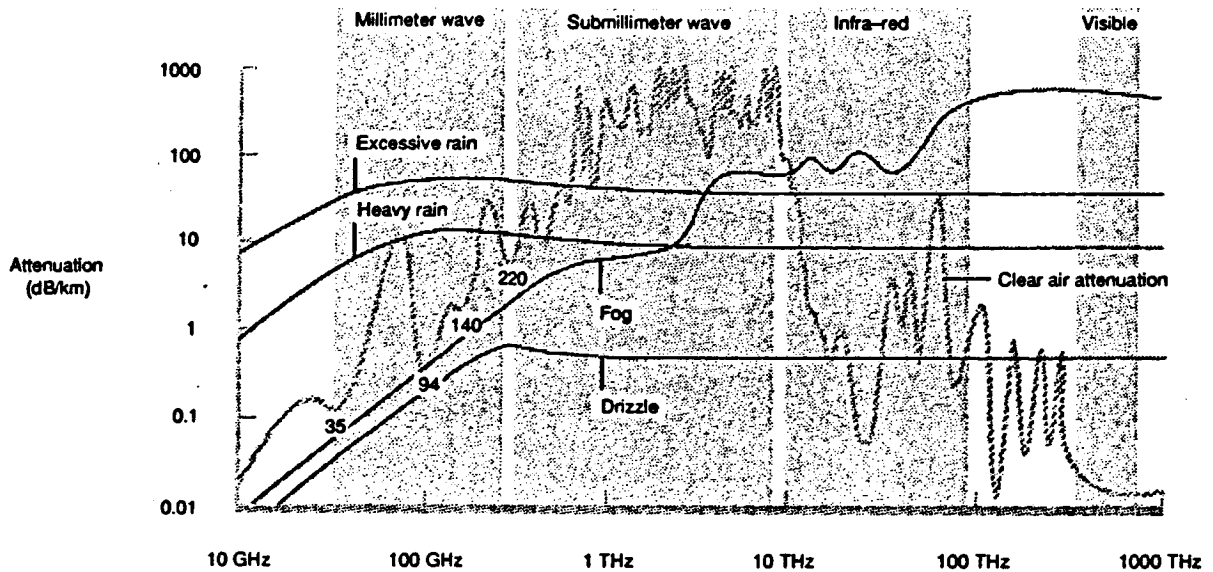
Figure 1. Atmospheric effects on electromagnetic radiation [4].
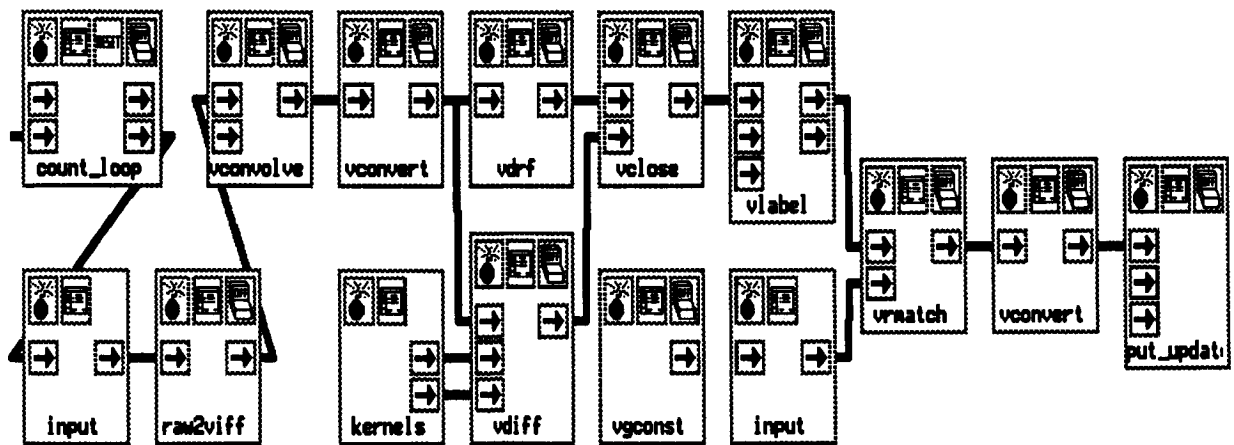
Figure 2. Block diagram of the image analysis and tracking operations presented as a *Cantata* workspace.

127
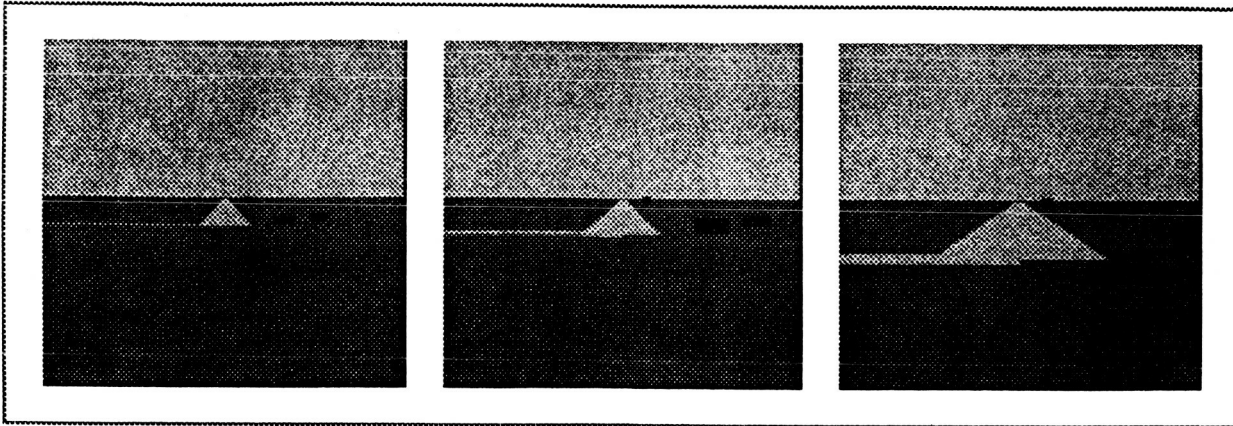
Figure 3. Frames 1, 16, and 30 in the sequence of simulated images.
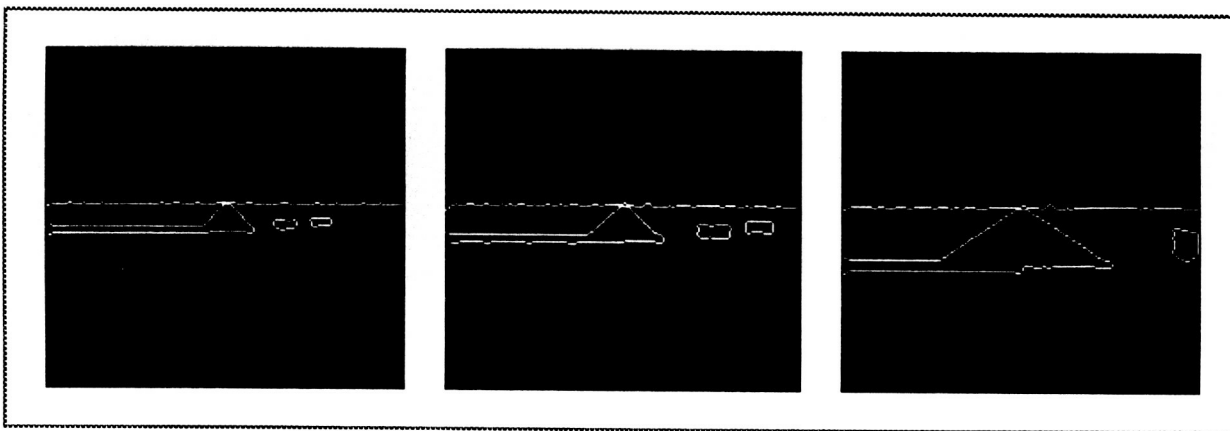
Figure 4. Runway, taxiway, horizon, and buildings delineated in the images of Figure 3.
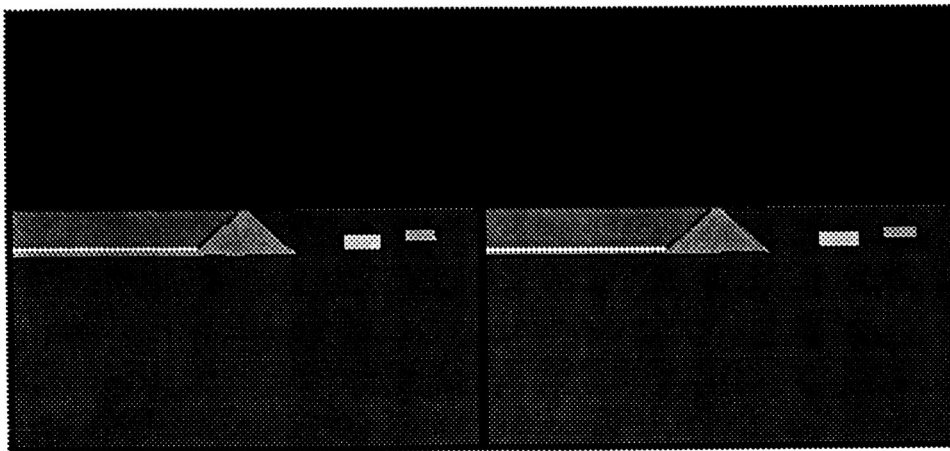
Figure 5. Two consecutive frames in the image sequence after detection and tracking of objects; corresponding objects in the two images are given the same gray level.

128

SQUEEZE FLOW AND COMPACTION BEHAVIOR OF TOUGHENED POLYIMIDE MATRIX COMPOSITES

by

B. L. Lee, Associate Prof. of Eng. Sci. and Mechanics
Pennsylvania State Univ., Univ. Park, PA

(In Collaboration with R. Pater and M. D. Soucek, MD/PMB)

As a means of increasing the resistance of fiber composites against *microcracking* or *matrix damage accumulation*, past efforts of toughening brittle thermoset resins with the inclusion of ductile secondary domain or the reduction of crosslink density were successful to various extents. For example, the use of elastomer-toughened epoxy resin matrix became a standard practice of composite prepreg industry. In the case of brittle thermoset polyimide matrix composites, several promising approaches such as the increase of molecular weight between crosslinks (Mc) or the formation of semi-interpenetrating network with thermoplastic polyimide were shown to toughen the matrix very effectively. However, their effectiveness has been limited by the lack of resin flow, the difficulty of removing solvent or other processing difficulties.

In view of the above-discussed limitations, a new research program on the processing science of toughened polyimide matrix composites has been proposed with the 1991 Summer Faculty Research Project (SFRP) as a preliminary phase. The main objectives of the program are: (a) to determine optimum processing conditions for toughened polyimide matrix composites in compression molding as well as filament winding based on the understanding of *squeeze flow, kinetics of cure, kinetics of volatile removal*, and *compaction behavior* of material elements, and (b) to define the roles and interaction of the degree of compaction (void/resin content) and residual stresses at the fiber-matrix interface in controlling the microcrack resistance of toughened polyimide matrix composites.

In the 1991 SFRP, main emphasis was placed upon the squeeze flow and compaction behavior of LaRC-RP series polyimide matrix composites. The composite prepregs were prepared with unsized IM7 graphite fibers and the following matrix resins of varied Mc (and therefore of varied fracture toughness):

	Mc
RP48	1 100
RP46	1 500
RP52	* 2:1 IPN of RP48/RP49
RP50	9 950
RP51	* 1:1 IPN of RP48/RP49
RP47	15 000
RP49	21 000

The measurement of squeeze flow behavior was performed by a plastometer which monitors the change of thickness of a prepreg specimen laid between two parallel plates under the specified temperature and pressure history. A critical evaluation of the plastometer data was attempted by examining the morphology of the specimen at various points during the squeeze flow. The effects of Mc of resin, imidization (B-staging) condition and pressure on the squeeze flow behavior were examined. The following facts were learned:

(1) The plastometer data under static loading provide three key results: melt transition temperature of linear polyimide resins, the degree of resin squeeze flow, and processing window.

(2) In estimating the degree of squeeze flow, an initial specimen thickness has to be defined before B-staging or imidization. The imidization step results in the increase of prepreg thickness because of resin foaming and the reduction of prepreg width. The use of the prepreg thickness after imidization as a baseline leads to serious errors in the estimation of the degree of flow. Higher prepreg thickness after imidization is observed with increasing Mc of resins.

(3) In the plastometer curve, the initial half of the region with sudden thickness drop is caused by the softening of materials. Morphology study showed no flow in that region. The resin flow occurs in the second half of the thickness drop region. The melt transition temperature can be defined by extrapolating the drop region and the plateau of final thickness (Figure 1).

(4) A separate study indicated that the application of pressure at the melt transition temperature maximizes the squeeze flow (Figure 2). When the pressure is applied in the plateau region (Figures 1 and 2), a lesser amount of squeeze flow is observed due to the onset of crosslinking.

(5) The melt transition temperature, which constitutes the lower bound of processing window, is independent of Mc of resins but highly dependent on the degree of imidization. The upper bound of processing window is determined by the occurrence of gelation.

(6) Slower heating in cure cycle lowers the melt transition temperature and lengthens the gelation time of resin, thus widening the processing window.

(7) The increase of Mc of resin reduces the degree of matrix squeeze flow (Figure 3). The reduction of matrix resin flow can be counterbalanced by the application of higher pressure or the use of prepreg systems with higher volatile contents. The prepreg systems with higher volatile contents are prepared by B-staging at lower temperature.

130

IM7 / LaRC-RP46 Polyimide
Unidirectional 8-ply

Static Loading: 3.45 MPa
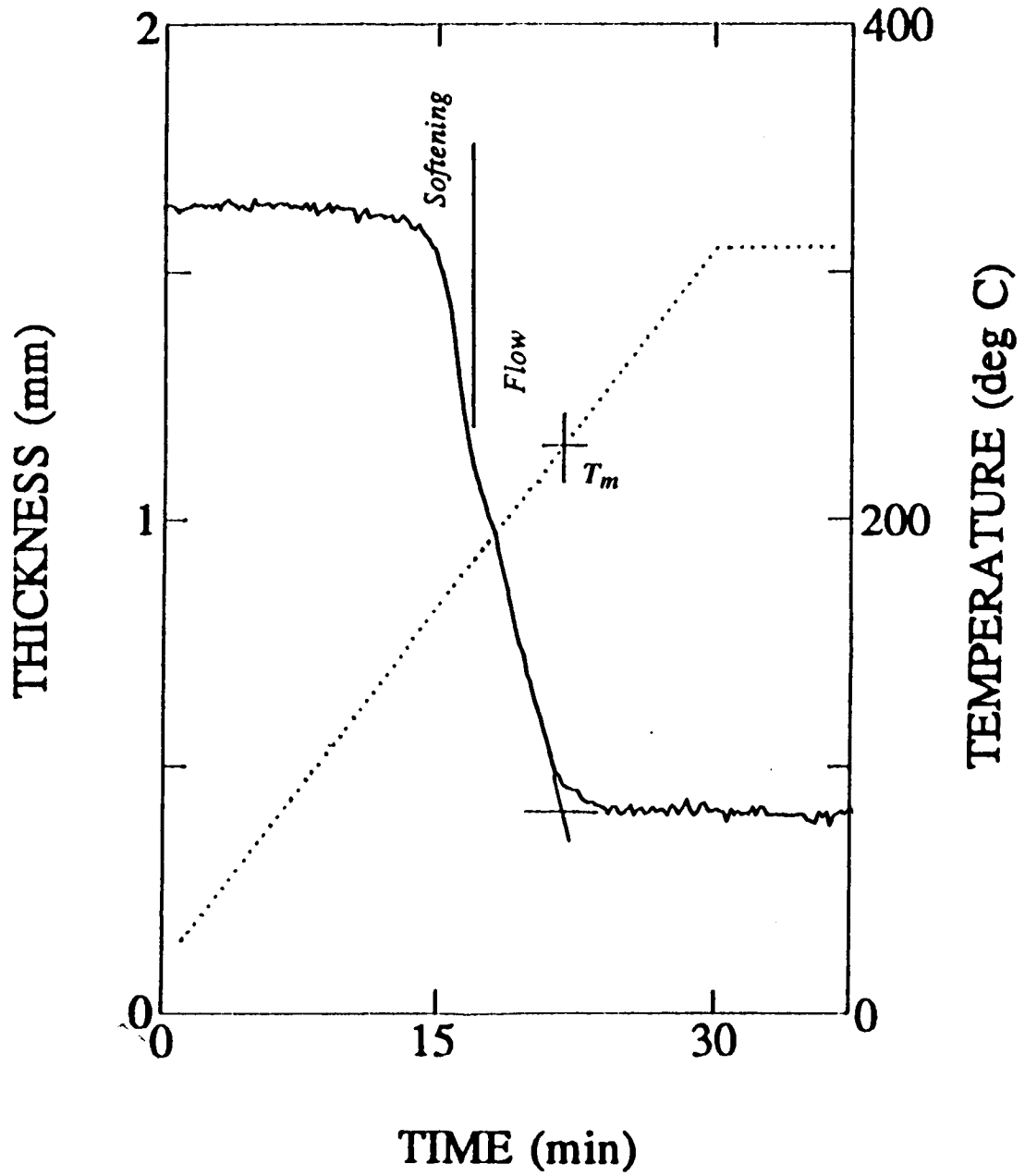
IM7 / LaRC-RP Series Polyimide
Unidirectional 8-ply

Quasi-Static Loading: 3.45 MPa

B-staging condition:
204 deg C for 1 hr

T_m

$M_c = 15\,000$ (*RP47*)

$M_c = 1\,500$ (*RP46*)

FINAL THICKNESS (mm)

TEMPERATURE (deg C)

TIME AT LOADING (min)

DEGREE OF FLOW (%)

PRESSURE (10³ psi)

IM7 / LaRC-RP Series Polyimide Composites:

		Mc
RP49	21 000	Mc
RP47	15 000	
RP51	1:1 IPN of RP48/49	
RP50	9 950	
RP52	2:1 IPN of RP48/49	
RP46	1 500	
RP48	1 100	

B-staging condition:
204 deg C for 1 hr

FINAL THICKNESS (mm)

PRESSURE (MPa)

133
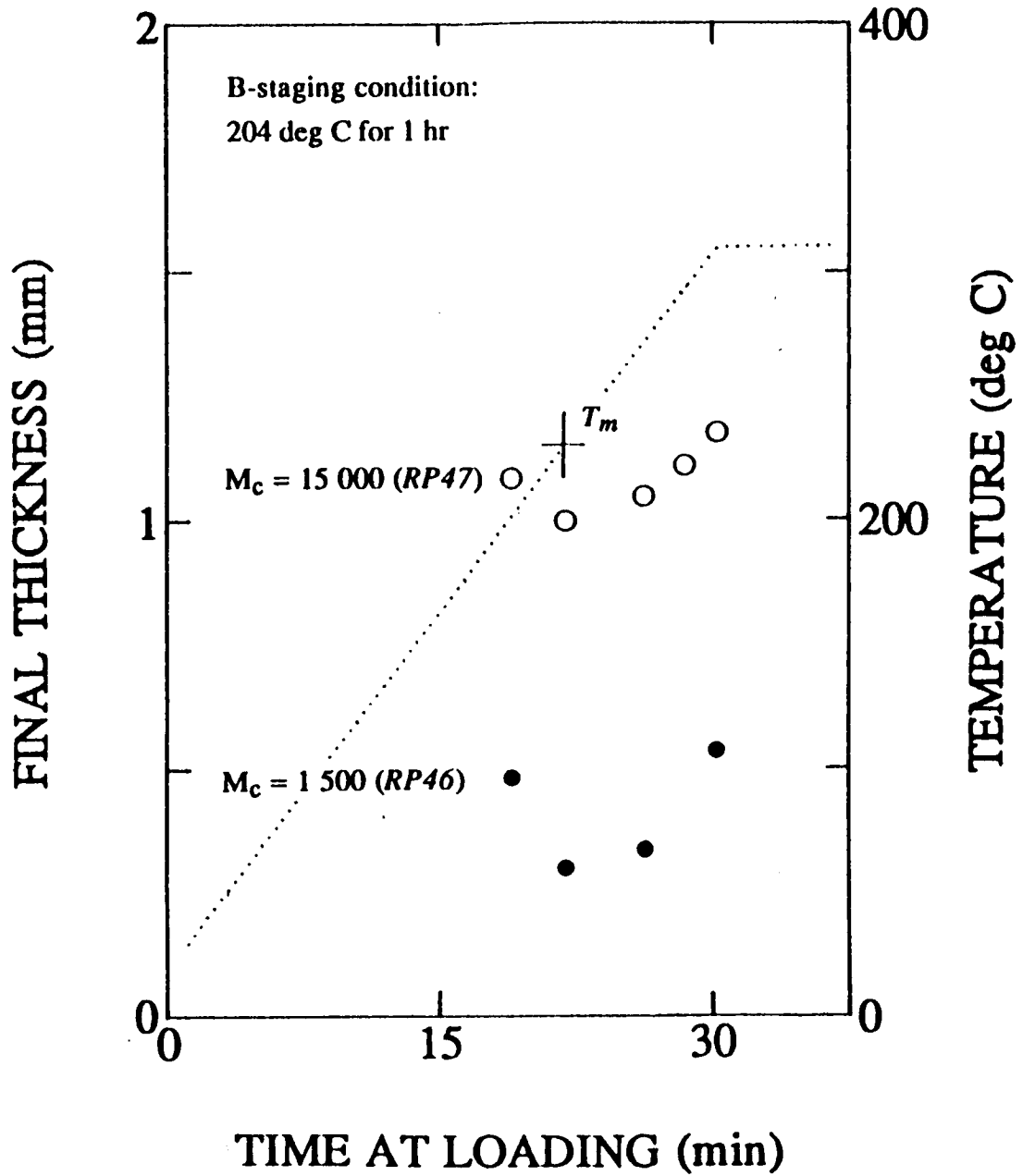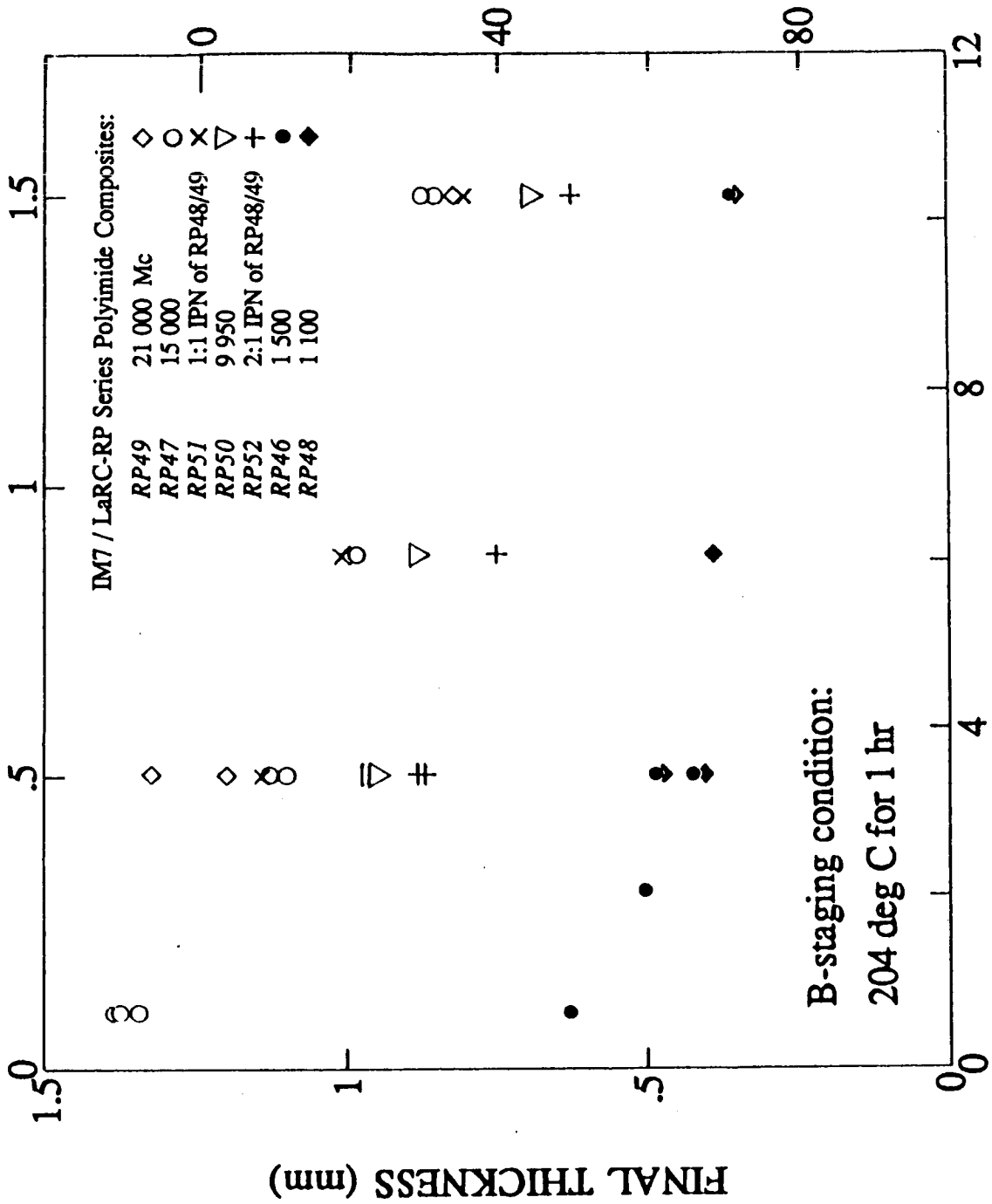
APPLICATION OF MULTIPLE CRITERIA DECISION METHODS IN

SPACE EXPLORATION INITIATIVE DESIGN AND PLANNING

Abu S. M. Masud, Ph.D., P.E.
Industrial Engineering Department
The Wichita State University
Wichita, Kansas 67208

My 1991 NASA/ASEE Summer Faculty Fellowship activities at the Langley Research Center (LaRC) were directed towards the identification of the opportunities for application of Multiple Criteria Decision Making (MCDM) techniques in the Space Exploration Initiative (SEI) domain. I identified several application possibilities and proposed demonstration application in these three areas: (1) evaluation and ranking of SEI architectures, (2) space mission planning and selection, and (3) space system design. Due to page limitations, this report describes only the results of my research efforts directed towards the first problem. A more detailed report about all three problems would be issued later.

SEI Architectures

SEI represents the focused efforts by NASA in meeting President Bush's challenge to the American's, made on the 20th anniversary of first manned Moon landing, to go "..back to the Moon.. (and this time) to stay... and a manned mission to Mars." Accordingly, several studies have been conducted to define strategies about how this can be accomplished. One of the first detailed report discussing scenarios (called "architectures") for Mars missions is the "90-day Study" report by NASA[1]; and, the most recent one is the report of the "Synthesis Group" set up by Vice-President Quayle[2]. NASA would now be conducting additional technical studies to arrive at a baseline SEI architecture. My research was aimed towards demonstrating that MCDM methods can assist in this. The following five architectures were chosen for evaluation and ranking:

A : Architecture I (Mars Exploration) of the Synthesis Group Report.
B : Architecture II (Science Emphasis for the Moon and Mars) of the Synthesis Group Report.
C : Architecture III (Moon to Stay and Mars Exploration) of the Synthesis Group Report.
D : Architecture IV (Space Resource Utilization) of the Synthesis Group Report.
E : Modified Reference Architecture of the 90-Day Study Report.

Evaluation Criteria

Several researchers from the SEI Office at LaRC participated in the development of a two-level, hierarchically structured set of general evaluation criteria. Specific, technical criteria were not deemed to be relevant at this early stage of architectural concepts. Table 1 shows the developed criteria set.

Relative Importance of the Evaluation Criteria

Many approaches for the development of relative importance weights are available[3]. We have used the concept proposed by Saaty for Analytic Hierarchy Process (AHP). Using the scale shown in Table 2, SEI researchers first made pairwise comparisons of the major criteria. Weights for these major criteria were then computed from these comparisons; see column 2 of Table 3. Next, they made pairwise comparisons of the sub-criteria under each major criterion. Weights from these comparisons and the weights of the major criteria computed previously were used to determine the absolute weights of each sub-criterion. Finally, sub-criteria with only marginal effects were combined, to reduce the set of the evaluation criteria. Table 3 shows the resultant reduced set of evaluation criteria and the corresponding weights.

Evaluation of the Architectures

Each of the five architectures were then evaluated by the SEI researchers with respect to each the sub-criterion. The scale in Table 4 was used in these evaluations, and the results are shown in Table 5.

Rank Ordering of the Architectures

Different rank ordering methods, such as Simple Additive Weighing, ELECTRE and TOPSIS, are available. We have used TOPSIS by Hwang and Yoon[3]. TOPSIS uses the Euclidian distance of each alternative from an "Ideal Solution" (constructed from the best achieved value with respect to each criterion by any of the alternatives under consideration) and a "Negative Ideal Solution" (constructed from the worst criteria values of all the alternatives) to compute a closeness measure, C_*. The closeness measure for an alternative equals 1 when it coincides with the "Ideal Solution" and the measure equals 0 when the alternative coincides with the "Negative Ideal Solution." Table 6 shows the computed closeness measure values for all five of the architectures, and their final ranking.

Concluding Remarks

The most meaningful result from this analysis is the wide separation between the top two ranked architectures, indicating a significant preference difference between them. It must also be noted that the final ranking reflects, to some extent, the biases of the evaluators and their understanding of the architectures.

REFERENCES

1. Report of the 90-Day Study on Human Exploration of the Moon and Mars. NASA Internal Report, Johnson Space Center (Aaron Cohen, Study Leader), November, 1989.
2. America at the Threshold : America's Space Exploration Initiative. Final report of the Synthesis Group (Thomas Stafford, Group Leader), May, 1991.
3. Hwang, C.L. and K. Yoon, Multiple Attribute Decision Making : Methods and Applications. Springer-Verlag, New York, 1981.

Table 1. Evaluation Criteria

Criterion	Sub-criterion	Explanation

Maximize the following criteria (i.e., the more the better)

1. Utility/Benefit

	1.1 Economical	Potential national economic payoffs
	1.2 Technological	Technological Payoffs/spinoffs
	1.3 Educational	Impact on national education system
	1.4 Scientific	Impact on scientific knowledge
	1.5 Commercial	Potential for commercial payoffs
	1.6 Synergy	Positive (synergistic) effect on other SEI/Civilian space projects
	1.7 Visibility	Public visibility and appeal
	1.8 International Cooperation	Degree of International cooperation that may be achieved
	1.9 Political	Political appeal and attractiveness

2. Feasibility

	2.1 Technical	Soundness and reasonableness of the technological state-of-the-art assumptions
	2.2 Schedule	Functionality and reasonableness of the schedule
	2.3 Political	Potential for public/congress support

3. Flexibility

	3.1 Launch Date	Flexibility in launch date
	3.2 Budget	Flexibility in the required budget
	3.3 Schedule	Flexibility in the overall schedule (resiliency in the schedule)
	3.4 Mission	Adaptability to changes in the mission goal, focus, etc.
	3.5 Design	Robustness of the architectural design

4. Manageability

	4.1 Developmental	Degree of difficulty in the management of the development efforts
	4.2 Operational	Degree of difficulty in the management of the mission operations

Minimize the following criteria (i.e., the less the better)

5. Risk/Uncertainty

	5.1 Crew Safety	Potential risk in crew safety and health
	5.2 Technological	Risk that the expected technology would not be developed at all or in a timely manner
	5.3 Economical	Economic risk/uncertainty (potential, and degree thereof, for the budget to increase)
	5.4 Schedule	Robustness of the schedule (level of uncertainty in the schedule)
	5.5 Performance	Potential uncertainty about achieving the expected performance

6. Cost

	6.1 Life Cycle Cost	Total developmental and operating cost
	6.2 Conflict	Potential for detrimental effect on other SEI/Civilian space projects?

136

Table 2. <u>Pairwise Preference Measurement Scale</u>

<u>Intensity of Importance of criterion C_i over criterion C_j</u>	<u>Definition</u>	<u>Explanation</u>
1	Equal importance	C_1 and C_2 are equally important
3	Weak importance	Experience & judgement slightly favor C_1 over C_2
5	Essential or strong importance	Experience & judgement strongly favor C_1 over C_2
7	Demonstrated importance	C_1 is strongly favored & its dominance is demonstrated in practice
9	Absolute importance	The evidence favoring C_1 over C_2 is of the highest possible order of affirmation
2,4,6,8	Intermediate values	When compromise is needed between two adjacent judgements

137

Table 3 Final Weights of Evaluation Criteria

Criterion	Weight	Sub-criterion	Weight	
			Relative	Absolute
Utility/Benefit	0.0754			
		Economical/ Technological/ Educational	0.2279	0.0172
		Scientific	0.2314	0.0175
		Visibility	0.2511	0.0189
		Political	0.2896	0.0218
Feasibility	0.3179			
		Technical	0.2211	0.0703
		Schedule	0.4600	0.1462
		Political	0.3190	0.1014
Flexibility	0.0774			
		Launch Date/ Schedule	0.2192	0.0170
		Mission	0.6095	0.0471
		Design	0.1713	0.0133
Manageability	0.0331			0.0331
Risk/Uncertainty	0.3610			
		Crew Safety	0.6544	0.2362
		Technological/ Performance	0.1690	0.0610
		Economical/ Schedule	0.1766	0.0638
Cost	0.1349			
		Life Cycle Cost	0.9000	0.1214
		Conflict	0.1000	0.0135

Table 4. Architecture Evaluation Scale

For Cost Attributes				For Benefit Attributes
	0	-	0	
very high	1.0	-	1.0	very low
high	3.0	-	3.0	low
average	5.0	-	5.0	average
low	7.0	-	7.0	high
very low	9.0	-	9.0	very high
	10.0	-	10.0	

Table 5. <u>Architecture Evaluation Matrix</u>

(Sub) Criterion	Architecture Evaluation				
	A	B	C	D	E
Econ/Tech/Educ Benefit	6	7	8	7	6
Scientific Benefit	6	9	8	5	5
Visibility Benefit	6	8	9	6	6
Political Benefit	6	7	6	7	6
Technical Feasibility	7	5	6	3	9
Schedule Feasibility	4	2	1	2	9
Political Feasibility	5	5	1	5	8
Launch/Schedule Flexibility	5	5	3	5	7
Mission Flexibility	7	5	8	5	7
Design Flexibility	6	6	6	6	7
Manageability	6	5	4	5	8
Crew Safety Risk	6	6	4	6	6
Techn/Performance Uncertainty	4	4	3	4	6
Econ/Schedule Uncertainty	5	3	3	2	7
Life Cycle Cost	5	2	5	7	7
Conflict Cost	3	2	1	2	5

Table 6. <u>Ranking of the Architectures</u>

Architecture	Separation Measures		Relative Closeness $C_{i\bullet}$	Rank
	(From A^*) $S_{i\bullet}$	(From A^-) S_{i-}		
A	0.08135	0.11308	0.5816	2
B	0.12002	0.05481	0.3135	4
C	0.14060	0.03552	0.2017	5
D	0.11353	0.07253	0.3898	3
E	0.00724	0.15107	0.9543	1

The Use of Artificial Neural Networks In
Experimental Data Acquisition and Aerodynamic Design

by

Andrew J. Meade, Jr.
Assistant Professor
Department of Mechanical Engineering and Materials Science
Rice University
Houston, TX 77251-1892

During the ASEE summer tenure at NASA Langley I participated in two projects that were of mutual interest to myself and the staff of the Transonic Aerodynamics Branch. The primary project was the numerical simulation, by a finite element/finite difference method, of the viscous flow about an airfoil [1]. This project is currently funded by the branch and is considered a long term project. The secondary project was a feasibility study on the use of artificial neural networks (ANN) in experimental data acquisition and the design of aerodynamic components. Preliminary results from the secondary project are presented.

An appreciable amount of work done by the Transonic Aerodynamics Branch's (TAB) Applied Aerodynamics Group is in the design of aerodynamic components in the transonic regime. The tools used for design include both physical experimentation and computational fluid dynamics (CFD). The considerable costs in money and manpower in the collection of experimental data and the construction and use of numerical models greatly hampers high-risk, innovative research. The use of an ANN data acquisition system and the resulting construction of the data base could significantly reduce those costs.

Traditionally programmed digital computers can process numbers at great speed; however, they do not easily recognize patterns, nor can they deal with imprecise or contradictory data. Artificial neural networks [2] exhibit an adaptive behavior that makes them capable of self-learning. Instead of being programmed, neural networks are trained by exposing them to repeated examples. When networks are trained with correct examples from available data, they accurately supply missing information and can even extrapolate the information. Consequently, a neural network is an attractive method for encoding and compressing empirical knowledge. ANN models have been studied for many years in the hope of achieving human-like performance in the complex problems of real-time pattern recognition (i.e. speech and vision). The proposed application to aerodynamics would be comparatively modest.

It is proposed that an artificial neural network be used to construct an intelligent data acquisition system. The benefits of the proposed "smart" acquisition system would be:

- The neural network, with proper hardware and software, could possibly in real time steer the experimentalist away from the parameter combinations that give well behaved and well known results, and towards combinations that give interesting phenomena. This may save a considerable amount of time and effort in the wind tunnel.

- The resulting neural net model could then be used as an easily accessible and easily usable data base. This data base code could find numerous uses, including CFD validation.

Currently table lookups, statistical packages, and curve fitting interpolation codes are used on data bases for aerodynamic problems. The ANN model has a potential for replacing these traditional procedures as well as use in CFD validation. Some of the potential advantages of the ANN model for aerodynamics are as follows:

1. The ANN model would not store experimental data for interpolation but would rely upon the trained neural network to store the pattern with relatively little memory requirement. This includes data generated from highly nonlinear processes.

2. ANN adaptation provides a degree of robustness by compensating for minor variabilities (noise) in the experimental data. Traditional statistical techniques are not adaptive but typically process all training data simultaneously before being used with new data. As a result, the statistical techniques can be memory intensive and slow.

3. The trained neural network can be widely distributed to other users and function within a traditional computer environment.

As proof of concept the author [3] modeled a NACA 0012 airfoil (Fig. 1), at specific conditions, using the neural network simulator "NETS" developed by James Baffes of the NASA Johnson Space Center [4]. The code does not require special hardware and runs on virtually any digital computer with an ANSI-C compiler. Fig. 2 illustrates a typical backpropagation network topology.

The experimental chordwise coefficient of pressure (C_p) distribution curves for the NACA 0012 airfoil were taken from the actual experimental data [5] and tabulated for use by the neural network. The curves used were taken at $Re = 3.0 \times 10^6$, based on chord, and at angle of attack $\alpha = -0.14°$. Turbulent transition was fixed on the airfoil at 0.05 x/c. The nominal freestream Mach numbers M_∞ were 0.30, 0.35, 0.50, 0.55, 0.60, 0.65, 0.70, 0.74, and 0.76. The backpropagation topology used for the test consisted of one input node for M_∞, thirty seven hidden nodes and thirty eight output nodes for the thirty eight components of the C_p distribution vector. The net was trained to a maximum rms error of approximately 0.008 using the data sets at $M_\infty = 0.30, 0.50, 0.70$, and 0.76. A comparison of the neural net prediction (triangles) at $M_\infty = 0.74$ with the actual data is shown in Fig. 3. The C_p plot of Fig. 4 compares the ANN results with data from a training set sample ($M_\infty = 0.76$).

Artificial neural networks can provide an elegant and valuable class of mathematical tools for data analysis. Since the hardware, software, and expertise already exist in other fields, such as computer science and electrical engineering, it is thought then that the use of neural networks, and the accompanying hardware, would be more of an application problem than basic research. The feasibility study will continue.

References

1. Meade, A.J., "Semidiscrete Galerkin Modeling of Compressible Viscous Flow Past an Airfoil", NASA/ASEE Summer Faculty Fellowship Program 1990, NASA Contractor Report 182092, 1990.

2. Rumelhart, D.E., and McClelland, J.L., "Parallel Distributed Processing: Explorations in the Microstructure of Cognition", MIT Press, Cambridge, M.A., 1986.

3. Meade, A.J., Cheatham, J.B., and Adnan, S., "An Artificial Neural Network Application In Aerodynamics", to appear in Application of Neural Networks in Engineering conference (ANNIE '91), University of Missouri-Rolla, Rolla, Missouri, November 1991.

4. Baffes, Paul T., "NETS User's Guide, Version 2.0 of NETS", Software Technology Branch, Johnson Space Center, JSC-23366, 1989.

5. Harris, Charles D., "Two-Dimensional Aerodynamic Characteristics of The NACA 0012 Airfoil In The Langley 8-Foot Transonic Pressure Tunnel", NASA TM 81927, 1981.
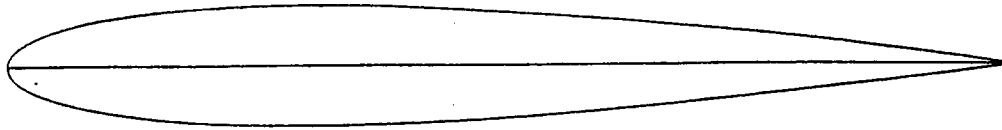
Fig. 1 Sketch of a NACA 0012 Airfoil
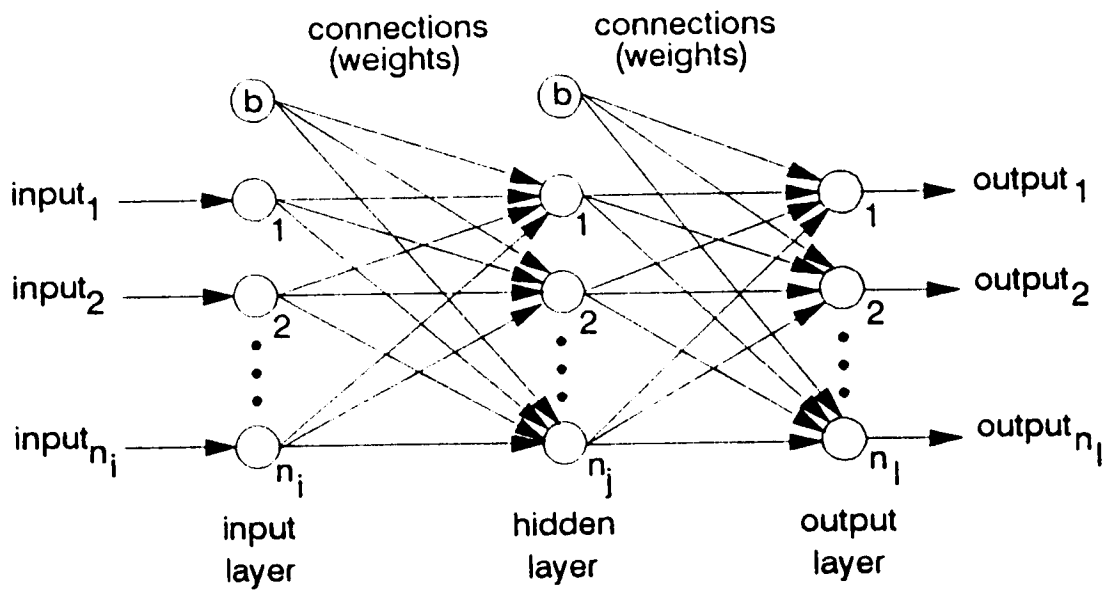
Fig. 2 Typical Backpropagation Topology
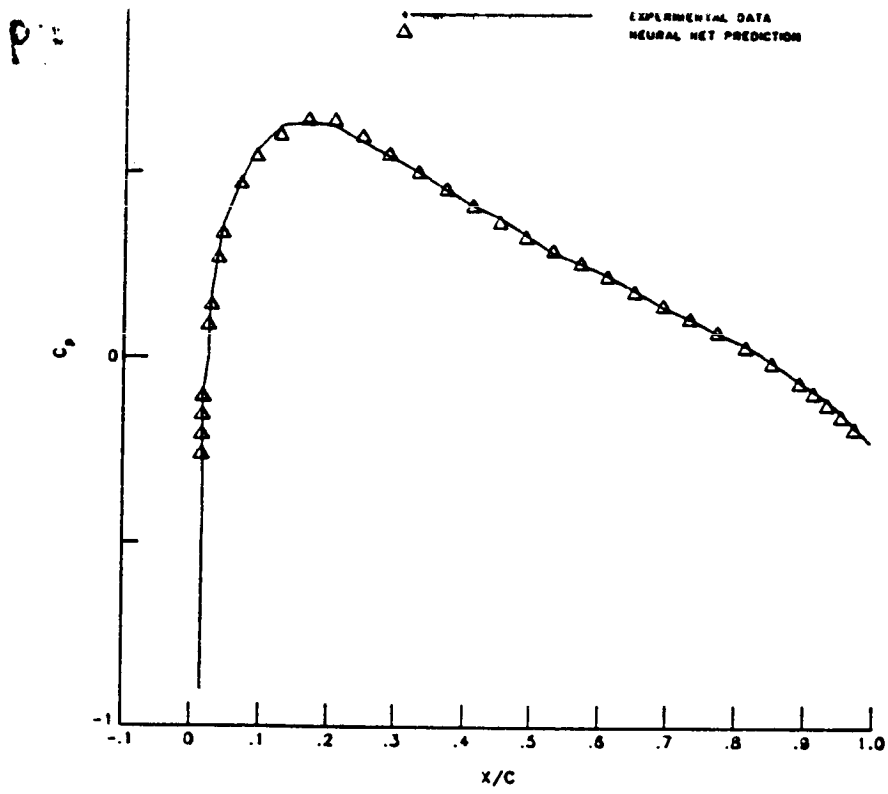
Fig. 3   NACA 0012 AIRFOIL $M_\infty = 0.74$
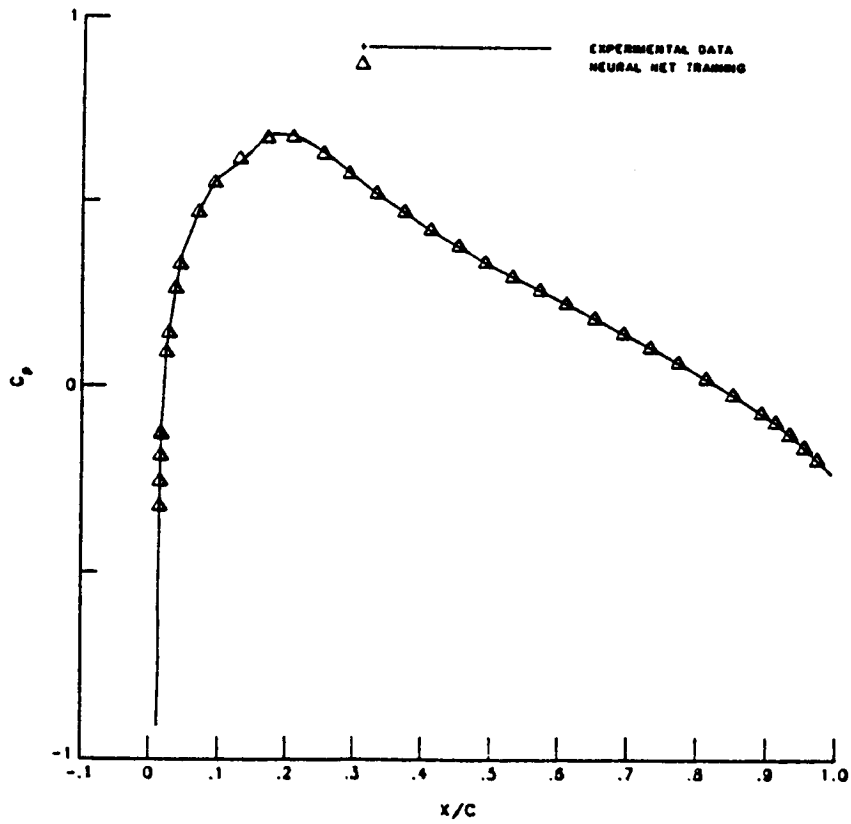
Fig. 4   NACA 0012 AIRFOIL $M_\infty = 0.76$

AN EVALUATION OF PRELIMINARY
DOPPLER GLOBAL VELOCIMETRY MEASUREMENTS

by

L. Scott Miller
Assistant Professor
Aerospace Engineering Department
The Wichita State University
Wichita, KS 67226

Doppler Global Velocimetry (DGV) is a new and evolving method for making aerodynamic measurements. The technique, which was invented at Northrop Research and Technology Center, is currently undergoing development and evaluation at the NASA Langley Research Center (LaRC). Future DGV system applications planned include F-18 flight tests at NASA Ames and wind tunnel investigations at LaRC.

DGV is a very attractive technique since it potentially offers the capability for making simultaneous three-component velocity measurements within a flow plane region. The basic operating principle is very simple. References 1-4 provide a more detailed description. In summary, a laser is used to generate a plane of light within the flow field region of interest. Particles, or seeds, present in the moving flow scatter this light with a frequency determined by the Doppler effect. Scattered light frequency measurement from a specific direction can thus allow single flow velocity component identification. This frequency discrimination is performed using an optically transparent Absorption Line Filter (ALF) which has a transmission behavior similar to that shown in Figure 1. The laser is normally tuned to operate in the mid (5th mode location) linear ALF transmission range. Flow field velocity changes, which cause scattered light frequency changes due to the Doppler effect, are simply measured as intensity levels by a CCD camera viewing the illuminated flow through the ALF. A second CCD camera views the same flow region and is used to identify intensity variations which have nothing to do with Doppler frequency effects. The signal from each camera is acquired by processing electronics which provide as output a normalized image describing the velocity within the illuminated flow. To make three-component measurements three camera and ALF sets are required to view the light sheet region from three separate directions. A simple one-component system schematic is shown in Figure 2.

A number of very basic tests have been performed in the past to identify DGV performance and capability. Recently, however, a more challenging investigation using a one-component DGV system was conducted on a thin 75 degree swept delta wing in the NASA LaRC Basic Aerodynamic Research Tunnel (BART). It is the purpose of this paper to discuss and evaluate the BART test results and to provide recommendations as necessary for future DGV test activities.

Initial BART results evaluations were somewhat discouraging. Figure 3 shows a direct comparison between DGV and baseline data for the flow velocity (resolved into the measured DGV direction) along a horizontal line through each wing vortex core. In this figure, the solid continuous line represents baseline data, from references 5 and 6, and the discontinuous lines represents DGV data. The DGV data is not continuous since seeds or particles were not present at all points in the flow. Two points of concern surface from the comparison made in Figure 3. Specifically, the DGV data shows rapid high frequency variations and the general velocity trends appear incorrect.

146

Careful data examination indicates that the two camera images were not exactly aligned. This misalignment can result in the introduction of high frequency variations during normalization. Camera position differences, CCD array differences or ALF image distortions may have introduced the alignment problems. It appears likely that careful camera aiming or image processing (FFT or Convolution) procedures can be used to remove the image variations.

Output simulations were performed to identify potential BART DGV velocity trend problems. To explore the possibility that the laser may have been improperly tuned, a simple nonlinear ALF transfer function model was applied to the baseline data to generate simulated DGV output data. Direct comparison of these results with actual DGV data suggests that the DGV system was indeed operating in a nonlinear condition during the BART investigation. An elaborate and complex scheme was developed to "correct" the DGV data for nonlinear effects. Figure 4 shows a comparison between the corrected and baseline results. As can be seen these results compare much better than those previously shown in Figure 3. Unfortunately some differences, which are likely due to the difficulty associated with properly correcting the nonlinear source data, still exist.

In summary, a review of DGV data obtained during wind tunnel tests on a 75 degree swept delta wing was performed. High frequency variations observed in normalized image files are attributed to image alignment problems. Unfortunately, initial DGV velocity data compared poorly with baseline reference data. Nonlinear DGV system operation during the tests is the likely source of this problem. Corrected data compares much more favorably and suggests that DGV is a valid measurement technique. Future DGV investigations should include a method or means for monitoring laser frequency relative to the ALF transfer function behavior.

References

1) Komine, H., Brosnan, S.J., Litton, A.H. and Stappaerts, E.A., "Real-Time Doppler Global Velocimetry," AIAA 29th Aerospace Sciences Meeting, AIAA-91-0337, Reno, NV., Jan. 1991.

2) Meyers, J.F. and Komine, H., "Doppler Global Velocimetry A New Way to Look at Velocity," ASME Fourth International Conference on Laser Anemometry, Cleveland, Ohio, Aug. 1991.

3) Komine, H. and Brosnan, S.J., "Instantaneous Three-Component Doppler Global Velocimetry," ASME Fourth International Conference on Laser Anemometry, Cleveland, Ohio, Aug. 1991.

4) Meyers, J.F., Lee, J.W. and Cavone, A.A., "Signal Processing Schemes for Doppler Global Velocimetry," IEEE 14th International Congress on Instrumentation in Aerospace Simulation Facilities, Rockville, Maryland, Oct. 1991.
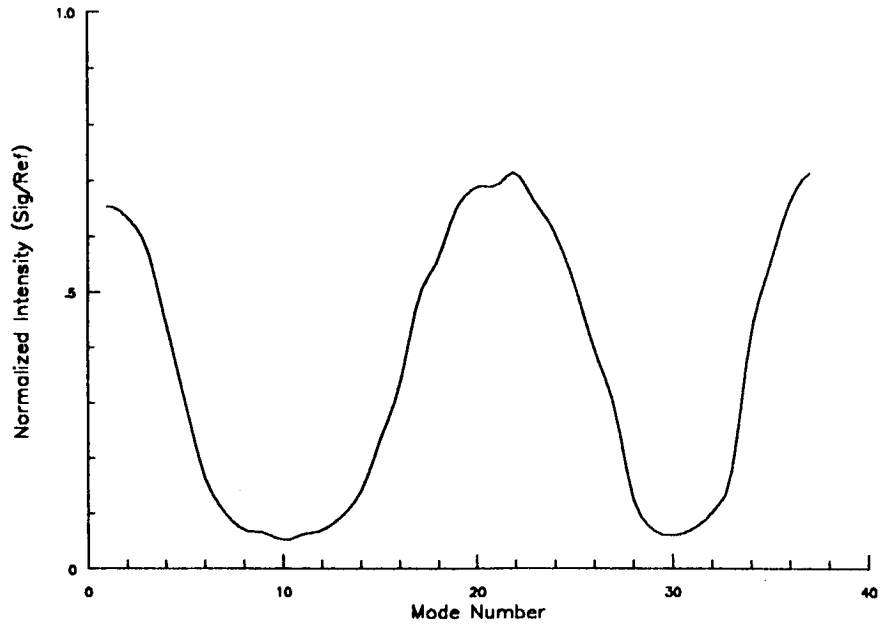
Figure 1. Example of an Absorption Line Filter (ALF) transfer function.
(The vertical axis represents normalized transmission and the horizontal axis represents laser frequency in terms of mode number.)
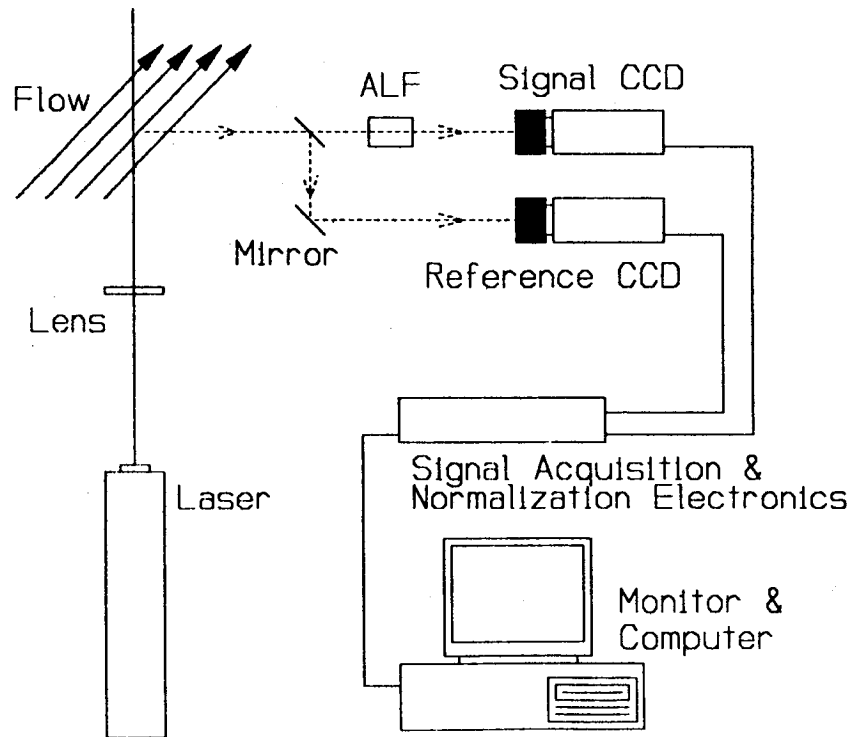
Figure 2. A schematic diagram of a one-component DGV system.
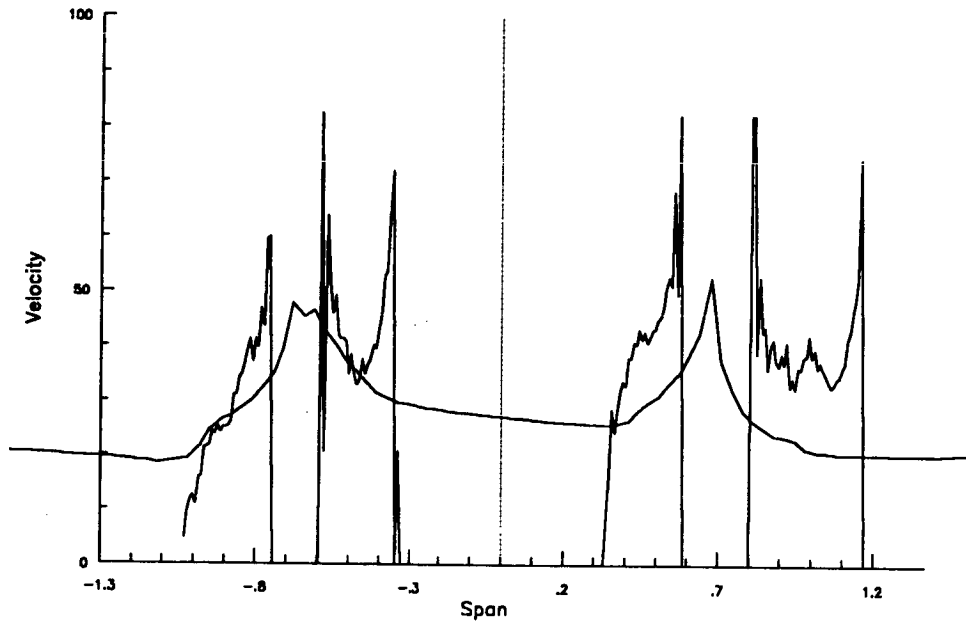
Figure 3.   Comparison between initial DGV and baseline data.
(The vertical axis represents velocity in meters/second and the horizontal axis represents normalized wing span.)
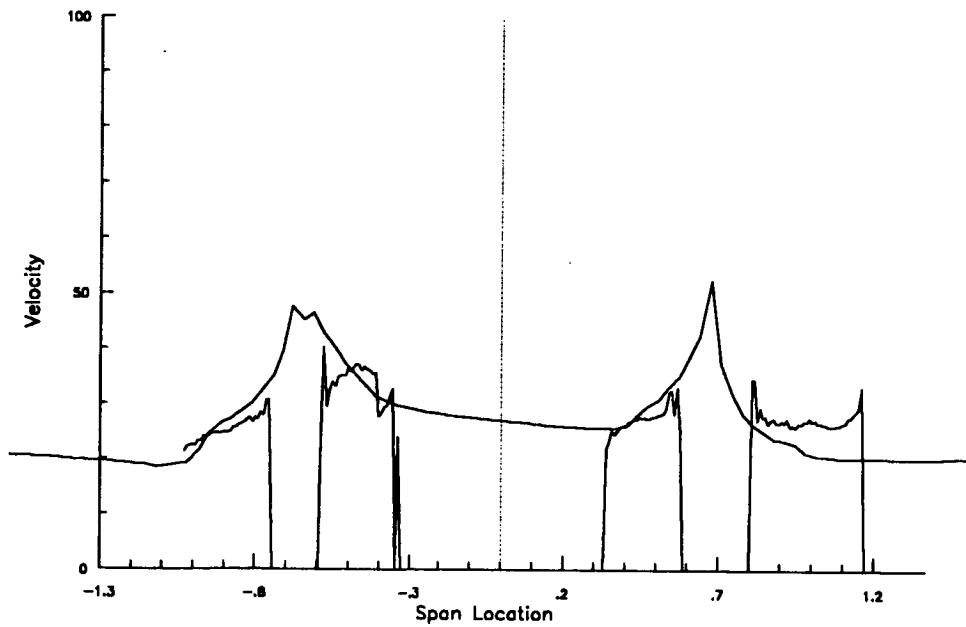
Figure 4.   A comparison between corrected DGV and baseline data.
(Axes are as described in figure 3.)

ASEE FINAL REPORT

An Examination of the
1991 Langley Aerospace Research
Summer Scholars Program (LARSS)
June 3, 1991 - August 9, 1991
Langley Research Center
Hampton, VA

By: Dr. Lois S. Miller

For: Dr. Surendra N. Tiwari
      ASEE Director

Date: August 2, 1991

SUMMARY OF THE 1991 LANGLEY AEROSPACE RESEARCH SUMMER SCHOLARS PROGRAM (LARSS)

The LARSS Program was established in 1986 as as incentive for college/university upper level engineering and science students to enhance their interest in aerospace research. In addition, it is the Program's intent to strongly encourage students to pursue and earn their graduate degrees.

The 1991 ten-week LARSS Program successfully met its goals through the assignment of research projects to be conducted at NASA, a Federal research laboratory, under the guidelines of selected mentors; through a lecture series (see Appendix C) composed of outstanding researchers at NASA; and through a Career and Graduate Education Conference (see Appendix D).

Vital statistics derived on the LARSS participants follow:

Classification of Students	N
Juniors	37
Seniors	33
Graduate	13
Other	7

Racial Distribution of Students (See Appendix E "Minorities Participating in 1991 LARSS Program")	N
Non Minority	66
Black	15
Hispanic	5
Asian	3
American Indian	1

Gender Distribution of Students	N
Male	63
Female	27

Universities Represented (6 HBCUs) (See Appendix F)	N = 45
Home States Represented (Plus Puerto Rico)	N = 22
Mean GPA	3.40

Academic Majors	N
Aeronautical Engineering	2
Aerospace Engineering	15
Airway Science Administration	1
Applied Math	1
Biology	1
Chemical Engineering	2
Civil Engineering	4
Computer Engineering	3
Computer Science	8
Electrical Engineering	15
Engineering	2
Industrial Psychology	1
Management Information Science	1
Materials Engineering	3
Materials Science & Engineering	2
Mathematics	1
Mechanical Engineering	14
Physics	8
Polymer Science	1
Psycho-Biology	1
Psychology	2
Systems Engineering	1

APPENDIX

1991

NASA/ASEE/LARSS

ACTIVITIES SCHEDULE

DATE	ACTIVITY	TIME
June 3	Orientation	9 a.m.
June 11	Lecture Series - Global Warming	10 a.m.
June 14	Unnual University Affairs Picnin	4 p.m.
June 18	Lecture Series - High Speed Civil Transport	10 a.m.
June 25	Lecture Series - Long Duration Exposure Facility	10 a.m.
June 26	NASA Bus Tour - Board at Activity Center	1:30 p.m.
July 2	Lecture Series - Nondestructive Evaluation: What's Up Doc?	10 a.m.
July 5	Free Day - - - No Work - - - HAPPY HOLIDAYS	
July 9	Lecture Series - HL 20 Personnel Launch System ***Group Pictures for both LARSS and ASEE after lecture - Please plan to be present.**	10 a.m.
July 10	Peninsula Pilots Baseball Game ($1.75/person) 1889 Pembroke Avenue	7 p.m.
July 12	LARSS Career and Graduate Education Conference	9:15 - 4 p.m.
July 16	**NO LECTURE TODAY**	
July 23	Lecture Series - Artificial Neural Networks	10 a.m.
July 26	The Spirit of Norfolk Moonlight Cruise Board Cruiser at Waterside Dock - Waterside Drive	11:30 p.m.
August 5	Banquet - Langley Officer's Club Cash Bar Dinner	6 p.m. 7 p.m.

ORIENTATION

ASEE SUMMER FACULTY FELLOWSHIP PROGRAM
and
LARSS PROGRAM

NATIONAL AERONAUTICS and SPACE ADMINISTRATION

LANGLEY RESEARCH CENTER

Location: Building 1222
Time: 9 a.m. - 12 noon
Date: Monday, June 3, 1991

Time	Topic	Speaker
9:00	Registration/Coffee & Doughnuts Badge and Pass Photos and Processing	
9:40	Introduction of Center Director	Dr. Michael F. Card Chief Scientist
9:45	Welcoming Remarks	Mr. Richard Petersen Director, Langley Research Center
9:50	Langley Overview Video	
10:20	Visitor's Center Briefing	Dr. Mark Nataupsky Director, Visitor's Center
10:30	Library Briefing	Mr. George Roncaglia, Head Technical Library Branch
10:40	Cafeteria Briefing	Mr. Richard C. Weeks, Manager
10:50	Computational Facilities Briefing	Dr. John Shoosmith Chief Scientist Analysis and Computation Division
11:00	Security Briefing	Mr. O. J. Cole, Chief
11:10	Safety Briefing	Mr. Clarence Breen, Safety Specialist Safety Management Section
11:20	Activities Center Briefing	Mrs. Pam Verniel, Manager
11:30	Occupational Health Services	Mr. Peter Edgette, Head
11:40	Introductions: ASEE - Co-Director LARSS - Associate Director LARSS - Project Director	 Dr. Surendra Tiwari, ODU Dr. John Whitesides, GWU Dr. Lois S. Miller, ODU
11:50	Introduction to Langley Associates	Mr. Ed Prior Technical Asst. to Chief Scienctist
12:00	Depart to Worksite	

1991

NASA Langley Aerospace Research Summer Scholars

LECTURE SERIES

Location: Activities Center Auditorium, Bldg. 1222

Time: 10:00 a.m. - 11:00 a.m. - Lecture
11:00 a.m. - 11:15 a.m. - Questions and Answers

DATE	TOPIC	SPEAKER
June 11	Global Warming	Dr. Joel Levine Atmospheric Sciences Division - Space Directorate
June 18	High Speed Civil Transport	Donald Maiden Advanced Vehicles Division - Aeronautics Directorate
June 25	Long Duration Exposure Facility	Dr. William Kinard Materials Division - Structures Directorate
July 2	Nondestructive Evaluation: What's Up Doc?	Dr. Joseph Heyman Instrument Research Division - Electronics Directorate
July 9	HL 20 Personnel Launch System	Dr. Kelli Willshire Information Systems Division - Flight Systems Directorate
July 23	Artificial Neural Networks	Donald Soloway Information Systems Division - Flight Systems Directorate

6/5/91

LARSS CAREER AND GRADUATE EDUCATION CONFERENCE

ACTIVITIES CENTER
BLDG 1222
JULY 12, 1991

9:15-9:30 REGISTRATION

9:30-10:00 OPENING REMARKS   Dr. Mary Lewis
Employee Development
Specialist
Human Resource
Management Division

Session I---CAREERS

10:00-10:30 A. The NASA Experience   Former LARSS Participants
Now Working at NASA

Robert D. Braun
Aerospace Technologist
Space Systems Division

Christyl M. Chamblee
Aerospace Technologist
Flight Electronics Division

Jerry L. Garcia
Aerospace Technologist
Flight Electronics Division

Glenn D. Hines
Aerospace Technologist
Flight Electronics Division

Luther N. Jenkins
Aerospace Technologist
Fluid Mechanics Division

Stephanie A. Wise
Aerospace Technologist
Flight Electronics Division

10:30-10:45	Question and Answer Session	
10:45-11:30	B. Employment Opportunities at NASA	Mr. Don Petrine Head, Personnel Management Section - Human Resource Management Division
11:30-1:00	LUNCHEON	
	Guest Speaker Advantages of Graduate Education	Dr. Theodore Habarth Vice President, Educational Programs - Director, GEM Programs John Hopkins University

Session II---GRADUATE EDUCATION

1:00-1:30	A. Making a Sound Choice of Graduate School	Dr. Demetrius Venable Director, Graduate School Hampton University
1:30-1:45	B. NASA's Financial Aid for Graduate Education	Dr. Samuel E. Massenberg University Affairs Officer
1:45-2:00	C. The Joint Institute for Advancement of Flight Sciences (JIAFS) Program	Dr. Michael K. Myers George Washington University
2:00-2:15	D. Graduate Opportunities	Dr. Oktay Baysal Director, Graduate Programs Old Dominion University
2:15-2:45	E. Fellowship Programs	Ms. Christine O'Brien Program Supervisor Ford Foundation Programs National Research Council
2:45-3:00	Question and Answer Session	

MINORITIES PARTICIPATING IN 1991 LARSS PROGRAM

	University	Ethnicity
1.	Christopher Newport College	Black - 1 American Indian - 1
2.	Elizabeth City State University	Black - 1
3.	Fayetteville State University	Black - 1
4.	Florida International University	Hispanic - 1
5.	Hampton University	Black - 4
6.	Norfolk State University	Black - 3
7.	North Carolina A&T State University	Black - 2
8.	North Carolina State University	Black - 1
9.	Old Dominion University	Black - 1
10.	University of Oklahoma	Asian - 1
11.	University of Puerto Rico, Mayaguez	Hispanic - 4
12.	University of Virginia	Asian - 1 Black - 1
13.	Virginia Polytechnic Institute & State University	Asian - 1

(26.6%)

HBCUs PARTICIPATING IN 1991 LARSS PROGRAM

UNIVERSITY	NO. OF PARTICIPANTS	
Elizabeth City State University	1	
Fayetteville State University	1	
Florida A & M University	1	
Hampton University	4	
Norfolk State University	3	
North Carolina A&T State University	2	
Total HBCU Participants	12	(13%)

Convection in vertical Bridgman configurations

by

Ranga Narayanan
Professor of Chemical Engineering
University of Florida, Gainesville, Fl 32611

Vertical Bridgman growth of compound semiconductors is associated with natural convection. The natural convection is of two types viz: buoyancy driven and surface tension gradient driven. The former (Rayleigh) is of importance under earth's gravity and may be due to adverse temperature or solutal gradients in the liquid melt. Surface tension gradient or Marangoni convection is important when we have liquid encapsulated Bridgman growth. In this configuration a viscous but lighter fluid overlies the melt of the compound semi-conductor in question. This provides a suitable diffusion barrier of volatile constituents but in the process an interface between the liquids is formed and this in turn can generate convection. This convective phenomenon arises because of surface tension gradients that ar promoted through a potential such as temperature or concentration gradients. We are interested in tracing the convective profiles in two configurations- these are the pure Rayleigh convective mode and the combined Rayleigh - Marangoni mode. In order to do so we conducted a numerical investigation that involved a 'finite volume' calculation. The governing equations were integrated about a cell volume, using the Gauss Theorem and the volume variables like temperature and velocity were related to the surface variables. In order to solve for the pressure field we employed the continuity equation and the residuals resulted in a Poisson equation. The results and comments for the Rayleigh and Marangoni problems in a vertical cylinder or Bridgman configuration were as follows:

a)   Three- dimensional and two- dimensional disturbances on the three dimensional equations were examined. The steady solutions converged to two- dimensional axisymmetric motion for cylinders that had an aspect ratio of unity or less (aspect ratio is defined as height/radius). The flows were three dimensional for aspect ratios greater than unity.

b)   The results were compared to those of Neumann (1990). The total energy of the flow was computed as a function of problem time. It was observed that the energy reached a steady state much sooner than the individual velocity components. The criterion for convergence used by Neumann is therefore suspect.

c)   The calculations were repeated for the pure Marangoni problem and the results of Vrentas, Narayanan and Agrawal (1981) were verified.

On a separate level, linearized stability calculations for the onset conditions for Rayleigh - Marangoni in a laterally unconstrained bilayer were performed and the results are given below:
a)   Liquid bilayers heated from above become more stable as the gravitational level is increased. As a result bottom- seeded crystal growth is better performed on earth.

b)   Liquid bilayers that are heated from below become more stable as the gravitational level is decreased.

c)   The above results will change for narrow geometries and so this raises the important question on what effect side walls will have on the stability of the flow.

References:

1) Neumann.G.,"Three-dimensional numerical simulation of buoyancy-driven convection in vertical cylinders heated from below.",J.Fluid.Mech.(1990),**214**,pp 559-578

2) Vrentas J.S.,Narayanan R. and Agrawal S.S., "Free surface convection in a bounded cylindrical geometry",Int. J. heat and Mass Transfer,**24**, (1981),pp. 1513-1529

Implementation Of The Lanczos Eigen-Solver For The CSI Code

On High Performance Computers

by

Duc T. Nguyen
Associate Professor
Department of Civil Engineering
Old Dominion University
Norfolk, VA 23529-0241

EXTENDED ABSTRACT

Lanczos algorithm for the solution of generalized eigenvalue problems have been receiving a lot of attention in recent years [1 - 7] due to its computational efficiency.

The basic steps involved in the Lanczos algorithm are summarized in Table 1 [6]. In Table 1, M is the structural mass matrix, and K_σ is defined as

$$K_\sigma = K - \sigma M$$

were σ is the shift factor and K is the structural stiffness matrix.

The focus of this research work is to implement a Lanczos algorithm for the Control-Structure Interaction (CSI) code which can exploit both parallel and vector capabilities provided by modern, high performance computers (such as the Alliant, and Cray-YMP). A partial restoring orthogonality scheme is also developed and incorporated into the basic Lanczos algorithm.

From Table 1, major computational time in the Lanczos algorithm can be identified as:
I.   Matrix-vector multiplication (see steps 1b, 1d, and 2e)
II.   Matrix factorization (see step 2a)
III. Forward/Backward elimination (see step 2a)

Step 2a (in Table 1) involves the solution for system of simultaneous linear equations. It should be emphasized here that factorization of the matrix K_σ need be done only once. The forward/backward elimination phase, however, needs to be done repeatedly.

The solution for system of simultaneous linear equations in step 2a can be obtained very effectively by incorporating the newly developed Parallel Vector equation SOLVEr [8], PVSOLVE, into the Lanczos procedure. Furthermore, to be consistent with the data structure for PVSOLVE, the structural mass matrix M also needs to be stored in a row-oriented, variable-band fashion.Effective (mass) matrix-vector multiplication which exploits

both parallel and vector speed has also been developed.

The numerical performance (in terms of accuracy and efficiency) of the proposed parallel-vector Lanczos algorithm is demonstrated by solving for the frequencies and modeshapes of the Phase Zero CSI model [9, 10] as shown in Figure 1 on the Alliant and Cray-YMP multi-processor high performance computers. The superior performance of the Lanczos algorithm is illustrated in Table 2.

References

1. C. Lanczos, "An Iteration Method for the Solution of the Eigenvalue Problem of Linear Differential and Integral Operator," *Journal of Research of the National Bureau of Standards*, 45 (1950), 255-281.

2. G. Golub, R. Underwood, and J.H. Wilkinson, "The Lanczos Algorithm for the Symmetric $Ax = \lambda Bx$ Problem," Tech. Rep. STAN-CS-72-720, Computer Science Department, Stanford University, 1972.

3. B.N. Parlett and D. Scott, "The Lanczos Algorithm with Selective Orthogonalization," *Mathematics of Computations*, 33, No. 145 (1979), 217-238.

4. B. Nour-Omid, B.N. Parlett, and R.L. Taylor, "Lanczos versus Subspace Iteration for Solution of Eigenvalue Problems," *International Journal for Numerical Methods in Engineering*, 19 (1983), 859-871.

5. B. Nour-Omid and R.W. Clough, "Dynamic Analysis of Structures Using Lanczos Coordinates," *Earthquake Engineering and Structural Dynamics*, 12 (1984), 565-577.

6. T.J.R. Hughes, *The Finite Element Method: Linear Static and Dynamic Finite Element Analysis*, Prentice-Hall, Inc. (1987).

7. O.O. Storaasli, S.W. Bostic, M. Patrick, U. Mahajan, and S. Ma, "Three Parallel Computation Methods for Structural Vibration Analysis," *Proceedings of the AIAA/ASME/ASCE/AHS 29th Structures, Structural Dynamics and Materials Conference*, Williamsburg, VA, April 18-20, 1988, pp. 1401-1411, AIAA Paper No. 88-2391.

8. T.K. Agarwal, O.O. Storaasli, and D.T. Nguyen, "A Parallel-Vector Algorithm for Rapid Structural Analysis on High-Performance Computers," *Proceedings of the AIAA/ASME/ASCE/AHS 31st Structures, Structural Dynamics and Material Conference*, Long Beach, CA, April 2-4, 1990, AIAA Paper No. 90-1149. Also appeared in NASA Technical Memorandum 102614 (For early Domestic Dissemination only), April 1990.

9. W.K. Belvin, K.E. Elliott, A. Bruner, J. Sulla, and J. Bailey, "The LaRC CSI Phase-0 Evolutionary Model Testbed: Design and Experimental Results," Presented at the 4th Annual NASA/DOD Conference on Control/Structures Interaction Technology, November 5-7, 1990, Orlando, Florida.

10. P.G. Maghami, S.M. Joshi, and S. Gupta, "Integrated Control-Structure Design for a Class of Flexible Spacecraft," Presented at the 4th NASA/DOD CSI Technology Conference, November 5-7, 1990, Orlando, Florida.

TABLE 1: The Lanczos Algorithm
Given an Arbitrary vector r_0 then:

1. Set

   a. $q_0 = 0$

   b. $\beta_1 = \left(r_0^T M r_o \right)^{1/2}$

   c. $q_1 = \dfrac{r_0}{\beta_1}$

   d. $p_1 = M q_1$

2. For $j = 1, 2, \ldots$, repeat:

   a. $\bar{r}_j = K_a^{-1} p_j$

   b. $\hat{r}_j = \bar{r}_j - q_{j-1} \beta_1$

   c. $a_j = q_j^T M \hat{r}_j = p_j^T \hat{r}_j$

   d. $r_j = \hat{r}_j - q_j \alpha_j$

   e. $\bar{p}_j = M r_j$

   f. $\beta_{j+1} = (r_j^T M r_j)^{1/2} = (\bar{p}_j^{-T} r_j)^{1/2}$

   g. if enough vectors, then terminate the loop

   h. $q_{j+1} = \dfrac{1}{\beta_{j+1}} r_j$

   i. $p_{j+1} = \dfrac{1}{\beta_{j+1}} \bar{p}_j$

Figure 1: Phase Zero CSI Finite Element Model
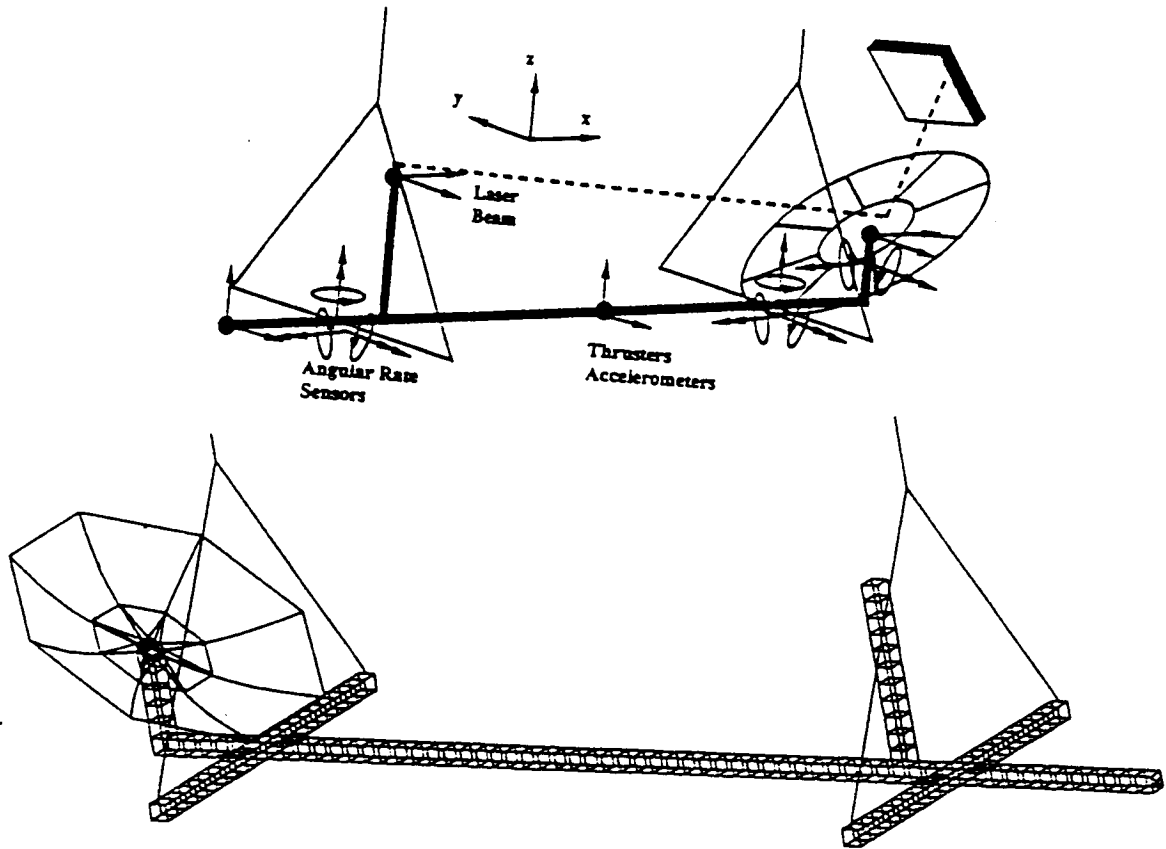
TABLE 2: Alliant CPU Time Comparison of Subspace and Lanczos algorithms for the Phase Zero CSI Model

No. of Requested Eigen-pairs	Subspace Elapsed Time (Use PVSOLVE) on ALLIANT	Lanczos Elapsed Time (Use PVSOLVE) on ALLIANT
10	50.3^{sec}	38.3^{sec}
15	68.3	41.3
20	79.2	46.9
50	421.2	89.1
100	2083.9	209.5
	$\lambda_{100} = 193.878334$	$\lambda_{100} = 193.875783$

MECHANICAL PROPERTIES OF 2D AND 3D BRAIDED TEXTILE COMPOSITES

by

Timothy L. Norman
Department of Mechanical and Aerospace Engineering
West Virginia University
Morgantown, WV 26506

Textile composite materials are receiving recognition as potential candidate materials for increased damage tolerant designs on future aircraft. Design for damage has become especially important as the fleet of aircraft age beyond their design fatigue life. Textile composites can be designed to any layup providing strength tailoring capabilities. Fibers and resins can be changed to optimized materials performance. Thus, there are a large number of material combinations, layup configurations and fiber architectures to chose from which provide a large array of potential material candidates. Common examples of textile composite materials are: stitching, knitting, 2D and 3D weaving and braiding. Textile composites offer through-the-thickness reinforcement which is the key feature for preventing propagation of damage. A number of publications are available in the literature which describe general topics in textiles such as manufacturing, nomenclature and fiber architecture (Chou and Ko, 1989; Ko, 1989; Ko et al., 1986, Ko and Pastore, 1990; Mohamed, 1990; and, Zawislak and Maiden, 1988).

Although through-the-thickness reinforcement increases damage tolerance, the performance of textile composites, e.g. strength, stiffness, toughness, is not clearly understood. In the manufacturing process, bundles of fibers called yarns are distorted to provide the through the thickness geometry. This distortion may have detrimental effects on other mechanical properties, i.e. decrease stiffness and strength.

The purpose of the summer research was to determine the mechanical properties of 2D and 3D braided textile composite materials. Specifically, 2D and 3D braided textile materials designed for tension or shear loading were tested under static loading to failure to investigate the effects of braided. The overall goal of this work was to provide the structural designer with an idea of how textile composites perform under typical loading conditions.

A test program was developed around 2D and 3D textile composite materials of two fiber architectures, one designed for end load (tension) and one designed for shear, using two resin systems, PEEK and and an epoxy applied through RTM. Specimens were tested in the following configurations: unnotched tension, open hole tension, unnotched compression and compression after impact. After testing, ultimate stress, ultimate strain, elastic modulus, and Poisson's ratio were determined from stress-strain curves. A typical stress-strain curve is shown in Figure 1. Table 1 shows the results of tests conducted.

From test results for unnotched tension, it was determined that the 2D is stronger, stiffer and has higher elongation to failure than the 3D. It was also found that the PEEK resin system was stronger, stiffer and had higher elongation at failure than the RTM epoxy. Open hole tension tests were important to determine the effect of notches in braided composites. Results showed that PEEK resin is more notch sensitive than RTM epoxy. Of greater significance, it was found that the 3D is less notch sensitive than the 2D. The literature suggests that the shear design specimen is less notch sensitive than the tension design specimen, however no data was available here to make this comparison. Strain gages mounted on the specimen showed strain magnitudes as expected: stress concentration at the hole, remote stresses at the edge gage. Unnotched compression tests indicated, as did the tension tests, that the 2D is stronger, stiffer and has higher elongation at failure than the 3D. It was also found as before that the PEEK was stronger, stiffer and has higher elongation at failure than the RTM epoxy. Results also indicated that the tension specimen was stronger and stiffer than the shear specimen, however the shear specimen had higher elongation at failure as expected. Poisson's ratio found from the longitudinal and transverse gages was determined to be large, variable and nonlinear, much different than conventional composite materials. The most encouraging results were from the compression after impact. The 3D braided composite showed a compression after impact failure stress equal to 92% of the un-impacted specimen. The 2D braided composite failed at about 67% of the un-impacted specimen. Compression after impact is a primary motivation for using textile performance, i.e. higher damage tolerance is observed in textiles over conventional composite materials. This is observed in the above results, especially in the 3-D braided materials.

REFERENCES

Chou, Tsu-Wei, and Ko, F. K., *Textile Structural Composite,* Elsevier, New York, 1989.

Ko, F. K., "Preform Fiber Architecture for Ceramix-Matrix Composites," *Ceramic Bulletin,* Vol. 68, No. 2, 1989.

Ko, F. K., Chu, H., and Ying, Edwina, "Damage Tolerance of 3-D Braided Intermingled Carbon/PEEK Composites," In *Advanced Composites: The Latest Developments; Proceedings of the Second Conference,* Dearborn, MI, Nov. 18-20, 1986, pp. 75 - 88.

Ko, F. K., Pastore, C. M., *Atkins & Pearce Handbook of Industrial Braiding,* Atkins & Pearce, Covington, KY, October, 1989.

Mohamed, M. H., "Three-dimensional Textiles", *American Scientist,* Vol. 78, pp. 530-541, Nov.-Dec., 1990.

Zawislak, S.P., and Maiden, J. R., "Advanced Weaving concepts for complex Structural Preforms", *Fiber-Tex,* pp. 91-111, Sept. 13-15, 1988.

10) UT 2-A-1-1 PEEK

Legend:
- AXIAL STRAIN
- TRANS STRAIN
- Exten
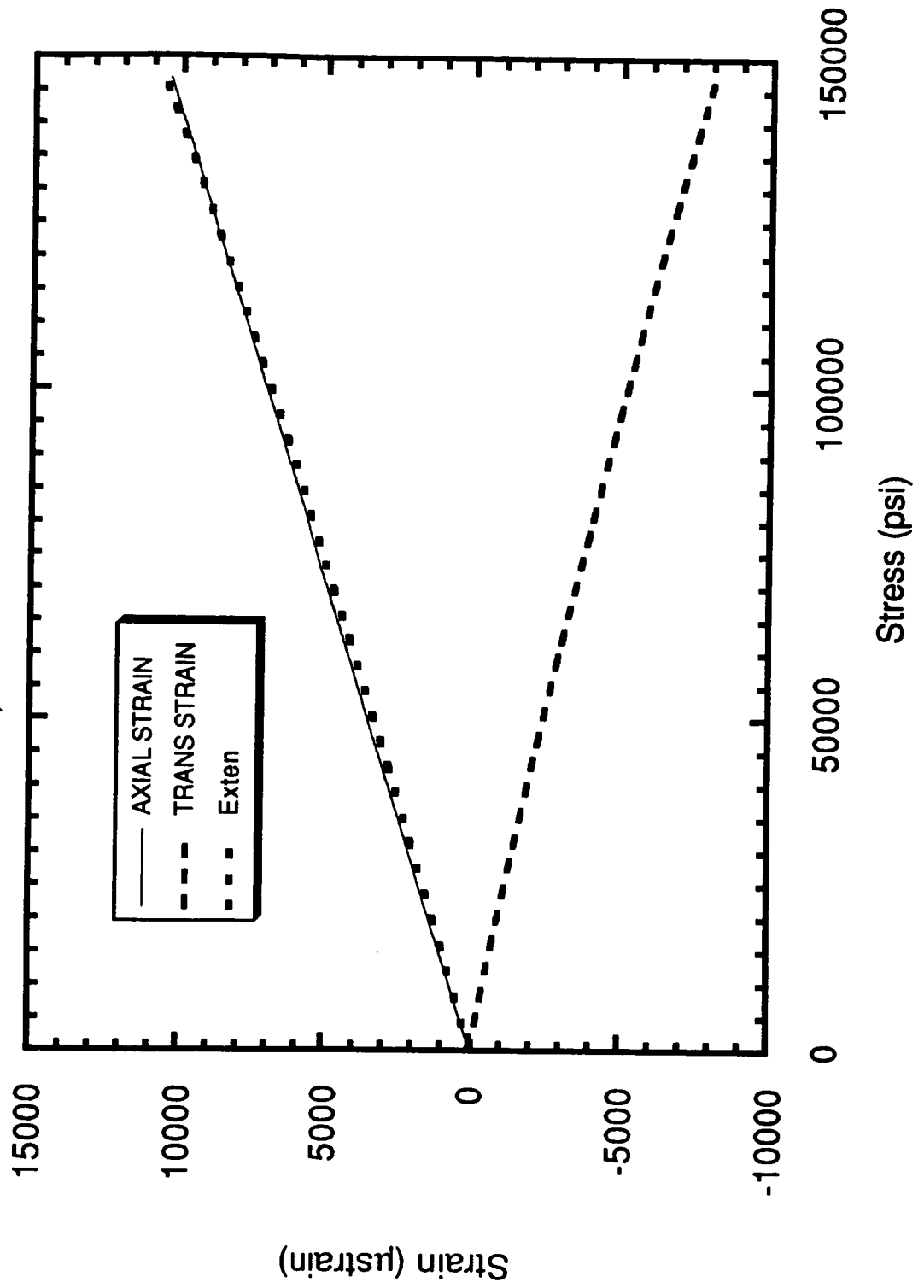
Figure 1. Stress-Strain curves for 2D tension specimen with PEEK resin.

171

Table 1: 2-D and 3-D Braided Average Mechanical Properties

Fiber Architecture	Loading	Failure Stress (ksi)	Failure Strain (μstrain)	Modulus (Msi)	Poisson's Ratio
2-D Graphite/PEEK Architecture A	Unnotched Tension	137.9	10,262	13.39	.4 - .82
	Open Hole Tension	81.7	5631	13.82	---
	Unnotched Comp.	71.1	5256	14.59	.56 - .65
	CAI	47.7	---	---	---
Architecture B	Unnotched Comp.	31.4	5672	6.72	.5 - .9
2-D Graphite/RTM Architecture A	Unnotched Tension	106.2	8624	11.94	.78 - 1.3
	Open Hole Tension	73.3	5313	13.43	---
3-D Graphite/PEEK Architecture A	Unnotched Tension	92.0	9665	10.44	.45 - .60
	Open Hole Tension	67.8	5263	12.98	---
	Unnotched Comp.	62.3	5551	12.05	.57 - .71
	CAI	57.4	---	---	---
Architecture B	Unnotched Comp.	39.5	5557	8.99	.43 - 1.6
3-D Graphite/RTM Architecture B	Unnotched Tension	77.8	11,076	7.40	.57 - 1.3
	Open Hole Tension	57.0	10,881	6.50	---
	Unnotched Comp.	20.9	3941	6.52	.7-.82

A - Braided geometry optimized for end load [60% Braided at 20 Degrees, 40% 0 Degrees]
B - Braided geometry optimized for shear [100% Braided at 35 Degrees]

172

Incorporating Affective Bias in Models of Human Decision Making

by

Thomas E. Nygren
Associate Professor
Department of Psychology
Ohio State University
Columbus, Ohio 43210

Research on human decision making has traditionally focused on three issues: (1) process or how people actually make decisions, (2) quality or how good their decisions are, and (3) improvement or can decision behavior be made better. Despite a rapid growth in decision making research over the past two decades, theoretical and empirical work has been narrowly driven by models incorporating some form of the maximization of expected utility principle. For example, according to the current leading model, Kahneman and Tversky's [2] Prospect Theory model, alternatives are evaluated as a function of the psychological values of the outcomes of the decision alternatives multiplied by the subjective weights assigned to the corresponding probabilistic events that determine them.

Recent research suggests that this model is inadequate. Affective as well as cognitive components drive the way information about relevant outcomes and events is perceived, integrated and used in the decision making process. At least four categories of affective influences have been identified and studied including how the individual frames outcomes as "good" or "bad", whether the individual anticipates regret in a decision situation, the affective mood state of the individual, and the psychological stress level anticipated or experienced in the decision situation. A focus of the current work has been to propose empirical studies that will attempt to examine in more detail the relationships between the latter two critical affective influences, mood state and stress, on decision making behavior.

A second and equally important purpose of the research is to develop an experimental paradigm that goes beyond the traditional gambling or investment context in the decision making literature. One important complex environment that is rich in decision making and is well-suited for this type of research is that of flight. In addition to providing obvious face validity to the research, the many subtasks of flight make it particularly useful for studying the impact of workload and stress on decision making. A particularly useful tool for doing the research is the Multi-attribute Task Battery developed by Comstock (see Arnegard & Comstock [1]) at NASA LaRC. The MAT is a PC-based battery of tasks that incorporates activities analogous to those performed

in flight. Figure 1 illustrates the video monitor display of the tasks included in the MAT -- monitoring, tracking, auditory communications, and resource management.

Proposed Studies

Study 1 will attempt to calibrate the subtasks on the MAT according to their perceived levels of mental workload. In particular, approximately four levels of difficulty of each subtask will be developed. Individuals will be asked to evaluate combinations of the subtasks according to perceived levels of mental workload. Subjects' judgments will be scaled to obtain a standard baseline measure of workload levels that we and others may use to study workload in flight.

Study 2 will be an attempt to examine the effects of positive and negative affect or mood on MAT performance. In particular, we are interested in whether strong differences that have been previously found in the decision making behavior of people in good and bad moods will generalize to decision strategies used in this kind of monitoring task.

Study 3 will examine the effects of workload level on decision strategy in the monitoring task. We are interested in both the effects of very low sustained levels of workload (boring tasks) and very high levels. We hope to determine what comprises an optimal level of workload and whether this level might produce a "natural" positive affective state. Similarly, we will attempt to determine if very low and very high workload lead to different types of negative affect and/or stress. Is the effect of boredom or very low workload comparable to what has been labeled ambient stress -- stress due to variables independent of the task? Does it lead to fewer decision alternatives being examined and to more inconsistency in decisions? An additional component of Study 3 would be to vary training on the resource management subtask in an attempt to manipulate expertise.

A number of additional studies are being proposed in conjunction with anticipated results from the first three. The actual designs of these studies will become clearer as data becomes available.

References

1. Arnegard, R. J., and Comstock, J. R. "Multi-Attribute Task Battery: Applications in Pilot Workload and Strategic Behavior Research." Paper presented at the 6th International Symposium on Aviation Psychology, Columbus, Ohio, May, 1991.

2. Kahneman, D., and Tversky, A. "Prospect Theory: An Analysis of Decisions Under Risk." Econometrika, 47, 1979, 263-291.
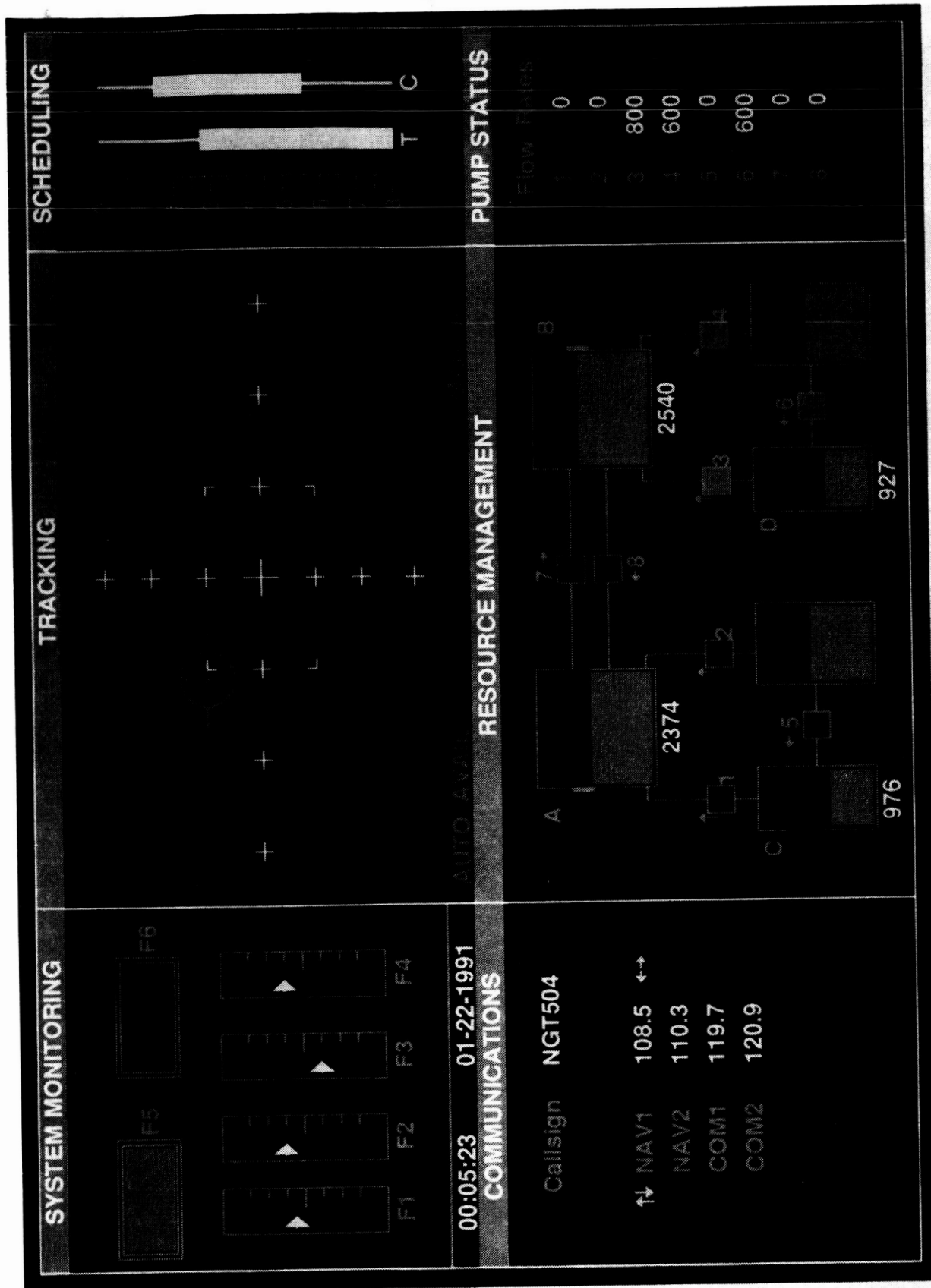
Figure 1. The Multi-Attribute Task Battery Display

The Use of Carboranes as Oxidation Inhibitors for Carbon-Carbon Composites

by

Dr. John T. Petty
Assistant Professor
Department of Natural Sciences
Longwood College
Farmville, Virginia 2390

Carbon-carbon composites have many beneficial properties for use in aerospace applications including their high specific strength and modulus at elevated temperatures. Unfortunately, they share with all carbon based substances a strong tendency to burn when heated in air. In order to exploit their good qualities, it is necessary to slow or prevent their oxidation during use.

The are two methods of protecting the composites, coating the composite and adding inhibitors directly to the resin. An effective coating must adhere well to the carbon-carbon material over a broad temperature range (0 - +1700 °C) Since the composites have very low coefficients of thermal expansion, this results in cracking and spalding of the coatings. Commercially available coatings try to overcome this problem by including some form of boric oxide glass to act as a sealant for these cracks.

The second method is to add inhibitors directly to the composite. Commercial inhibitors are usually based on boron carbide or pure boron along with other glass forming compounds. Since these materials are generally insoluble in the resins, they tend to settle out of the resin during heating, and there are problems with the undissolved material abrading the fibers during molding.

Molecular inhibitors could offer the same kind of protection, with the added advantage of being able to form a homogeneous solution with the resin. Since boron oxides are known to provide the desired kind of protection, molecular compounds based on boron seem reasonable candidates to test as inhibitors.

Dicarbadodecaborane (12), more commonly referred to as "carborane", is a molecular compound with the chemical formula $C_2B_{10}H_{12}$. Carborane clusters have the shape of an icoshedron and exist in three isomeric forms depending on the relative positions of the two carbons in the cluster. (Figure 1) Derivatives are formed by

replacing the terminal hydrogens on either carbon or boron with other groups.

Carboranes have many properties to recommend their use as molecular inhibitors including a high mass percent boron and the ability to form solutions with the phenolic resins being tested. They are chemically very stable, resisting attack by strong acids or oxidizing agents and not decomposing thermally until >600°C. The latter is an important consideration since the non-carbon components being expelled from the resin at lower temperatures can react with other additives and remain trapped in the composite. The carboranes release their borons only after the matrix has been reduce to essentially carbon, thus limiting the formation of compounds to carbide type substances.

Samples containing from 5%-25% by mass of meta-carborane, 8%-17% by mass 1-methyl-ortho-carborane, 10% boron powder and the neat phenolic resin were prepared for testing. All the samples contained about 5 grams of resin, were cured in air and then pyrolyzed under nitrogen at >850°C to form a glassy carbon material. The pyrolyzed samples were cut into rectangular pieces and their rates of oxidation measured in a thermal gravimetric analyzer (TGA) in flowing air (20 torr), at temperatures of 700°C and 900 °C. The results for representative samples are shown in Figures 2 & 3.

All the inhibited samples initially showed substantial reductions in the rate of oxidation compared to the uninhibited material. A more significant development became apparent only after the samples had been partially oxidized. The samples which originally had contained a high mass percent carborane continued to improve until their rates were less than 5% of that of the uninhibited material.

An examination of the oxidized samples using both a microscope and a scanning electron micrograph (SEM) demonstrated that all the inhibitors had responded to oxygen attack by forming partial coatings of boron oxides, but the surface of the sample which originally contained 10% boron powder showed many larger and deeper pits then any of the samples inhibited with carboranes. Clearly, the carboranes had done a better job of distributing their boron uniformly through out the matrix and so these samples showed much less damage on their exposed surfaces.

In conclusion, the carboranes have been shown to be excellent materials for obtaining high uniform loadings of boron inhibitors in glassy carbon materials and thus reducing their rates of oxidation. Further, there are is evidence that the use of substituted derivatives could provide more complete and thorough forms of protection.

Figure 1.
Dicarbadodecaborane (12)

$C_2B_{10}H_{12}$
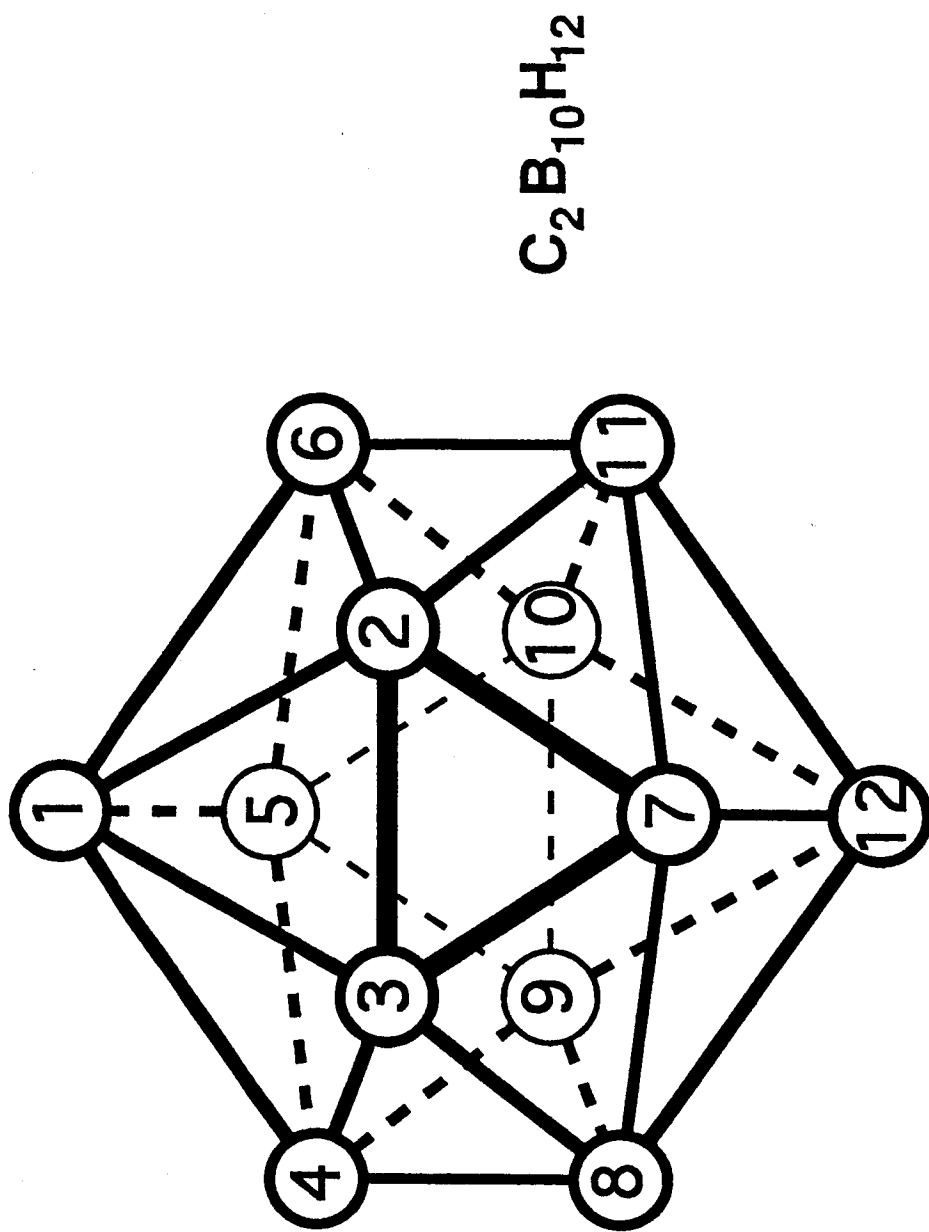
Three Isomers: 1,2 = Ortho-Carborane

1,7 = Meta-Carborane

1,12 = Para-Carborane

Figure 2.

Oxidation Rates of Pyrolyzed Resin Containing Various Inhibitors at 900 Celsius in Air

179
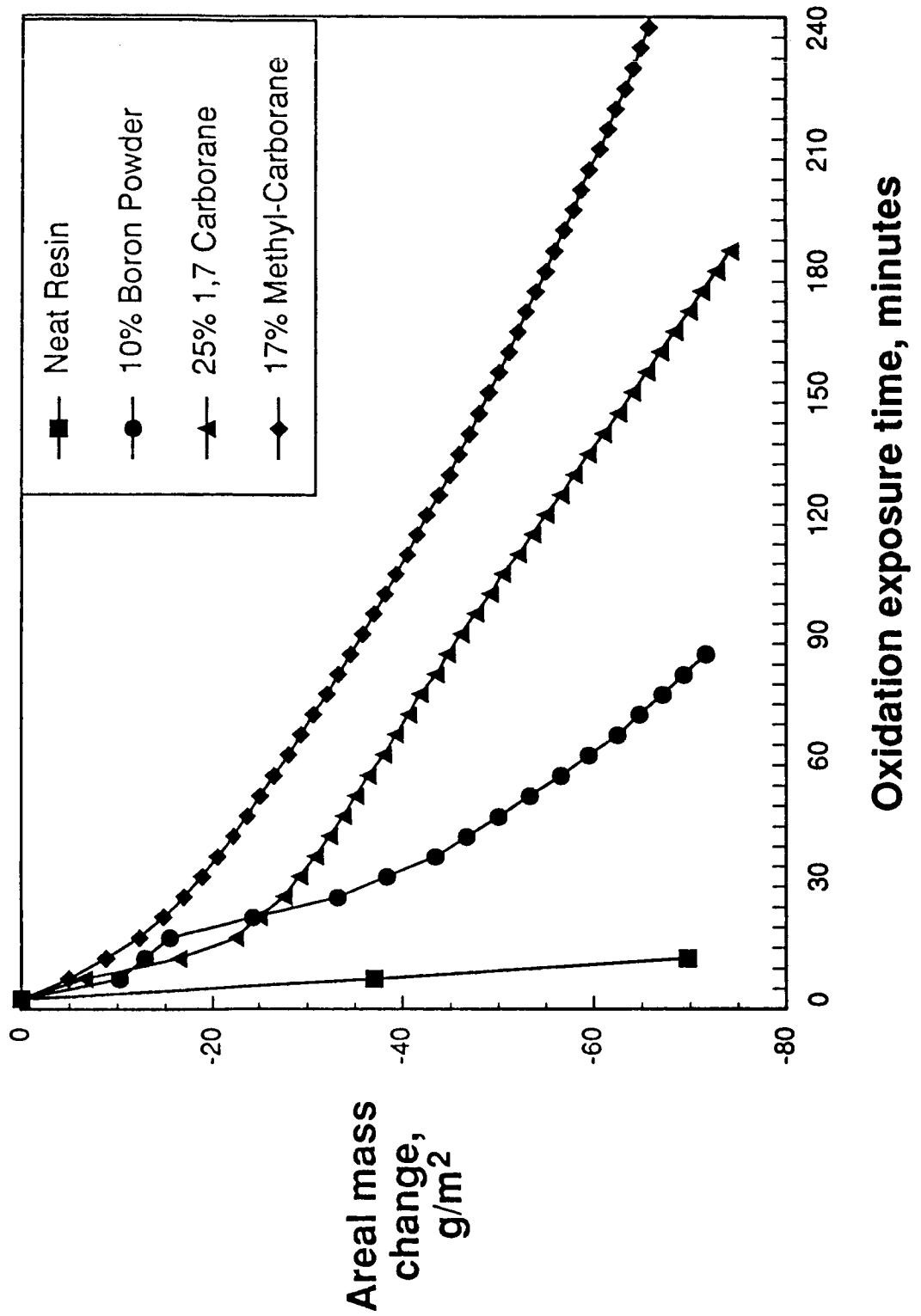
Figure 3.

Rates of Oxidation of Pyrolyzed Resin with Various Inhibitors at 700 Celsius in Air
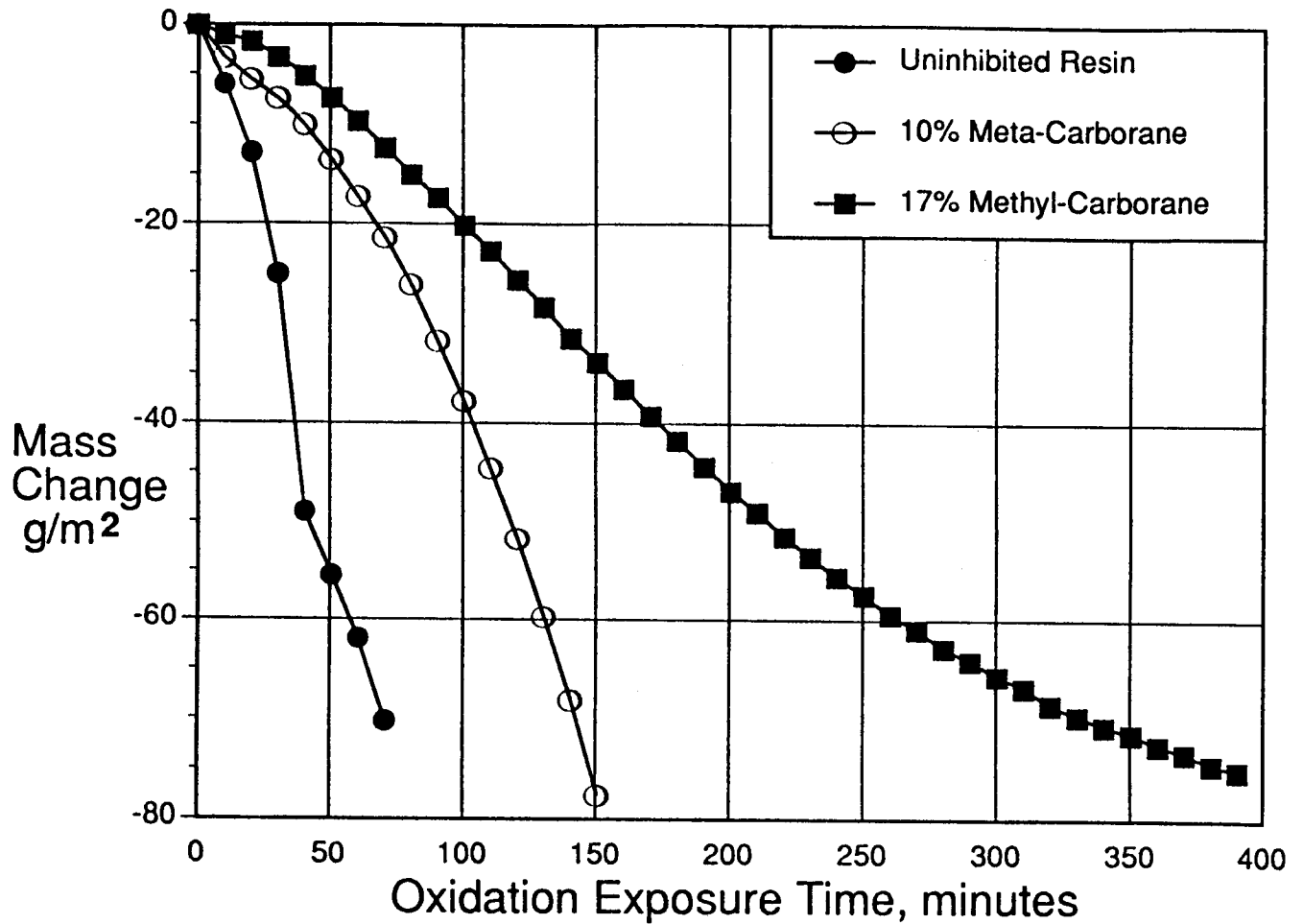
Naturally Induced Secondary Radiation in Interplanetary Space: Preliminary Analyses for Gamma Radiation and Radioisotope Production from Thermal Neutron Activation

by

Heriberto Plaza-Rosado
Professor
Department of Electrical and Computer Engineering
University of Puerto Rico
Mayaguez Campus
Mayaguez, Puerto Rico   00709

Thermal neutron activation analyses were carried out for various space systems components to determine gamma radiation dose rates and food radiation contamination levels. The space systems components selected were those for which previous radiation studies existed. These include: manned space vehicle radiation shielding, lunar habitat regolith shielding, liquid hydrogen propellant tanks for a Mars mission, and food supply used as space vehicle radiation shielding.

The computational method used is based on the fast neutron distribution generated by the BRYNTRN and HZETRN transport codes for GCR at solar minimum conditions and intense solar flares in space systems components. Fast neutrons slow down to thermal energies and their transport is assumed to be described satisfactorily by thermal neutron diffusion theory. Thermal neutron losses due to capture in (n, γ), (n, α) and (n,p) reactions is accounted for in a set of neutron activation differential equations which describes the formation of the radioactive isotopes. In shielding analysis only the (n, γ) reaction is considered, and prompt as well as delayed gamma rays are included in the volumetric radiation sources.

The gamma dose rates for soft tissue are calculated for water and aluminum space vehicle slab shields considering volumetric source self-attenuation and exponential buildup factors. In the case of the lunar habitat with regolith shielding a completely exposed spherical habitat was assumed for mathematical convenience and conservative calculations. Table I summarizes the gamma dose rates for the various space systems analyzed, and for comparison purposes the GCR and solar flares dose rates for the same components are given. Note that the gamma dose rates in all cases is not very significant.

Activation analysis of food supply used as radiation shielding is presented for four selected nutrients: potassium, calcium, sodium, and phosphorus. Radioactive isotopes that could represent a health hazard if ingested are identified and their concentrations determined. The results are presented in Tables II and III. For nutrients soluble in water it was found that all induced radioactivity was below the accepted maximum permissible concentrations.

References

1. Simonsen, L. C. ; and Nealy, J. E.; 1991: Radiation Protection for Human Missions to the Moon and Mars. NASA-TP 3079.

2. Townsend, L. W.; Nealy, J. E.; Wilson, J. W.; and Simonsen, L. C.; 1990: Estimates of Galactic Cosmic Ray Shielding Requirements During Solar Minimum. NASA-TM 4167.

3. Chilton, A. B.; et al.; C1984: Principles of Radiation Shielding, Prentice-Hall, Inc.

4. Sauer, H. H.; Zwickl, R. D., Ness, M. J. 1990: Summary Data for the Solar Energetic Particle Events of August through December 1989. Space Environment Lab, National Oceanic and Atmospheric Adm., Feb. 21.

5. Nealy, J. E.; Wilson, J. N.; and Townsend, L. W. , 1989: Preliminary Analyses of Space Radiation Protection for Lunar Base Surface Systems. SAE Tech. Paper ser. 891487, July

6. Nealy, J. E., et al.; Qualls, G. D.; Schnitzler, B. G.; and Gates, M. M.: Radiation Exposure and Dose Estimates for a Nuclear Powered Manned Mars Sprint Mission; 8th Symposium on Space Nuclear Power Systems, Jan 1991.

7. Weast, R. C.; CRC Handbook of Chemistry and Physics, 68th Edition, 1987-1988, CRC Press.

8. Chart of the Nuclides; Knolls Atomic Power Laboratory; General Electric Corp.; Naval Reactors; U. S. Department of Energy, 13th Edition, 1983.

Table I. Preliminary Results of Gamma Dose Rates Calculations Versus GCR or Solar Flares Dose Rates

Space System Component	Gamma dose Rates	GCR or Solar Flares Dose Rates
Manned Space Vehicle Shielding		
• GCR: aluminum slab (18.5 cms)	18.54 mrem/yr	30.9 rem/yr
• GCR: water slab (50 cms)	2.64 mrem/yr	22.9 rem/yr
• Solar flares: aluminum slab (18.5 cms)	7.60 mrem for 1 day	~ 10 rem for 1 day
Lunar Spherical Habitat Shielding		
• GCR: Lunar regolith (50 cms)	< 1 rem/yr	12 rem/yr
Liquid Hydrogen Tank		
• GCR: cylinder (r = 5.5 m, = 21.1 m)	< 0.2 for a 500 day mission	(27.8 - 36.7) rem for 500 day mission

Table II. Concentration of Radioisotopes from Thermal Neutron* Activation of Food Nutrients

Nutrient	Isotope	Relative Concentration**		Saturation Time	Half-life
		1 Year Period	Saturation Time		
Potassium (K^{39}, K^{40}, K^{41})	K^{42}	10^{-60}	10^{-19}	∞	12.36 hr
	Cl^{36}	10^{-35}	10^{-12}	∞	3×10^5 yr
	Cl^{38}	$\ll 10^{-35}$	10^{-22}	∞	37.2 min
Calcium (Ca^{40}, Ca^{42}, Ca^{43}, Ca^{44}, Ca^{46})	Ca^{45}	10^{-88}	10^{-27}	∞	165 days
	Ca^{47}	10^{-123}	10^{-42}	∞	4.5 days
Sodium (Na^{23})	Na^{24}	10^{-20}	10^{-20}	150 hr	15 hr
Phosphorous (P^{31})	P^{32}	10^{-18}	10^{-18}	140 days	14 days

*10^8 neutrons/cm^2-yr

**atoms/atoms of nutrient, order of magnitude given

Table III. Concentration of Radioisotropes from Thermal Neutron Activation of Food Nutrients Versus Maximum Permissible Concentrations (MPC) Values

Nutrient	Isotope	Concentration (1 year period) (μC_i/gm of nutrient)	Fluid milk (nonfat) (μC_i/gm of H_2O)	MPC* (μC_i/gm of H_2O)
Sodium	N_a^{24}	10^{-7}	1.26×10^{-9}	10^{-6}
Phosphorus	p^{32}	10^{-7}	2.47×10^{-8}	5×10^{-4}

* Occupational exposure; for nutrients soluble in water

Analysis of Pressure-Broadened Ozone Spectra
in the 3-μm Region

Eleanor S. Prochaska
Department of Mathematics and Computer Science
Western Carolina University
Cullowhee, N.C.

The presence of a layer of photochemically produced ozone in the stratosphere has long been recognized as vital to life on earth, as it provides a shield from the harmful ultraviolet component of sunlight. A deficit in the ozone layer was observed over Antarctica in the mid 1980's, motivating considerable effort to improve and standardize methods of measuring and monitoring ozone in the atmosphere. More recently, increased atmospheric ozone at the earth's surface has been found to be of significant environmental concern. Spectroscopic methods are the basis for remote sensing techniques to measure atmospheric content of many chemical species, including ozone, on both global and regional scales. As technology continues to improve, the understanding of the spectra of these species becomes increasingly important in accurate retrieval of atmospheric composition data obtained by remote sensing techniques.

The Molecular Spectroscopy Lab at NASA-Langley has been involved in a long term effort to carefully and fully characterize the infrared spectra of small molecules of atmospheric interest, including methane, water vapor, carbon dioxide, and ozone, and their isotopic counterparts. High resolution gas phase infrared spectra are obtained using both a tunable diode laser system, and the McMath Fourier transform spectrometer at the Kitt Peak Solar Observatory. Spectra are obtained at various sample pressures and temperatures, both for pure gas samples, and for samples containing mixtures of the species of interest diluted in nitrogen, oxygen, or air. Air-diluted samples simulate the atmosphere at different altitudes, by varying temperature and pressure. Nitrogen- and oxygen-diluted samples allow theoretical studies of the interactions of ozone with these air components individually. Spectral parameters are modeled to the observed spectra by a non-linear least squares fitting technique. Position, intensity and half-width are determined for each well-isolated feature of reasonable intensity in the spectra. These parameters are of interest in theoretical studies, as well as in allowing more accurate interpretation of remote sensing data.

This work involves the analysis of a series of McMath FTIR spectra of ozone broadened by mixing with air (four different pressures), nitrogen (three pressures), or oxygen (three pressures). Each spectrum covers the region from 2396 to 4057 cm^{-1}. This study has focused on the $3\nu_3$ band in t 3000 to 3060 cm^{-1}

region. The band is analysed by first dividing its region into small (0.5 to 2.0 cm^{-1}) intervals containing a few well isolated absorption lines of reasonable intensity. Each of these small intervals is "fit" by multiple iterations of the non-linear least squares program until residuals (difference between calculated and observed spectrum, as a percent of the strongest intensity in the interval) are minimized to a "reasonable" value which corresponds to the noise level of the measured spectrum. Position, intensity and half-width are recorded for later analysis.

From the measured half-widths, a pressure broadening coefficient has been determined for each absorption line. These broadening coefficients are shown in Figure 1 as a function of lower state rotational quantum number. The broadening coefficients show a slight decrease with increasing rotational quantum number. Pressure shifts have been determined by comparing observed line positions in the spectra of the diluted ozone samples to tabulated line positions determined from spectra of pure gas samples. Pressure shifts are shown as a function of quantum number in Figure 2, and show little dependence on rotational quantum number. Broadening and shift coefficients for this absorption band have not been examined before, but comparisons can be made to similar studies of other ozone bands. In particular, it is noteworthy that the observed shifts for the $3\nu_3$ band are on the order of three times the shifts for the ν_1 band (1), showing a dependence on the energy of the vibration, as ν_1 occurs at about 1100 cm^{-1} and $3\nu_3$ at about 3000 cm^{-1}. It is also of interest that the broadening coefficient for air is between those of nitrogen and oxygen. In particular, the broadening coefficient for air can be expressed as a weighted average of those for nitrogen and oxygen, where the weighting coefficients are those of the relative abundance of each gas in air. Comparisons to other work on ozone (2,3,4,5) indicate that the broadening and shift coefficients determined in this study are consistent with those determined in other spectral regions.

(1) M. A. H. Smith, C. P. Rinsland, V. Malathy Devi, D. Chris Benner, and K. B. Thakur, *J. Opt. Soc. Amer. B.* 5, 585-592 (1988).

(2) M. N. Spencer and C. Chackerian, Jr., *J. Mol. Spectrosc.* 146, 135-142 (1991).

(3) J. J. Plateaux, S. Bouazza, and A. Barbe, *J. Mol. Spectrosc.* 146, 314-325 (1991).

(4) A. Barbe, S. Bouazza, and J. J. Plateaux, *Applied Optics* 30(18), 2431-2436 (1991).

(5) J. M. Hartmann, C. Camy-Peyret, J. M. Flaud, J. Bonamy, and D. Robert, *J. Quant. Spectrosc. Radiat. Transfer* 40(4), 489-495 (1988).
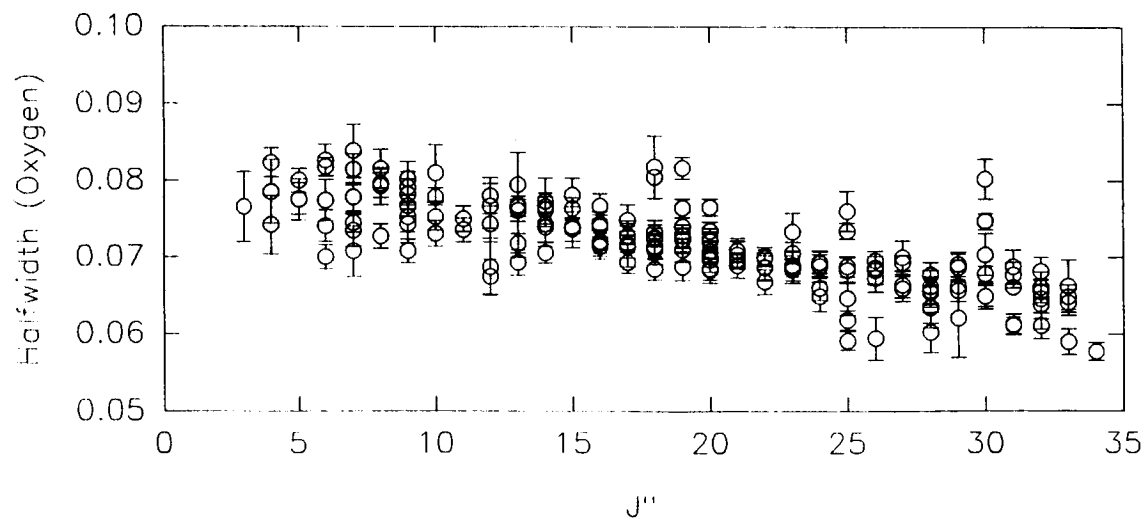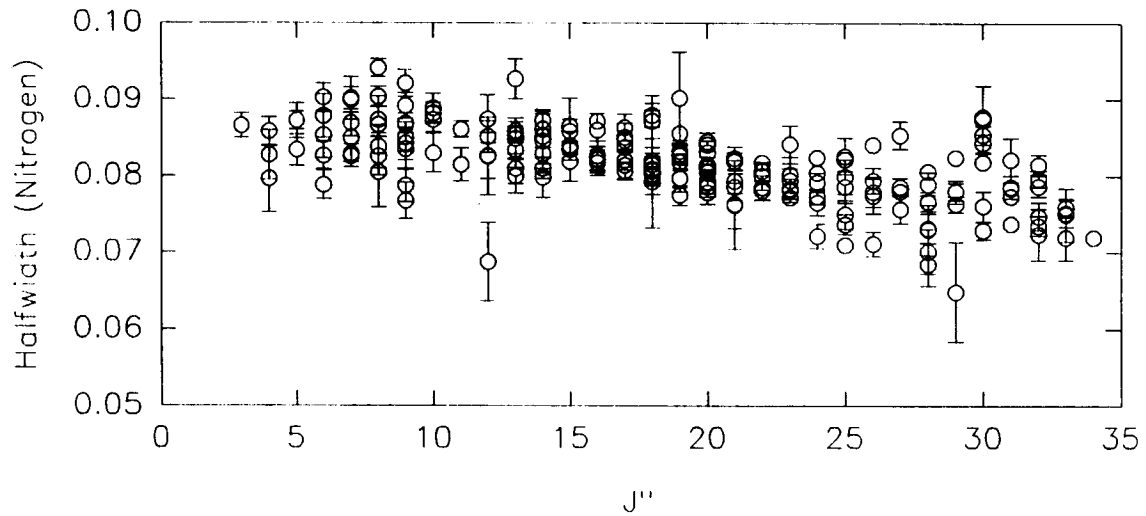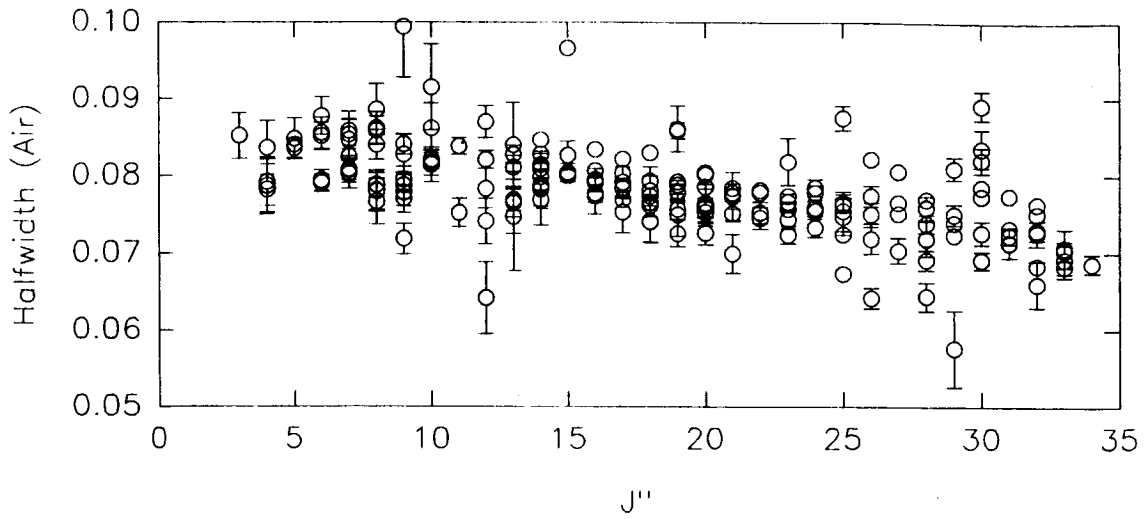
Figure 1. Broadening Coefficient $(cm^{-1}atm^{-1})$ vs Rotational Quantum Number
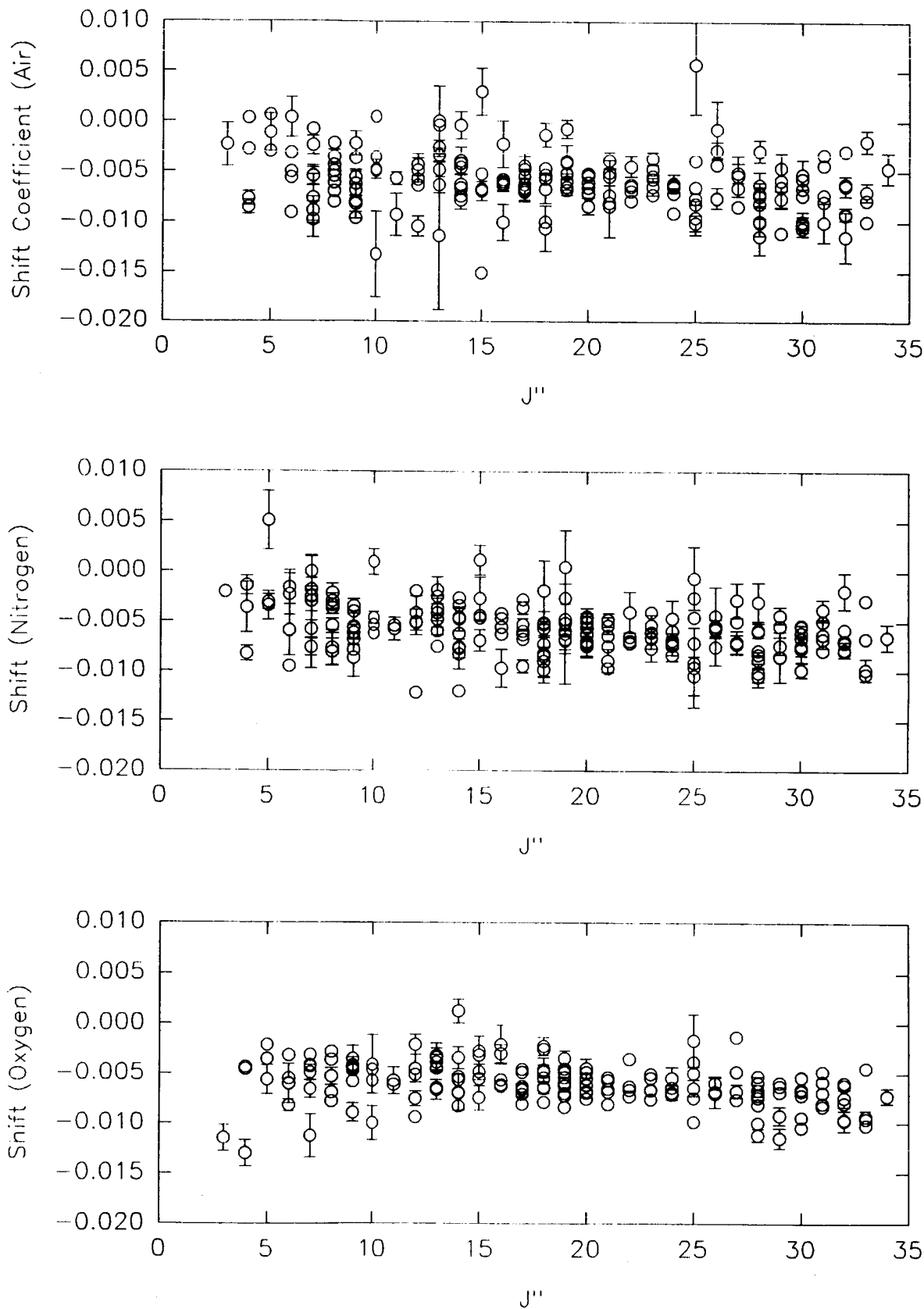
Figure 2. Shift Coefficients (cm^{-1}atm^{-1}) vs Rotational Quantum Number

Critical Problems of Computational Aeroacoustics

By

Joel C. W. Rogers
Department of Mathematics
Polytechnic University
Brooklyn, New York 11201

The discipline of aeroacoustics is concerned with the propagation of sound in air. This is a fluid phenomenon, for the description of which the Navier-Stokes equations (or the Euler equations in the inviscid case) have been shown to be adequate. Hence the possibility arises of solving these equations as a predictive tool for determining sound fields due to particular sources, and also as a tool for the design and control of sources of sound. The application of computational techniques to the solution of equations governing aeroacoustic phenomena is known as computational aeroacoustics (CAA).

A special difficulty facing CAA is the fact that the sound levels of interest generally comprise only a small perturbation on the underlying flow field. For example, rather noisy environments are characterized by acoustic pressures which are only about 10^{-5} times the ambient atmospheric pressure [1]. Accordingly, extremely accurate solutions of the governing equations are needed, so that the sound field is not lost in the error in computing the whole field.

A particular simplification which occurs in many, but by no means all, aeroacoustic problems is that Mach numbers are low and there are no shocks. From the numerical point of view, flows without shocks are more regular than those with shocks, and it is possible to compute them with greater accuracy than would be the case for shocked flows, for the same computational effort.

We have been guided by an internal NASA report [2] on special problems which are considered to distinguish CAA from the discipline of computational fluid dynamics. The report cited advocates the establishment of research tools to be used in the discipline of CAA. In the spirit of the report, our effort this summer has focused initially on critical problems of CAA, solutions of which would be part of a stable of tools at the disposal of researchers in CAA. The problems we have settled on are listed in Figure 1.

The first problem listed is that of aeroacoustics in the absence of rigid boundaries. Lighthill [3] gave a formulation of this problem in which he showed that the sources of the acoustic field were quadrupole in nature. We have preferred a different formulation of the problem, in which the quadrupoles are sources for a nonlinear wave equation, as opposed to the linear one used by Lighthill. This is given in Figure 2. The figure also gives further details of a solution procedure for the Euler equations appropriate for the aeroacoustic problem and motivated by the analysis of Crow [4]. In accordance with our formulation, we contend that an algorithm for accurate solutions of an inhomogeneous nonlinear wave equation is of prime importance.

The second problem concerns the effects of rigid boundaries. In this case one has to distinguish two types of flows: those immersed in a stream with upstream and downstream boundaries, and those which are not. A flow of the latter type would be flow in a shock tube, whereas pipe flows and jet flows would be of the former type. For pipe and jet flows the proper choice of upstream and downstream boundary conditions has not always been clear-cut [5]. Now there is a theory for inviscid incompressible flows which treats the prescription of boundary conditions as a control problem [6,7]. We consider the numerical implementation of boundary conditions in accordance with this theory to be a high-priority item for CAA, and also the extension of the theory to viscous and compressible subsonic flows is considered to be important.

A third problem would be computation of the interference and diffraction of sound waves. In this case one needs very precise information about the phases of the waves. A capability in this area would enable one to design devices to reduce noise by canceling out sound waves.

Further problems listed in Figure 1 are the scattering of sound waves and the control of noise.

The subsequent effort of the summer has focused on algorithms to solve the problems just described, beginning with the first one, aeroacoustics in free space. To date this has been the only one of the problems which has received special attention during the reporting period. Figures 3, 4, and 5 describe technical aspects of the numerical treatment proposed for an inhomogeneous nonlinear wave equation in the acoustic regime. Figure 3 describes a time discretization ("semigroup" formulation) of the problem; Figure 4 discusses the solution of the time-discretized equations by means of a further spatial discretization; and Figure 5 shows how the time-discretized equations can be given an integral formulation, in a manner close to the treatment of the linear wave equation.

References

1. Jay C. Hardin: Introduction To Computational Aeroacoustics and Its Applications, NASA Langley Research Center (1991).

2. K. Brentner, et al.: White Paper on Computational Aeroacoustics, NASA Langley Research Center (1990).

3. M. J. Lighthill: On Sound Generated Aerodynamically: 1. General Theory, Proc. Roy. Soc. 211A (1952).

4. S. C. Crow, Aerodynamic Sound Emission as a Singular Perturbation Problem, Studies in Applied Mathematics 49 (1970).

5. J. C. Hardin and D. S. Pope: Sound Generation by a Stenosis In a Pipe, AIAA 90-3919 (1990).

6. Joel C. W. Rogers: Boundary Conditions and Stability of Inviscid Plane-Parallel Flows, Quart. Appl. Math. 31 (1973).

7. Joel C. W. Rogers: The Control of Jets at the Upstream Boundary, Free Boundary Problems: Theory and Applications Pitman Publishing (1991).

1. Free space problems: nonlinear wave equation.

2. Boundary effects: numerical implementation of control theory for inviscid incompressible flows; extension of theory to viscous and subsonic flows.

3. Diffraction of sound waves: accurate phase calculations.

4. Scattering of sound waves.

5. Control of noise.

Figure 1. Critical Problems of Computational Aeroacoustics.

Given ρ and u at t = 0. ρ_t is obtained at t = 0 from $\rho_t + \nabla \cdot (\rho u) = 0$.

Update ρ by solving

$$\rho_{tt} - \nabla^2 p(\rho) = \sum \frac{\partial^2}{\partial x_i \partial x_j}(\rho u_i u_j)$$

Write $u = V + \nabla\phi$, where $\nabla \cdot V = 0$. V is a functional of
$\omega = \nabla \times u$: $V = \mathcal{F}\{\omega\}$.

To update V, update ω from

$$\frac{D}{Dt}\left(\frac{\omega}{\rho}\right) = \left(\frac{\omega}{\rho}\right)_t + u \cdot \nabla\left(\frac{\omega}{\rho}\right) = \frac{\omega}{\rho} \cdot \nabla u.$$

Let h_1 be given by
$$\nabla^2 h_1 = \nabla \cdot (u \times \omega) = -u \cdot \nabla \times \omega.$$

Then ϕ is updated by solving
$$\phi_t + \frac{1}{2}u^2 + h - h_1 = 0,$$
where
$$h = h(\rho) = \int \frac{dp(\rho)}{\rho}$$

Figure 2. Solution Procedure in Free Space

Rewrite as:

$$\hat{\rho}_t + \nabla \cdot q = 0$$

$$q_t + \nabla \hat{p} = F$$

$$\rho = \rho_0 + \hat{\rho}, p(\rho) = p_0 + \hat{p}, p_0 = p(\rho_0)$$

$$\frac{d}{dt}\int \hat{\rho}\,dx = 0, \frac{d}{dt}\int q\,dx = \int F\,dx$$

$$\hat{E}(\hat{\rho}) = \int_{\rho_0}^{\rho_0+\hat{\rho}} p(\rho)d\rho - p_0\hat{\rho}$$

$$\frac{d}{dt}\int\left(\hat{E} + \frac{q^2}{2}\right)dx = \int q \cdot F\,dx$$

"Semigroup" formulation:

$$\frac{\hat{\rho}^{n+1} - \hat{\rho}^n}{\Delta t} + \frac{1}{2}\nabla \cdot \left(q^{n+1} + q^n\right) = 0$$

$$\frac{q^{n+1} - q^n}{\Delta t} + \nabla\left(\frac{\hat{E}^{n+1} - \hat{E}^n}{\hat{\rho}^{n+1} - \hat{\rho}^n}\right) = \frac{1}{2}\left(F^{n+1} + F^n\right)$$

$$\int \hat{\rho}^{n+1}dx = \int \hat{\rho}^n dx, \int q^{n+1}dx = \int q^n dx + \frac{1}{2}\Delta t\int\left(F^{n+1} + F^n\right)dx$$

$$\int\left[\hat{E}^{n+1} + \frac{\left(q^{n+1}\right)^2}{2}\right]dx = \int\left[\hat{E}^n + \frac{\left(q^n\right)^2}{2}\right]dx$$

$$+\frac{1}{4}\Delta t\int\left(q^{n+1} + q^n\right) \cdot \left(F^{n+1} + F^n\right)dx$$

Figure 3. Treatment of Nonlinear Wave Equation

$$\hat{\rho}^{n+1} = \hat{\rho}^n - \Delta t \; \nabla \cdot q^n + \frac{1}{2}(\Delta t)^2 \nabla^2 \left(\frac{\hat{E}^{n+1} - \hat{E}^n}{\hat{\rho}^{n+1} - \hat{\rho}^n} \right)$$

$$- \frac{1}{4}(\Delta t)^2 \; \nabla \cdot \left(F^{n+1} + F^n \right)$$

Spatial discretization: $\Delta x = \Delta y = \Delta z = h$,

$$\left(\nabla^2 f \right)_{ijk} \cong (f_{i+1,j,k} + f_{i-1,j,k} + f_{i,j+1,k} + f_{i,j-1,k}$$

$$+ f_{i,j,k+1} + f_{i,j,k-1} - 6 f_{ijk}) / h^2$$

$$\xi^{(0)} = \hat{\rho}^n$$

$$G(\xi) = \xi + \frac{3(\Delta t)^2}{h^2} \frac{\hat{E}(\xi) - \hat{E}\left(\xi^{(0)}\right)}{\xi - \xi^{(0)}}$$

G monotone nonlinear, can solve $G(\xi) = g$ easily. Iterative solution:

$$G\left(\xi^{(i)}\right) = g\left(\xi^{(i-1)}\right)$$

$$\xi^{(i)} \xrightarrow[i \to \infty]{} \hat{\rho}^{n+1}$$

Figure 4. Solution of equations.

$$\nabla^2 f(x) \cong \frac{3}{2\pi} \oint_{|x-x^1|=c(x^1)\Delta t} \frac{f(x^1)}{\left(c(x^1)\Delta t\right)^3} \frac{1}{\left|x^1 - x - (\Delta t)^2 c(x^1)\nabla^1 c(x^1)\right|} dS^1$$

$$- \frac{6}{\left(\Delta t\, c(x)\right)^2} f(x)$$

Inserting into equation at top of Figure 4, we get new

$$\tilde{G}(\xi) = \xi + \frac{3}{\left(c(x)\right)^2} \frac{\hat{E}(\xi) - \hat{E}\left(\xi^{(0)}\right)}{\xi - \xi^{(0)}}.$$

$\tilde{G}$ is monotone and nonlinear
Iterative solution of equations:

$$\tilde{G}\left(\xi^{(i)}\right) = \tilde{g}\left(\xi^{(i-1)}\right)$$

$$\xi^{(i)} \xrightarrow[i\to\infty]{} \hat{\rho}^{n+1}$$

Formulation is close to Huyghens' construction in linear case $\frac{dp}{d\rho} = c_0^2$.

Figure 5. Integral Representation of $\nabla^2 f$.

Background Issues for On-Line Aircraft Documentation

by

C. Ray Russell
Assistant Professor
Department of Mathematical Sciences
Appalachian State University
Boone, NC 28607

Currently, almost all aircraft documentation in commercial aircraft cockpits is presented via hardcopy manuals. Several recent projects are aimed at eliminating all paper documentation in cockpits using "electronic libraries". Electronic libraries encompass diverse information bases including aircraft systems documentation, operations and procedures, checklists, maintenance logs, minimum equipment lists, maps and charts, and flight management information. These electronic libraries are envisioned to be embedded in the avionics so as to provide real time monitoring and display of information. The research presented here examines background issues--motivation, information retrieval models, and preliminary designs--for the on-line presentation of aircraft systems documentation including operations, procedures and checklists.

The primary motivation for the automation of aircraft documentation must be safety. While other motivations can be cited, flight safety must be primary. The incorporation of on-line documentation should provide faster access to more accurate, more easily understood information in a more reliable manner so as to increase pilot awareness and thus aid the pilot's decision making process. Designing on-line documentation which is better than hardcopy manuals will be no small task. Accomplishing this requires a study of safety issues and in particular how these issues relate to the delivery of aircraft documentation. Perrow [1] reviews accidents in a variety of domains and characterizes a class of accidents as "system accidents". This class is characterized by: 1) multiple failures, 2) tight coupling, 3) interdependence of events, and 4) impossibility of operators comprehending the sequence of events. Within this analysis of accidents, overcoming operator incomprehensibility would be an appropriate target of on-line documentation; however, embedding the documentation within the aircraft systems would increase the interdependence between the documentation and other systems (e. g., power supply). This fact, along with other limitations of on-line documentation, suggests that the new documentation must be carefully designed so as to capitalize on its strengths in order to truly improve aircraft safety.

NTSB Accident Reports and a database search including 469 reports (referencing systems documentation, manuals, or checklists) from the NASA Aviation Safety Reporting System provided the basis for an analysis of aircraft incidents (and accidents). This analysis indicates that aircraft incidents and accidents tend to involve many of the following elements:
1. subsystem failure(s),
2. inoperable items which do not ground the aircraft,
3. flight crew stress or fatigue,
4. complacency or over-reliance on maintenance, dispatch, other crew members, or equipment to perform functions flawlessly,
5. initial disregard of the seriousness of a warning,

6. lack of information regarding what happened or how to deal with the situation,
7. events "out of sync" (either rushed or delayed),
8. adverse weather, or
9. economic pressure to continue operation.

These are not necessary conditions for a serious accident; however, they probably comprise sufficient conditions.

How can on-line documentation address these issues? First, automated check-lists can allow for better tracking of exactly what has and has not been accomplished particularly when events are "out of sync" [2]. Second, faster access to accurate information about aircraft systems and procedures would help in addressing the lack of information. In many emergency situations, time is critical; the pilot has only seconds to react. On-line documentation could immediately display appropriate abnormal checklist. In time-critical situations, improved access to aircraft systems descriptions could have only indirect impact at best--the pilot must use information in his/her head and information immediately visible in the cockpit. However, many emergency situations have origins on the ground or at high altitudes where the pilot does have time to investigate the problem. In these cases, on-line documentation can speed access to the appropriate information and assist the decision making process.

Having identified two areas where on-line documentation could increase air-craft safety, design issues related to checklists and information retrieval have been addressed. First, a prototype, on-line checklist system has been developed (see Figs. 1 and 2). While targeted to a color, touch-sensitive monitor, the figures illustrate the marking of completed items (reverse video and checked), the next item to be done (boxed), and the items not accomplished (normal video). Pilots would indicate completion of items by touching the screen.

Second, to address the speed and accuracy of information retrieval, one must understand when and how pilots use aircraft systems documentation. Almost no one, including pilots, uses documentation unless there is no other choice. For pilots, accessing the manuals is a next-to-last resort (the last resort is to call the company operations office). Accessing the systems manual is only done when some problem arises for which the pilot does not have a solution in his/her head. Thus, retrieving information from a manual is always an embedded task guided by a specific context. Most models of information retrieval involve novice users and are inappropriate here. However, the constructs from a field of study called "search theory", while not originally intended as a model of operator behavior, may provide such a model [3]. Fig. 3 illustrates how these constructs can model an expert user searching for information within some information base.

Future research should investigate the utility of the search theory model of information retrieval, based on this model provide an overall architecture for an on-line documentation system, implement this system, and test the usability of the resulting system.

References
1. Perrow, C. Normal Accidents. New York: Basic Books, 1984.
2. Degani, A., and Wiener, E. L. "Human Factors of Flight-Deck Checklists: The Normal Checklist". NASA Contractor Report 177549, 1990.
3. Janes, J. W. "The Application of Search Theory to Information Science.". In Katzen, J., and Newby, G., Eds., ASIS '89: Managing Information and Technology. Washington, DC, Oct 30-Nov 2, 1989.

Normal Checklists

Taxi Checklist

1. Parking Brake.....................RELEASE ✓
2. Flaps.....................SET TO/APP ✓
3. Auto Brake.....................ON/MAX ✓
4. Flight Controls.....................CHECKED ✓
5. Long. Trim.....................SET _____ ✓
6. Auto Pilot/FD.............AS REQUIRED ✓
7. Takeoff Briefing..........COMPLETED ✓
8. Taxi Checklist.............COMPLETED ✓

Cockpit Prep.
Before Start
After Start
Taxi
Before Takeoff
After Takeoff
Descent/Appr.
Before Landing
After Landing
Parking
Leaving Cockpit
Abnormal
Emergency

Other Information

Expanded Checklist

Performance

Procedures

Systems

Information Index

Where Am I?

Aircraft Information

Checklists   Systems

Performance   Procedures

Figure 1.   Checklist with All Items Completed

Normal Checklists

After Takeoff Checklist

1. Landing Gear.....................UP ✓
2. Flaps.....................UP ✓
3. Landing Lights.....................OFF
4. Fuel Pumps.....................ON
5. Seat Belts.....................SET
6. After Takeoff Chklst..COMPLETED

Cockpit Prep.
Before Start
After Start
Taxi
Before Takeoff
After Takeoff
Descent/Appr.
Before Landing
After Landing
Parking
Leaving Cockpit
Abnormal
Emergency

Other Information

Expanded Checklist

Performance

Procedures

Systems

Information Index

Where Am I?

Aircraft Information

Checklists   Systems

Performance   Procedures

Figure 2.   Checklist with Some Items Not Completed

Target Description

Pilot Task: Characterize information sought in the context of the immediate problem

Research Questions:
1. How does the pilot characterize the target information?
2. What are the natural information classifications?
3. In what contexts is information most likely to be sought?

Target Distribution

Pilot Task: Determine where in the manual this target is likely to be found

Research Questions:
1. What organizations best fit the pilot's natural classifications?
2. What indicies should be available?
3. How can the sections in the manual best be described?

Effort Allocation

Pilot Task: Determine how much effort should be allocated to searching each section of the manual

Research Question:
1. What factors other than Target Distribution affect the amount of effort a pilot is willing to spend searching for information?

Detection

Pilot Task: Search a section of the manual for the target

Research Question:
1. How should the information be presented to optimize detection (page organization, readability, use of graphics, etc.)?

Successful Search

Unsuccessful Search

Figure 3. The Search Theory Model of Information Retrieval

Optical and Mechanical Response of High Temperature Optical Fiber Sensors

by

Jim Sirkis
Assistant Professor
Department of Mechanical Engineering
University of Maryland
College Park, Maryland 20742

The National Aerospace Plane (NASP) will experience temperatures as high as 2500 F at critical locations in its structure. Optical fiber sensors have been proposed as a means of monitor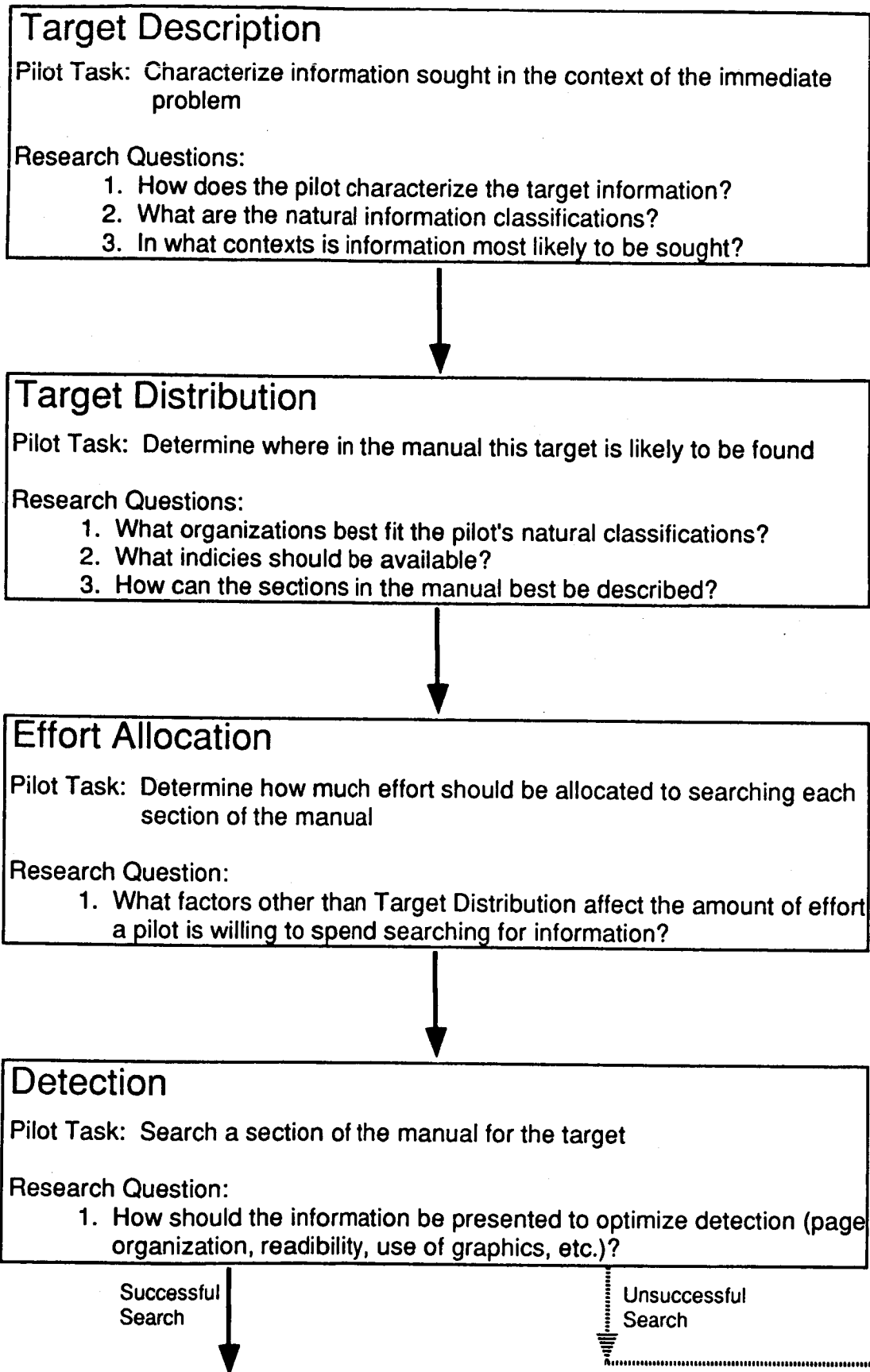ing the temperature in these critical regions by either bonding the optical fiber to, or embedding the optical fiber in, metal matrix composite components (MMC). Unfortunately the anticipated NASP temperature ranges exceed the glass transition region of the optical fiber glass. This study attempts to define the operating temperature range of optical fiber sensors from both optical and mechanical perspectives. The two underlying questions which are addressed ar "What are we measuring?" and "Will the fiber, bonding agent, and/or MMC survive the thermomechanical loading?" Both of these are issues define the usefulness of glass optical fibers for high temperature measurements. Glass transition is the phenomena where the material properties of the optical fiber drastically change during a well define temperature range (roughly 900 F to 1100 F). Properties such as coefficient of thermal expansion, Young's modulus, Poisson's ratio, fracture toughness, and refractive index can all change by as much as a order of magnitude. The behavior of these properties is a non-linear function of time and temperature, and as a result is highly dependent on the time-temperature history. A full non-linear optical analysis has been performed by modeling the optical response of an isolated sensor cyclically driven through the glass transition region. The mechanical analysis addresses the mechanical reliability of an optical fiber embedded in a transversely isotropic MMC. This analysis included non-linearities with temperature, but not with time.

Optical Response

The response of the optical phase lock loop (OPLL) sensor proposed by NASA LaRC for NASP applications is governed by optical path length. Optical path length is proportional to the refractive index and total length of the optical fiber. Under uniform thermal loading, the total length is governed by thermal expansion. The refractive index and thermal expansion can both be modeled

through glass transition using Narayanaswamy's [1] method of defining a reduced time and thermorheological simplicity. The parameters which govern this model for thermal expansion and refractive index are available in the literature for borosilicate glass [2,3], which is similar to the glass compositions used in optical fibers. Figures 1b through 1d show the response of the thermal expansion, refractive index, and optical signal to the temperature history shown in Fig. 1a. The competing hysteresis in the thermal expansion and refractive index results in a reduced hysteresis in the optical signal. The optical signal response to a symmetric, three cycle, saw-tooth temperature history is shown in Fig. 2 where the hysteresis has collapsed onto a closed curve. This collapse is important since it indicates that the "calibration" of the optical fiber sensor will settle into a repeatable function of time.

Mechanical Response

The mechanical response of an optical fiber sensor/MMC system is analyzed for the case of an uncoated optical fiber embedded in a transversely isotropic host, and subjected to a uniform temperature distribution. The possible failure mechanisms which are explored are brittle fraction of the fiber, and failure of host MMC. Time did not permit a full history dependent non-linear analysis of the optical fiber mechanics, so only a temperature dependent non-linear analysis is described. The thermomechanical properties of the fiber and MMC show strong temperature dependence. Figure 3, for example, shows the temperature dependence of Young's modulus, shear modulus, and fracture toughness for float glass [4]. Notice the abrupt change in the character of all of these curves as the glass transition region is breached. This analysis assumes the system is in a state of generalized plane strain. The resulting axial stresses in the fiber are used as the far field stresses in a classical fracture mechanics analysis. The fiber is assumed to have a circumferential crack whose depth is typical of the flaw sizes sighted in the optical fiber literature. The radial stresses on the fiber are not included in the fracture analysis since they are non-singular. Sih's strain energy density criterion [5] is adopted since this method is purported to be applicable to brittle, ductile, and fully non-linear materials and loading. These characteristics are desirable since the optical fiber is expected to transition form brittle to ductile failure as the temperature is increased. The host MMC is transversely isotropic with different tensile and compressive strength characteristics. The Tsai-Wu failure model [6] is adopted for this material.

The stresses in the matrix are determined in the generalized plane strain analysis, and are highest at the interface with the optical fiber. The region of stress concentration is localized within five fiber diameters of the optical fiber center. Figure 4 shows the failure criterion for the fiber and the fiber/host interface plotted as a function of the applied temperature field. Failure is

203

predicted in the fiber when Sih's strain energy density ratio, S/Sc, exceeds 1, and likewise in the MMC when the Tsai-Wu failure function, F, exceeds 1. Failure is predicted in the fiber around 800 F and in the MMC at around 1150 F. The nonlinearity in S/Sc for the fiber is due to the competing temperature response of the material properties.

[1] Narayanaswamy, O. S, Jou. Am. Cer. Soc., 54 (10), pp. 491-498, 1971.
[2] Spinner, S., et al, Jou. Res. Nat. Bur. Std., 70A (2), pp. 147-152, 1966.
[3] Scherer, G. W., Relaxation in Glass and Composites, Wiley, NY, 1986.
[4] Shinkai, N., et al., Jou. Am. Cer. Soc., 64 (7), pp. 426-430, 1971.
[5] Sih, G. C., Eng. Fract. Mechs., 5, pp. 1037-1040, 1973.
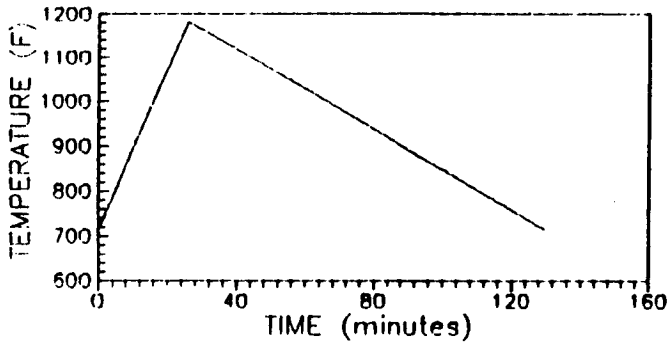[6] Tsai, S. W., and Wu, E. M, Jou. Comp. Mat., 5, pp. 58-80, 1971.

Figure 1a.

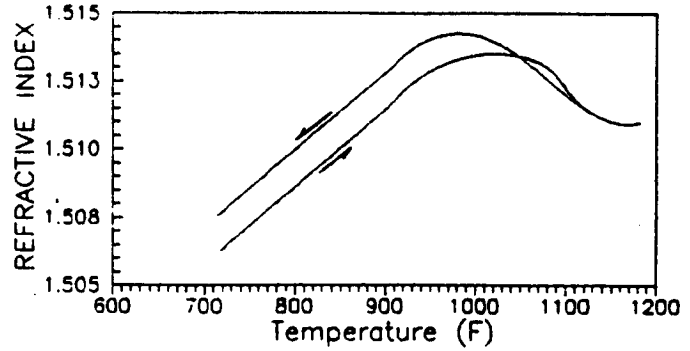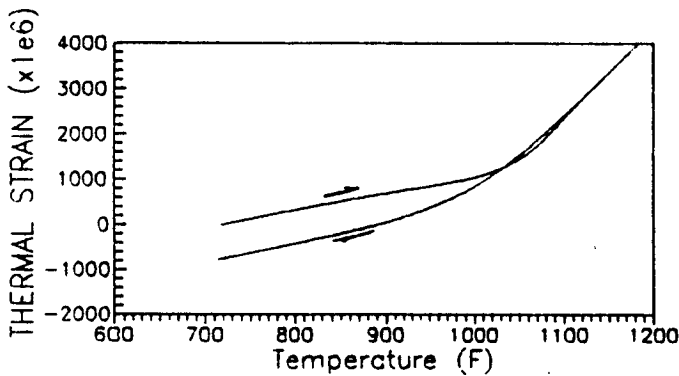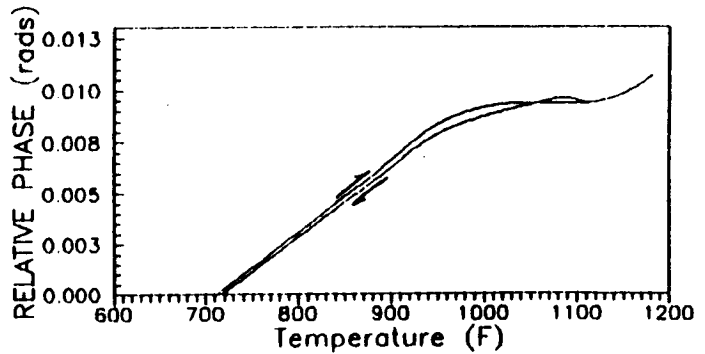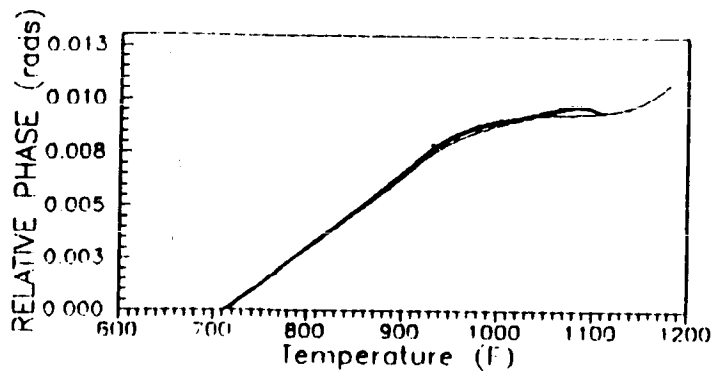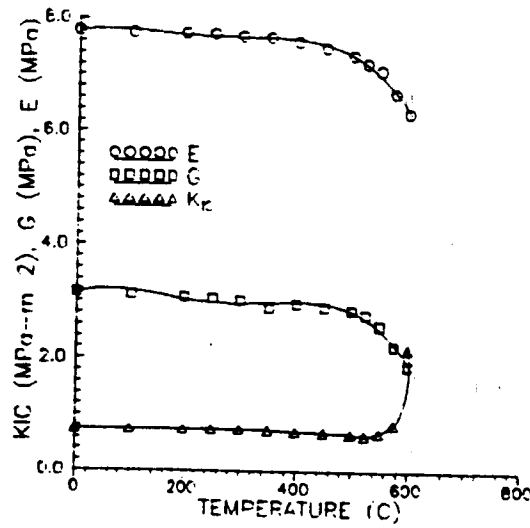Figure 1c.
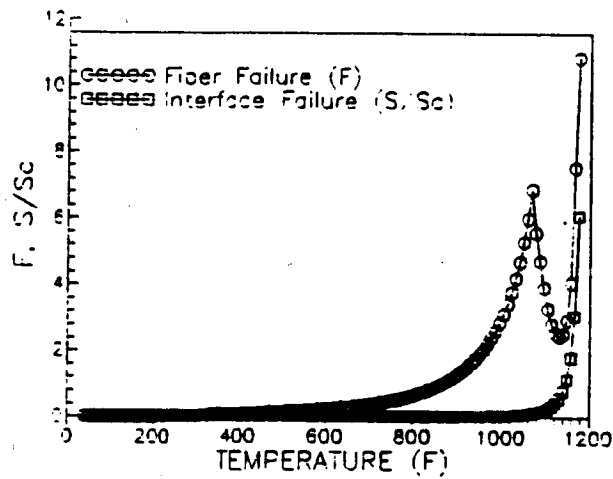
Figure 1b.

Figure 1d.

204

Figure 2.

Figure 3.

Figure 4.

Further Evaluation of the Constrained Least Squares Electromagnetic Compensation Method

by

William T. Smith
Assistant Professor
Department of Electrical Engineering
University of Kentucky
Lexington, Kentucky 40506-0046

Technologies exist for construction of antennas with adaptive surfaces that can compensate for many of the larger distortions caused by thermal and gravitational forces. However, as the frequency and size of reflectors increase, the subtle surface errors become significant and degrade the overall electromagnetic performance. Electromagnetic (EM) compensation through an adaptive feed array offers a means for mitigation of surface distortion effects.

This study looked into implementation of EM compensation with the measured surface errors of the NASA 15 meter hoop/column reflector antenna. There are two parts to the study. The first looked into a hybrid EM compensation technique. The second evaluated the performance of a given EM compensation method when implemented with discretized weights. Both parts were computer simulations.

Hybrid Compensation Bailey [1,2] developed a compensation technique in which an array feed is used to reduce the radiation pattern effects of the distorted surface for the NASA hoop/column reflector antenna. The method uses a constrained least squares (CSL) algorithm to derive excitation coefficients for the feed elements such that the aperture field of the reflector is approximated at specified match points. It is a global algorithm that attempts to correct for irregularities over a significant portion of the radiation pattern. Smith and Stutzman [3] proposed a pattern synthesis compensation (PSC) algorithm that works on localized portions of the radiation pattern. The thrust of the hybrid compensation study was to determine if the side lobe performance of the CSL method could be improved by superposing PSC corrections with the CLS feed excitations.

The hybrid compensation was implemented at 6 GHz. The results of the study showed that the CLS method works very well and that superposing the PSC excitations provided very little improvement in the resulting pattern. Further investigations will be performed at higher frequencies where the surface errors appear more severe and the CLS compensation side lobe levels are slightly higher.

Discretized Weights for the CLS Compensation Technique Most compensation algorithms determine the excitations of the feed elements assuming continuous values of the amplitudes and phases are available. In practice, discretized amplitude and phase weights will probably be used to implement the algorithms. This study evaluated the effects of the quantized excitations on the radiation performance of a compensated distorted reflector. Again, measured surface data from the hoop/column antenna were used.

The quantization study was performed for a frequency of 6 GHz. The exact compensation coefficients were modified by a program which quantizes the amplitudes

and phases of the weights. The amplitude was quantized into 1 dB, 2 dB, 3 dB, and 4 dB bins. The phase was quantized into bins corresponding to the number of bits for digital phase shifters: 3 bits (45° bins), 4 bits (22.5° bins), ..., 8 bits (1.41° bins).

The effects of the discretization were judged using contour plots of the radiation patterns. Figure 1 shows the compensated radiation pattern for the distorted hoop/column reflector with a hexagonal 169 element feed array before quantization. The CLS algorithm was shown to be quite insensitive to amplitude quantization. The first sign of pattern degradation occurred for the somewhat coarse 3 dB amplitude bins. Figure 2 shows the pattern for the 3 dB bins where some new side lobes appear above the 30 dB contour. The CLS method was found to be fairly insensitive to phase quantization, also. Slight pattern degradation first appeared when the number of bits was down to 4 (22.5° bins). Figure 3 shows the pattern for the 4 bit phase shifters.

The results of the analysis at 6 GHz showed that CLS compensation can be implemented with discretized weights and can withstand a reasonable amount of quantization error. The analysis is just at the one frequency, however. Work is in progress to evaluate the quantization effects at higher frequencies where the surface errors appear to be more severe.

References

1. M. C. Bailey, "Electronic Compensation for Reflector Surface Distortion to Improve Radiation Pattern Characteristics of Antenna," NASA Technical Memorandum, no. 100652, February, 1989.

2. M. C. Bailey, "Determination of Array Feed Excitation to Improve Performance of Distorted or Scanned Reflector Antennas," 1991 Antennas and Propagation Society Symposium Digest, London, Ontario, pp. 175-178, June, 1991.

3. W. T. Smith, W. L. Stutzman, "A Pattern Synthesis Technique for Array Feeds to Improve Radiation Performance of Large Distorted Reflector Antennas," to be published in the IEEE Trans. on Ant. and Prop..
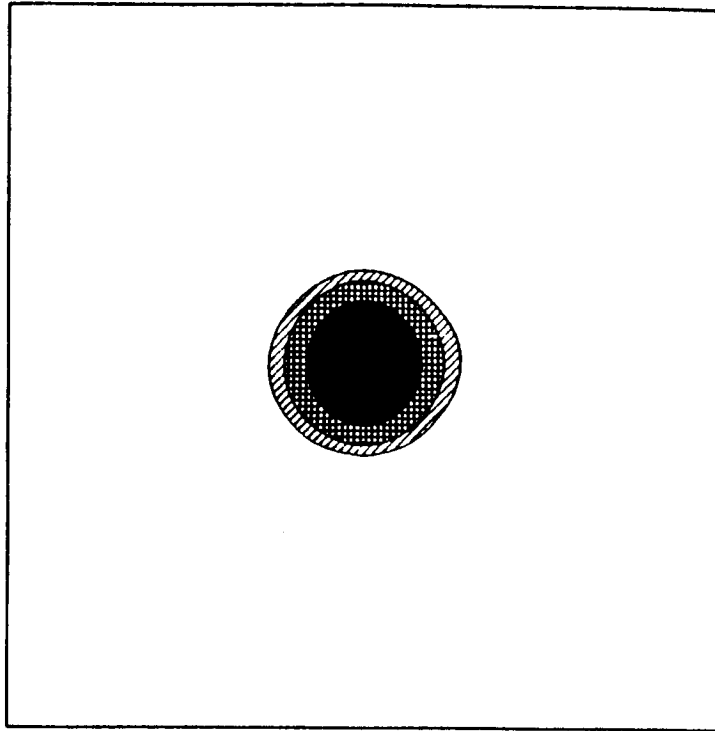
Figure 1 Compensated radiation pattern for the hoop/column reflector antenna without quantization (10 dB - solid; 20 db - crossed; 30 dB - slanted lines). The feed array has 169 elements.
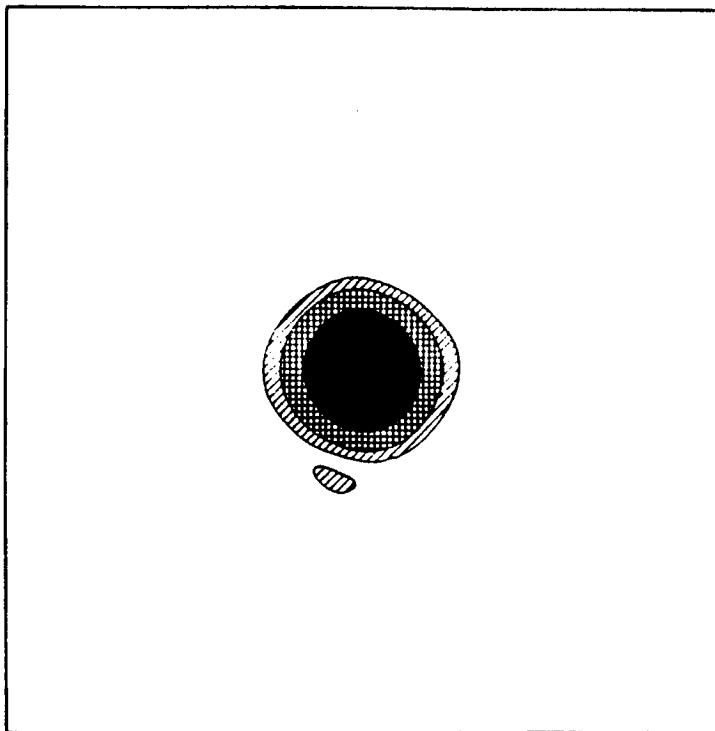
Figure 2 Compensated radiation pattern with 3 dB amplitude quantization (10 dB - solid; 20 dB - crossed; 30 dB - slanted lines).
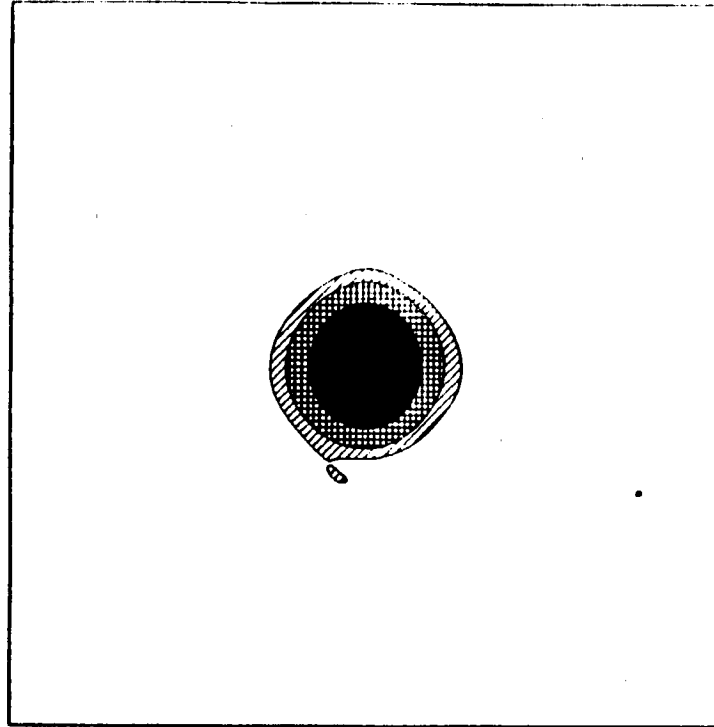
Figure 3 Compensated radiation pattern with phase quantization of 4 bits (22.5° bins) (10 dB - solid; 20 dB - crossed; 30 dB - slanted lines).

Constant–Temperature Anemometry Measurements in Hypersonic Boundary Layers

by
Prof. Eric F. Spina
Department of Mechanical and Aerospace Engineering
Syracuse University
Syracuse, NY 13244

One of the major unresolved issues in fluid dynamics is the nature of apparent stresses, called Reynolds stresses, which occur in turbulent boundary layers. In hypersonic boundary layers, the flow physics is further complicated by the large temperature and density fluctuations and the concomitant contamination of the Reynolds stresses by "fictitious" terms. Because of the severe flow environment and the extraordinary demands on sensors and instruments, the turbulence characteristics of hypersonic boundary layers have been studied in only a cursory fashion. The plans for supersonic (HSCT) and hypersonic (NASP) vehicles have made supersonic flow physics one of the critical pacing technologies in aerospace science. In particular, experimental data is needed to verify candidate computer models and to reach an improved understanding of the turbulence physics. The research performed this summer at NASA–Langley's Experimental Flow Physics Branch is the start of a substantial effort to refine existing instrumentation and develop experimental techniques to measure the various components of the Reynolds stress in hypersonic boundary layers.

The few fluctuating velocity measurements which have been made in hypersonic boundary layers have been acquired using constant–current hot–wire anemometry (CCA). While CCA is able to separate contributions from various turbulence modes, it cannot be used to acquire instantaneous signals because it must be operated at several different over-heat settings during the same run. Constant–temperature hot–wire anemometry (CTA) does not suffer from this shortcoming (although some assumptions must be made to reduce the data), but the frequency response of this type of system was thought to be considerably lower than the CCA system. Since a frequency response in excess of 400 KHz is needed to resolve the high–frequency spectral content of hypersonic boundary layers, this instrument had generally been ignored for high–speed flows. The approach used in this study, however, was to determine whether the frequency response of the easier–to–use CTA system could be optimized, so that a significant portion of the energy spectrum could be captured.

Customized hot–wire probes were built in an effort to reduce the probe impedance and thus increase the system frequency response. Copper–plated tungsten wire 2.5 μm in diameter was soft-soldered onto the probe prongs, and a 0.5 mm active length was etched using a sulfuric acid solution. The hot–wire frequency response was deduced using square–

wave injection, and a $-3\ dB$ point of 700 KHz was regularly achieved in the freestream of a Mach 10 helium pilot tunnel. The single normal wire was operated in a symmetric bridge at an overheat ratio, τ, of about one, so that, as a first estimate, stagnation temperature fluctuations could be neglected. In addition to the extraordinary frequency response, the absence of the "strain gauging" phenomenon and the survivability of the hot wires illustrate the potential applicability of CTA to hypersonic flows.

The Mach 10 pilot tunnel was also used to determine the recovery temperature of the unheated 2.5 μm wires, and to investigate the heat transfer relationship of the heated wires. The recovery factor, η, was found to be slightly greater than one, and is in agreement with other transitional and free-molecular flow data when end-conduction effects are considered. Despite the relatively high Knudsen number of the flow (Kn_0 as high as 5), a well-behaved and repeatable cooling law was found: $Nu_0 = Af(\tau) + Bg(\tau)Re_0^{0.73}$, where $f(\tau)$ and $g(\tau)$ were determined by calibrating at various overheat ratios, and A & B are constants which have a slight dependence on wire geometry. The attached figure shows the results of a typical calibration, achieved by varying the tunnel stagnation pressure from 900 psi to 100 psi. The subsonic continuum form of this cooling law, known as "King's Law", has a Reynolds number exponent of 0.5, and the free-molecular form correlates with $Re_0^{1.0}$. The wires used in this study are in the overlap region between continuum and free-moecular flow, and thus have a Reynolds number dependence somewhere between that of the two regimes.

The goal for the remainder of the summer is to obtain mass-flux fluctuation profiles across the transitional and turbulent boundary layers of the High-Reynolds-Number Mach 20 Helium Tunnel. The study will be done on a 4° wedge, with a flow Mach number of 10 behind the shock. The hot wires will be calibrated in the Mach 10 pilot tunnel, and the data reduced using the recovery factor and the cooling law found earlier. In the long term, this study will be followed by the development of dual-wire probes, crossed-wire probes, and a hybrid laser and hot-wire technique, all to be applied to the Mach 10 helium boundary layer. One type of dual normal-wire probe, with the wires separated by 0.5 mm and operated at two different overheat ratios, will be used to simultaneously determine both T_0' and u'. With such a probe, there is no need to resort to assumptions about the relative sensitivity of the CTA system to mass-flux and stagnation temperature, and the questionable Strong Reynolds Analogy is not needed to deduce u'. Dual normal-wire probes with a larger separation will be used to study the large-scale structure of the boundary layer, and the crossed-wire probe will allow measurement of the Reynolds shear stress, $u'v'$. The hybrid technique, employing single-point Rayleigh scattering and closely-spaced normal wires, will provide measurements of u', T_0', ρ', and p'. These would be the first measurements of fluctuating pressure within a boundary layer, and may be important in understanding hypersonic boundary layer physics.

Nusselt vs Wire Reynolds Number

RUN NURE23
η = 1.00
τ = 0.757

Nu_0

$Re_0^{0.73}$

c1=0.1579 c0=0.0083
error= 0.723
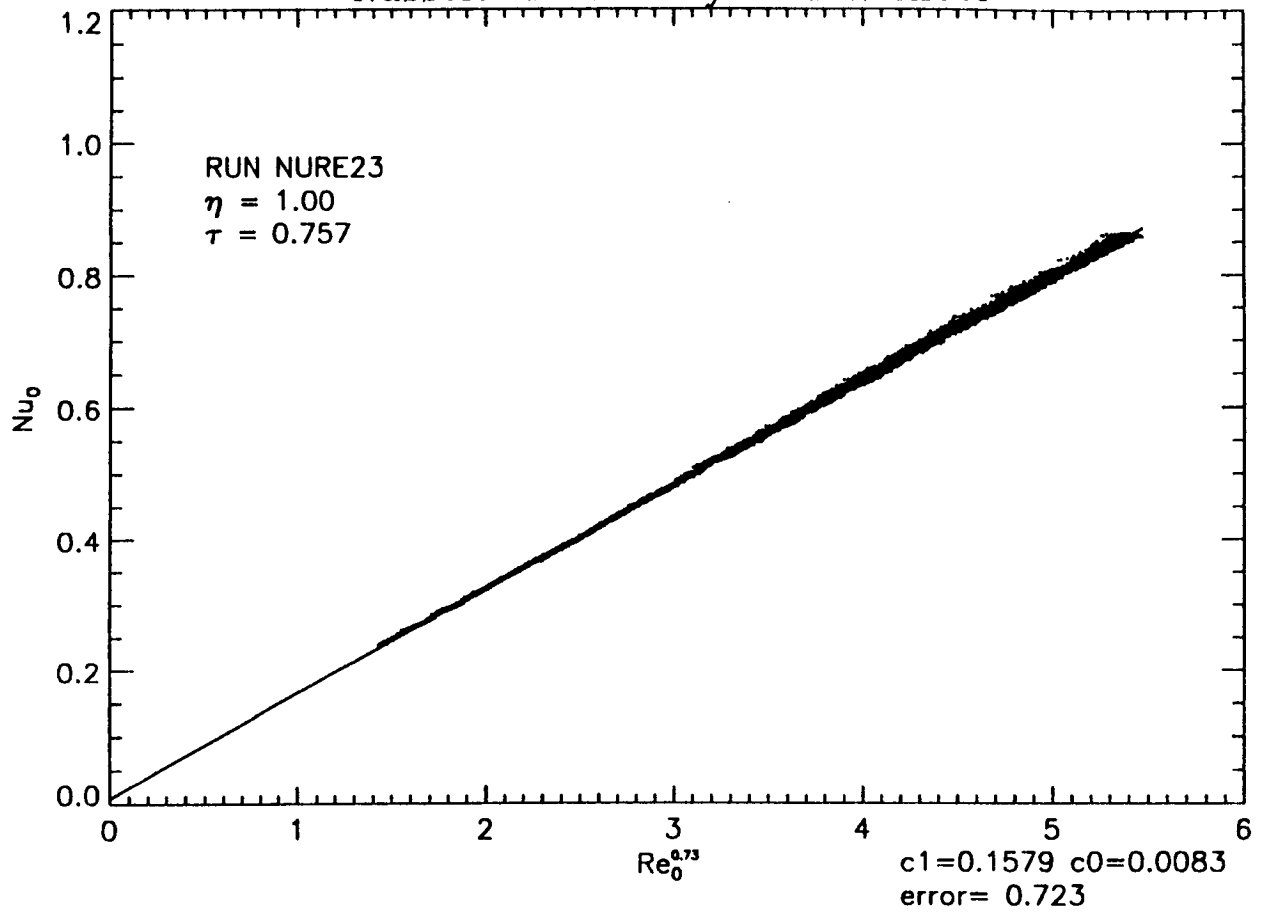
POTENTIAL APPROACHES TO THE SPECTROSCOPIC CHARACTERIZATION OF HIGH PERFORMANCE POLYMERS EXPOSED TO ENERGETIC PROTONS AND HEAVY IONS

by

N. K. SULEMAN
Assistant Professor
Department of Chemistry
Hampton University
Hampton, Virginia 23668

The general plans for the human exploration of space over the next several decades are clearly set forth in the Space Exploration Initiative (SEI), and in the 90-Day Report. Deployment of the Space Station Freedom in the mid-1990's will be followed by a permanent presence on the moon early in the next century. A manned mission to Mars is planned during the period 2010-2020 [1].

A potential limitation to human activity on the lunar surface or in deep space is the exposure of the crew to unacceptably high levels of penetrating space radiations [2]. The radiations of most concern for such missions are high-energy protons emitted during solar flares, and galactic cosmic rays which are high-energy ions ranging from protons to iron (in the case of the higher atomic number species, the ions are highly charged as well, e.g. Fe^{+26}).

The interactions of such high-energy radiations with matter are not well understood at present. However, it is clear that the physical characteristics of the radiation fields are altered through nuclear and electromagnetic interactions when traversing bulk matter [3]. For HZEs (the high-charge, high-energy component of galactic cosmic rays), the modification in the propagating fields includes energy loss due to nuclear coulomb scattering, nuclear elastic scattering and nuclear fragmentation. In the case of nuclear fragmentation, subsequent-generation particles are formed and the isotopic composition of the transported radiation field is altered. The incident radiation may also cause electronic excitation and ionization in bulk media via collision with atomic electrons.

The development of materials for effective shielding from energetic space radiations will clearly require a greater understanding of the underlying mechanisms of radiation-induced

damage in bulk materials. This can be accomplished in part by the detailed spectroscopic characterization of bulk materials that have been exposed to simulated space radiations. An experimental database thus created can then be used in conjunction with existing radiation transport codes in the design and fabrication of effective radiation shielding materials.

Electron Paramagnetic Resonance (EPR) Spectroscopy has proven very useful in elucidating radiation effects in polymers (high performance polymers are often an important component of structural composites) [4]. One of the major goals of the ASEE term was thus to repair and to bring back on line an existing EPR spectrometer. In excess of eighty percent of the total period was devoted to this activity. The remainder of the term was committed to conducting literature searches and to program planning.

Considerable progress has been made toward meeting these goals. As of 7/30/91, the EPR system is fully operational. Literature searches are almost complete, and future activities are currently being mapped out. It is expected that experimental activity will commence as soon as the energetic (1-2 MeV) proton facility is available at NASA LaRC.

References

1. Report of the 90-Day Study, NASA, 1989.
2. Townsend, L. W., Wilson, J. W., and Nealy, J. E., "Space Radiation Shielding Strategies and Requirements for Deep Space Missions," SAE Paper No. 891433, 1989.
3. Townsend, L. W., and Wilson, J. W., "Interaction of Space Radiation with Matter," 41st Congress of The International Astronautical Federation, 1990, Dresden, GDR.
4. Ranby, B. and Rabek, J. F., ESR Spectroscopy in Polymer Research, Springer-Verlag Publishing Co., New York, 1977, pp 173-248.

Condensational Growth and Trace Species Scavenging in Stratospheric Sulfuric Acid/Water Aerosol Droplets

by

Robert V. Tompson, Jr.
Research Assistant Professor
Nuclear Engineering Program
Particulate Systems Research Center
University of Missouri-Columbia
Columbia, Missouri 65211

The Earth's atmosphere can generally be divided into two parts, the troposphere at lower levels and the stratosphere at higher levels. These two levels are separated by the tropopause and generally have very different properties. The height of the tropopause depends upon the latitude and varies from about 9 km at 60°N/S to about 13 km at 20°N/S.

Stratospheric aerosols were discovered about 1961 [Junge et al.] and have since been recognized to play a significant role in the environment. The composition of stratospheric aerosol is believed to be a liquid solution of sulfuric acid (H_2SO_4) and water (H_2O) with numerous trace species [Rosen; Hamill et al.]. Of these trace species, ozone (O_3) in particular has been recognized as being very important in its role of shielding the environment from harmful ultraviolet radiation. Also among the trace species are HCl and $ClONO_2$, the so called 'chlorine reservoir' species and various oxides of nitrogen such as NO, NO_2, and N_2O_5.

The quantity of stratospheric aerosol and its particle size distribution determines, to a large degree, the chemistry present in the stratosphere. $ClONO_2$ and HCl react with water and N_2O_5 on droplet surfaces to produce the ozone reactive species HOCl, Cl_2, and $ClNO_2$ (eqn. 1) which subsequently destroy the ozone [Watson et al.]. A principal product of these reactions is nitric acid (HNO_3) which is generally lost through absorption by the aerosol droplets. This results in a 'denitrification' of the stratosphere [Van Doren et al.]. Loss of these nitrogen compounds suppresses the reformation of the chlorine reservoir species and thus enhances ozone depletion. The NO and NO_2 species play a role in both ozone production and removal but have their own removal mechanisms involving the formation of HNO_3 [Mozurkewich and Calvert]. This removal represents a further denitrification of the stratosphere.

Aerosols experience three types of growth: nucleation, condensation, and coagulation. The term 'growth' in this context also encompasses the corresponding size decreasing mechanisms of disintegration, evaporation, and fragmentation. Nucleation and condensation have probably been studied the most extensively. In particular, extensive work has been done on the nucleation of stratospheric sulfuric acid/water droplets [e.g. Yue; Singh et al.]. Much generic work has been done on the problem of condensation [e.g. Tompson and Loyalka; Loyalka et al.]. The current effort seeks to apply the latter work [Loyalka et al.] to the specific problem of stratospheric aerosols.
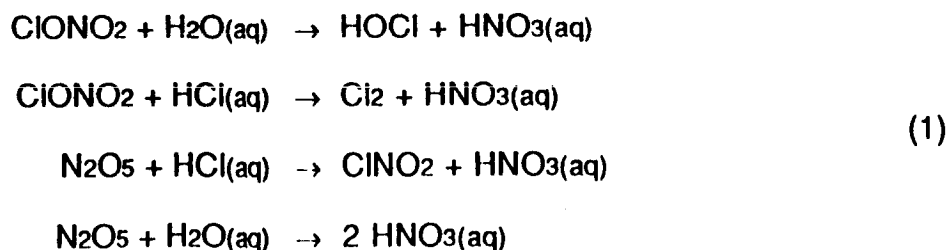
The transport of various trace gas species to and from a droplet can be thought of as condensation and evaporation. The ultimate driving term for each species'

condensation is the gradient of its density at the surface of the droplet or, more simply, the difference between its bulk background density and its saturation density at the droplet surface. Many things can modify these density gradients and each factor would have to be considered in a comprehensive model. For the present we simply consider these densities to be known.

The previous results that are followed [Loyalka et al.] are the numerically calculated condensation rates for a vapor species diffusing through some noncondensing background gas. Where the vapor is incident on a spherical droplet it is assumed to condense and to reach thermal equilibrium with the droplet. The vapor is assumed to have a much lower density than the background gas such that the velocity distribution function for the vapor is determined by a linear form of the transport equation (Boltzmann's equation; eqn. 2) with appropriate boundary conditions (eqn. 3). The boundary conditions are interpreted to mean that all of the incident vapor molecules reach thermal equilibrium as stated previously and that far from the droplet the usual continuum theory (Diffusion theory) applies. Discretization of the above problem leads to an expression for the condensation rate (eqn. 4) and a series of appropriate iterative formulas (eqn. 5). Table 1 lists the results of this previous work in a convenient dimensionless form. As can be seen, these results are generic in that they do not apply to any specific combination of gases.

In this work, the previous results have been employed to obtain values of the condensation rates for specific trace species in the stratosphere. The values thus determined assume a background gas of N_2 and are listed in Table 2. Work is currently underway to integrate these values into a reasonably comprehensive, dynamic model of stratospheric droplet behavior. The droplet sizes in the above results have been expressed in units of the molecular mean free path.

Hamill, P., Toon, O.B. and Kiang, C.S. (1977) "Microphysical processes affecting stratospheric aerosol particles," *J. Atmos. Sci.* **34**, 1104-1119.

Junge, C.E., Chagnon, C.W. and Manson, J.E. (1961) "Stratospheric aerosols," *J. Met.* **18**, 81-108.

Loyalka, S.K., Hamoodi, S.A. and Tompson, R.V. (1989) "Isothermal condensation on a spherical particle," *Phys. Fluids A* **1(2)**, 358-362.

Mozurkewich, M. and Calvert, J.G. (1988) "Reaction probability of on aqueous aerosols," *J. Geophys. Res.* **93(D12)**, 15889-15896.

Rosen, J.M. (1971) "The boiling point of stratospheric aerosol," *J. Appl. Meteorol.* **10**, 1044-1046.

Singh, J.J., Smith, A.C. and Yue, G.K. (1980) "Experimental study of cluster formation in binary mixture of H_2O and H_2SO_4 vapors in the presence of an ionizing radiation source," NASA Technical Paper #1735.

Tompson, R.V. and Loyalka, S.K. (1988) "Condensation on a spherical droplet - III," *J. Aerosol Sci.* **19(3)**, 287-293.

Van Doren, J.M., Watson, L.R., Davidovits, P., Worsnop, D.R., Zahniser, M.S. and Kolb, C.E. (1991) "Uptake of N_2O_5 and HNO_3 by aqueous sulfuric acid droplets," *J. Phys. Chem.* **95**, 1684-1689.

Watson, L.R., Van Doren, J.M., Davidovits, P., Worsnop, D.R., Zahniser, M.S. and Kolb, C.E. (1990) "Uptake of HCl molecules by aqueous sulfuric acid droplets as a function of acid concentration," *J. Geophys. Res.* **95(D5)**, 5631-5638.

Yue, G.K. (1980) "The formation and growth of sulfate aerosols in the stratosphere," *Atmos. Environment* **15**, 549-556.

$$CIONO_2 + H_2O_{(aq)} \rightarrow HOCl + HNO_{3(aq)}$$

$$CIONO_2 + HCl_{(aq)} \rightarrow Cl_2 + HNO_{3(aq)}$$

$$N_2O_5 + HCl_{(aq)} \rightarrow ClNO_2 + HNO_{3(aq)} \tag{1}$$

$$N_2O_5 + H_2O_{(aq)} \rightarrow 2\,HNO_{3(aq)}$$

$$\mathbf{c} \cdot \frac{\partial h_m}{\partial \mathbf{r}} = \hat{L} h_m \tag{2}$$

$$h_m(R, c, \mu) = 0, \quad \mu > 0$$

$$\tag{3}$$

$$\lim_{r \to \infty} h_m(r, c, \mu)$$

$$= \left(\frac{n_{asy}(r) - n_s}{n_s} \right) + \mathbf{c}\phi_d(c) \cdot \frac{1}{n_s} \frac{d}{d\mathbf{r}} n_{asy}(r) = \left(\frac{n_\infty - n_s}{n_s} \right) + \hat{u}(r)\frac{1}{r}\left(-1 + \frac{\mathbf{c} \cdot \mathbf{n}_r}{r}\phi_d(c) \right)$$

$$\hat{u}(R) = \left(\frac{n_\infty - n_s}{n_s} \right)\left(\frac{\sqrt{\pi}}{R^2} - 4\pi^{3/2} \sum_{j=1}^{J} c_j^2 w_j \sum_{m=2,4,\ldots}^{N} \omega_m \mu_m \psi_{mj}^{1/2} \right)^{-1} \tag{4}$$

---

for $\mu_m = -1$,

$$\bar{\psi}_{-1j}^{i+1/2} = \frac{(A_{i+1} + A_i)\psi_{-1j}^{i+1} + V_{i+1/2}q_{-1j}^{i+1/2}}{(A_{i+1} + A_i) + V_{i+1/2}\sigma_j}$$

$$\tag{5a}$$

for $-1 < \mu_m < 0$,

$$\bar{\psi}_{mj}^{i+1/2} = \frac{-\mu_m(A_{i+1} + A_i)\psi_{mj}^{i+1} + (1/\omega_m)(a_{m+1j}^{i+1/2} + a_{m-1j}^{i+1/2})\psi_{m-1j}^{i+1/2} + V_{i+1/2}q_{mj}^{i+1/2}}{-\mu_m(A_{i+1} + A_i) + (1/\omega_m)(a_{m+1j}^{i+1/2} + a_{m-1j}^{i+1/2}) + V_{i+1/2}\sigma_j}$$

for $\mu_m > 0$,

$$\bar{\psi}_{mj}^{i+1/2} = \frac{\mu_m(A_{i+1} + A_i)\psi_{mj}^{i-1} + (1/\omega_m)(a_{m+1j}^{i+1/2} + a_{m-1j}^{i+1/2})\psi_{m-1j}^{i+1/2} + V_{i+1/2}q_{mj}^{i+1/2}}{\mu_m(A_{i+1} + A_i) + (1/\omega_m)(a_{m+1j}^{i+1/2} + a_{m-1j}^{i+1/2}) + V_{i+1/2}\sigma_j}$$

$$\psi_{mj}^{l} = 2\bar{\psi}_{mj}^{l+1/2} - \psi_{mj}^{l+1}$$

$$\psi_{m+1j}^{l+1/2} = 2\bar{\psi}_{mj}^{l+1/2} - \psi_{m-1j}^{l+1/2}$$

$$\sigma_j = \sigma(\beta c_j)$$

$$A_i = 4\pi r_i^2$$

$$V_{i+1/2} = (4\pi/3)(r_{i+1}^3 - r_i^3)$$

$$a_{1j}^{l+1/2} = a_{2N+1j}^{l+1/2} = 0$$

$$a_{m+1j}^{l+1/2} = a_{m-1j}^{l+1/2} - \omega_m \mu_m (A_{i+1} - A_i)$$

(5b)

$$q_{mj}^{l} = \epsilon \exp(-c_j^2) \sum_{l=0}^{L} \frac{2l+1}{2} P_l(\mu_m)$$

$$\times \sum_{j'=1}^{J} c_{j'} \cdot w_{j'} \cdot k_l(c_j, c_{j'}) \sum_{m'=2,4,...}^{2N} \omega_{m'} \cdot \psi_{m'j'}^{ll},$$

$$\psi_{mj}^{ll} = P_l(\mu_m) \tfrac{1}{2}(\psi_{mj}^{l-1/2} + \psi_{mj}^{l+1/2})$$

$$\psi_{mj}^{l} \triangleq \psi_{mj}^{l0}.$$

Table 1: The dimensionless condensation rate from [Loyalka et al.].

R	$\beta^2=0.1$	$\beta^2=0.5$	$\beta^2=1.0$	$\beta^2=10.0$
0.1	0.9884	0.9782	0.9770	0.9734
0.25	0.9490	0.9415	0.9401	0.9342
0.5	0.8765	0.8706	0.8688	0.8612
0.75	0.8060	0.8012	0.7990	0.7908
1.0	0.7410	0.7374	0.7353	0.7273
1.25	0.6824	0.6802	0.6783	0.6710
1.5	0.6304	0.6293	0.6279	0.6215
1.75	0.5845	0.5842	0.5832	0.5779
2.0	0.5440	0.5443	0.5436	0.5392
3.0	0.4224	0.4223	0.4226	0.4214
5.0	0.2885	0.2887	0.2891	0.2894
10.0	0.1594	0.1594	0.1595	0.1598
20.0	0.0834	0.0834	0.0835	0.0836
50.0	0.0342	0.0342	0.0343	0.0343
100.0	0.0172	0.0172	0.0172	0.0173

Table 2a: The dimensionless condensation rates for stratospheric vapor species.

R	H_2O	H_2SO_4	SO_2	HCl
0.01	0.9967	0.9974	0.9975	0.9963
0.02	0.9945	0.9959	0.9956	0.9941
0.05	0.9876	0.9911	0.9896	0.9874
0.07	0.9829	0.9878	0.9855	0.9829
0.1	0.9758	0.9826	0.9793	0.9760
0.2	0.9514	0.9577	0.9550	0.9520
0.5	0.8670	0.8733	0.8713	0.8689
0.7	0.8110	0.8172	0.8155	0.8131
1.0	0.7332	0.7391	0.7378	0.7359
1.2	0.6871	0.6922	0.6914	0.6897
1.5	0.6265	0.6299	0.6295	0.6286
1.7	0.5903	0.5930	0.5928	0.5922
2.0	0.5429	0.5442	0.5443	0.5441
3.0	0.4229	0.4223	0.4223	0.4224
5.0	0.2895	0.2886	0.2887	0.2889
7.0	0.2027	0.2018	0.2019	0.2020
10.0	0.1596	0.1594	0.1594	0.1594
20.0	0.0836	0.0834	0.0834	0.0834
50.0	0.0344	0.0342	0.0342	0.0342
70.0	0.0178	0.0176	0.0176	0.0177
100.0	0.0173	0.0172	0.0172	0.0172

Table 2b: The dimensionless condensation rates for stratospheric vapor species.

R	HOCl	Cl_2	$ClNO_2$	$ClONO_2$
0.01	0.9975	0.9974	0.9973	0.9974
0.02	0.9954	0.9956	0.9956	0.9959
0.05	0.9889	0.9899	0.9904	0.9911
0.07	0.9845	0.9860	0.9868	0.9877
0.1	0.9777	0.9801	0.9812	0.9826
0.2	0.9538	0.9557	0.9566	0.9577
0.5	0.8703	0.8718	0.8724	0.8732
0.7	0.8146	0.8159	0.8164	0.8171
1.0	0.7372	0.7382	0.7386	0.7391
1.2	0.6909	0.6916	0.6919	0.6922
1.5	0.6292	0.6296	0.6297	0.6299
1.7	0.5927	0.5929	0.5929	0.5930
2.0	0.5443	0.5443	0.5443	0.5442
3.0	0.4223	0.4223	0.4223	0.4223
5.0	0.2887	0.2886	0.2886	0.2886
7.0	0.2019	0.2018	0.2018	0.2018
10.0	0.1594	0.1594	0.1594	0.1594
20.0	0.0834	0.0834	0.0834	0.0834
50.0	0.0342	0.0342	0.0342	0.0342
70.0	0.0177	0.0176	0.0176	0.0176
100.0	0.0172	0.0172	0.0172	0.0172

Table 2c: The dimensionless condensation rates for stratospheric vapor species.

R	HNO3	NO	NO2	N2O5
0.01	0.9976	0.9971	0.9968	0.9975
0.02	0.9956	0.9949	0.9947	0.9961
0.05	0.9896	0.9881	0.9881	0.9915
0.07	0.9855	0.9835	0.9837	0.9883
0.1	0.9791	0.9764	0.9768	0.9834
0.2	0.9549	0.9524	0.9529	0.9583
0.5	0.8712	0.8687	0.8697	0.8737
0.7	0.8154	0.8128	0.8140	0.8175
1.0	0.7378	0.7354	0.7367	0.7394
1.2	0.6914	0.6893	0.6905	0.6924
1.5	0.6295	0.6281	0.6290	0.6300
1.7	0.5928	0.5918	0.5925	0.5930
2.0	0.5443	0.5438	0.5442	0.5442
3.0	0.4223	0.4225	0.4223	0.4223
5.0	0.2887	0.2890	0.2888	0.2886
7.0	0.2019	0.2021	0.2019	0.2018
10.0	0.1594	0.1595	0.1594	0.1594
20.0	0.0834	0.0835	0.0834	0.0834
50.0	0.0342	0.0343	0.0342	0.0342
70.0	0.0176	0.0177	0.0177	0.0176
100.0	0.0172	0.0172	0.0172	0.0172

All values of the dimensionless condensation rate can be multiplied by the appropriate value of the free molecular condensation rate from the below equation to obtain the actual, dimensionally correct condensation rate for any specific system of interest:

$$\tilde{u}_{fm}(\tilde{R}) = \pi \tilde{R}^2 \rho_0 \left(\frac{8\,k\,T}{\pi\,m} \right)^{1/2} \left(\frac{n_\infty - n_s}{n_s} \right)$$

where:

$\tilde{u}_{fm}(\tilde{R})$ is the free molecular condensation rate

$\tilde{R}$ is the droplet radius

ρ_0 is the vapor saturation mass density

k is Boltzmann's constant

T is the system temperature

m is the mass of a vapor molecule

n_∞ is the bulk number density of the vapor

n_s is the saturation number density of the vapor

Preparation of Atomic Oxygen Resistant Polymeric Materials

by
Victor J. Tortorelli*
Chemistry Department
Ursinus College
Collegeville, PA 19426

in association with
P. M. Hergenrother and J. W. Connell
Polymeric Materials Branch
NASA Langley Research Center
Hampton, VA 23665

Polyphenylquinoxalines (PPQs) are an important family of high performance polymers that offer good chemical and thermal stability coupled with excellent mechanical properties.[1] These aromatic heterocyclic polymers are potentially useful as films, coatings, adhesives, and composite materials for applications that demand stability in harsh environments.

PPQs are generally synthesized by the solution polymerization of aromatic bis(o-diamine)s and aromatic bis(phenyl-α-diketone)s (see figure 1). The properties of the resulting polymer can vary depending on the structure of either monomer. The overall objective was to develop polymeric materials with resistance to atomic oxygen for potential space applications. PPQs are the materials of choice because of their inherent stability and the ease at which substituted versions could be synthesized.

Previous work has demonstrated that a protective silicon oxide coating applied to a polymer surface substantially decreases the erosion rate of the polymer from attack by atomic oxygen.[2] Polyimides containing siloxane units in the backbone have been shown by both ground-based and flight experimentation to form a protective surface coating when exposed to atomic oxygen.[3] The oxygen presumably reacts preferentially with silicon to form thermodynamically stable silicon-oxygen bonds. This coating protects the underlying polymer from further erosion by atomic oxygen. However, since the siloxane unit is in the polymer backbone, cleavage of the siloxane by atomic oxygen causes a decrease in the polymer's molecular weight with a corresponding reduction in properties. If the siloxane units are attached as pendent groups their cleavage by atomic oxygen results in the polymer backbone remaining intact, thus preserving the properties of the polymer and forming a resilient silicate layer to protect the polymer (see figure 2). Recently at NASA, novel polyimides with pendent siloxane groups were prepared and exhibited superior properties to polyimides with siloxane segments in the backbone after exposure to atomic oxygen.[4]

Our approach was to prepare PPQs with pendent siloxane groups using the appropriate chemistry and then evaluate these polymers before and after exposure to simulated atomic oxygen (Asher). Either monomer, the bis(o-diamine)s or the bis(α-diketone)s can be synthesized with a hydroxy group to which the siloxane chain will be attached.

Bis(3,4-diaminophenyl)methanol was prepared by the sodium borohydride reduction of 3,3',4,4'-tetraaminobenzophenone.[5] This compound was then reacted with 1,4-bis(phenylglyoxylyl)benzene to form the PPQ as shown in figure 3. This polymer has a Tg of approximately 275°C. Reaction of this polymer with heptamethylhydrotrisiloxane in the presence of chloroplatinic acid should result in the formation of a siloxane containing PPQ. Unfortunately, the molecular weight of this polymer, as indicated by inherent viscosity, was too low to cast good films.

Preparation of a hydroxy-containing bis(α-dicarbonyl) compound is shown in figure 4. Polymerization with a tetraamine and subsequent reaction with a hydrotrisiloxane would result in a siloxane substituted PPQ (see figure 5). Work is continuing in this area and no results on this polymer are yet available.

Work to date has resulted in the preparation of several novel materials. The PPQ shown in figure 3 has been prepared and once quality film is obtained, then the siloxane derivative will be prepared. The hydroxy containing monomer, 1,4-bis(p-hydroxyphenyl-glyoxylyl)benzene, has been prepared. Reaction of this tetracarbonyl monomer with a tetraamine will result in the formation of a new PPQ. Reaction of this PPQ with the hydrosiloxane will be attempted.
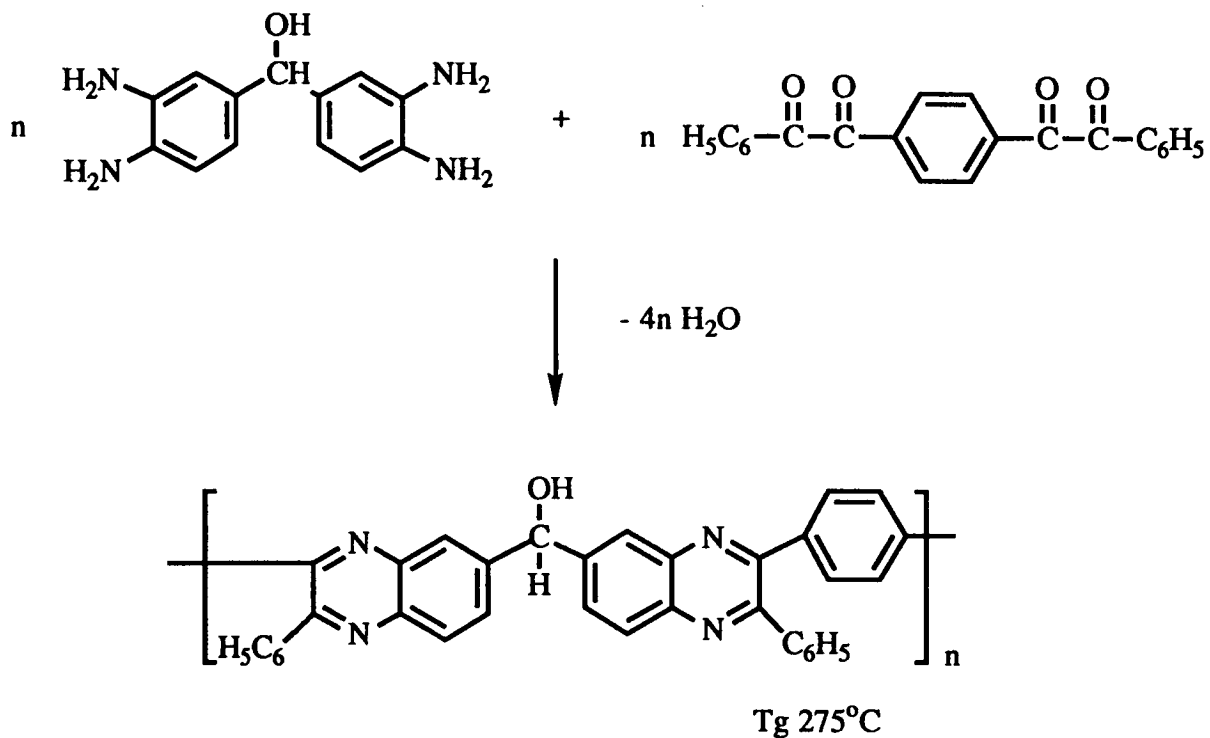
Future work will involve testing of the siloxane containing PPQs with atomic oxygen (Asher), preparation of other silicon containing PPQs, and investigation of methods to simplify the synthetic path to these PPQs.
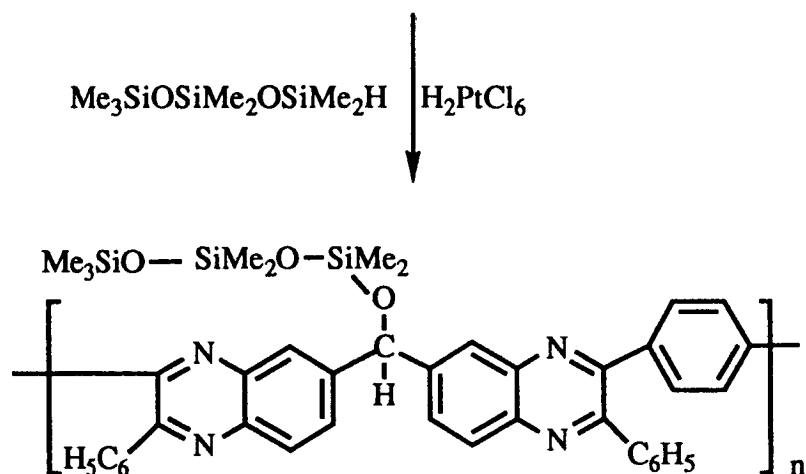
References

1. P. M. Hergenrother, **Encyclopedia of Polymer Science and Technology**, 2nd edition, Vol. 13, pp. 55-87, 1988.
2.a)D. G. Zimcik, M. R. Wertheimer, K. G. Balmain, and R. C. Tennyson, *Surface and Coatings Technology*, **39/40**, 617-626 (1989).
 b) I. Ritchie and H. B. Gjerde, *Surface and Coatings Technology*, **39/40**, 599-605 (1989).
3. J. McGrath, Virginia Poytechnic Institute and State University, unpublished results.
4. J. W. Connell, personal communication.
5. P. M. Hergenrother, *AFML TR-73-68*, 1973.

figure 1 Preparation of Polyphenylquinoxalines (PPQs)

Pendent Siloxane

Backbone Siloxane

figure 2 Pendent vs Backbone Siloxane Containing Polymers

Synthesis of Hydroxy Containing PPQ

Synthesis of Siloxane Substituted PPQ

Me = CH$_3$

figure 3

HOOCCH₂—⟨benzene⟩—CH₂COOH →(SOCl₂) Cl–C(=O)–CH₂—⟨benzene⟩—CH₂–C(=O)–Cl   89 %

+ 2 ⟨benzene⟩–OCH₃

AlCl₃ | CH₂Cl₂

68 %   ←(SeO₂ / CH₃COOH)—   79 %

HBr | CH₃COOH

mp 223°C
70 %
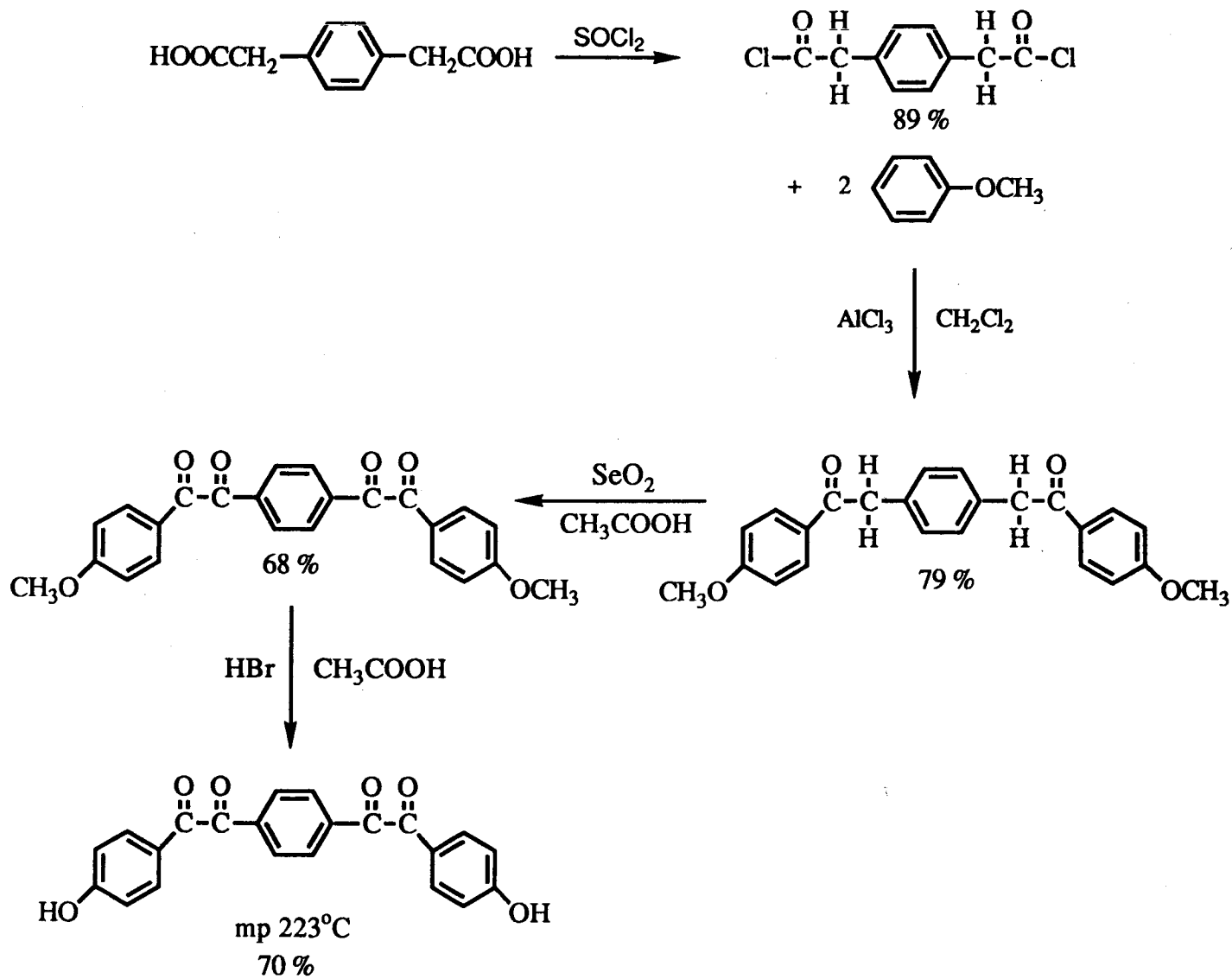
figure 4   Preparation of Dihydroxy bis(α-carbonyl) Monomer

% yields shown below each compound

Synthesis of Hydroxy Containing PPQ

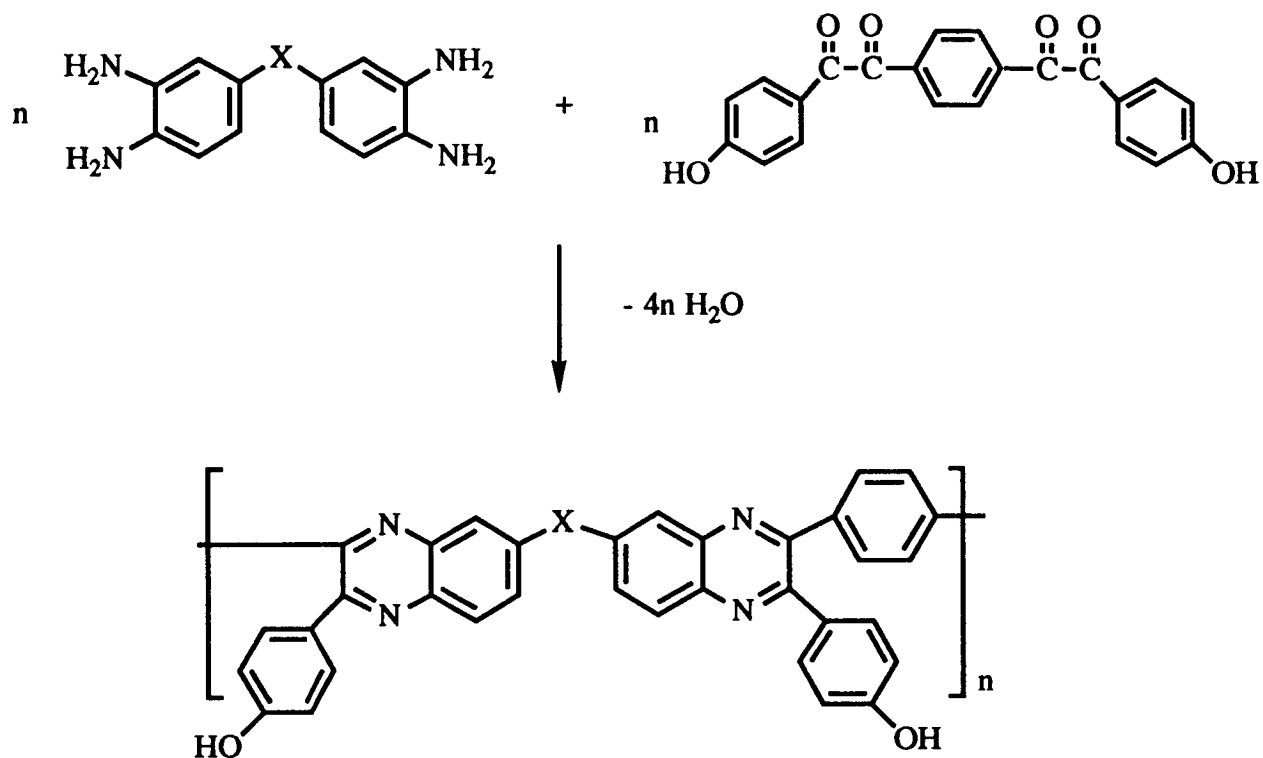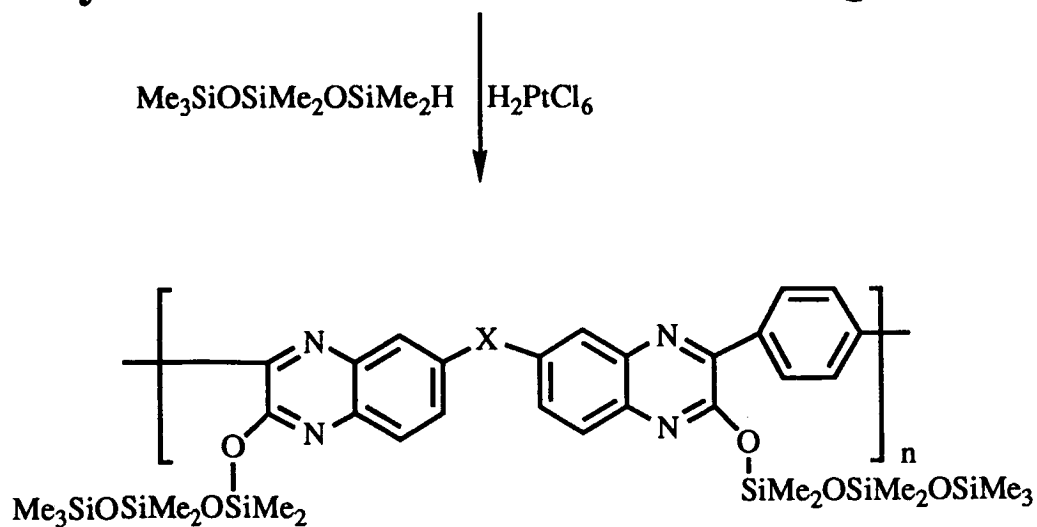## Synthesis of Siloxane Substituted PPQ

Me₃SiOSiMe₂OSiMe₂H   H₂PtCl₆

Me = CH₃

figure 5

SPACECRAFT DESIGN OPTIMIZATION USING TAGUCHI ANALYSIS

Dr. Resit Unal

Assistant Professor
Engineering Management Department
Old Dominion University
Norfolk, VA 23529

Reliable, readily available, and affordable space transportation systems have become the key to the success of future space missions. Congressional budget constraints and rising international competition dictate the need to design and build space systems at low cost even with increased performance, reliability and quality requirements. This implies that new philosophy, technology and advanced statistical tools must be employed to design and produce reliable, high quality space systems at low cost.

The quality engineering methods of Dr. Genichi Taguchi, employing design of experiments, are important statistical tools for designing high quality systems at reduced cost. Taguchi methods have been used successfully in Japan and the United States in designing reliable, high quality products at low cost in such areas as automobiles and consumer electronics. However, these methods are just begining to see application in the aerospace industry.

Taguchi methods provide an efficient and systematic approach to optimize designs for performance, quality, and cost. The objective is to determine the optimum levels for the controllable design parameters such that the system is functional, exhibits a high level of performance under a wide range of conditions, and is robust to noise factors.

Studying the design variables one at a time or by trial and error until a first feasible design is found, is a common approach to design optimization. However, this usually leads to either a very long and expensive time span for completing the design or a premature termination of the design process due to budget or schedule pressures. The result in most cases, is a product design which is far from optimal.

In contrast, the Taguchi method utilizes orthogonal arrays from design of experiments theory to study the design parameters simultaneously and their interactions. Using orthogonal arrays significantly reduces the number of experimental configurations to be studied. Furthermore, the conclusions drawn from a small scale of experiments are valid over the entire experimental region spanned by the control factors and their settings.

The Taguchi method reduces research and development costs by improving the efficiency of generating information. As a result, development time can be shortened significantly and, important design parameters affecting operation, performance, and cost can be identified.

This research effort utilized the Taguchi method for a weight optimization study for a lunar aerobrake. Aerobrakes are devices which use atmospheric drag instead of propulsion system thrust to modify the velocity and trajectory of a space vehicle.

Aerobraking is proposed for both Mars orbital insertion and for Earth orbit insertion following Lunar or Martian missions. The main advantage of aerobrakes is the significant reduction expected in propellant required as compared to a lunar/Mars orbit insertion using all propulsive braking. Yet, to date, there has been little structural evaluation or design of lunar/Mars aerobrakes to justify further consideration. The objective of this study was to identify viable minimal weight candidate lunar aerobrake structures, and those structural design parameters which have the most profound effect on the final structure weight.

The Taguchi method was utilized to study several simultaneous parameter level variations of an lunar aerobrake structure to arrive at the lightest weight configuration. Finite element analysis was used to analyze the unique experimental aerobrake configurations selected by the Taguchi method. The approach consisted of the following steps:

1. Identify the design parameters and their alternative levels,

2. Define the possible interactions between these parameters,

3. Select an appropriate Taguchi orthogonal array,

4. Create a linear graph and determine the parameter arrangement,

5. Conduct the matrix experiment using finite element analysis,

6. Create a response table and analyze the data,

7. Determine optimum levels for the design parameters,

8. Predict the performance under these levels and verify.

Using the above approach, important design parameters affecting weight and global buckling were identified and the lowest weight design configuration was selected. The study resulted in significant weight savings as compared with the initial (baseline) design configuration. Given the high cost of launching cargo into orbit, the weight reduction realized can result in large savings in cost.

Overall, the results suggest that Taguchi approach to design optimization is a powerful tool which can offer simultaneous improvements in performance, engineering productivity and cost.

Line Narrowing of AgGaSe$_2$
Optical Parametric Oscillator
by Injection Seeding

George H. Watson
Assistant Professor
Department of Physics and Astronomy
University of Delaware
Newark, Delaware 19716

Research Associates:
Norman Barnes
Keith Murray

The use of high-energy pulsed lasers has become the primary means for remote sensing of trace molecular constituents in the atmosphere. LIDAR (lightwave detection and ranging) is used routinely for spatial profiling of trace concentrations of ozone, for example. In particular, Differential Absorption LIDAR (DIAL) is used to provide greater sensitivity. Molecular selectivity is accomplished by wavelength tuning of the laser to a strong absorption of the desired molecular specie. Many strong absorption lines of interest are in the mid-infrared region (2 to 12 μm). Further, the spectral linewidths of these molecular absorptions are narrow in the gaseous state. Extension of DIAL to molecules such as greenhouse gases thus requires development of new narrow-linewidth pulsed sources of mid-IR radiation.

The Flight Electronics Division (FED) at NASA Langley Research Center is currently developing solid-state lasers for atmospheric applications. As part of this effort, optical parametric oscillators (OPO) are being investigated as sources of tunable radiation in the 2.5 to 12 μm range where development of conventional lasers is subject to numerous difficulties.[1] Parametric oscillation is a nonlinear optical technique for converting laser output to longer wavelengths. Incident photons, typically from a pulsed pump laser, are converted into two photons of longer wavelength, while satisfying energy conservation. The particular split of energy is determined by momentum conservation; the wavelength of interest is usually selected by angle orientation of the nonlinear material with respect to the direction of propagation of the pump beam.

Recently an OPO based on AgGaSe$_2$ has been under consideration by the Environmental Sensors Branch of the FED. This material possesses a strong nonlinear coefficient, optimal birefringence, and excellent transmission in the mid-IR. This OPO, pumped by a 1.73 μm Er:YLF laser, was shown to have low thresholds and high slope efficiencies and was observed to have a spectral

linewidth of $\sim$ 20 nm.[2] Line narrowing of the $AgGaSe_2$ OPO to the picometer level is desired.

Injection seeding is a technique commonly used to line narrow pulsed laser output. By injecting low intensity light from an external single-frequency laser (typically as low as μW) into a laser resonator, the spectral linewidth of the high energy laser can be reduced to that of the external source. Pulsed injection seeding has recently been demonstrated in a β-barium borate OPO in the visible.[3] Here we report cw injection seeding of a $AgGaSe_2$ OPO in the mid-IR.

Approximately 200 μW of 3.39 μm HeNe radiation was injected into the OPO, tuned to that wavelength, described in Ref. 2. The seed beam was mode-matched to the OPO resonator to maximize coupling with the pump laser . The HeNe laser operated predominately in a single longitudinal mode with a spectral linewidth less than 5 pm ($\sim$ 0.1 GHz), measured with a scanning Fabry-Perot interferometer.

The spectral behavior of each OPO output pulse was monitored with a 0.5 m monochromator and a pyroelectric camera. Although the monochromator was capable of 0.2 nm resolution and the camera/software combination provided an effective resolution of 0. 4nm/pixel, thermal bleeding to neighboring pixels limited the overall resolution to $\sim$ 1nm. The spectral response to the pump and seed beams are shown in Fig. 1, indicating the instrument resolution.

A typical unseeded OPO output was observed to extend over $\sim$ 20 nm, confirming previously observations.[2] On successful seeding, the OPO linewidth was seen to collapse to a value smaller than measurable by this spectroscopic technique.

Work in progress includes more accurate determination of the actual OPO linewidth on seeding by using interferometric techniques. In addition, the effects of seeding on the pulse time evolution interval are being examined. Investigation of line narrowing by other methods, $ZnGeP_2$ OPO work, and pumping with a 2.1 μm Ho:YAG laser are future projects.

1. N. P. Barnes, "Tunable Mid Infrared Sources Using Second Order Nonlinearites," *Nonlinear Optics*, in press (1991).

2. N. Barnes and K. Murray, "Er:YLF-Pumped $AgGaSe_2$ Optical Parametric Oscillator," *OSA Proceedings on Advanced Solid-State Lasers*, H. P. Jenssen and G. Drube, eds. (Optical Society of America, Washington, DC 1991), Vol. 6, pp. 322-328.

3. Y. X. Fan, R. C. Eckardt, R. L. Byer, J. Nolting, and R. Wallenstein, "Visible BaB_2O_4 Optical Parametric Oscillator Pumper at 355 nm by a Single-Axial-Mode Pulsed Source," *Appl. Phys. Lett.* **53**, 2014 (1988), J. G. Haub, M. J. Johnson, B. J. Orr, and R. Wallenstein, "Continuously Tunable, Injection-Seeded β-Barium Borate Optical Parametric Oscillator: Spectroscopic Applications," *Appl. Phys. Lett.* **58**, 1718 (1991).

a. Pump

| 1.73 μm

b. Seed

| 3.39 μm

c. Unseeded OPO

16 nm

| 3.54 μm

d. Seeded OPO

1 nm
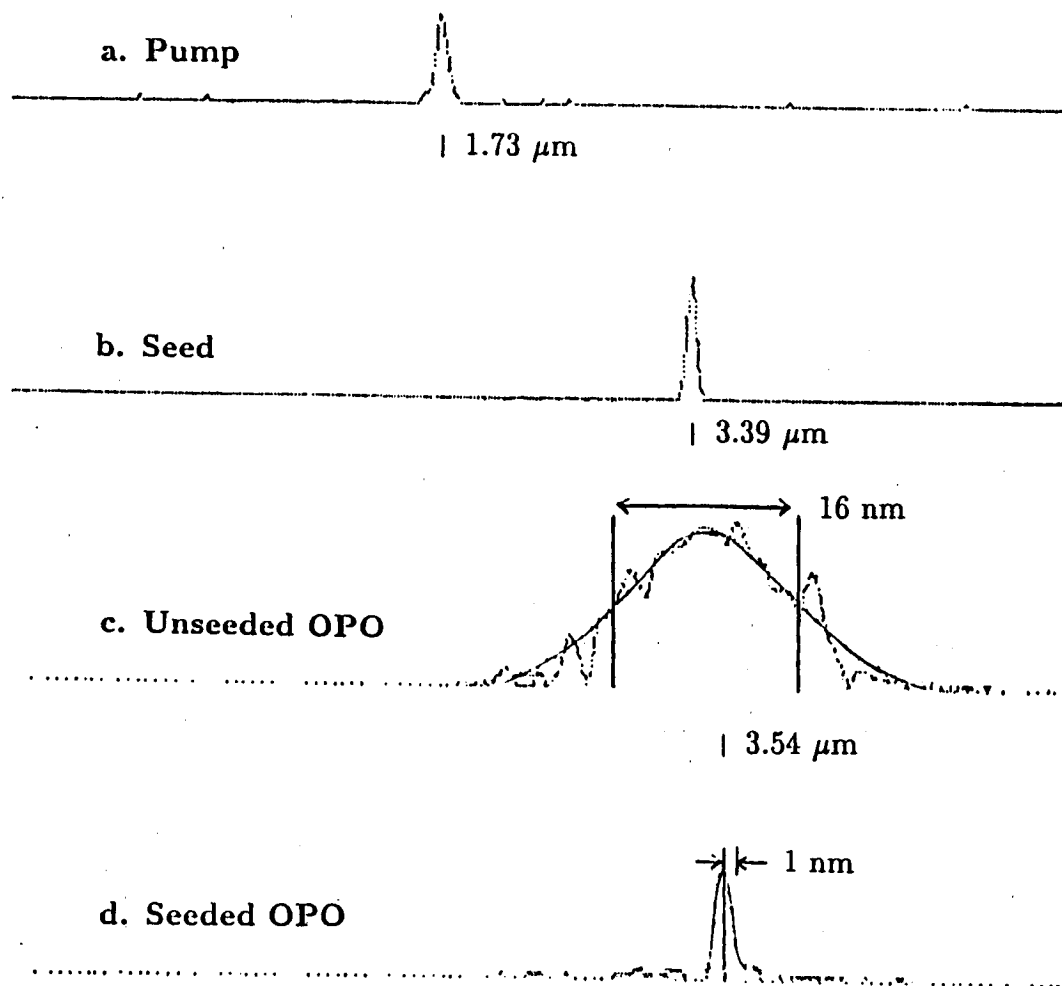
Fig. 1. *Line Narrowing as a Result of Injection Seeding AgGaSe₂ Optical Parametric Oscillator.* Observed linewidths of pump and seed beams are instrument limited. The output linewidth of the seeded OPO becomes narrower than the resolution limit.

THE EFFECT OF
A TYPE III AND TYPE IV SHOCK/SHOCK INTERACTION
ON HEAT TRANSFER IN THE STAGNATION REGION

by

Dennis Wilson
Associate Professor
Department of Mechanical Engineering
The University of Texas at Austin
Austin, Texas 78712

One of the major engineering challenges in designing the National Aerospace Plane, NASP, is to overcome augmented heating on the intake cowl lip from shock/shock interactions. The shock/shock interation arises when the bow shock from the craft's nose interferes with the bow shock from the cowl lip. Considering only the region immediately around the cowl lip, the problem geometry may be simplified as that of an oblique shock impinging on a bow shock from a circular cylinder. Edney [1] classified six different interference patterns resulting from an oblique-shock/curved-bow-shock interaction. Of these six types, the Type III and Type IV are most significant in that augmented surface heat transfer may be ten to thirty times greater than the case without the shock/shock interaction [2].

Several researchers, [3] and [4], have attempted to numerically compute the flowfield created by the shock/shock interaction. Their results for the Type III and Type IV interactions have always underpredicted the maximum surface heat transfer in the stagnation region. Empirical correlations could be used, but again these relationships only interpolate known data for the range which experiments have been performed. If viscous effects are included, a global flowfield computation would require excessive computational time and grid points to accurately resolve the shear layer and boundary layer to obtain accurate surface flux quantities. A more rational approach which considers only the boundary layer and a finite number of parameters to characterize the shear layer is described in this abstract.

The objective of this research was to begin to develop a mathematical model which is capable of predicting the effect of a Type III and Type IV shock/shock interaction in the stagnation region of an arbitrary two-dimensional body. This model must be capable of predicting the maximum surface heat flux and the surface stagnation point pressure once the outer (effectively inviscid) flowfield is given. Therefore, it must capture the unsteady physics of the impinging shear layer.

The approach taken here will be to solve the unsteady equations for the stagnation-point region on the surface of a blunt body in a Type III shock/shock interaction flowfield. Figure 1 [4] displays a schematic of the overall flowfield for a Type III shock/shock interaction. Figure 2 displays in greater detail where the shear layer impinges upon the boundary layer. Essentially this is an oblique reattaching shear layer forming an unsteady stagnation-point flow. The key to the success of the method is to accurately characterize the large-scale, quasi-periodic structures in the impinging shear layer. Recent success with a simpler but physically similar flowfield, [5] and [6], gives cedibility to this approach.

The computational domain of interest is illustrated in Figure 2. To quantify the boundary layer edge condition of the computational domain the flow outside of the boundary layer is assumed to be inviscid. This assumption will allow the outer flow to be characterized by the compressible form of the Euler equations. The boundary-layer edge velocity is assumed to be composed of pulsations, oscillations, and a term to account for obliqueness and vorticity in the incoming flow. The details of constructing this phenomenological model are somewhat involved and are omitted from this abstract. It is important to point out that the parameters which appear in the edge velocity models will be determined a priori using experimental data from compressible shear layers. Ultimately, these model parameters will depend only upon the characteristic Mach numbers of the shear layer, M_2 and M_4, and the characteristic length of the shear layer. The near wall flowfield will be modeled using the unsteady, compressible forms of the Navier-Stokes and thermal energy equations as applied to a stagnation region.

REFERENCES

1. Edney, B., "Anomalous Heat Transfer and Pressure Distributions on Blunt Bodies at Hypersonic Speeds in the Presence of an Impinging Shock", FFA Report 115, Aeronaut. Res. Inst. of Sweden (1968).
2. Nowak, R.J., M.S. Holden, and A.R. Wieting, "Shock/Shock Interference on a Transpiration Cooled Hemispherical Model", AIAA Paper 90-1643 (1990).
3. Klopfer, G.H., and H.C. Yee, "Viscous Hypersonic Shock-On-Shock Interaction on Blunt Cowl Lips", AIAA Paper 88-0233 (1988).
4. Glass, C.E., "Computer Program To Solve Two-Dimensional Shock-Wave Interference Problems With an Equilibrium Chemically Reacting Air Model", NASA TM-4187 (1990).
5. Wilson, D.E., and P.K. Philips, "A Phenomenological Model for the Near Wall Structure due to a Turbulent Reattaching Flow behind a Backward Facing Step", Computers and Experiments in Fluid Flow; Proceedings of the fourth International Conference on Computational Methods and Experimental Measurements, Computational Mechanics Publications, Southampton, U.K. (1989) pp. 171-180.
6. Wilson, D.E., and A.J. Hanford, "The Effect of Spatial and Temporal Freestream Fluctuations on Stagnation Point Heat Transfer", Report 90-108, The Fluid Dynamics Group, Bureau of Engineering Research, The University of Texas, Austin, TX (1990).
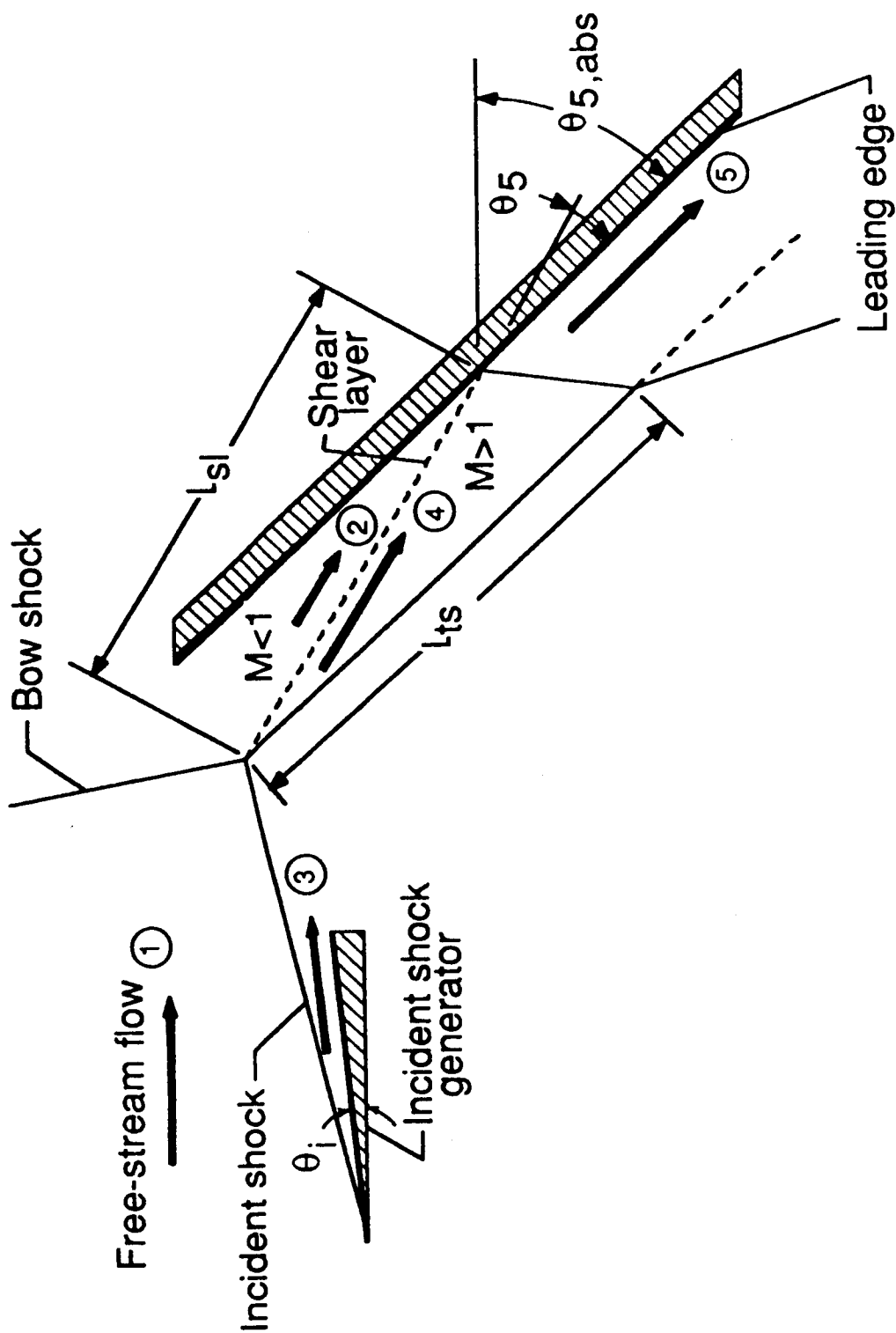
Figure 1: Overall flowfield for a Type III shock/shock interaction (from reference [4]).
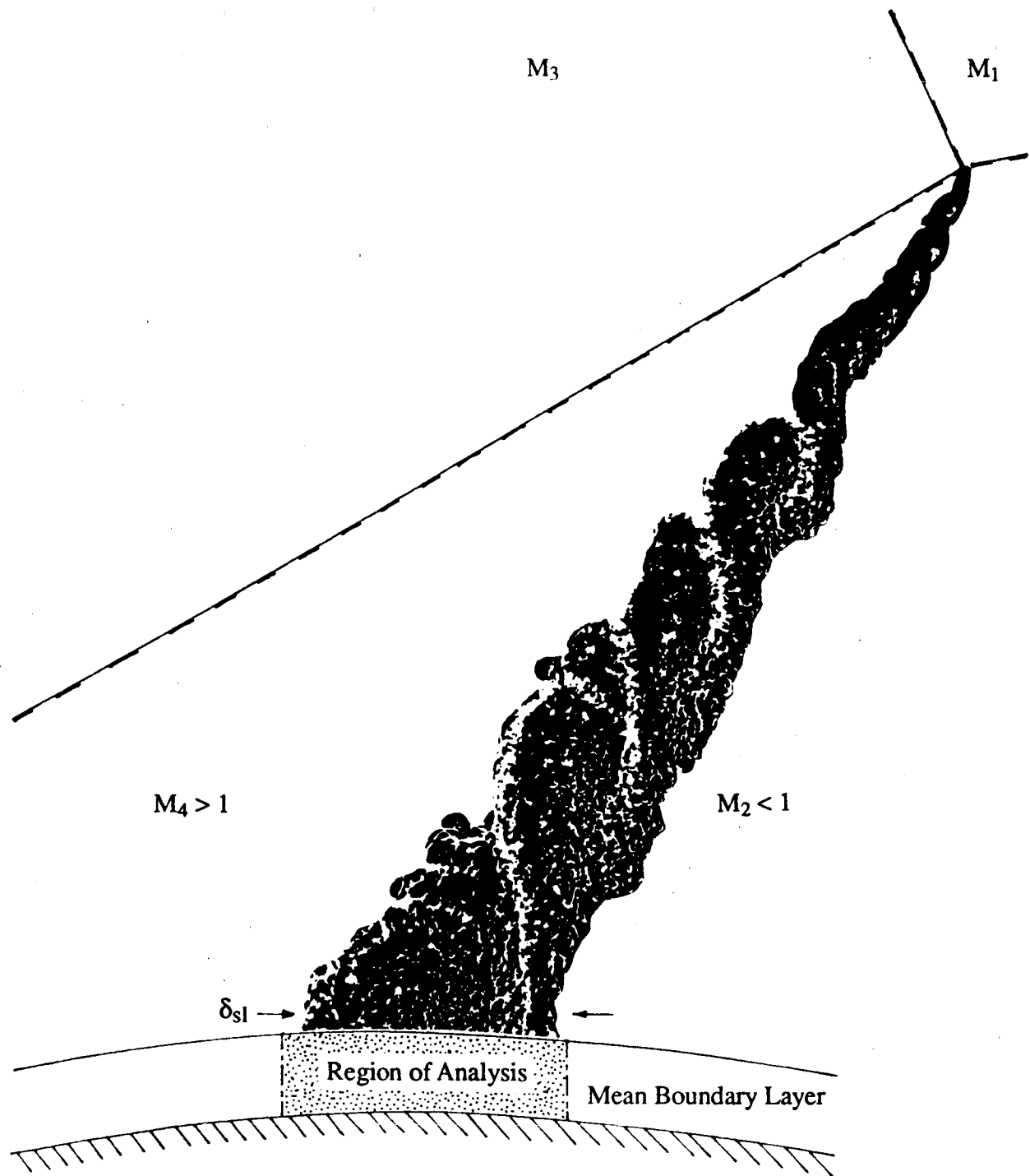
Figure 2: Schematic of the local flowfield in the stagnation region showing the impingement of the large-scale, quasi-periodic structures in the shear layer.

Navier-Stokes Calculation of Transonic Flow Past the NTF 65-deg Delta Wing

by

Chivey C. Wu
Associate Professor of Mechanical Engineering
California State University, Los Angeles
Los Angeles, CA 90032

Models of four delta wings were built and tested in the 8 foot by 8 foot transonic wind tunnel at the National Transonic Facility, NASA Langley Research Center. The wings are identical in planform shape with a swept-back angle of 65 degrees, but bear different leading edge profiles. The models were tested under pressurized and cryogenic conditions to simulate true flight Reynold's numbers. Data on the aerodyanamic forces and pressure distributions at various locations on the wings were taken at various flight Mach numbers and angles of attack. Effects of high Reynold's number and leading edge radius on the aerodynamic characteristics of the wings are being accessed.

A preliminary analytical study was done at MIT, but it was limited to the case of low Reynold's number, thin layer laminar flow over one of the wings [1]. To thoroughly understand the turbulent, vortical flow around the wings, an effort to perform computational aerodynamic analysis is being committed. The objective of the analysis is to supplement and validate the experimental data and explain the high Reynold's number and leading edge effects. GRIDGEN, a software developed by General Dynamics, is being used to generate the grid topology for the flow field around the wings. The flow solver to be used is CFL3D, a computational fluid dynamics code developed by the Computational Aerodynamics Branch at Langley.

Based on the geometric description of the wings [2], a Fortran program called WINGSURF has been written to generate the databases defining the surface geometry of the wings. To match the true geometry of the models in the wind tunnel for realistic comparision with experimental results, databases defining the sting support for the wing models have also been created by two other Fortran programs, STINJOIN and STINREAR. Listing of the programs are attached and the geometry of a typical wing model with the sting support is shown in Fig. 1.

From the geometric databases, the computational grid for each wing both with and without the sting was created interactively on an IRIS Graphics Workstation employing the single block approach. A computational domain of 20 times the chord length of the wing in all directions was taken. Figs. 2 and 3 show the grid topology on

a typical wing surface and in the entire computational domain, respectively, for free flight (no sting) condition. Figs. 4 and 5 show similar grid topology for a typical wing model attached to the sting. For ease of future comparision with experimental data, the grid on the wing surface is generated in such a way that the grid lines at 20%, 40%, 60% and 80% chord always coincide with the pressure orifices on the models.

With the single block approach, however, the grid lines extending from the sting tip to the wing apex have to collapse into a singular grid surface right on top of the centerline of the wing, resulting in a loss of a large number of computational grid points. Also, changing the leading edge profile would require a complete regeneration of the volume grid in the entire computational domain. This means excessive computing time.

For better computing efficiency, a multi-block approach is being employed to modify the grids involving the sting. The computational domain is divided into seven blocks, as shown in Fig. 6 (near field) and Fig. 7 (far field). Since the multi-block approach allows different computational dimensions among different blocks, the collapsed grid surface is easily eliminated by placing the sting in a separate block. The leading edge surface now only appears in two of the blocks, making it much more efficient to change leading edge and regenerate the grids in these two block while leaving the grids in the other blocks intact.

Surface grids for each block are in the process of being generated. Upon obtaining the surface grids, the GRIDGEN3D module in GRIDGEN can be run on the Cray to create the volume grid in each block, resulting in a complete volume grid for the entire computational domain. The flow solver can then be applied to compute flow properties in the domain. Results will be used to compare with wind tunnel data and to access effects of high Reynold's number and leading edge radius.

Due to lack of time and change of blocking strategy, the volume grids are not yet complete and calculation of flow properties has not been attempted. A research proposal is being prepared to request future support for continuation of the project at the university.

References

1. Becker, T. M., "Hybrid 3-D Euler/Navier-Stokes Calculations of Transonic Vortex Flows over the NTF Delta Wing", MIT CFDL-TR-89-7, August, 1987.

2. Luckring, J. M., "NTF Delta Wing Geometry", Model Description, NASA Langley, 1987.

```fortran
      program wingsurf
      dimension a(4),b(4),c(4),d(4),x(22,22),z(22,22),y(22,22)
      pi = 4.*atan(1.)
      del = 65./180.*pi
      rc = 12.*tan(del)
      xle = .15*rc*cos(del)
      xte = .1*rc
      data b1/.510024/, c1/-.19819008/, d1/.025671542/
      data a/.4935262, .34897572, .20148123, 0.0/
      data b/.080048085, .29224873, .5087712, .804546399243/
      data c/-.19710469, -.28382228, -.37230603, .49317707317/
      data d/.046323876, .062270923, .078542758, .100770498643/
      do 900 k=1,4
      do 100 j=2,22
      xj = (22-j)/20.
      xn = xle*(exp(5.*xj)-1.)/(exp(5.)-1.)
      x(1,j) = xn/cos(del)
      y(1,j) = 0.
      z(1,j) = a(k)*xn**.5 + b(k)*xn + c(k)*xn**2 + d(k)*xn**3
 100  continue
      z(1,2) = b1*xte + c1*xte**2 + d1*xte**3
      x(1,1) = .15*rc
      x(2,1) = .2*rc
      x(3,1) = .4*rc
      x(4,1) = .6*rc
      x(5,1) = rc - 9.395
      x(6,1) = .8*rc
      x(7,1) = .9*rc
      do 110 i=1,7
      y(i,1) = 0.
      z(i,1) = z(1,2)
 110  continue
      do 130 i=8,22
      xi = (22-i)/15.
      xi = xte*(exp(4.*xi)-1.)/(exp(4.)-1.)
      x(i,1) = rc - xi
      y(i,1) = 0.
      z(i,1) = b1*xi + c1*xi**2 + d1*xi**3
 130  continue
      do 115 i=2,22
      do 115 j=2,22
      x(i,j) = x(i,1)
      y(i,j) = (x(i,j)-x(1,j))/tan(del)
 115  continue
      do 120 i=2,7
      do 120 j=2,22
      z(i,j) = z(1,j)
 120  continue
      do 125 i=8,22
      do 125 j=2,22
      z(i,j) = z(i,1)*z(7,j)/z(7,2)
 125  continue
      if (k.eq.1) open (7,file='bluntlo.dba')
      if (k.eq.2) open (7,file='interlo.dba')
      if (k.eq.3) open (7,file='sharplo.dba')
      if (k.eq.4) open (7,file='extralo.dba')
      write (7,*) 22,22
      write (7,*) ((x(i,j)/rc,i=1,22),j=1,22),
     1            ((y(i,j)/rc,i=1,22),j=1,22),
     2            ((-z(i,j)/rc,i=1,22),j=1,22)
      close (7)
 900  continue
      end
```

238

```fortran
      program stinjoin
      dimension x(30,10),z(30,10),y(30,10)
      pi = 4.*atan(1.)
      del = 65./180.*pi
      rc = 12.*tan(del)
      xte = .1*rc
      data b1/.510024/, c1/-.19819008/, d1/.025671542/
      data as/.3094608214/, bs/.3327982281/, cs/-.04163681011/,
     1     ds/.001507294514/
      tmax = b1*xte + c1*xte**2 + d1*xte**3
      do 100 j=1,10
      x(1,j) = rc-10.022+.627
      y(1,j) = 0.
      z(1,j) = tmax
      do 120 i=2,15
      xi = (i-1)/14.
      xi = .627 + (9.395-xte)*(exp(3.*xi)-1.)/(exp(3.)-1.)
      r = as*xi**.5 + bs*xi + cs*xi**2 + ds*xi**3
      t = tmax
      ang = (pi/2.-asin(t/r))/9.*(j-1)
      x(i,j) = rc-10.022+xi
      y(i,j) = r*sin(ang)
      z(i,j) = r*cos(ang)
      if (j.eq.10) z(i,j) = tmax
120   continue
      do 130 i=16,30
      xi = (i-15)/15.
      xi = 10.022-xte+xte*(exp(-4.*xi)-1.)/(exp(-4.)-1.)
      r = as*xi**.5 + bs*xi + cs*xi**2 + ds*xi**3
      if (xi.gt.9.5) r=1.65
      xt = 10.022-xi
      t = b1*xt + c1*xt**2 + d1*xt**3
      ang = (pi/2.-asin(t/r))/9.*(j-1)
      x(i,j) = rc - xt
      y(i,j) = r*sin(ang)
      z(i,j) = r*cos(ang)
130   continue
100   continue
      z(30,10) = 0.
      open (7,file='jointup.dba')
      write (7,*) 30,10
      write (7,*) ((x(i,j)/rc,i=1,30),j=1,10),
     1            ((y(i,j)/rc,i=1,30),j=1,10),
     2            ((z(i,j)/rc,i=1,30),j=1,10)
      close(7)
      end
```

```fortran
      program sting
      dimension x(10),y(10,10),z(10,10)
      pi = 4.*atan(1.)
      open (7,file='stingup2.dba')
      del = 65./180.*pi
      rc = 12.*tan(del)
      x(1) = rc
      x(2) = rc + 4.5
      do 100 i=1,2
      do 100 j=1,10
      y(i,j) = 1.65*sin(pi/18.*(j-1))
      z(i,j) = 1.65*cos(pi/18.*(j-1))
100   continue
      do 200 i=3,6
      x(i) = x(i-1)+.5
      r = 52.57-(50.92**2-(.5*(i-2))**2)**.5
      do 200 j=1,10
      y(i,j) = r*sin(pi/18.*(j-1))
      z(i,j) = r*cos(pi/18.*(j-1))
200   continue
      x(7) = rc + 17.59
      do 300 j=1,10
      y(7,j) = 2.125*sin(pi/18.*(j-1))
      z(7,j) = 2.125*cos(pi/18.*(j-1))
300   continue
      x(8) = rc + 19.5
      do 400 j=1,10
      y(8,j) = 2.875*sin(pi/18.*(j-1))
      z(8,j) = 2.875*cos(pi/18.*(j-1))
400   continue
      x(9) = rc + 25.7
      r = 2.875 + 6.2*tan(2.*pi/180.)
      do 450 j=1,10
      y(9,j) = r*sin(pi/18.*(j-1))
      z(9,j) = r*cos(pi/18.*(j-1))
450   continue
      x(10) = 20.*rc
      r = 2.875 + (19.*rc - 19.5)*tan(2.*pi/180.)
      do 500 j=1,10
      y(10,j) = r*sin(pi/18.*(j-1))
      z(10,j) = r*cos(pi/18.*(j-1))
500   continue
      do 600 i=1,10
      z(i,10) = 0.
600   continue
      write (7,*) 10,10
      write (7,*) ((x(i)/rc,i=1,10),j=1,10),


     1 ((y(i,j)/rc,i=1,10),j=1,10),((z(i,j)/rc,i=1,10),j=1,10)
      close (7)
      end
```
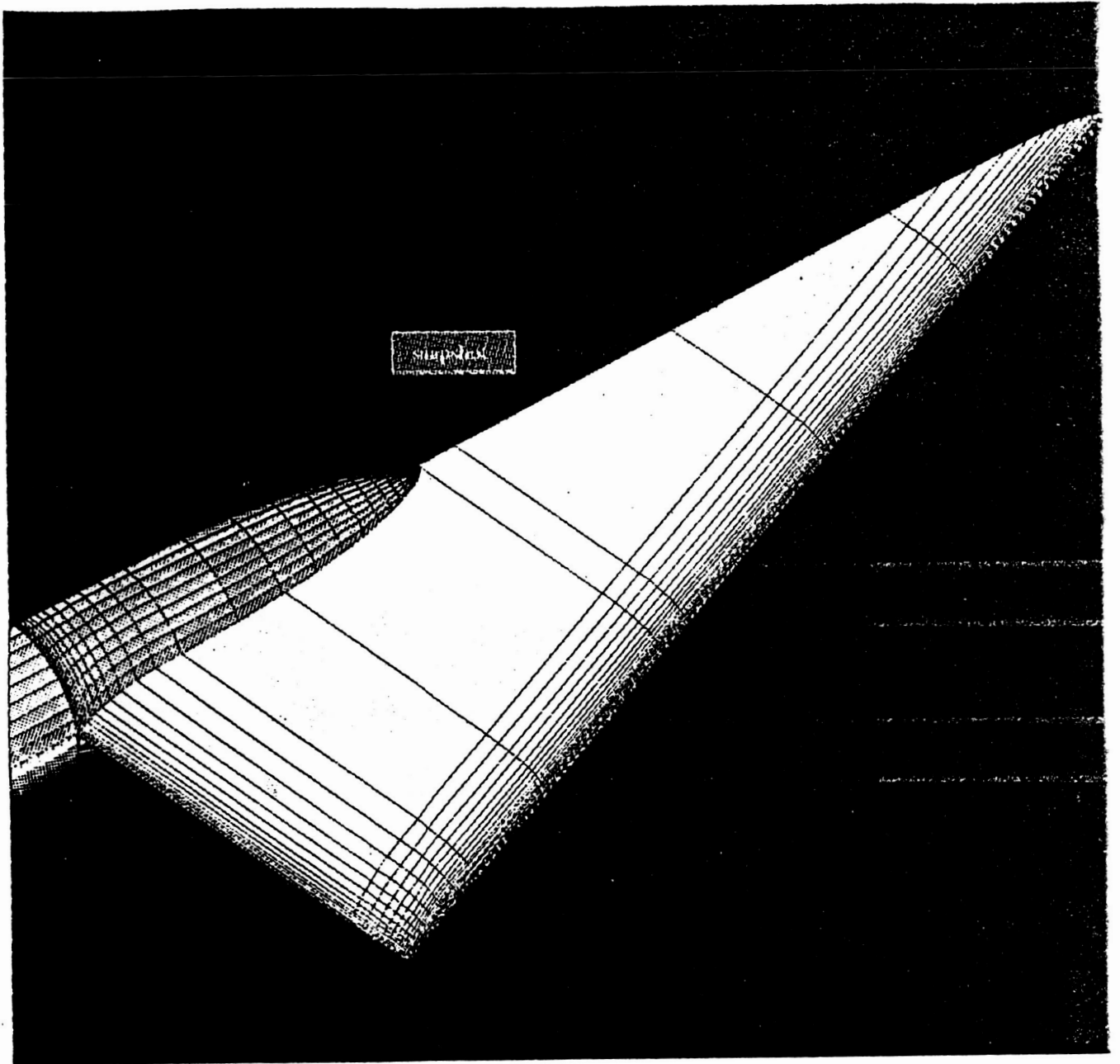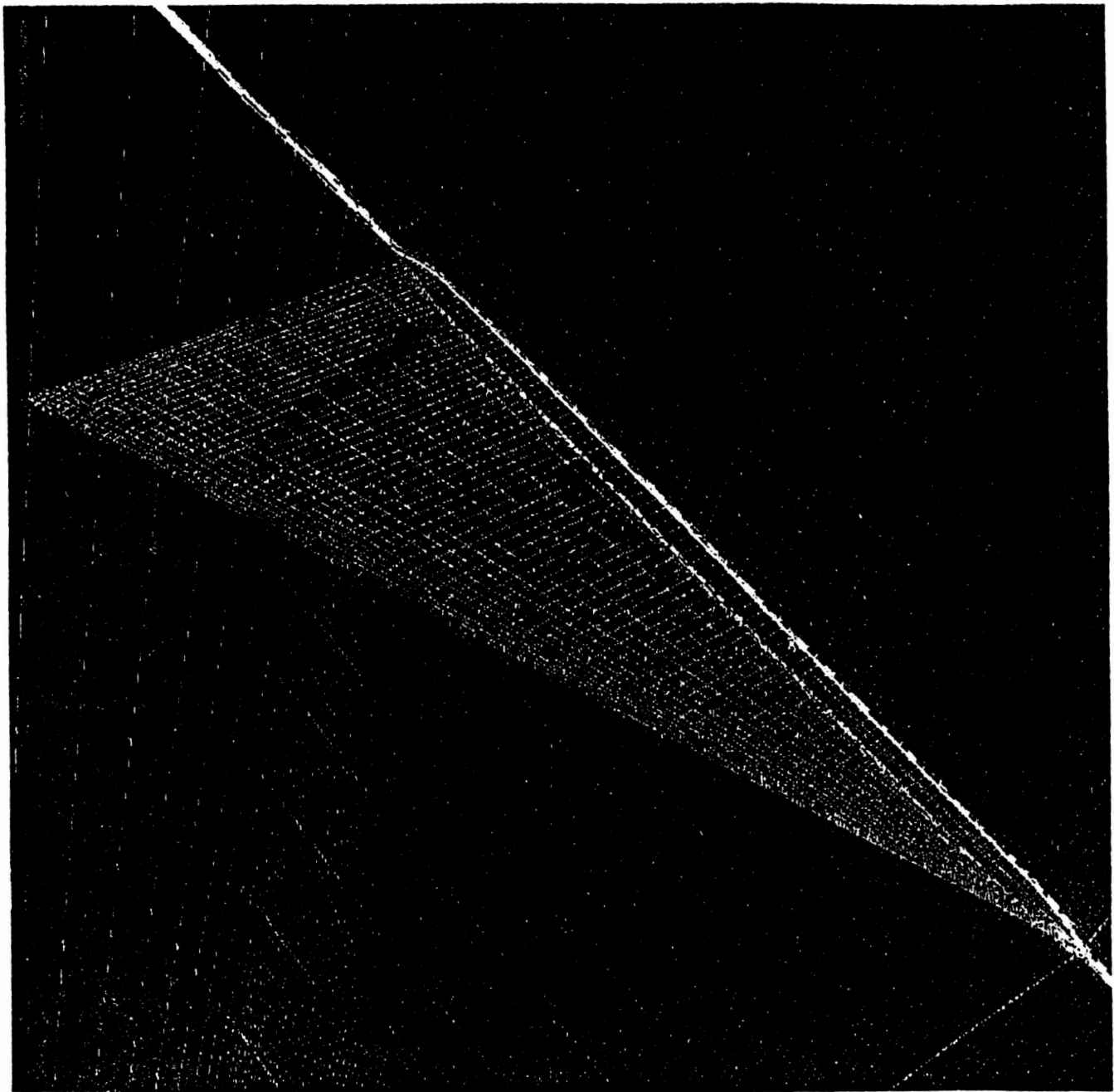
Fig. 1   Wing and Sting Geometry (Right Half)
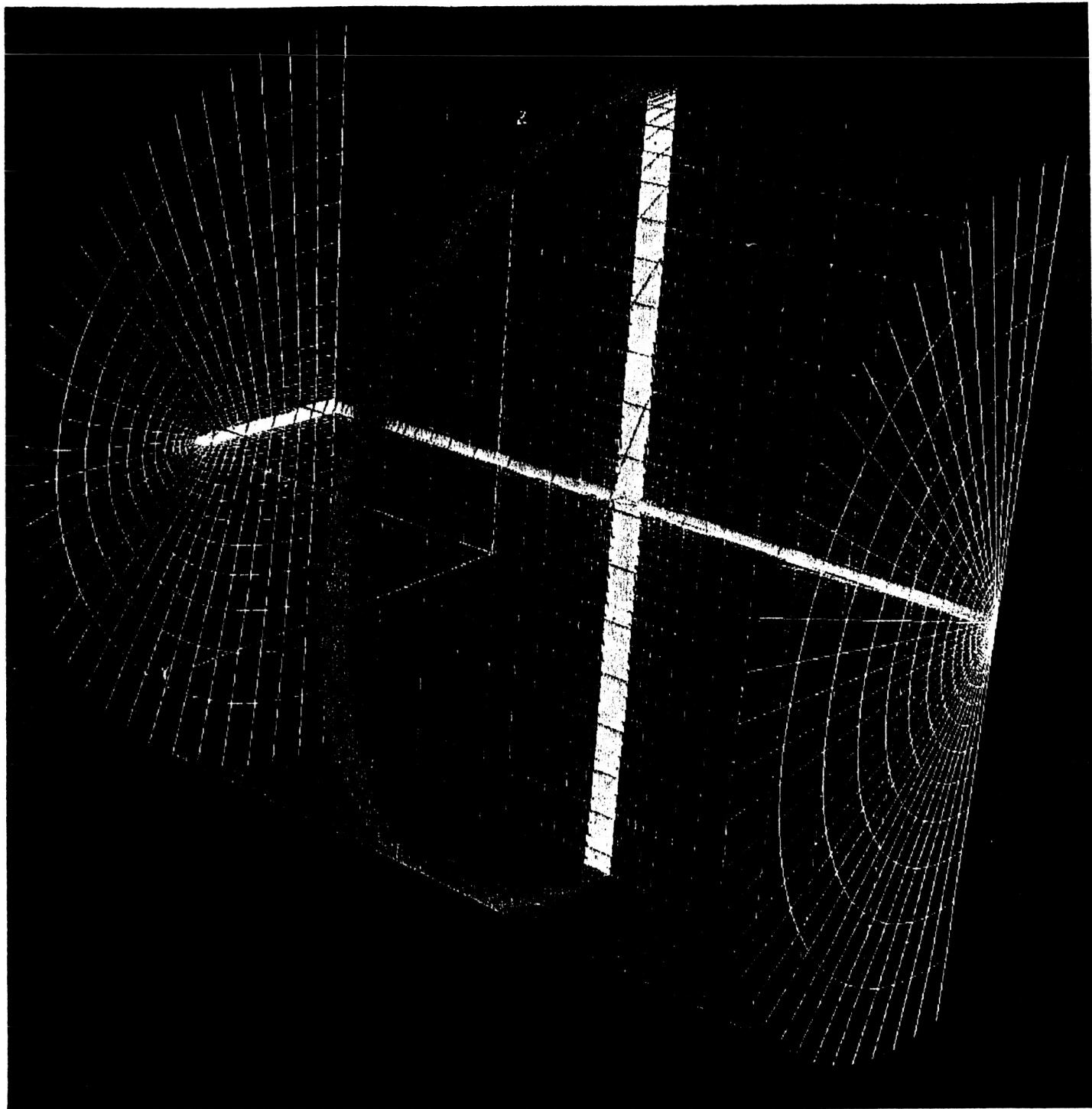
Fig. 2   Grid on Wing Surface

242

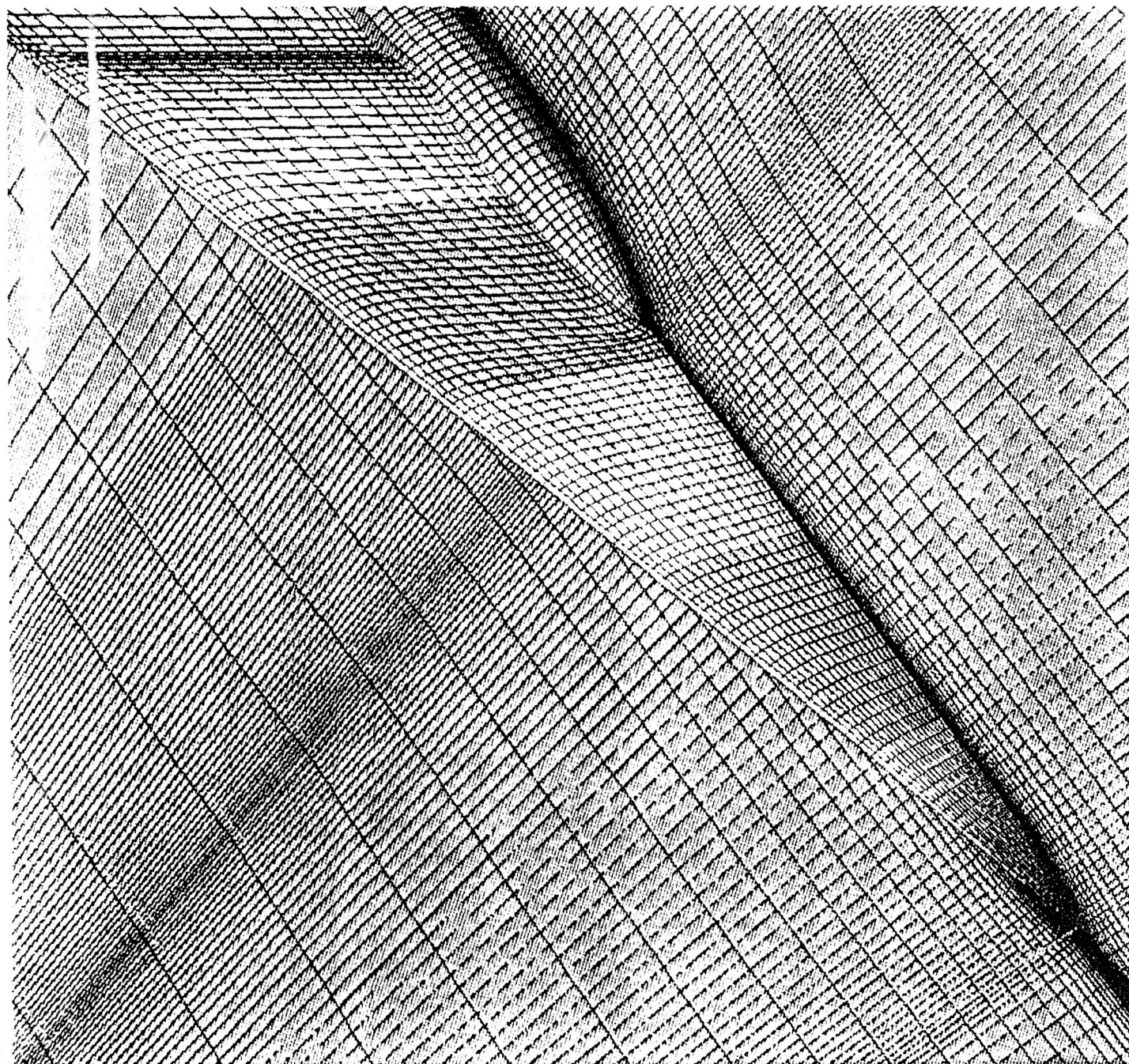Fig. 3 Grid for Entire Computational Domain Around Wing Alone

243

Fig. 4   Grid on Wing and Sting Surfaces
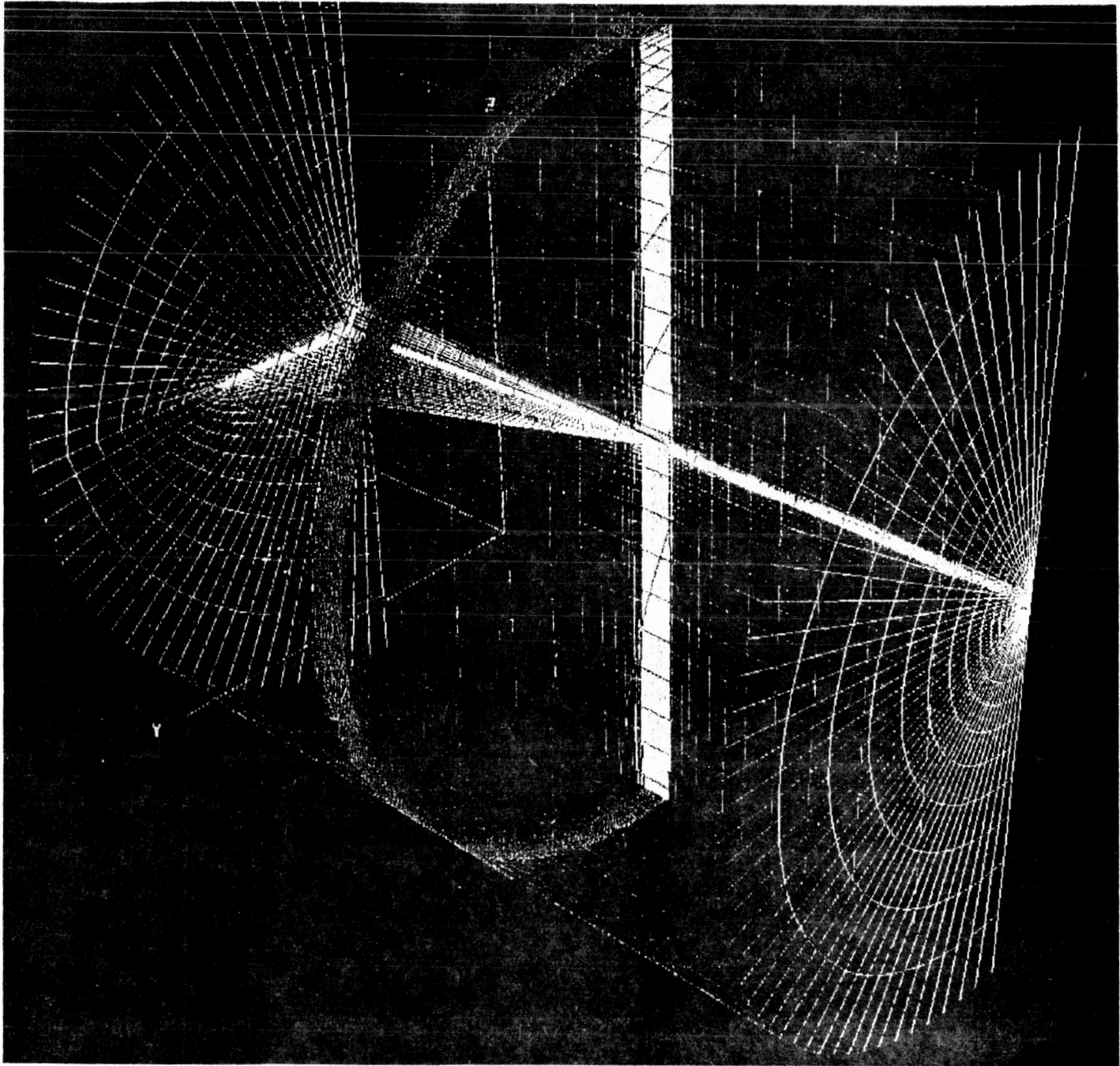
Fig. 5   Grid for Entire Computational Domain around Wing with Sting

245
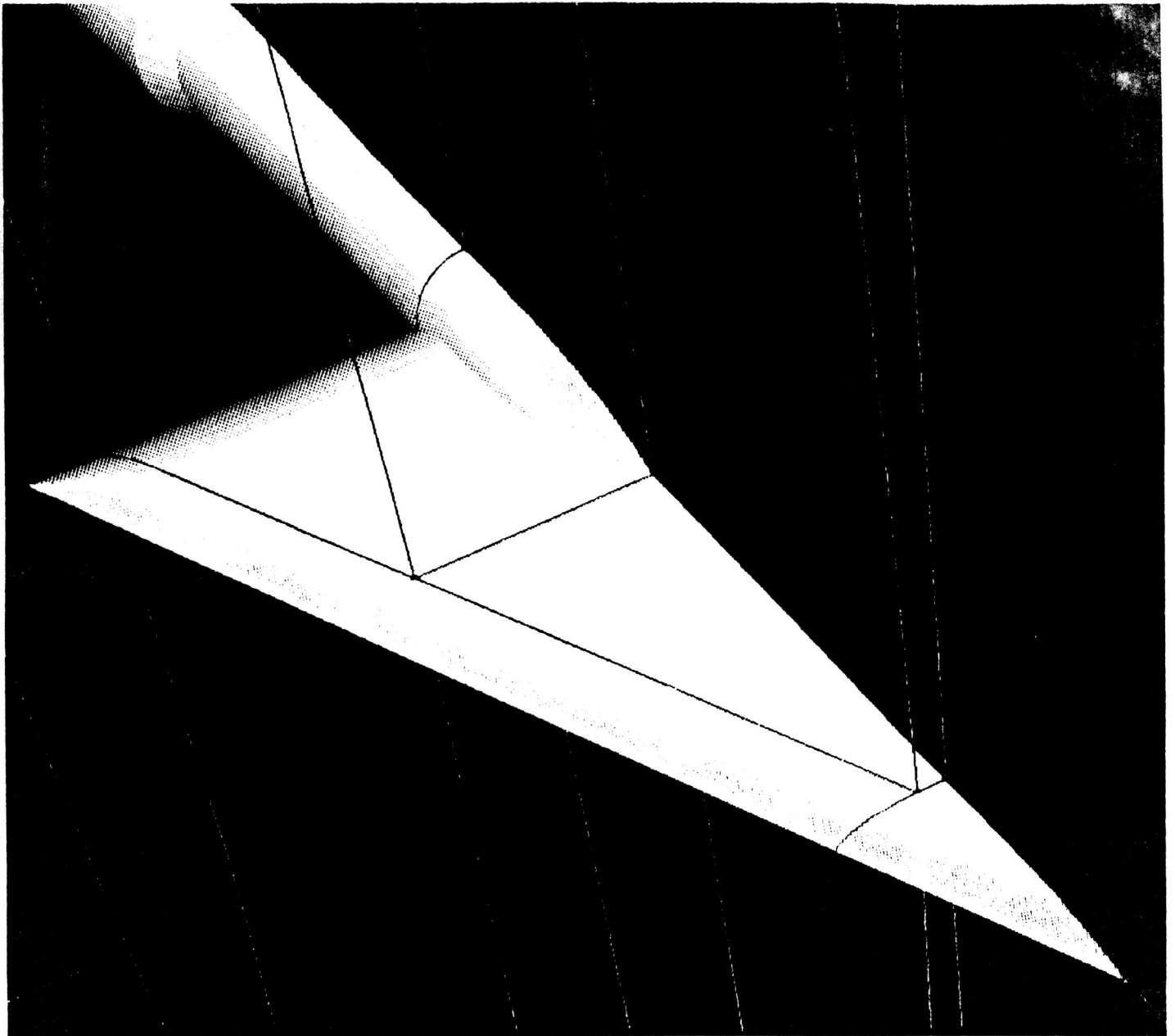
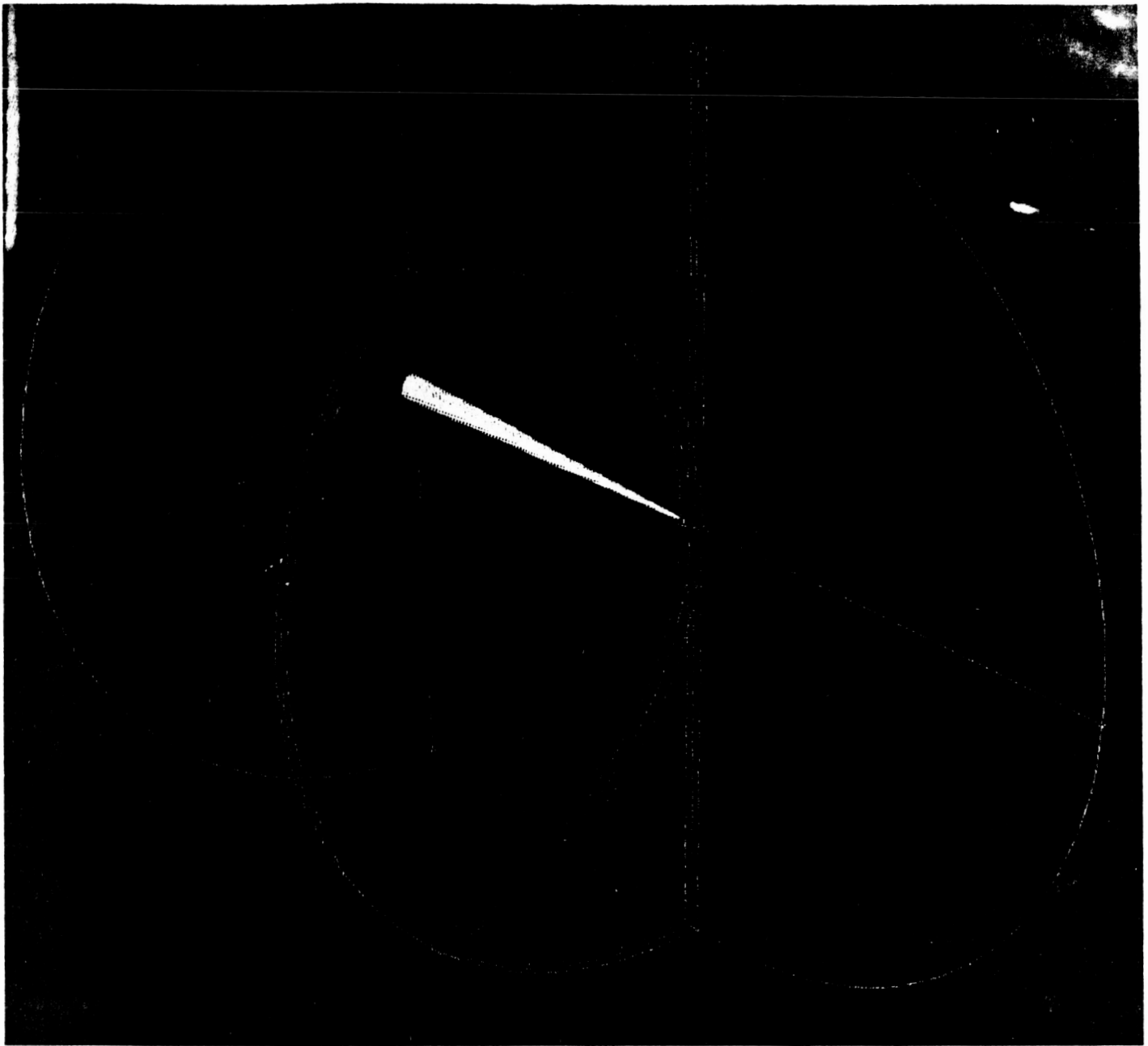Fig. 6   Blocking Strategy for Wing Model with Sting

Fig. 7   Seven-Block System for Entire Computational Domain

247

Object Oriented Development of Engineering Software
Using CLIPS

C. John Yoon
Assistant Professor
Department of Civil Engineering
Polytechnic University
Brooklyn, NY 11201

Object oriented approaches have emerged as one of the most promising paradigms for developing softwares that are reliable, flexible and maintainable[1]. During the early 1980's, there was much debate on what is object oriented programming; that debate is now more or less settled. Currently, active research centers around effective software design and development methodology using an object oriented programming paradigm [2].

The origins of CLIPS, the C Language Integrated Production System, date back to 1984 at NASA's Johnson Space Center and as the acronym indicates, it started as an expert system shell [3]. CLIPS is now used by over 3000 users throughout the public and private community including all NASA sites, branches of the military, numerous federal bureaus, government contractors, universities and many companies. CLIPS has grown to accommodate many other functions, such as utilities for embedded applications. The most recent release of CLIPS, version 5.0, introduces object oriented programming with COOL (CLIPS Object Oriented Language).

The work during the tenure involved (1) critical evaluation of COOL as an object oriented language, (2) investigation of object oriented software design and development methodolgy for engineering software and (3) implementation of a method for optimal sensor placement proposed by Kammer[4] with COOL.

As an object oriented language, COOL is more powerful than other widely used object oriented languages such as Smalltalk and C++. In Smalltalk, literally everything in it is an object and in that sense, Smalltalk is a pure object oriented language. Because a construct such as a class in COOL is not an object, COOL is not a pure object oriented language. However, COOL supports inheritance, encapsulation, abstraction, polymorphism, and dynamic binding - the five primary characteristics generally agreed that an object oriented language must support. COOL provides a rich set of utilities and tools, such as browsers, that are essential in developing an object oriented program. Lack of these tools

has been a criticism for many existing object oriented languages such as C++.

Engineering applications involve numeric complexity and manipulations of a large amount of data. Traditionally, numeric computation has been the concern in developing an engineering software. As engineering application software became larger and more complex, management of resources such as data, rather than the numeric complexity, has become the major software design problem. Object oriented design and implementation methodologies can improve the reliability, flexibility and maintainability of the resulting software; some tasks, however, are better solved with the traditional procedural paradigm. CLIPS, with deffunction and defgeneric constructs, supports procedural paradigm. The natural blending of object oriented and procedural paradigms has been cited as the reason for popularity of the C++ language. COOL's object oriented features are more versatile than C++'s. A software design methodology based on object oriented and procedural approaches appropriate for engineering software, and to be implemented in CLIPS, has been outlined. A method for sensor placement for Space Station Freedom that was proposed by Kammer is being implemented in COOL as a sample problem.

References

1. Cox, B.J., Object Oriented Programming, Addison-Wesley, Reading, MA, 1986.

2. Yoon, C.J., "An Object Oriented Design and Implementation of a Finite Element and Graphics Data Translation Facility", accepted for publication, special issue of the ASCE Journal of Computing in Civil Engineering devoted to object oriented concepts and applications.

3. Giarratano, J.C., CLIPS User's Guide, Version 5.0, Vol. 2, NASA Johnson Space Center, May 1991.

4. Kammer, D.C., "Sensor Placement for On-Orbit Modal Identification and Correlation of Large Space Structures", Journal of Guidance, Control, and Dynamics, Vol. 14, No. 2, Mar-Apr 1991.

ON THE CONTROL ASPECT OF LASER FREQUENCY STABILIZATION

By

Omar   Zia, Ph.D. , P.E.
Associate Professor
Electronic Engineering Technology
California Polytechnic State University
San Luis Obispo, Ca 93407

Realization of frequency stable lasers is viewed as key to progress in many areas of research and therefore, search for more effective techniques of frequency stabilization has intensified significantly in recent years. Investigating and validating the fundamental linewidth and frequency stability limits of a Nd:YAG laser oscillator, locked to a high finesse reference cavity in the microgravity and vibration-free environment of space, is the objective of a NASA project called" **SUNLITE**" at Langley Research Center. As part of this project NASA engineers have designed and built a space qualified system for measuring the linewidth and stability limits of an ultra-stable laser oscillator in space. In order to achieve greater stability and better performance, not only passive but also active frequency control, requiring use of feedback control loop has been applied. In this technique of frequency stabilization, based on basic property of feedback control theory, the intrinsic frequency noise and drift of the laser are expected to be reduced to the measurement noise level.

The objective of this paper   is to further investigate the application of feedback control theory in active frequency control as a frequency stabilization technique and determine the most appropriate control strategy to be used in general and in SUNLITE project in particular.

ACTIVE FREQUENCY CONTROL VIEWED AS A CONTROL SYSTEM PROBLEM.

The plant is the laser, the process that needs to be monitored and controlled is the frequency of the laser, which is a function of the optical path length of the laser. Optical path length of the laser can be varied by:
*   Temperature control of the laser gain medium.
*   Control of the current supplied to the diode laser pump.
*   Use of a Piezo-electric transducer.
While the first two methods have proven to be too slow for this application, use of piezo-electric transducer has received general acceptance as a practical method to this date. The block diagram for the active frequency control system presently applied in the SUNLITE project is given in Fig.1. For the sake of simplicity of analysis, the combination of converter, multiplier and low pass filter has been represented by frequency discriminator Fig. 2. The role of the discriminator is to monitor and convert the optical frequency fluctuations into voltage fluctuations.

ROLE OF FEEDBACK LOOP IN NOISE REDUCTION AND MEASUREMENT

There are several noise sources that cause the phase of the laser to wander leading to an output signal not a perfect sinusoid, resulting in instantaneous frequency variation and drift. In an attempt to minimize the noise, the block diagram of Fig. 3. was analyzed. It was concluded that for sufficiently large K_c (controller's gain) the output noise can be reduced to a minimum as shown in Eq. 1. Use of block diagram given in Fig. 4. which is a very crude approximation of the system in Fig. 3. for the purpose of measuring the laser noise, $S_{f, laser}$, is inaccurate at best. The effect of large K_c on the stability of the control loop was examined next. Attempt was made to identify system components with crucial impact. The transfer function of the controller was derived (Eq. 2), which indicates that R_x can have significant effect on the K_c, provided that R_F is chosen to be equal to R_1 as is the case in SUNLITE project.

FUTURE WORK

1. Digital versus analogue control

Replacement of the analogue controller $G_c(S)$, by a digital predictor/controller as shown in Fig. 5, is certainly an option, specially in the case of the SUNLITE project. Implementation of the control algorithm by the TMS320C30 microprocessor which is being used in the system for other purposes, is very much tempting and must be perused. Ofcourse it is essential to obtain an appreciation of the possible effects of the quantization. However, it must be reminded that in almost every control application, the inability to place controller poles with perfect precision, due to finite word length of the computer used for implementation, is quite insignificant in the overall design.

2. Alternative control approaches

System identification and noise cancellation, using adaptive linear algorithm or NEURAL-NET approach is definitely worth trying. Adaptive linear algorithms, including the least mean square algorithm (LMS) and the Kalman filter algorithm, can be used effectively in different types of tasks provided the systems being monitored or controlled are reasonably linear. Noisy situations where the source signals are not ever available in noiseless form, have not yet been handled by neural network algorithms.

REFERENCES

1. SUNLITE project Preliminary Design Review, Electronic Brunch, Flight Electronics Division, LaRC, NASA, 1990
2. Timothy Day, "Frequency Stabilized Solid State Laser for Coherent Optical Communication", Ph.D. Dissertation, Stanford University, Stanford California, 1990
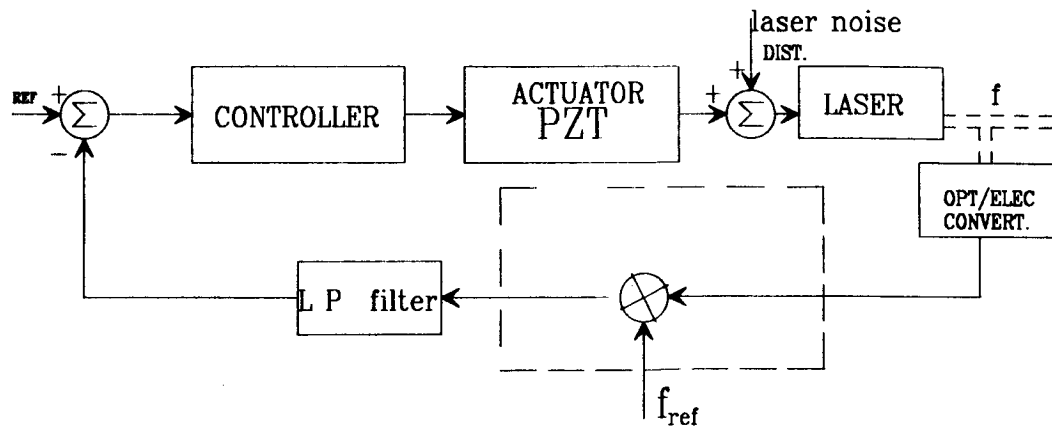
Fig. 1. Block diagram of the active control loop in frequency stabalization system.
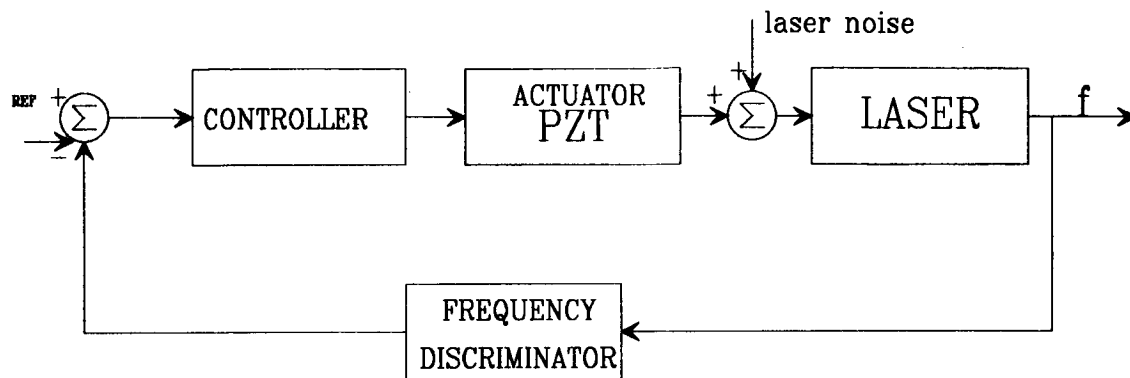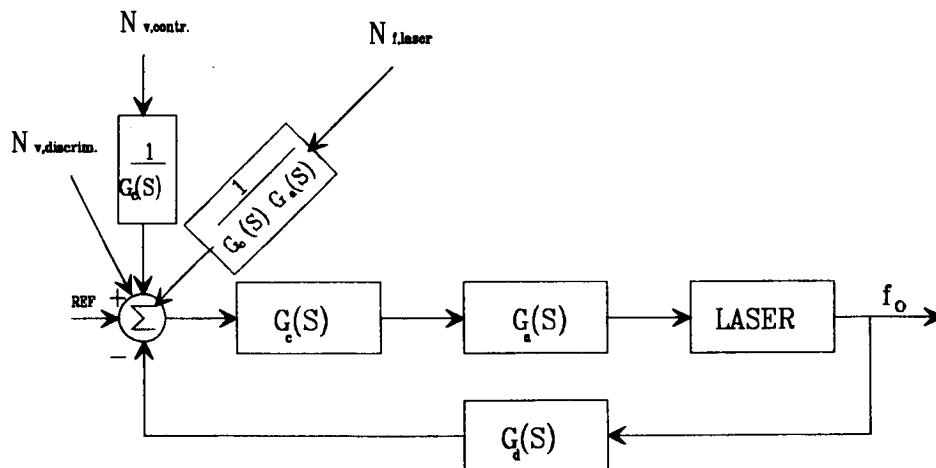

Fig. 2. Simplified block diagram of fig. 1.

Fig. 3. Use of feedback loop for noise reduction

$$\left|\Delta f_o\right| = \frac{\left|N_{v,discrim} * K_c * K_a\right|}{\left|1 + K_c * K_a * K_d\right|} = \frac{N_{v,discrim}}{K_d} \quad \ldots \ldots \text{Eq. 1.}$$

$$K_c \gg K_a > 1$$

252

$$G_c(S) = \frac{\dfrac{R_F}{R_1} \dfrac{R_F}{R_X} \left(1 + \dfrac{S}{1/R_1 C_1}\right)}{\left(1 + \dfrac{S}{1/R_F C_F}\right) \left(1 + \dfrac{S}{1/R_F C_F}\right)} \qquad \ldots\ldots\ldots \text{Eq. 2..}$$

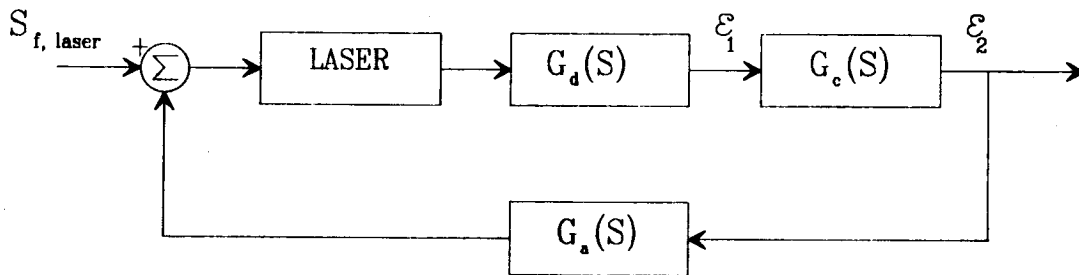$$R_1 = R_F = 1 \text{ MEG} \qquad C_1 = 33pF \qquad C_F = 0.0047UF$$

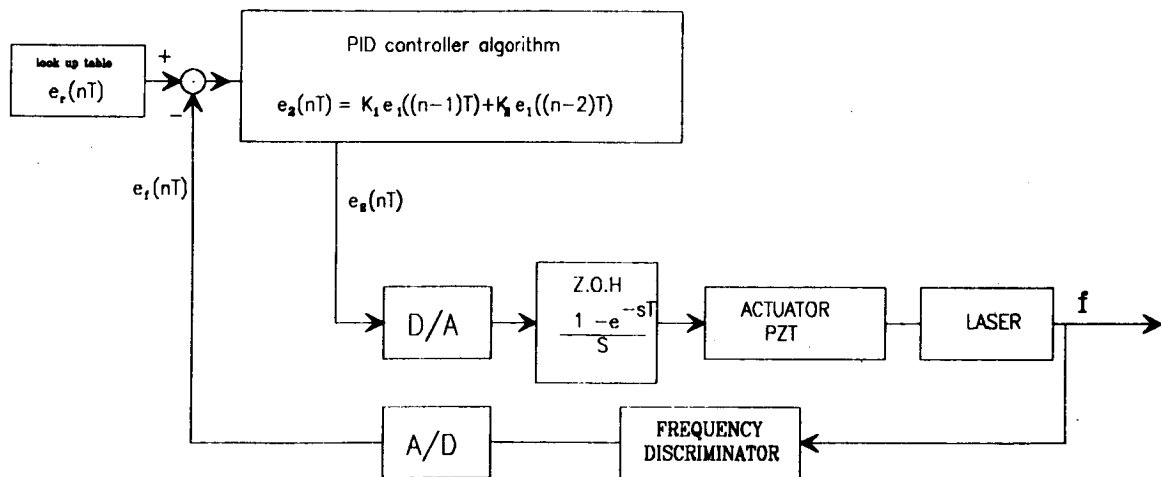Fig. 4. Laser noise treated as the only input to the system

Fig. 5. Proposed discrete controller

253

APPENDIX XI

SAMPLE QUESTIONNAIRES

NASA-ASEE

SUMMER FACULTY RESEARCH PROGRAM

QUESTIONNAIRE FOR RESEARCH ASSOCIATES

Please complete and return to Mary Fagley by August 2, 1991, NASA MS 105A.

1. Would you say that your Fellow was adequately prepared for his/her research assignment?

   YES   NO   (Circle One)

   Comments:_____

   _____

   _____

   _____

2. Would you comment on the diligence, interest, and enthusiasm with which your Fellow approached his/her research assignment.

   Comments:_____

   _____

   _____

   _____

3. Would you be interested in serving as a Research Associate Again?

   YES   NO   (Circle One)

   Comments:_____

   _____

   _____

   _____

4. Would you be interested in having your Fellow (if eligible) return a second year?

   YES   NO   (Circle One)

   Comments:_____

   _____

   _____

   _____

5. Any recommendations regarding improvement of the program will be appreciated.

   Comments:_____

   _____

   _____

   _____

   _____

   _____

   _____

   Signature_____

American Society for Engineering Education

NASA/ASEE Summer Faculty Fellowship Program
Evaluation Questionnaire

(Faculty Fellows are asked to respond to the following questions)

Name: _____

Birthdate: _____

Social Security Number: _____

Permanent Mailing Address: _____

_____

_____

_____

Home Institution: _____

NASA Center and (Laboratory) Division: _____

Name of Research Associate: _____

Brief Descriptive Title of Research Topic: _____

257

A. | Program Objectives

1. Are you thoroughly familiar with the research objectives of the research (laboratory) division you worked with this summer?

   Very much so _____
   Somewhat _____
   Minimally _____

2. Do you feel that you were engaged in research of importance to your Center and to NASA?

   Very much so _____
   Somewhat _____
   Minimally _____

3. Is it probable that you will have a continuing research relationship with the research (laboratory) division that you worked with is summer?

   Very much so _____
   Somewhat _____
   Minimally _____

4. My research colleague and I have discussed follow-up work including preparation of a proposal to support future studies at my home institution, or at a NASA laboratory.

   Yes _____   No _____

5. What is the level of your personal interest in maintaining a continuing research relationship with the research (laboratory) division that you worked with this summer?

   Very much so _____
   Somewhat _____
   Minimally _____

B. Personal Professional Development

1. To what extent do you think your research interests and capabilities have been affected by this summer's experience? You may check more than one.

   Reinvigorated _____
   Redirected _____
   Advanced _____
   Just maintained _____
   Unaffected _____

2. How strongly would you recommend this program to your faculty colleagues as a favorable means of advancing their personal professional development as researchers and teachers.

   With enthusiasm _____
   Positively _____
   Without enthusiasm _____
   Not at all _____

3. How will this experience affect your teaching in ways that will be valuable to your students? (you may check more than one)

   By integrating new information into courses _____

   By starting new courses _____

   By sharing research experience _____

   By revealing opportunities for future employment in government agencies _____

   By depending your own grasp and enthusiasm _____

   Will affect my teaching little, if at all _____

4. Do you have reason to believe that those in your institution who make decisions on promotion and tenure will give you credit for selection and participation in this highly competitive national program?

   Yes _____   No _____

C. | Administration

1. How did you learn about the Program? (Please check appropriate response)

_____ Received announcement in the mail.

_____ Read about in a professional publication.

_____ Heard about it from a colleague.

_____ Other (explain). _____
_____
_____

2. Did you also apply to other summer faculty programs?

Yes _____   No _____

_____ DOE

_____ Another NASA Center

_____ Air Force

_____ Army

_____ Navy

3. Did you receive an additional offer of appointment from one or more of the above? If so, please indicate from which.   No _____   Yes _____

_____

4. Did you develop new areas of research interest as a result of your interaction with your Center and laboratory colleagues?

Many _____
A few _____
None _____

260

5. Would the amount of the stipend ($900 per week) be a factor in your returning as an ASEE Fellow next summer?

Yes _____
No _____
If not, why _____
_____

6. Did you receive any informal or formal instructions about submission of research proposals to continue your research at your home institution?

Yes _____   No _____

7. Was the housing and programmatic information supplied prior to the start of this summer's program adequate for your needs?

Yes _____   No _____

8. Was the contact was your research colleague prior to the start of the program adequate?

Yes _____   No _____

9. How do you rate the seminar program?
Excellent _____
Very good _____
Good _____
Fair _____
Poor _____

10. In terms of the activities that were related to your research assignment, how would you describe them on the following scale?

Check one per activity			Time Was	
Activity	Adequate	Too Brief	Excessive	Ideal
Research				
Lectures				
Tours				
Social/Recreational				
Meetings				

11. What is your overall evaluation of the program?

Excellent _____

Very good _____

Good _____

Fair _____

Poor _____

12. If you can, please identify one or two significant steps to improve the program.

_____
_____
_____
_____

13. For second-year Fellows only. Please use this space for suggestions no improving the second year.

_____
_____
_____
_____

D. Stipend

1. To assist us in planning for appropriate stipends in the future would you indicate your salary at your home institution.

   $ _____ per Academic year _____ or Full year _____. (check one)

2. Is the amount of the stipend the primary motivator to your participation in the ASEE Summer Faculty Fellowship Program?

   Yes _____   No _____   In part _____

3. What, in your opinion, is an adequate stipend for the ten-week program during the summer of 1991?

   $ _____

E. American Society for Engineering Education (ASEE) Membership Information

1. Are you currently a member of the American Society for Engineering Education?
   Yes _____   No _____

2. Would you like to receive information pertaining to membership in the ASEE?
   Yes _____   No _____

PLEASE USE THIS PAGE FOR YOUR COMMENTS TO ANY QUESTION

_____
_____
_____
_____
_____
_____
_____
_____
_____
_____
_____
_____
_____
_____
_____
_____
_____
_____
_____
_____
_____
_____
_____
_____

NASA
National Aeronautics and Space Administration

Report Documentation Page

1. Report No. NASA CR-187598	2. Government Accession No.	3. Recipient's Catalog No.
4. Title and Subtitle NASA/American Society for Engineering Education (ASEE) Summer Faculty Fellowship Program 1991		5. Report Date September 1991
		6. Performing Organization Code
7. Author(s) Surendra N. Tiwari (Compiler)		8. Performing Organization Report No.
		10. Work Unit No.
9. Performing Organization Name and Address Old Dominion University Norfolk, VA 23508		11. Contract or Grant No. NGT 47-003-029
		13. Type of Report and Period Covered Contractor Report 3 June - 9 August 1991
12. Sponsoring Agency Name and Address National Aeronautics and Space Administration Langley Research Center Hampton, VA 23665-5225		14. Sponsoring Agency Code

15. Supplementary Notes

Langley Technical Monitor: Dr. Samuel E. Massenberg

16. Abstract Since 1964, the National Aeronautics and Space Administration (NASA) has supported a program of summer faculty fellowships for engineering and science educators. In a series of collaborations between NASA research and development centers and nearby universities, engineering faculty members spend 10 weeks working with professional peers on research. The Summer Faculty Program Committee of the American Society for Engineering Education supervises the programs.
Objectives: (1) To further the professional knowledge of qualified engineering and science faculty members; (2) To stimulate and exchange ideas between participants and NASA; (3) To enrich and refresh the research and teaching activities of participants' institutions; (4) To contribute to the research objectives of the NASA center. Program Description: College or university faculty members will be appointed as Research Fellows to spend 10 weeks in cooperative research and study at the NASA Langley Research Center. The Fellow will devote approximately 90 percent of the time to a research problem and the remaining time to a study program. The study program will consist of lectures and seminars on topics of interest or that are directly relevant to the Fellow's research topics. The lectures and seminar leaders will be distinguished scientists and engineers from NASA, education, or industry.

17. Key Words (Suggested by Author(s)) ASEE-NASA Summer Faculty Fellowship Program ASEE-NASA Administrative Report	18. Distribution Statement Unclassified - unlimited Subject Category - 80		
19. Security Classif. (of this report) Unclassified	20. Security Classif. (of this page) Unclassified	21. No. of pages 271	22. Price A12

NASA FORM 1626 OCT 86